

**Dissertation**

submitted to the  
Combined Faculties for the Natural Sciences and for Mathematics  
of the Ruperto-Carola University of Heidelberg, Germany

for the degree of  
Doctor of Natural Sciences

**presented by**

M.Sc. (Mol. Medicine) Gerd Christian Quack  
born in: Cologne, Germany

Oral examination: \_\_\_\_\_



# **Targeting MAPK Signaling in Hepatocellular Carcinoma**

-

## **Implications for Cell Fate, Microenvironment and Immune Recognition**

Referees: Prof. Dr. Stephan Urban  
Prof. Dr. Christine Falk



*Für meine Eltern*

---



# Table of Contents

<b>List of Figures</b> .....	<b>iv</b>
<b>List of Tables</b> .....	<b>vi</b>
<b>List of Abbreviations</b> .....	<b>vii</b>
<b>Summary</b> .....	<b>1</b>
<b>Zusammenfassung</b> .....	<b>2</b>
<b>1 Introduction</b> .....	<b>3</b>
1.1 Liver Immunology .....	5
1.1.1 Function of the immune system in the liver.....	5
1.1.2 Hepatic cytokine milieu .....	8
1.2 Hepatocellular Carcinoma .....	12
1.2.1 Oncogenic signaling in HCC .....	13
1.2.2 NK cells and the recognition of hepatocellular carcinoma cells.....	17
1.2.3 Overview of immunological and signaling treatment options .....	21
<b>2 Goals of the Thesis</b> .....	<b>24</b>
<b>3 Materials</b> .....	<b>26</b>
3.1 Cell Culture.....	26
3.2 Antibodies.....	27
3.3 Buffers, Chemicals, Reagents and Special Machines.....	28
<b>4 Methods</b> .....	<b>30</b>
4.1 Cell Culture.....	30
4.2 Tissue Preparation .....	34
4.3 Flow Cytometry .....	36
4.4 Detection of Cell Proliferation.....	38
4.5 Detection of Apoptosis .....	41
4.6 Multiplex Analysis of Cytokines and Phosphorylated Proteins .....	42
4.7 Enzyme-Linked Immunosorbent Assay (ELISA) .....	45
4.8 Western Blot Analysis .....	45
4.9 Signaling Pathway Drawing .....	46
4.10 Generation of Classification Trees .....	46
4.11 Statistics .....	46

<b>5</b>	<b>Results .....</b>	<b>47</b>
5.1	Signaling Pathways in HCC and Small Molecule Inhibitors.....	47
5.1.1	Comparison of MAPK inhibitors at the phosphorylation level .....	49
5.1.2	Effects of MAPK inhibitors on other signaling pathways .....	52
5.1.3	MAPK inhibition limits proliferation of HCC cells.....	57
5.1.4	Some MAPK inhibitors induce apoptosis in HCC.....	62
5.2	Immunological Side Effects of MAPK Inhibitors .....	72
5.2.1	Characterization of hepatocellular carcinoma cell lines .....	72
5.2.2	Influence of MAPK inhibition on HLA, NK receptor ligands and adhesion molecule expression.....	75
5.2.3	Consequences of altered HLA class I and NK ligand expression for NK cell degranulation.....	80
5.2.4	Lymphocytes in normal, cirrhotic and HCC liver.....	84
5.2.5	MAPK inhibitors modulate chemokine and growth factor secretion in HCC cells .....	88
5.3	Modulation of MAPK Pathway in Healthy and HCC Tissue.....	93
5.3.1	Hepatic microenvironment.....	93
5.3.2	Modulation of cytokine and chemokine secretion by MAPK inhibitors in <i>ex vivo</i> hepatic tissue.....	99
<b>6</b>	<b>Discussion and Conclusions .....</b>	<b>105</b>
6.1	Signaling Pathways.....	105
6.1.1	MEK/ERK signaling in HCC cells .....	106
6.1.2	Akt, JNK and p38 signaling pathways.....	108
6.1.3	Proliferation .....	110
6.1.4	Apoptosis .....	112
6.1.5	Conclusion .....	117
6.2	Immunological Side Effects .....	118
6.2.1	Modulation of immune cell recognition following MAPK inhibition.....	118
6.2.2	Hepatic NK and T cells.....	122
6.2.3	Secretion of chemokines and growth factors by HCC cells.....	125

6.2.4	Conclusion .....	129
6.3	HCC and MAPK Pathway in the Tissue.....	130
6.3.1	Hepatic microenvironment.....	130
6.3.2	Modulation of the microenvironment by MAPK inhibitors .....	132
6.3.3	Conclusions .....	134
<b>7</b>	<b>References.....</b>	<b>135</b>
	<b>Acknowledgements.....</b>	<b>150</b>
	<b>List of Publications.....</b>	<b>151</b>
	<b>Conference Abstracts.....</b>	<b>151</b>
	<b>Appendix .....</b>	<b>152</b>

## List of Figures

Figure 1: Development of hepatocellular carcinoma. ....	3
Figure 2: Structure of hepatic lobule. ....	6
Figure 3: Hallmarks of cancer. ....	12
Figure 4: MAPK signaling pathway. ....	15
Figure 5: Activation of NK cells. ....	18
Figure 6: Schematic overview of molecular targeted therapy in HCC. ....	22
Figure 7: Chemical structures of MAPK inhibitors. ....	32
Figure 8: CFSE labeling of the cell. ....	39
Figure 9: xCELLigence technology and derivation of the cell index. ....	40
Figure 10: Apoptosis measurement with sub-G1 peak method. ....	42
Figure 11: Principle of multiplex analysis. ....	44
Figure 12: MAPK family and Akt signaling pathway and inhibitors of the MAPK pathway. ....	48
Figure 13: Modulation of MEK1 and ERK1/2 after treatment with MAPK inhibitor. ....	51
Figure 14: JNK, p38 and Akt phosphorylation after treatment with MAPK inhibitor. ....	55
Figure 15: c-Jun and ATF-2 phosphorylation after treatment with MAPK inhibitor. ....	57
Figure 16: Cell count of MAPK inhibitor-treated HCC cells. ....	58
Figure 17: xCELLigence profile of HCC cells treated with MAPK inhibitors. ....	59
Figure 18: MAPK inhibitor-mediated inhibition of cell division of HCC cells. ....	61
Figure 19: MAPK inhibitors induce apoptosis in HCC cell lines to a different extent. ....	63
Figure 20: p53 phosphoplex and WB analysis in HCC cells after MAPK inhibition. ....	65
Figure 21: p53 expression is modulated by MAPK inhibitors in HepG2 cells. ....	66
Figure 22: p53 family members p53, p63 and p73 are altered by sorafenib. ....	67
Figure 23: Death receptor expression on HCC cells. ....	68
Figure 24: MAPK inhibition increase CD95 expression in HepG2 cells. ....	69
Figure 25: Expression of Mcl-1 and Bcl-xL is reduced after sorafenib treatment. ....	70
Figure 26: Mcl-1 and Bcl-xL are partly modulated by MAPK inhibitors in Hep3B cells. ....	71
Figure 27: HLA and c-Met surface molecule expression of HCC cells. ....	73
Figure 28: NKG2D ligand surface molecule expression of HCC cells. ....	73
Figure 29: CD155 (PVR) and adhesion molecule expression of HCC cells. ....	74
Figure 30: HLA class I is altered by certain MAPK inhibitors in HCC cells. ....	75
Figure 31: c-Met surface molecule expression is altered by MAPK inhibitors in HCC cells. ....	76
Figure 32: ULBP2 and ULBP4 expression is altered by MAPK inhibitors in HCC cells. ....	77

Figure 33: CD155 expression is partly increased by sorafenib, AZD6244 and PD0325901 treatment.....	78
Figure 34: Adhesion molecules are altered by MAPK inhibitors in HCC cells .....	79
Figure 35: Degranulation of NK cells against HCC cells treated with MAPK inhibitors .....	81
Figure 36: Degranulating NK cells downregulate CD16 expression.....	82
Figure 37: CD16 and CD56 phenotype of NK cells is altered after long-term co-cultivation with HCC cells .....	83
Figure 38: Hepatic NK cells differ to peripheral NK cells regarding CD16 and CD6 expression.....	86
Figure 39: Hepatic T cells differ to peripheral T cells regarding the ratio between CD4 <sup>+</sup> and CD8 <sup>+</sup> T cells.....	87
Figure 40: Secretion of chemokines is modulated by MAPK inhibitors .....	88
Figure 41: Secretion of growth factors is modulated by MAPK inhibitors .....	90
Figure 42: Secretion of soluble adhesion molecules is modulated by MAPK inhibitors .....	91
Figure 43: Soluble MICB secretion is partially reduced by MAPK inhibitors.....	92
Figure 44: Chemokine milieu in healthy liver, liver resection of colorectal metastases, cirrhosis and HCC. ....	94
Figure 45: Cytokine milieu and adhesion molecules in healthy liver, liver resection of colorectal metastases, cirrhosis and HCC. ....	95
Figure 46: Classification tree of analyzed cytokines, chemokines and growth factors. ....	97
Figure 47: Sorafenib alters the chemokine milieu in HCC tissue.....	100
Figure 48: Sorafenib alters the chemokine milieu in healthy liver. ....	101
Figure 49: Sorafenib alters the cytokine milieu and adhesion molecules in HCC.....	102
Figure 50: Sorafenib alters the cytokine milieu and adhesion molecules in healthy liver....	103
Figure 51: Effects of MAPK inhibitors on MEK/ERK signaling in HCC cells. ....	107
Figure 52: Effects of MAPK inhibitors on cell cycle progression.....	111
Figure 53: Schematic drawing of regulation of apoptosis by MAPK and death receptor signaling pathways. ....	115
Figure 54: Scheme of surface molecule expression regulated by MAPK pathway. ....	120
Figure 55: Schematic diagram of T and NK cell population in liver tissue and peripheral blood.....	123
Figure 56: Regulation of chemokines and growth factors by different signaling pathways..	126
Figure 57: Possible regulation mechanisms of MIF in HCC cells.....	128

## List of Tables

Table 1: CC and CXC chemokine classification and corresponding receptors. ....	10
Table 2: Human activating and inhibitory NK cell receptors. ....	19
Table 3: Medium for cell culture.....	26
Table 4: Cell lines. ....	26
Table 5: Primary antibodies. ....	27
Table 6: Secondary antibodies. ....	27
Table 7: Western blot antibodies.....	28
Table 8: Sub-G1 method. ....	28
Table 9: Western blot buffers.....	28
Table 10: Bio-Plex. ....	28
Table 11: Phosphoplex.....	29
Table 12: ELISA. ....	29
Table 13: MAPK inhibitors.....	29
Table 14: Special machines.....	29
Table 15: Proportion of peripheral blood NK and T cells in HCC. ....	84
Table 16: Proportion of hepatic NK and T cells in healthy, cirrhotic and tumor tissue. ....	85

## List of Abbreviations

AP-1	Activating protein 1
APC	Antigen presenting cell
ASH	Alcoholic steatohepatitis
ATP	Adenosine-triphosphate
CFSE	Carboxy-fluorescein succinimidyl ester
CI	Cell index
DC	Dendritic cell
DMSO	Dimethyl sulfoxide
DNAM-1	DNAX accessory molecule-1
EGF	Epidermal growth factor
ERK	Extracellular signal-regulated kinase
FACS	Fluorescence activated cell sorting
FGF	Fibroblast growth factor
FSC	Forward scatter
GDP	Guanosine diphosphate
GI tract	Gastrointestinal tract
GPCR	G-protein coupled receptor
GRB2	Growth factor receptor bound 2
GTP	Guanosine triphosphate
HBV	Hepatitis B virus
HCC	Hepatocellular carcinoma
HCV	Hepatitis C virus
HGF	Hepatocyte growth factor
HLA	Human leukocyte antigen
HRP	Horse reddish peroxidase
HSC	Hepatic stellate cell
ICAM-1	Inter-cellular adhesion molecule 1
IFN	Interferon
IGF	Insulin-like growth factor
IL	Interleukin
KIR	Killer cell immunoglobulin-like receptor
LAMP-1	Lysosomal-associated membrane protein-1
LFA-3	Lymphocyte function-associated antigen 3
LSEC	Liver sinusoidal endothelial cells
MAPK	Mitogen-activated protein kinase
MDSC	Myeloid-derived suppressor cell
MEK	MAPK ERK kinase
MFI	Median fluorescence intensity
MHC	Major histocompatibility complex
MIF	Macrophage migration inhibitory factor
M-CSF	Macrophage colony stimulating factor
mTOR	Mammalian target of rapamycin
NASH	Non-alcoholic steatohepatitis
NCR	Natural cytotoxicity receptors
NK cell	Natural killer cell
NKT cell	Natural killer T cell

PBL	Peripheral blood leukocytes
PBMC	Peripheral blood mononuclear cells
PDGF	Platelet-derived growth factor
PFA	Paraformaldehyd
PH domain	Pleckstrin homology domain
PI3K	Phosphatidylinositol 3-kinases
PIP2	Phosphatidylinositol-4,5-bisphosphate
PIP3	Phosphatidylinositol-3,4,5-trisphosphate
p-protein	Phosphorylated protein
PVR	Polio-virus receptor
RANTES	Regulated upon Activation, Normal T-cell Expressed, and Secreted
RT	Room temperature
RTCA	Real-time cell analyzer
RTK	Receptor tyrosine kinase
SAPE	Streptavidin-PE
SCGF	Stem cell growth factor
SOS	Son-of-Sevenless
SSC	Side scatter
TGF $\beta$	Transforming growth factor $\beta$
TM	Tumor medium
TNF	Tumor necrosis factor
t-protein	Total protein
TRAIL	Tumor necrosis factor related apoptosis inducing ligand
Tregs	Regulatory T cells
VEGF	Vascular endothelial growth factor
wt	Wild-type

Abbreviations exclusively used in figures or tables are explained in the respective figure and table legends.

## Summary

Hepatocellular carcinoma (HCC) is one of the most lethal tumors worldwide. So far, the only treatment option for unresectable HCC is the multikinase inhibitor sorafenib, an inhibitor of the Raf/MEK/ERK (MAPK) signaling pathway, which is one of the major pathways implicated in HCC. Although HCC cannot be cured by sorafenib treatment, targeting the MAPK pathway may be a promising strategy for HCC therapy. In order to improve HCC treatment, it is of particular importance to understand the action of sorafenib in more detail. Therefore, a comprehensive analysis of its effects was performed in HCC cells and tissue and compared to specific inhibitors of the MAPK pathway. In my thesis, the following aspects could be demonstrated:

1. Both, Sorafenib and MEK-specific inhibitors repressed the MAPK signaling pathway, but had partially opposite effects on other signaling pathways like Akt signaling. As a consequence, HCC cell numbers were reduced after sorafenib and MEK inhibitor treatment, but cell division was mainly inhibited by sorafenib and to a low extent by the MEK inhibitors. In contrast, apoptosis was stronger induced by the MEK inhibitors, but differences were observed between the cell lines. This suggests that in HCC besides the MAPK pathway other signaling pathways play an important role and need to be targeted in addition to the MAPK pathway.
2. HCC cell lines expressed a variety of surface molecules which are associated with tumor progression. In addition, they secreted several chemokines and growth factors which favor tumorigenesis and angiogenesis. Inhibition of the MAPK pathway modulated both surface molecule expression and secretion of several chemokines and growth factors, whereby, tumor progression is inhibited.
3. NK cells are supposed to be important for fighting against HCC, but in HCC tumor tissue, NK cells were almost absent. There, the microenvironment was altered with an increase of several chemokines and angiogenic factors. These alterations might account for the decreased numbers of NK cells. *In vitro* treatment of resected HCC tissue with sorafenib resulted in a substantial decrease in the concentration of these increased factors. This indicates that alterations of the microenvironment might be also induced by sorafenib in HCC patients and, thereby, affecting recruitment of immune cells, NK cells in particular, into the tumor tissue.

## Zusammenfassung

Das Hepatozelluläre Karzinom (HCC) ist einer der bösartigsten Tumore weltweit. Das bisher einzige erfolgreiche Medikament ist der Multi-Kinase-Inhibitor Sorafenib, der eines der Hauptsignalwege des HCC, den Raf/MEK/ERK (MAPK) Signalweg, hemmt. Obwohl Sorafenib nur zu einer gewissen Verlängerung des Überlebens der HCC-Patienten führt, stellt die Hemmung des MAPK-Signalweges dennoch eine vielversprechende Strategie da. Um in Zukunft aber die HCC Behandlung zu verbessern, ist es notwendig den Wirkmechanismus von Sorafenib auch jenseits der Signalkaskaden zu verstehen. Daher wurde eine umfassende Analyse von Sorafenib im Bezug auf die Wirksamkeit bei HCC Tumorzellen und im HCC-Gewebe durchgeführt, wobei eine Besonderheit in dem direkten Vergleich mit spezifischen MEK-Inhibitoren besteht. In meiner Arbeit konnte folgendes gezeigt werden:

1. Sowohl Sorafenib als auch die MEK-Inhibitoren hemmen den MAPK Signalweg, aber haben teilweise unterschiedliche Effekte auf andere Signalwege wie Akt. Dies hat zur Folge, dass Tumorzellzahlen durch Sorafenib und den MEK-Inhibitoren gesenkt wurden, aber die Zellteilung wurde hauptsächlich von Sorafenib und weniger durch die MEK Inhibitoren gehemmt. Im Gegensatz induzierten die MEK-Inhibitoren stärker Apoptose, wobei es aber Unterschiede zwischen den verschiedenen Zelllinien gab. Dies deutet darauf hin, dass neben dem MAPK-Signalweg auch andere Signalwege eine wichtige Rolle spielen und für eine erfolgreiche Behandlung des HCC zusätzlich inhibiert werden müssen.
2. Zum einen exprimieren HCC Zellen eine Vielzahl an Oberflächenmolekülen, welche z.T. bei der Tumorprogression beteiligt sind. Zum anderen sekretieren sie Chemokine und Wachstumsfaktoren, welche das Tumorwachstum weiter fördern. Die Hemmung des MAPK-Signalweges durch Sorafenib bzw. MEK-Inhibitoren verändert die Expression dieser Oberflächenmoleküle und reduziert vor allem die Sekretion der Chemokine und Wachstumsfaktoren, was sich inhibierend auf die Tumorprogression auswirkt.
3. NK Zellen spielen bei der Tumorbekämpfung eine zentrale Rolle und sind im HCC Tumorgewebe stark reduziert. Im HCC ist das Mikromilieu verändert, wobei einige Chemokine und Wachstumsfaktoren signifikant erhöht sind. Diese Veränderung könnte auch ein Grund für den Ausschluss der NK Zellen im HCC-Gewebe sein. Bei *in vitro* Behandlungen von reseziertem HCC-Gewebe mit Sorafenib, konnte eine signifikante Senkung dieser Faktoren erzielt werden, was darauf hindeutet, dass auch in Patienten eine Veränderung des Mikromilieus durch Sorafenib hervorgerufen werden könnte und die Rekrutierung der NK Zellen beeinflusst.

# 1 Introduction

Hepatocellular carcinoma (HCC) is the 5<sup>th</sup> most prevalent cancer worldwide and represents the 3<sup>rd</sup> most lethal cancer with 500,000 to 600,000 deaths per year, worldwide (El-Serag and Rudolph, 2007; Llovet *et al.*, 2003). The incidence of HCC is increasing in Europe and in the United States mainly due to hepatitis C virus (HCV) infection with an estimated fivefold increase until 2015 (Severi *et al.*, 2010). HCC does not only arise as a result of HCV infections, but can also develop through hepatitis B virus (HBV) infections or non-infectious destructive conditions like alcohol intoxication, which is called alcoholic steatohepatitis (ASH), or fat deposition, called non-alcoholic steatohepatitis (NASH) (Figure 1) (Korangy *et al.*, 2010a; Severi *et al.*, 2010). Moreover, in most of the cases, HCC is associated with advanced fibrosis or with cirrhosis, which makes the situation for the patient even more difficult (Severi *et al.*, 2010). Because the development of cirrhosis and progression towards HCC are poorly understood, intensive research still has to be performed.

The main problem in HCC therapy is that conventional chemotherapy has failed in terms of curing the disease. Surgical resection or liver transplantation would be the most effective treatment for improving survival of the patients, but only few patients are candidates for these operations due to diagnosis of HCC at stages too advanced for a curative therapy. Because of this and a lack of treatment options, patients with unresectable HCC typically have a very poor prognosis with a five year survival of only 5% – 9% (Farazi and DePinho, 2006; Mendez-Sanchez *et al.*, 2008). In this situation, the small molecule sorafenib (Nexavar) is the

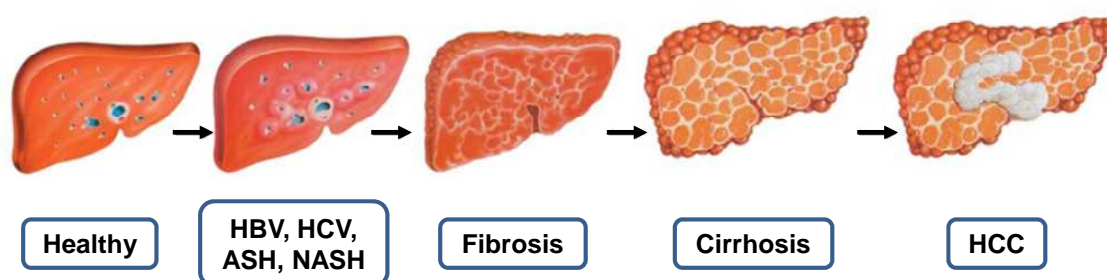


**Figure 1: Development of hepatocellular carcinoma.** Hepatocellular carcinoma (HCC) can develop through HBV and HCV infections or non-infectious destructive conditions like alcohol intoxication (alcoholic steatohepatitis, ASH) or fat deposition (non-alcoholic steatohepatitis, NASH). This might lead to liver fibrosis and cirrhosis, which then can transform into HCC. Figure was modified from (Korangy *et al.*, 2010a).

only treatment option for unresectable HCC which showed a survival benefit compared to non-treated patients with an average of three to four months.

Due to the fact that sorafenib is not a curative therapy but has effects for unresectable HCC, it is of particular importance to understand its mechanism of action. This will help to understand how to improve drug development and drug administration. Therefore, it is very important to have a comprehensive analysis of the mechanism of the action of sorafenib in order to understand where sorafenib benefits are and where HCC treatment can be improved. Sorafenib is a multikinase inhibitor targeting the Raf/MEK/ERK (MAPK) signaling pathway, as well as growth factor receptors (receptor tyrosine kinases). Because it is thought that the antitumor effect is mainly achieved through the inhibition of the Raf/MEK/ERK signaling pathway, sorafenib is compared to specific inhibitors of the MEK kinase and a specific B-Raf inhibitor, which are currently used in clinical and pre-clinical evaluations. With this comparison, it can be concluded which effects are mediated through the MAPK pathway and whether inhibition of only this pathway is sufficient for successful treatment of HCC.

To get a broad view of how the inhibitors work, analyses were performed regarding their effects on (1) *different signaling pathways*, how the inhibitors influence *cell proliferation*, to what extent they induce *apoptosis*, and (2) how they modulate the *immune cell recruitment* and *cytotoxicity*. Moreover, the change of the (3) *hepatic microenvironment* in HCC and changes *in vitro*-treated HCC tissue will be investigated. In this thesis, significant findings in this respect are presented that contribute to this comprehensive analysis of HCC and signaling pathway inhibitors.

Before showing the results, the basic principles about liver immunology and hepatocellular carcinoma are introduced, as far as they are important for a better understanding of the results and the discussion. Section 1.1 gives an overview of the importance of the liver for the immune system with its diversity of cells and distinct cytokine and chemokine milieu (microenvironment). Section 1.2 explains the pivotal signaling pathways in HCC and the importance of natural killer cells, which play a central role for tumor cell killing, with their mechanisms of tumor recognition. Moreover, an overview of currently tested signaling pathway inhibitors for the treatment of HCC will be given.

## 1.1 Liver Immunology

The liver is one of the largest human organs with a daily blood flow of more than 2000 liters (Gershwin *et al.*, 2007c). This is necessary, because the function of the liver is to regulate the composition of the blood by detoxification of harmful substances, metabolism of carbohydrates, lipids, and proteins, storage of glycogens, uptake of amino acids, and the production of uric acid. Furthermore, the liver is involved in the clearance of bacterial products and toxins from the blood (Knolle and Gerken, 2000). Moreover, the liver produces and secretes bile, which is stored in the gallbladder. Besides this, the liver plays a pivotal role for the immune system. In the following section (1.1.1), the basic function and mechanisms of the immune system in the liver are described. Section 1.1.2 explains the communication signals of the cells in the liver.

### 1.1.1 Function of the immune system in the liver

The liver is the first organ, which receives blood from the gastrointestinal (GI) tract, but it also gets the blood from the systemic circulation. Its central location in the body and the position as the first checkpoint for substances from the GI tract makes the liver an important organ also for the immune system since it represents a boarder for foreign substances (Racanelli and Rehmann, 2006). The blood from the GI tract and the systemic circulation enter the liver through the portal vein and the hepatic artery, respectively, and flows together into the hepatic sinusoids (Figure 2) (Adams and Eksteen, 2006; Fox, 2006). This mixed blood in the hepatic sinusoids is then transported to the central veins, which collect the blood into the vena cava inferior. Therefore, via these routes, the liver receives antigen-rich (e.g. from pathogens) blood from the gut but also from the stomach, spleen, and pancreas. In the sinusoids the blood flow is slow, which leads to a vivid exchange of molecules between the sinusoidal space and cells of the liver (Adams and Eksteen, 2006). The sinusoids are lined by liver sinusoidal endothelial cells (LSECs), which have open “fenestrae” to allow the antigens to pass the LSEC layer (Figure 2). Kupffer cells, which are liver-resident macrophages, are attached to the endothelial cells. Hepatic stellate cells (HSCs) and dendritic cells (DCs) are found in the space of Dissé, the location between the endothelial cells and the hepatocytes (Figure 2). Through the fenestrates of the LSECs, DCs and HSCs can reach into the sinusoids

and get in contact with circulating antigens and lymphocytes (Adams and Eksteen, 2006). They are important liver-resident antigen-presenting cells (APCs) that can take up antigens from the blood stream or from the liver tissue and present them to lymphocytes, primarily CD8<sup>+</sup> and CD4<sup>+</sup> T cells (Racanelli and Rehermann, 2006; Winau *et al.*, 2008).

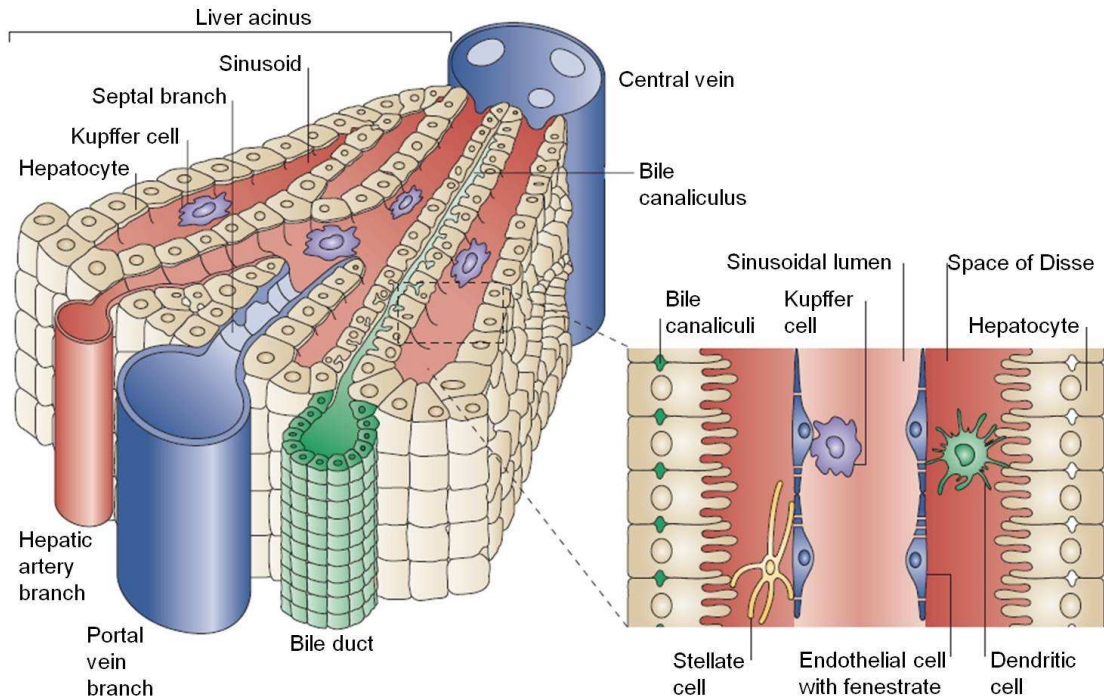


**Figure 2: Structure of hepatic lobule.** The liver is perfused by the blood from the gut and the systemic circulation flowing through the portal vein and the hepatic artery, respectively, into the hepatic sinusoids. In the hepatic sinusoids the blood from the portal vein and hepatic artery is mixed and transported to the central veins, which collect the blood into the vena cava inferior. In the sinusoids a vivid exchange of molecules occurs between the sinusoidal space and cells of the liver. The sinusoids are lined by liver sinusoidal endothelial cells, which have open fenestrae. Kupffer cells are attached to the endothelial cells and hepatic stellate cells and dendritic cells are found in the space of Dissé, the location between the endothelial cells and the hepatocytes. Figure was adapted from (Adams and Eksteen, 2006).

---

Through the blood stream, not only pathogen-derived antigens are transported to the liver, the liver itself can also be a target of potentially harmful pathogens under infectious conditions. In the liver, hepatocytes, APCs and effector cells of the innate (NK and NKT cells) and adaptive (T and B cells) immune system are able to induce an immune response (Klein and Crispe 2006). Hepatocytes, which account for about two-third of all hepatic cells, can secrete acute-phase proteins and complement components, which are important for the first line defense during infections (Weiler-Normann and Rehermann, 2004). Moreover, they play an

important role for the induction of the innate immune system by the secretion of pattern recognition receptors. These proteins bind to pathogens and lead to their clearance by activation of the complement system and marking them for the uptake by phagocytes (Gao *et al.*, 2008).

Hepatic NK cells account for 30-50% of all liver lymphocytes and are located in the lumen of the hepatic sinusoid (Gao *et al.*, 2008; Lotze and Thomson, 2010; Norris *et al.*, 1998). They carry out a major part of the hepatic innate immune response by fighting against viruses, intracellular bacteria and parasites, and in the defense against primary liver tumors and liver metastases (Gao *et al.*, 2008; Racanelli and Rehermann, 2006). Moreover, NK cells are important for the recruitment of T and B cells, and neutrophils to the liver, where several cytokines and chemokines are involved (Crispe, 2003).

For the recognition of presented antigens of infected cells, T lymphocytes play an important role. In the liver, regarding the classical T lymphocytes, CD8<sup>+</sup> T cells outnumber CD4<sup>+</sup> T cells, which is in contrast to the distribution in the blood, where CD4<sup>+</sup> T cells are almost twice as much as CD8<sup>+</sup> T cells (Crispe, 2003). For the recognition of non-peptide antigens, natural killer T (NKT) cells play a pivotal role in the liver. They recognize non-peptide antigen targets such as glycolipids in the context of the non-classical antigen-presenting molecule CD1d. They contribute to immune responses against bacteria, viruses, and tumors (Kawano *et al.*, 1997; Kronenberg, 2005).

Besides antigens from pathogens, food-derived antigens are transported to the liver and taken up by APCs and presented to the immune system (Crispe, 2003). Since food-derived antigens are constantly present, it is mandatory to avoid an activation of the immune system to prevent damage of the liver and other organs (Gershwin *et al.*, 2007c). This is achieved by inhibiting the immune system by peripheral tolerance against these antigens (Knolle and Gerken, 2000). In the liver, mainly LSECs, but also DCs, NKT cells, and regulatory CD4<sup>+</sup> CD25<sup>+</sup> T cells (Tregs) play an important role for the induction of tolerance towards oral antigens (Gershwin *et al.*, 2007c; Kronenberg, 2005; Weiler-Normann and Rehermann, 2004).

This shows that the liver is able to induce an immune response but also maintain peripheral tolerance. This intra-hepatic balance between inflammatory and tolerogenic conditions is maintained by an intensive crosstalk between the different cells of the liver. For this crosstalk,

signal molecules like cytokines and chemokines are essential among other factors. Modifications of the cytokine and chemokine secretion can cause a shift in the balance between inflammatory and tolerogenic conditions. These modifications play a role in liver diseases like HCC, but the exact mechanisms have to be elucidated. Therefore, it is important to understand the regulation of cytokines and chemokines and the alterations during disease progression especially in HCC.

### 1.1.2 Hepatic cytokine milieu

The communication between the different hepatic cells is obligatory to maintain a coordinative interaction with their environment in order to react immediately when conditions change. In this scenario, cytokines and chemokines play an essential role. In general, most of the cytokines and chemokines are not constitutively produced and in the liver the normal cytokine production is rather at a low level (Gershwin *et al.*, 2007a). Under pathogenic stimulation, various cells are activated and release cytokines as a consequence of activation.

Cytokines are a diverse group of small soluble cell signaling proteins, which are secreted by different hematopoietic cells, including lymphocytes, monocytes, and granulocytes in response of an activation impulse. Cytokines and their receptors are grouped according to their structure. The large cytokine superfamily is separated in the hematopoietic family with four alpha-helices, which includes many interleukins (IL), the IL-1 family, gp130 utilizing cytokines (IL-6 family), the IL-12 family, the IL-10 superfamily, IL-17, interferons (IFNs) and tumor necrosis factor (TNF) superfamily. They are distinct from the chemoattractant families, called chemokines (Commins *et al.*, 2010; Janeway *et al.*, 2005).

Binding of a cytokine to its corresponding receptor on the target cell triggers an intracellular signal transduction cascade which leads to proliferation and to a rapid change in gene expression. Cytokines act on different cell types and have partly overlapping effects on the cell. They play major roles in immunity and inflammation, but also in lymphoid development, differentiation, and homeostasis. Many cytokines also regulate cell cycle transition and can protect cells from going into apoptosis (Gururaj and Kumar, 2005).

Several cytokines like IL-2, IL-15, IL-16, IL-21, TNF $\beta$  and IFN $\gamma$  can induce cell-mediated immunity, whereas other cytokines like IL-1 receptor antagonist (IL-1RA), transforming

growth factor  $\beta$  (TGF $\beta$ ) and IL-10 are involved in anti-inflammatory effects (Steinke and Borish, 2006).

In contrast to cytokines, chemokines play an important role in tissues, especially the liver, because they are needed to attract leukocyte subsets to specific tissue sites and, thereby, play a pivotal role for the maintenance of the cellular constellation in the liver. Moreover, they recruit immune cells to the liver and influence the immune responses including intrahepatic inflammation (Oo and Adams, 2010). However, chemokines also play an important role for liver regeneration and angiogenesis, but they are also “abused” during tumor development, progression and tumor angiogenesis (Keeley *et al.*, 2011; Simpson *et al.*, 2003). During tumor development, chemokine secretion is changed in such a way that the balance between inflammatory and tolerogenic conditions is shifted to a more tolerogenic microenvironment which supports tumor growth. One of the key chemokines acting as a double-edged sword is CXCL8 (IL-8), which has been shown to recruit immune cells and to promote tumor growth.

Chemokines, which were first named mostly according to their defined function, were newly classified according to their structure (Table 1). They are separated into four families, the C, CC, CXC and CX<sub>3</sub>C chemokines, which are based on the position of the conserved first two cysteine residues close to the N-terminus (Keeley *et al.*, 2011). Most of them fall into the group of CC and CXC chemokines (Table 1). The C and CX<sub>3</sub>C chemokines only consist of one member each, XCL1 (lymphotactin) and CX<sub>3</sub>CL1 (fractalkine), respectively. The CC and CXC chemokines differ from each other that the CC chemokines have two cysteine residues lying next to each other, while the CXC chemokines have also two cysteine residues, but these are separated by one non-conserved amino acid (Keeley *et al.*, 2011; Simpson *et al.*, 2003). The CXC chemokines are even further sub-grouped, depending on being ELR-positive or ELR-negative (Table 1). ELR is a motif of the three amino acids glutamine (E), leucine (L) and arginine (R), which lies immediately next to the CXC motif.

All chemokines achieve their activities through the binding to specific G-protein-coupled seven-transmembrane receptors (GPCR). The difference to other cytokines is that chemokines can bind to and therewith activate several related receptors (Table 1) (Platanias, 2005). Many chemokines bind to the same chemokine receptor. For example, most ELR-positive chemokines bind to the CXC chemokine receptor 1 (CXCR1) and/or CXCR2, while the ELR-

negative chemokines bind to CXCR3 and some also to CXCR4 (Simpson *et al.*, 2003). The most common chemokines and their receptors are listed in Table 1.

ELR-positive CXC chemokines and several CC chemokines like CCL2 (MCP-1), CCL11 (Eotaxin) and CCL16 (NCC-4) are potent promoters for the induction of angiogenesis, which are also called angiogenic chemokines (Keeley *et al.*, 2011). In contrast, ELR-negative CXC chemokines often inhibit angiogenesis (angiostatic). Moreover, the ELR-negative CXC chemokines can induce IFNs and promote Th1-dependent immunity by the recruitment of CXCR3<sup>+</sup> T and NK cells (Keeley *et al.*, 2011).

**Table 1: CC and CXC chemokine classification and corresponding receptors.**

CC Chemokines			CXC Chemokines			
Systemic nomenclature	Old nomenclature	Receptor	Systemic nomenclature	Old nomenclature	Receptor	ELR motif
CCL2	MCP-1	CCR2	<b>Angiogenic</b>			
CCL3	MIP-1 $\alpha$	CCR1, CCR5	CXCL1	Gro- $\alpha$	CXCR2	+
CCL4	MIP-1 $\beta$	CCR5	CXCL2	Gro- $\beta$	CXCR2	+
CCL5	RANTES	CCR1, CCR3, CCR5	CXCL3	Gro- $\gamma$	CXCR2	+
CCL7	MCP-3	CCR1, CCR2, CCR3	CXCL5	ENA-78	CXCR2	+
CCL8	MCP-2	CCR2, CCR3, CCR5	CXCL6	GCP-2	CXCR2	+
CCL11	Eotaxin	CCR3	CXCL7	NAP-2	CXCR2	+
CCL12	MCP-5	CCR2	CXCL8	IL-8	CXCR2	+
CCL13	MCP-4	CCR1, CCR2, CCR3	<b>Angiostatic</b>			
CCL14	HCC-1	CCR1	CXCL4	PF-4	CXCR3	-
CCL15	HCC-2 / leukotactin	CCR1, CCR3, CCR5	CXCL9	Mig	CXCR3	-
CCL16	LEC / NCC-4	CCR1	CXCL10	IP-10	CXCR3	-
CCL17	TARC	CCR4	CXCL11	I-TAC	CXCR3/CXCR7	-
CCL18	MIP-4	unknown	<b>Others / Unknown</b>			
CCL20	LARC / MIP-3 $\alpha$	CCR6	CXCL12	SDF-1	CXCR4/CXCR7	-
CCL21	SLC	CCR7	CXCL13	BCA-1	CXCR5	-
CCL22	MDC	CCR4	CXCL14	BRAK	?	-
CCL24	Eotaxin-2	CCR3	CXCL15	Lungkine	CXCR6	+
CCL25	TECK	CCR9				
CCL26	Eotaxin-3	CCR3				
CCL27	CTACK	CCR3, CCR2, CCR10				

In the liver, many different cytokines, chemokines and growth factors like IFNs, IL-10, CXCL8 (IL-8), CXCL10 (IP-10), TGF $\beta$ , vascular endothelial growth factor (VEGF) and hepatocyte growth factor (HGF) are produced by the liver-resident hepatocytes, APCs and cells of the innate and adaptive immune system for the balance of immune response and tolerogenic conditions. For example, Kupffer cells, which are important phagocytes in the liver, can be secretors of inflammatory cytokines like IL-1, IL-6 and TNF $\alpha$  and chemokines like CCL2 (MCP-1), CCL3 (MIP-1 $\alpha$ ) and CCL5 (RANTES), but also express IL-10 and TGF $\beta$  in response to LPS (Germano *et al.*, 2008; Gershwin *et al.*, 2007b; Knolle and Gerken, 2000). Hepatic NK cells can produce IFN $\gamma$  and at low levels TNF $\alpha$ , but rarely IL-2 (Simpson *et al.*, 2003). Through the secretion of IL-10 and TGF $\beta$  by Kupffer cells and LSECs, hepatic

DCs become tolerogenic. These resting DCs can then inhibit the proliferation of tissue-infiltrating lymphocytes through the expression of inhibitory molecules like CTLA-4 and PD-1. When DCs get activated, they downregulate these molecules and migrate to the extrahepatic lymph nodes to activate the immune response (Racanelli and Rehermann, 2006).

In general, the cytokine and chemokine microenvironment of the liver plays an important role for the recruitment of immune cells. In HCC, the cytokine and chemokine milieu, which is important for a good balance of immune response and tolerance, is changed in such a way that the tumor can escape the immune system and is able to induce angiogenesis for its own oxygen and nutrient supply. The initial alterations can be caused by factors like HBV or HCV infection which first lead to cirrhosis and can progress towards to HCC (Figure 1). Although a lot of research is performed in this area, surprisingly little is still known about the altered cytokine and chemokine milieu during cirrhosis and HCC. Therefore, it is mandatory to analyze the cytokine and chemokine milieu in the healthy liver in comparison to liver cirrhosis and HCC and the consequences for the recruitment of cells to the liver. The initial steps of tumor development which can lead to a change in the cytokine and chemokine milieu are often caused by mutations in the cell within central regulators of the signal transduction or the cell cycle. These mutations often affect signaling pathways which regulate many cell functions including cell proliferation, induction of apoptosis, as well as secretion of cytokine and chemokines. Therefore, it is also very important to elucidate how the signaling pathways regulate these cellular functions and how they are altered during HCC tumorigenesis.

## 1.2 Hepatocellular Carcinoma

As described at the beginning, hepatocellular carcinoma is one of the most prevalent and lethal tumors worldwide with increasing incidences. Due to the lack of treatment options and diagnosis at a late unresectable stage, patients with HCC have a very poor survival prognosis. As shown in Figure 1, HBV and HCV infections or alcohol intoxication and fat deposition can lead to liver fibrosis and cirrhosis, which then can transform into HCC.

For the development of HCC, a tumor cell or the whole tumor respectively, needs to acquire several modifications, which were classified by Hanahan and Weinberg as the hallmarks of cancer as depicted in Figure 3 (Hanahan and Weinberg, 2000; Hanahan and Weinberg, 2011). They include sustained proliferative signaling, evasion from growth suppressors, resistance against programmed cell death (apoptosis), acquisition of replicative immortality, induction of angiogenesis, tissue invasion and metastasis. Moreover, recently the hallmarks were extended with two enabling hallmarks, which are genome instability and tumor-promoting inflammation, and two emerging hallmarks, which are reprogramming energy metabolism and avoiding immune destruction.

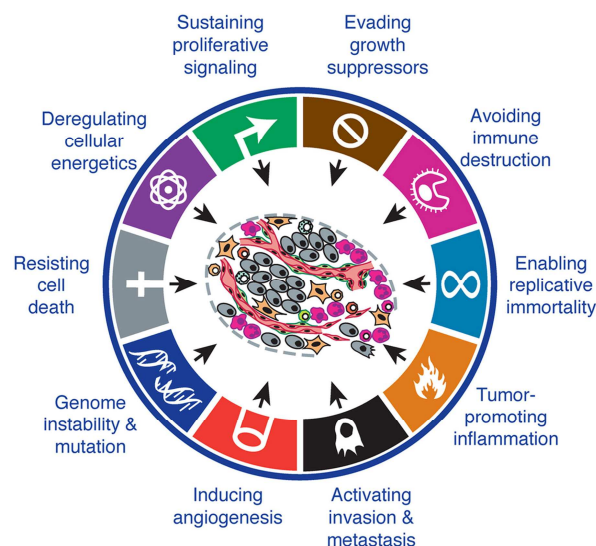


**Figure 3: Hallmarks of cancer.** Hanahan and Weinberg suggested this “hallmark of cancer” in 2000, which include 6 essential hallmarks. In 2011 they were extended with two enabling hallmarks: the genome instability and tumor-promoting inflammation, and the two emerging hallmarks: reprogramming energy metabolism and avoiding immune destruction. Figure was modified from (Hanahan and Weinberg, 2011).

This shows that the development of a tumor like HCC occurs in several steps with frequent mutations. Since these mutations often include players of signaling pathways, which are important for the regulation of the cell fate, the main altered signaling pathways of HCC are described in section 1.2.1. Moreover, tumor cells are altered in such a way that they can escape the immune system. Since NK cells play a pivotal role for the elimination of tumor cells, their regulation and main function are described in section 1.2.2. As the growth factor signaling pathways are often altered or mutated in HCC, they represent a promising target for therapy. Section 1.2.3 summarizes potential signaling inhibitors for the treatment of HCC.

### 1.2.1 Oncogenic signaling in HCC

For the reason that a variety of molecular mechanisms and signaling pathways can be altered in hepatocarcinogenesis, it is important to understand the main signaling pathways. In HCC, alterations are mostly seen in the growth factor receptor-mediated MAPK (mitogen activated protein kinase) signaling pathway (Ras/Raf/MEK/ERK), the wnt/ $\beta$ -catenin pathway and the p53 gateway (Aravalli *et al.*, 2008; Breuhahn *et al.*, 2006; Llovet and Bruix, 2008).

The MAPK signaling cascade (Figure 4) is one of the major pathways implicated in HCC (Whittaker *et al.*, 2010). At the time this pathway was elucidated, the groups of Rony Seger and Edwin Krebs described the MAPK signaling cascade as an information highway, used by many extracellular signals, e.g. growth factors, to trigger intracellular targets mediated by a network of interacting proteins that regulate a large number of cellular processes (Seger and Krebs, 1995). It is a constitutively present signal transduction pathway that regulates central cellular processes, including proliferation, differentiation, angiogenesis and survival (Gollob *et al.*, 2006).

The MAPK pathway lies downstream of various growth factors and bind to their corresponding receptors at the cell surface, i.e. receptor tyrosine kinases (RTKs), which include VEGF receptor (VEGFR), epidermal growth factor receptor (EGFR), fibroblast growth factor receptor (FGFR), HGF receptor (HGFR or c-Met) and insulin-like growth factor receptor (IGFR) (Figure 4). Upon binding of the growth factor, the receptor dimerizes and gets activated by trans-phosphorylation of tyrosine residues. This leads to an activation of an adaptor molecule complex composed of growth factor receptor bound 2 (GRB2), SH2

domain protein C (SHC) and Son of Sevenless (SOS). The complex, in turn, activates the Ras/Raf/MEK/ERK pathway, which releases a cascade of specific phosphorylation events (Avila et al., 2006). Within this pathway, activated SOS leads the removal of GDP from a member of the inactivated plasma membrane-bound small GTPase Ras subfamily including KRas, NRas, and HRas (Friday and Adjei, 2008). Ras can then bind GTP and becomes active, while binding of GTP leads to a conformational change of Ras and allows binding and activation of different effector molecules like Raf for the MAPK pathway and phosphatidylinositol 3-kinases (PI3K) for the Akt pathway (Figure 4).

The lipid kinase PI3K also regulates a number of cellular processes, like transcription, migration, angiogenesis, cell growth, proliferation and apoptosis, which, in turn, can play an important role in cancer (Osaki *et al.*, 2004). PI3K phosphorylates phosphatidylinositols of the cell membrane, e.g. phosphatidylinositol-4,5-bisphosphate (PIP<sub>2</sub>) to phosphatidylinositol-3,4,5-trisphosphate (PIP<sub>3</sub>). PIP<sub>3</sub> at the cell membrane recruits protein kinases such as Akt, which bind with their pleckstrin homology (PH)-domain to PIP<sub>3</sub> (Hennessy *et al.*, 2005; Tanaka and Arai, 2010; Whittaker *et al.*, 2010). Akt in turn, phosphorylates a variety of cellular signaling molecules like MDM2, mTOR and modulates several pro- and anti-apoptotic molecules. MDM2 can bind to p53 leading to ubiquitination and degradation of p53 (Figure 4). Phosphorylation of p53 at serine 15, however, protects p53 from MDM2-mediated degradation, therefore, the phosphorylation status of these molecules contribute to their stabilization and degradation respectively. Alterations in PI3K/Akt signaling components are frequent in HCC and thus, contribute to hepatocarcinogenesis (Huynh, 2010; Whittaker *et al.*, 2010).

In the Raf/MEK/ERK pathway, the serine/threonine kinase Raf, consisting of three main isoforms A-Raf, B-Raf and C-Raf, is recruited by one of the Ras proteins to the plasma membrane (Whittaker *et al.*, 2010). Raf was shown to bind efficiently to Ras only when Ras is bound to GTP, not GDP. It is postulated that Raf is activated through phosphorylation upon binding to Ras (Friday and Adjei, 2008). This phosphorylation locks Raf into an activated conformation that is then independent of binding to Ras for the continued activity of Raf. From Raf, the signal is transmitted via the cascade of MAPK and ERK kinases 1 and 2 (MEK1/2). MEK1/2 is activated through serine phosphorylation in its activation loop (Ser217/Ser221 and Ser222/Ser226). The activated MEKs are dual specificity kinases (act as

both tyrosine and serine/threonine kinases) and activate ERK1/2 through phosphorylation of threonine and tyrosine residues at Thr202/Tyr204 (ERK1) and Thr185/Tyr187 (ERK2) in the activation loop. ERK phosphorylates several substrates in the cytosol and in the nucleus, many of them involved in cell proliferation and survival (Keshet and Seger, 2010).

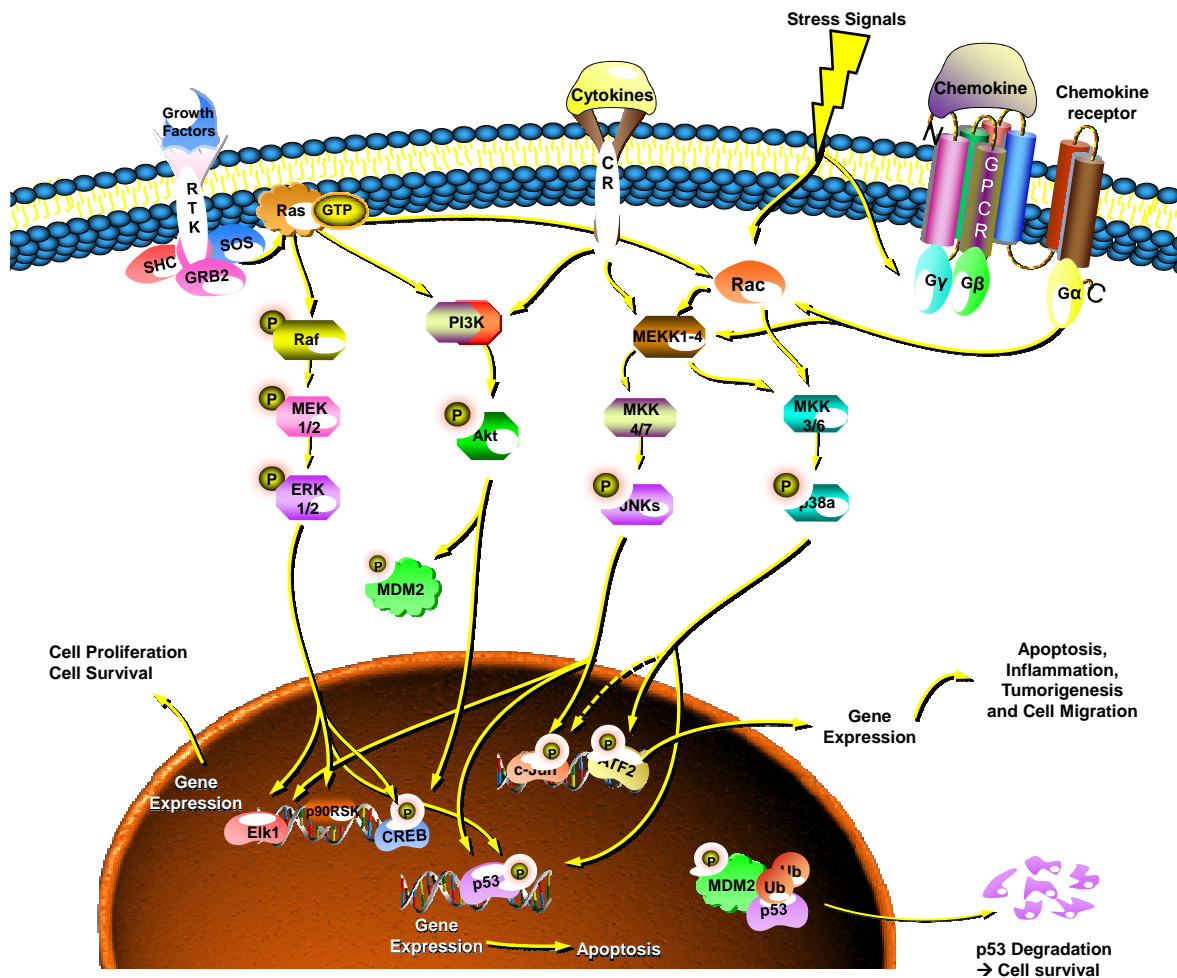


**Figure 4: MAPK signaling pathway.** Extracellular growth factors bind to the receptor tyrosine kinase (RTK). This results in Ras activation through the adaptor molecule complex GRB2/SHC/SOS, which then can activate Raf and PI3K. Binding of cytokine like MIF to its receptor leads to an activation of PI3K and MEKK1-4. Raf phosphorylates and activates MEK, which then phosphorylates and activates ERK. PI3K ultimately leads to Akt activation. Stress signals induce the activation of JNK and p38 signaling pathway. Several transcription factors like p90RSK, CREB, p53, c-Jun and ATF-2 are activated through these signaling pathways leading to cell proliferation or apoptosis. P: phosphorylation; RTK: receptor tyrosine kinase; CR: Cytokine receptor; GPCR: G-protein-coupled receptor. Pathway was generated with the pathway builder from [www.proteinlounge.com](http://www.proteinlounge.com).

The p38 and JNK signaling pathways, which also belong to the MAPK family, play an important role in the response to stress stimuli, immune responses and inflammation. These two cascades are induced by several stress factors and ligands that activate different receptors including death receptors, GPCRs and RTKs (Figure 4) (Keshet and Seger, 2010). JNK and p38 phosphorylate and therewith activate several transcription factors like ATF-2, ELK-1, and c-Jun. p38 also activates p53 and c-Jun, but the activation of c-Jun is controversially discussed (Hui *et al.*, 2007; Keshet and Seger, 2010). The duration and intensity of signaling pathway activity affects the cellular response to extracellular signals such as growth factors for instance. Therefore, it is important to study several pathways in parallel in order to get a more comprehensive view on signal events and their consequences for the microenvironment.

The abnormal regulation of these MAPK cascades has been shown to contribute to tumor development and other human diseases. It was described that the MAPK expression and activity is increased in primary human hepatocellular carcinoma (Schmidt 1997). This overexpression or increased activation of components of the MAPK pathway is believed to contribute to tumorigenesis, tumor progression and disease metastasis in a variety of solid tumors (Leicht *et al.*, 2007). For example, it has been reported that from all tested HCC samples, 100% of the MEK1/2 proteins were activated, i.e. constitutively phosphorylated (Huynh *et al.*, 2003).

The increased activation of the Raf/MEK/ERK pathway in solid tumors (HCC) usually occurs by two main mechanisms. The first mechanism is mediated by oncogenic mutations within the NRas gene primarily, which lead to constitutive pathway activation through Raf (Gollob *et al.*, 2006). Oncogenic Ras mutations occur in about 30% of HCC (Downward, 2003; Gollob *et al.*, 2006). The second main mechanism for activating the Raf/MEK/ERK pathway is a constitutive Raf activation due to overexpression of either growth factors (VEGF, EGF, IGF or c-Met) or their receptors (e.g. VEGFR, EGFR, IGFR or c-Met) (Gollob *et al.*, 2006; Lachenmayer *et al.*, 2010). Mutations in the Raf gene are only a rare event in HCC as compared to other tumors like melanoma or papillary thyroid cancer (Friday and Adjei, 2008). Since in HCC the MAPK pathway is constitutively activated by these mutations or overexpression, it represents a good target for therapeutic intervention.

There are also other genetic changes besides the activation of the MAPK pathway, which are involved in the pathogenesis of HCC. The PI3K/Akt pathway is often constitutively activated

in HCC, which is mostly due to anomalies of the PTEN function, the inhibitor of Akt (Whittaker *et al.*, 2010). This activation of the PI3K/Akt pathway is correlated with a poor prognosis in HCC (Schmitz *et al.*, 2008). Additional mutations are found in the tumor suppressor gene p53 and in the WNT signaling pathway (Hussain *et al.*, 2007). P53 and its family members p63 and p73 are central players for several cellular functions. It is a transcription factor that mediates cellular responses to diverse stresses, e.g. DNA damage, which include cell cycle arrest, apoptosis, senescence, DNA repair or alteration of metabolism (Muller *et al.*, 2006). Therefore, mutations of p53 can often lead to resistance to apoptosis as well as to changes in gene expression.

Besides having a major influence on cell proliferation and apoptosis, the MAPK family, PI3K/Akt pathways and the p53 family are involved in the regulation of a broad variety of cellular functions like cell differentiation, cell migration and adhesion, cytokine and chemokine secretion, and regulation of cell surface molecule expression, which is important for the recognition by immune cells. Therefore, it is important to understand the alterations of the signaling pathways leading to the development of HCC.

### **1.2.2 NK cells and the recognition of hepatocellular carcinoma cells**

Natural killer (NK) cells, which represent a lymphocytic population, are important players of the first line defense in the body, the so-called innate immune system, which is able to kill virus-infected or malignant cells. Moreover, NK cells are classified as innate immune effector cells because in contrast to T cells they do not need priming for activation and their receptors are not generated via the process of somatic recombination. Recent data, however, suggest that NK cells also have functions of the adaptive immune system and even may seem to have a memory (Paust *et al.*, 2010; Vivier *et al.*, 2011).

NK cells can kill target cells by cytotoxicity, i.e. secretion of perforins and granzymes, or by receptor-mediated apoptosis induction via Fas ligand (CD95L) or Tumor Necrosis Factor Related Apoptosis Inducing Ligand (TRAIL). It has been described that a subset of human hepatic NK cells may have a reduced effector function, but under appropriate inflammatory conditions develops into potent killers (Norris *et al.*, 1998). In another study it could be shown that hepatic NK cells can “spontaneously” without prior activation lyse NK-sensitive

HLA class I negative K562 target cells (Doherty *et al.*, 1999). Besides their cytotoxic functions, NK cells can secrete a variety of pro- and anti-inflammatory cytokines like IFN $\gamma$ , TNF $\alpha$ , GM-CSF and IL-10 and chemokines like CCL3-5, CXCL9 and CXCL10, which leads to an indirect modulation of the immune response by shaping the microenvironment (Di Santo, 2006).

Human peripheral blood NK cells can be divided into CD56<sup>dim</sup> CD16<sup>+</sup> (~90%) and CD56<sup>bright</sup> CD16<sup>-</sup> (~10%) NK cells. As described in 1.1.1, NK cells are enriched in the liver tissue and it could be shown that the liver comprises a different distribution of CD56<sup>dim</sup> CD16<sup>+</sup> and CD56<sup>bright</sup> CD16<sup>-</sup> NK cells, but the exact characterization of hepatic NK cells has to be analyzed (Cai *et al.*, 2008; Moroso *et al.*, 2010).

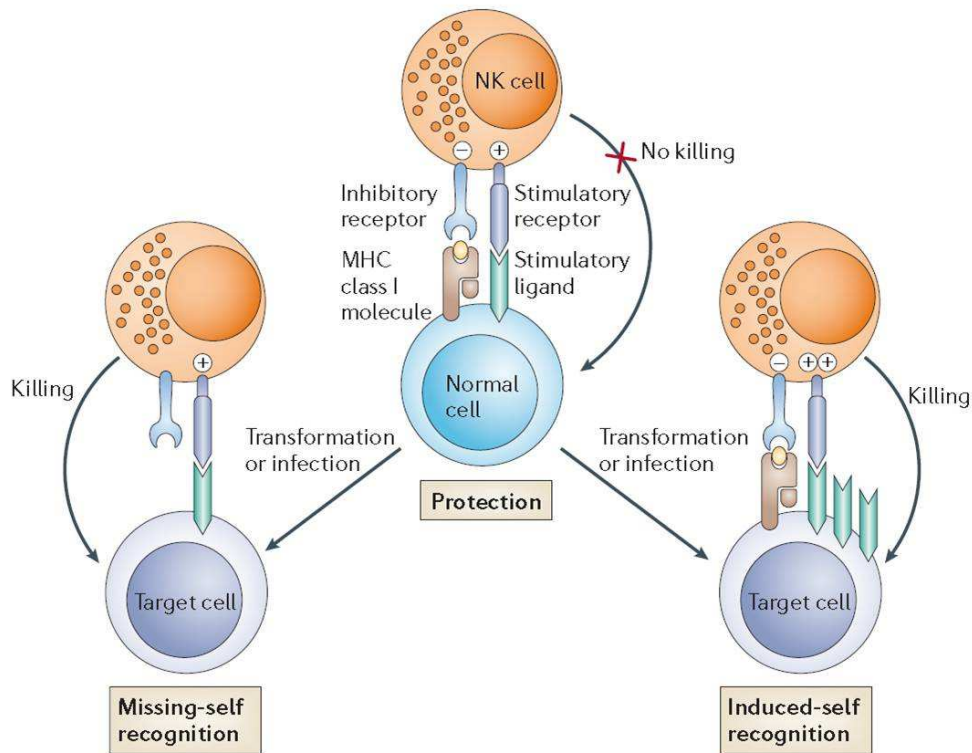


**Figure 5: Activation of NK cells.** Normal cells bind both the stimulatory and the inhibitory NK cell receptors. Signals delivered through the inhibitory receptors dominate and prevent NK cell activation and the lysis of normal cell. Transformed or infected cells downregulate expression of inhibitory ligands (“missing self recognition”) and/or up-regulate ligands for activating NK cell receptors (“induced-self recognition”) allowing NK cell activation and killing of the target cell. Figure was adapted from (Raulet and Vance, 2006).

**Table 2: Human activating and inhibitory NK cell receptors.**

Receptors	Cellular ligands	Receptors	Cellular ligands
<b>Activating receptors</b>		<b>Inhibitory receptors</b>	
NKG2D	ULBP1-6, MICA and MICB	KIR2DL2 / KIR2DL3	HLA-C1 group
CD94/NKG2C	HLA-E	KIR2DL1	HLA-C2 group
NKp30	B7-H6	KIR3DL1	HLA-Bw4
NKp44	ND	KIR3DL2	HLA-A3 and HLA-A11
NKp46	HA	CD85/LIR-1/ILT-2	several HLA class I molecules
NKp80	AICL	KLRG1	Cadherins
DNAM1 (CD226)	CD155 (PVR) and CD112 (nectin-2)	NKR-1A (CD161)	LLT1
CD96	CD155 (PVR) and CD112 (nectin-2)	CD94/NKG2A	HLA-E
CD16 (FcγRIIIA)	IgG	siglec 7/9	sialic acid
KIR2DS1	HLA-C2 group	<b>Receptors with dual functions</b>	
KIR2DS2,3	HLA-C1 group	2B4	CD48
KIR3DS1	ND	NTB-A	NTB-A
KIR2DS4	HLA-C1 group	KIR2DL4	HLA-G (soluble)
CD2	LFA-3 (CD58)		

Table was adapted and modified from (Ljunggren and Malmberg, 2007).

The activity of NK cells is regulated via a large variety of activating and inhibitory receptors on their cell surface. This is a tightly regulated balance, because the up- and downregulation of the ligand binding to the activating and inhibitory receptor will determine the function of NK cells (Figure 5). Negative regulatory receptors on NK cells, that interact with MHC ligands and inhibit target cell destruction by NK cells, were first described by Klas Kärre in his *missing-self hypothesis* (Figure 5) (Ljunggren and Karre, 1990). As depicted in Table 2, there are several classes of inhibitory receptors with MHC ligands, including the killer cell immunoglobulin-like receptor (KIR) family and the CD94/NKG2A complex (Di Santo, 2006). These inhibitory receptors mostly bind to HLA class I molecules, but do not depend on specific peptides presented by HLA class I. This interaction between self MHC and inhibitory ligand causes NK cell “tolerance” of HLA class I positive, “self”, cells. The inhibitory receptors are each differently expressed by a subset of NK cells and most NK cells have at least one inhibitory receptor on their surface. In the *disarming model* proposed by Raulet, it has been described that NK cells that do not have any inhibitory receptors for self-MHC get “shut down” or inactivated (“self-tolerance”) (Fernandez *et al.*, 2005). In the *licensing model*, the group of Yokohama describes that NK cells become only functionally competent when inhibitor receptors have interacted with self-MHC molecules during NK cell development and acquisition of full functional competence (Kim *et al.*, 2005). In another model, the group of Vivier postulated that NK cells require an *education* to complete their development (Anfossi *et al.*, 2006). In this model, NK cells only reach their full competence if they receive a signal by an inhibitory receptor binding to a self-MHC-molecule.

Besides the variety of inhibitory receptors, there are also several activating receptors (Table 2), because loss of the ligands for the inhibitory receptor is not always sufficient to trigger full NK cell activation. The activating receptors consist of NKG2D, DNAM-1, the CD94/NKG2C complex, the activating part of the KIR family and the natural cytotoxicity receptors (NCR, Nkp46, 44, 30). These receptors recognize a variety of different ligands on target cells which are in part higher expressed on infected, transformed and stressed cells or are derived from pathogens (Figure 5). However, several ligands for these receptors are still unknown. The NKG2D receptor binds to MHC class I like ligands, which consist of eight molecules: MICA/B and ULBP1-6 (Eagle *et al.*, 2009a; Eagle *et al.*, 2009b; Nausch and Cerwenka, 2008). These are stress induced ligands, which are usually not expressed or only to a low level on healthy cells. During infection or malignant transformation, these ligands are expressed at the cell surface and can be recognized by NK cell through NKG2D. This binding triggers lytic activity as well as the production of cytokines. Another important activating receptor is DNAM-1 (CD226), which binds to CD155 (polio-virus receptor, PVR) and CD112 (Nectin-2). These ligands are expressed by several tumors like HCC.

In general, NK cell triggering occurs through an imbalance of stimulating and inhibitory ligands (Figure 5). In this setting, cytokines and costimulatory molecules are also important for the regulation of NK cell activity (Carayannopoulos and Yokoyama, 2004). Tumor cells or virus-infected cells often lose or downregulate their MHC class I molecules in order to evade cytotoxic T cell response, which requires the peptide / MHC class I complex for recognition and subsequent activation. NK cells are in some situations important to fight against the tumor also through direct killing of the tumor cells. It has been reported that hepatic NK cells show higher cytotoxicity against tumor cells than peripheral blood or splenic NK cells (Gao *et al.*, 2008). This observation underlines the difference between peripheral and hepatic NK cells both in phenotype and function, also in the human situation (Moroso *et al.*, 2010). Of note, tumor cells and virus-infected cells have evolved mechanisms to avoid recognition and killing by NK cells. It was described that NK cells of patients with HCC have a reduced activity and HCV-infected hepatocytes can escape NK cells by inhibition of NK cell function (Cai *et al.*, 2008; Deignan *et al.*, 2002). Because NK cells are very important for fighting against tumor cells, the exact alterations of hepatic NK cells in cirrhotic and tumor tissue and the tumor evasion mechanisms of HCC against NK cells have to be analyzed in more detail. In consequence, tumor therapy is not only performed by influencing the tumor cells alone, but also needs to be analyzed in the content of the whole microenvironment. It is

still unknown, to what extent HCC treatment by small molecules, for instance, is influencing the immune system, the microenvironment and especially the killing capacity of hepatic NK cells towards tumor cells. In this hepatic environment, the tissue contribution to the local milieu in this organ should not be underestimated.

### 1.2.3 Overview of immunological and signaling treatment options

As described above, HCC is often diagnosed at an unresectable stage and chemotherapy has failed for HCC treatment. Therefore other treatment options are needed for HCC therapy. As one of the central players in hepatocarcinogenesis, the MAPK signaling pathway has been a focus of intense research for therapeutic targeting (Friday and Adjei 2008). Therefore, a number of new drugs, mostly small molecules or monoclonal antibodies, which target molecules involved in HCC tumorigenesis, are under clinical investigations (Greten *et al.*, 2009; Huynh, 2010). The multikinase inhibitor sorafenib (Nexavar) is the first and so far only approved small molecule for the treatment of advanced HCC. In a randomized phase III double-blind placebo-controlled clinical trial (SHARP trial), it was shown that patients with advanced HCC had an increased median overall survival of about three months when they were treated with sorafenib compared to the control group (Llovet *et al.*, 2008). Sorafenib inhibits B-Raf and C-Raf, but also the autophosphorylation of several receptor tyrosine kinases like VEGFR1,2 and 3, FGFR1, platelet-derived growth factor receptor (PDGFR), c-kit and others, making it a broad acting substance (Figure 6) (Wilhelm *et al.*, 2006; Wilhelm *et al.*, 2004). It has been reported that sorafenib induces antitumor effects in HCC through the inhibition of angiogenesis, which is done by the blockage of the receptor tyrosine kinases. In addition, sorafenib inhibits cell proliferation and induces apoptosis of the tumor cells (Whittaker *et al.*, 2010). Although several mechanisms of sorafenib antitumor activity have been revealed, many are still unclear and need to be discovered.

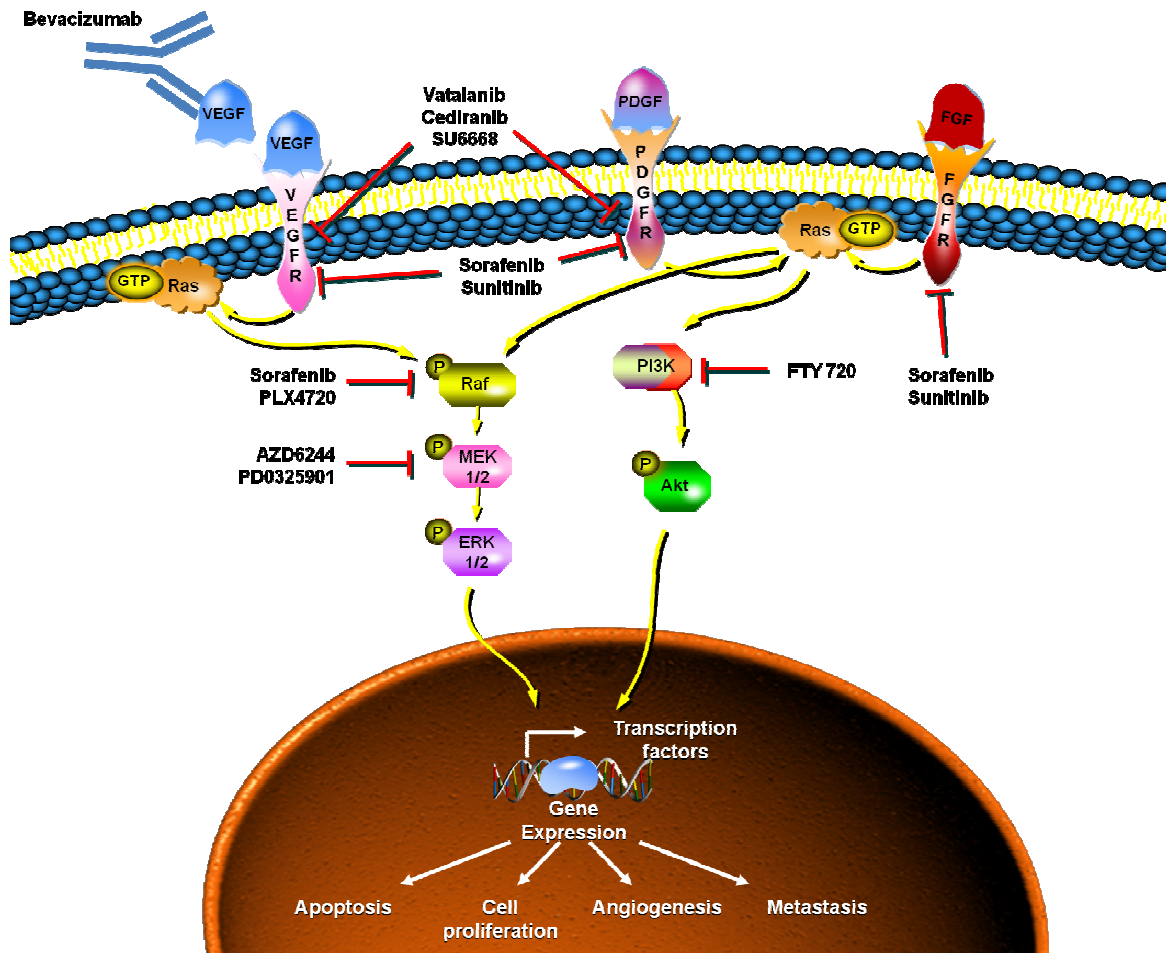


**Figure 6: Schematic overview of molecular targeted therapy in HCC.** Signaling pathway and targeted therapy was partly adapted from (Greten *et al.*, 2009). Pathway was generated with the pathway builder from [www.proteinlounge.com](http://www.proteinlounge.com).

Since treatment with sorafenib showed that targeting kinases seems to be a promising strategy for the treatment of HCC, several other multikinase inhibitors or specific inhibitors are under clinical evaluation (Figure 6). Another promising therapeutic multikinase inhibitor for HCC was sunitinib (sutent, SU11248), which also inhibits receptor tyrosine kinase receptors such as VEGFR, PDGFR, c-kit and RET kinase. Sunitinib was positively evaluated for the treatment of HCC after a phase II clinical trial, but the open-label phase III clinical study was stopped in 2010 due to higher incidence of serious adverse events in the sunitinib-treated patient group compared to sorafenib (Pfizer, 2010). There are several other multikinase inhibitors targeting VEGFR and PDGFR, which are under clinical evaluation for treatment of HCC. They include vatalanib (PTK787), cediranib (AZD2171) and SU6668 (TSU-68) (Tanaka and Arai, 2010). It has to be shown whether these inhibitors have fewer side effects.

Besides multikinase inhibitors, also selective inhibitors are currently tested. Erlotinib is a specific inhibitor of EGFR and it was observed that it clinically mainly stabilized HCC disease. Monoclonal antibodies are also being tested for the treatment of HCC like bevacizumab (Avastin), which is directed against VEGF and has been approved for several other tumors (Greten *et al.*, 2009).

There are also some rather new specific inhibitors tested for targeting the MAPK pathway. Among different MEK inhibitors, AZD6244 (Selumetinib) showed high potency of MEK1/2 inhibition and good efficacy in *in vitro* and *in vivo* models (Yeh *et al.*, 2007). Currently, AZD6244 is tested in a phase II study for advanced or metastatic hepatocellular carcinoma. Another potent MEK inhibitor is PD0325901, which has shown promising results with decrease growth in HCC *in vitro* and in mouse model systems (Hennig *et al.*, 2010).

For the treatment of other tumors like melanoma, also mutant-specific inhibitors like the B-Raf<sup>V600E</sup> inhibitor has been developed (Tsai *et al.*, 2008). PLX4720 has been described as a specific inhibitor of B-Raf and the mutant V600E form. For melanoma treatment it is under clinical evaluation and shows promising effects, but there are also some reports which describe that PLX4720 can have some adverse effect with increase of the MAPK pathway and cell proliferation (Heidorn *et al.*, 2010; Poulikakos *et al.*, 2010). Its effect for the treatment of HCC has not yet been performed.

Besides single agent therapy, there are also several clinical and pre-clinical trials for the combination of sorafenib with other targeted and cytotoxic drugs. Sorafenib is currently tested in a randomized phase III study for the treatment of HCC in combination with the chemotherapeutic agent doxorubicin (Abou-Alfa *et al.*, 2010).

The testing of variety of drugs shows that the development of effective therapies for HCC is very important. But still, extensive research has to be performed to fully understand the mechanisms of action of the therapeutic drug and the reasons why there is such a remarkable discrepancy between experimental efficacy of a drug and its clinical success in terms of disease free survival or overall survival.

## 2 Goals of the Thesis

Therapy options for unresectable hepatocellular carcinoma are very poor with the multikinase inhibitor sorafenib being the only effective treatment. It shows survival benefits for HCC patients, however unresectable HCC cannot be cured by sorafenib treatment. In order to improve HCC treatment, it is of particular importance to understand the mechanism of the action of sorafenib especially in comparison with other MAPK inhibitors. In the long run, this will help to improve drug development and drug administration. Regarding this big problem for HCC therapy, a comprehensive analysis of the effects of sorafenib and other MAPK inhibitors was performed on HCC cells and tissues in my thesis and had the following goals:

1. In HCC, the MAPK pathway is often permanently activated, suggesting a pivotal role for this pathway in tumor development. This activation is often due to a mutation in upstream molecules of the cascade. Thus, targeting the MAPK pathways seems to be a potential target for the treatment of HCC. Several small molecules are under clinical evaluation for HCC. In my thesis, I analyzed the currently used multikinase inhibitor sorafenib with potential new MAPK inhibitors such as MEK inhibitors U0126, AZD6244 and PD0325901, and a new mutation specific B-Raf inhibitor PLX4720 for HCC treatment regarding their mechanism of action. Since in many tumor lines, additional pathways are usually activated, I unraveled the effects of the different MAPK inhibitors on several other signaling pathways. Moreover, inhibitors were compared for their potency regarding the inhibition of cell proliferation and induction of apoptosis, which are important requirements of effective anti-tumor drugs.
2. Many surface molecules, also those which are important for cell-cell interaction and recognition by the immune cells, are regulated by the MAPK and closely linked pathways. Because these signaling pathways are often activated in HCC, I investigated the differences in surface molecules between HCC cell lines. Moreover, I determined whether treatment of HCC cells with MAPK inhibitors can alter the surface molecule expression in such a way that the tumor cell recognition and killing by NK cells is modulated. Due to the dependency on the chemokine and cytokine milieu for the infiltration of immune cells into the tumor, I examined the proportion of NK and T

cells in cirrhotic and HCC liver tissue in comparison to healthy liver. The secretion of cytokines, chemokine and growth factors are often regulated by the MAPK or related signaling pathways. Especially in HCC, many chemokines and growth factors are upregulated by the tumor cells. In my work, the secretion of chemokines and growth factors was analyzed in HCC cell lines and tested whether inhibition of the MAPK pathway by several MAPK inhibitors is able to alter the chemokine and growth factor secretion.

3. In the liver, the cytokine and chemokine microenvironment play an important role for the recruitment of immune cells and for organ function, in general. In hepatocellular carcinoma, the cytokine and chemokine milieu, which is important for a good balance of immune response and tolerance, seems to be changed in such a way that the tumor can escape the immune system and is able to induce angiogenesis. In a comprehensive analysis, I unraveled the alterations of the cytokine, chemokine and growth factor milieu in cirrhotic and HCC tissue in comparison to healthy liver tissue. In addition, I aimed to define the consequences of MAPK inhibition on the microenvironment.

## 3 Materials

### 3.1 Cell Culture

#### 3.1.1 Media

**Table 3: Medium for cell culture.** Medium used for cultivation of primary cells and cell cultures. NEAA: Non-Essential Amino Acids; FBS: Fetal Bovine Serum

Cell medium	Composition
RPMI III	RPMI 1640, 2 mM L-Glutamin, 1 mM Na-Pyruvat, 1x NEAA
TM	RPMI 1640, 10% FBS, 2 mM L-Glutamin, 1 mM Na-Pyruvat, 1x NEAA
HepG2 medium	DMEM, 10% FBS, 2 mM L-Glutamin, 1x NEAA, 1x HEPES buffer, 1x Gentamycin
Hep3B medium	MEM, 10% FBS, 2 mM L-Glutamin, 1x HEPES buffer, 1x Gentamycin
Huh-7 medium	DMEM, 10% FBS, 1x Pen/Strep
primary NK cell medium	RPMI III, 500 U/ml IL-2
NKL medium	RPMI III, 5% T cell growth factor (AG Falk), 15% FBS, 5% human serum, 100 U/ml IL-2
NK92 medium	RPMI 1640, 5% T cell growth factor (AG Falk), 15% FBS, 10% human serum, 200 U/ml IL-2

#### 3.1.2 Cell lines

**Table 4: Cell lines.**

Name	Origin	Medium	Source
HepG2	Human hepatoblastoma cell line from 15 year old caucasian male adolescent; NRas-mutant (Q61L); $\beta$ -catenin mutant	HepG2 medium	M. Müller-Schilling (University Hospital Heidelberg)
Hep3B	Human hepatocellular carcinoma cell line from a 8 year old black male juvenile; p53 <sup>-/-</sup> ; contains an integrated hepatitis B virus genome	Hep3B medium	M. Müller-Schilling (University Hospital Heidelberg)
Huh-7	Human hepatocellular carcinoma cell line from a 57 year old Japanese male adolescent; p53 mutant (Y220C)	Huh-7 medium	M. Müller-Schilling (University Hospital Heidelberg)
K562	Human erythroleukemia line, HLA class I negative	TM	D. Schendel (HZGU)
NK92	Human NK cell leukemia line	NK92 medium	M. Uhrberg (University Düsseldorf)
NKL	Human NK cell leukemia line	NKL medium	M. Lopez-Botet (UPF Barcelona, Spain)

RPMI 1640, DMEM, MEM, FBS, L-glutamine, sodium-pyruvate, 10x Pen/Strep, 10x HEPES buffer, 10x gentamycin and non-essential amino acids were purchased from Invitrogen. Cell lines have been tested for mycoplasma contaminations at least once a month.

## 3.2 Antibodies

**Table 5: Primary antibodies.** Antibodies used for direct or indirect flow cytometry. BD: Beckton Dickinson, BC: Beckman Coulter

Antigen	Conjugation	Isotype	Clone	Concentration	Source
Isotype control	-	IgG1	MOPC21	5 µg/ml	Sigma
Isotype control	-	IgG2a	UPC10	5 µg/ml	Sigma
Isotype control	-	IgM	MOPC104E	5 µg/ml	Sigma
HLA class I	-	IgG2a	W6/32	hybridoma supernatant	J. Johnson
HLA-A2 + B17	-	IgG1	HB54	hybridoma supernatant	ATCC
HLA-A24	-	IgM		5 µg/ml	One Lambda Inc.
HLA-DR	-	IgG	L243	hybridoma supernatant	J. Johnson
ULBP1	-	IgG2a	170818	5 µg/ml	R&D
ULBP2	-	IgG2a	165903	5 µg/ml	R&D
ULBP3	-	IgG2a	JFY02	5 µg/ml	R&D
ULBP4	-	IgG2a	7H7, Ratte	hybridoma supernatant	E. Kremmer
MICA	-	IgG2b	159227	5 µg/ml	R&D
MICB	-	IgG2b	236511	5 µg/ml	R&D
ICAM-1	-	IgG2a		hybridoma supernatant	J. Johnson
LFA-3	-	IgG		hybridoma supernatant	J. Johnson
CD155	-	IgG1	PV.404	5 µg/ml	BC
Apo1	-	IgG2a	AHO0152	5 µg/ml	Invitrogen
TRAIL-R2	-	IgG1	HS201	5 µg/ml	M. Müller-Schilling
TNF-R1	-	IgG1	16803	5 µg/ml	M. Müller-Schilling
Isotype control	FITC	IgG2b	MOPC19	2 µl	BD
Isotype control	PE	IgG2a	7T4-1F5	2 µl	BC
Isotype control	PerCP	IgG2a	X39	2 µl	BD
Isotype control	APC	IgG2a	X39	2 µl	BD
CD3	FITC	IgG1	UCHT1	2 µl	BC
CD4	APC	IgG1	13B8.2	2 µl	BC
CD6	PE	IgG1	M-T605	2 µl	BD
CD8	PE	IgG1	B9.11	2 µl	BC
CD16	FITC, Pacific Blue	IgG1	3G8	2 µl	BC
CD25	FITC	IgG2a	B1.49.9	2 µl	BC
CD44	FITC	IgG1	37.51.1	2 µl	BC
CD56	APC,	IgG1	NKH-1	2 µl	BC
CD107a	FITC, PE	IgG1	H4A3	10 µl	BD
CD166	PE	IgG1	3A6	2 µl	BC
c-Met	APC	IgG1	95106	4 µl	R&D Systems

**Table 6: Secondary antibodies.** Secondary antibodies used for indirect flow cytometry.

Antigen	Conjugation	Species	Concentration	Source
αMaus-IgG	PE	goat	1:100	Jackson ImmunoResearch
αMaus-IgG/M	PE	goat	1:100	Jackson ImmunoResearch

**Table 7: Western blot antibodies.** Primary and secondary antibodies used for western blot.

Antigen	Conjugation	Clone	Isotype	Source
Mouse anti-human p53	-	DO-1	IgG2a	Invitrogen
Mouse anti-human p63 (4A4)	-	sc-8431	IgG2a	Santa Cruz Biotechnology
Mouse anti-human p73	-	GC15	IgG	Upstate Biotechnology / Millipore
Rabbit anti-human Mcl-1 (S-19)	-	sc-819	IgG	Santa Cruz Biotechnology
Rabbit anti-human Bcl-x	-	E18	IgG	Epitomics
Mouse anti-human $\beta$ -actin	-	B11V08		Promokine
Goat anti-mouse IgG	Peroxidase			Jackson ImmunoResearch

### 3.3 Buffers, Chemicals, Reagents and Special Machines

**Table 8: Sub-G1 method.**

Sub-G1 Method	Components, Source
Nicoletti buffer	0.1% sodium citrate, 0.1% Triton X-100, pH 7.4
PBS	Invitrogen
Propidium Iodide	Sigma

**Table 9: Western blot buffers.**

Western Blot	Components, Source
Gel electrophoresis running buffer	NuPage MOPS SDS running buffer 20x NP0001
10x transfer buffer	120 mM Tris base, 960 mM glycine
1x transfer buffer	10% 10x transfer buffer, 20% methanol, 70% water
6x Laemmli buffer	150 mM Tris-HCl, pH 6.8, 6% SDS, 30% glycerine, 0.15% bromphenolblue, 0.3 M DTT
Blocking buffer	PBS, 0.1% Tween 20, 5% non fat dried milk, AppliChem A0830
Wash buffer	PBS, 0.05% Tween 20
First antibody dilution buffer	PBS, 5% BSA fraction V, 0.2% Tween 20
Second antibody dilution buffer	PBS, 2.5% nonfat dried milk, 0.1% Tween 20
Precision Plus Protein Standards All Blue	Bio-Rad 161-0373
Super Signal West Dura Extended Duration Substrate	Thermo Scientific 34075

**Table 10: Bio-Plex.** Buffers, cytokines and filter plates.

Cytokine multiplex measurements	Source
Reagent Kit A (wash buffer, assay buffer, detection antibody diluents)	Bio-Rad
Human cytokine tests: IL-1 $\beta$ , IL-RA, IL-2, IL-4, IL-5, IL-6, IL-7, IL-8, IL-9, IL-10, IL-12(p70), IL-13, IL-15, IL-17, Eotaxin, FGF basic, G-CSF, GM-CSF, IFN $\gamma$ , IP-10, MCP-1, MIP-1 $\alpha$ , MIP-1 $\beta$ , PDGF-bb, RANTES, TNF $\alpha$ , VEGF, CTACK, Gro- $\alpha$ , HGF, ICAM-1, IFN- $\alpha$ 2, IL-2R $\alpha$ , IL-3, IL-12(p40), IL-16, IL-18, LIF, MCP-3, M-CSF, MIF, MIG, $\beta$ -NGF, SCF, SCGF- $\beta$ , SDF-1 $\alpha$ , TNF $\beta$ , TRAIL, VCAM-1, IL-1 $\alpha$	Bio-Rad
96-well filter plates	Millipore

**Table 11: Phosphoplex.**

Phosphoprotein multiplex measurements	Source
Cell lysis kit + protease inhibitors	Bio-Rad
PMSF (Phenylmethylsulfonfluorid)	Sigma
Phosphoprotein reagent kit	Bio-Rad
96-well filter plates	Millipore
Total-protein tests:	Bio-Rad
Akt, p53, IκB-α, ATF-2, c-Jun, ERK1/2, JNK, MEK1, p38 MAPK, CREB	
Phospho protein tests:	Bio-Rad
Akt (Ser <sup>473</sup> ), GSK-3α/β (Ser <sup>21</sup> /Ser <sup>9</sup> ), p53 (Ser <sup>15</sup> ), IκB-α (Ser <sup>32</sup> /Ser <sup>36</sup> ), NF-κB p65 (Ser <sup>536</sup> ), ATF-2 (Thr <sup>71</sup> ), c-Jun (Ser <sup>63</sup> ), ERK1/2 (Thr <sup>202</sup> /Tyr <sup>204</sup> , Thr <sup>185</sup> /Tyr <sup>187</sup> ), JNK (Thr <sup>183</sup> /Tyr <sup>185</sup> ), MEK1 (Ser <sup>217</sup> /Ser <sup>221</sup> ), p38 MAPK (Thr <sup>180</sup> /Tyr <sup>182</sup> ), CREB (Ser <sup>133</sup> )	

**Table 12: ELISA.**

ELISA	Source
TGFβ	RnD Systems #DY240
MICA	RnD Systems #DY1300
MICB	RnD Systems #DY1599
Substrate solution	RnD Systems #DY995
Stop solution	RnD Systems #DY994
96-well plates	NUNC

**Table 13: MAPK inhibitors.**

MAPK Inhibitors	Source
DMSO (solvent)	Sigma (#472301)
Sorafenib (Nexavar, BAY 43-9006)	Bayer AG
PLX4720	Selleck Chemicals (#S152)
U0126	Promega (#V1121)
AZD6244 (Selumetinib, ARRY-142886)	Astra Zeneca / Selleck Chemicals (#S1008)
PD0325901	Selleck Chemicals (#S1036)

**Table 14: Special machines.**

Special machines	Source
xCELLigence system: RTCA-DP, E-Plate-16	Roche Diagnostics
Luminex 100 system	Bio-Rad
FACS Calibur	BD
FACS LSR II	BD
ELISA Reader TECAN sunrise	TECAN

## 4 Methods

### 4.1 Cell Culture

Cells were cultured in an incubator at 37°C with 5% CO<sub>2</sub>. In general, cells were frozen in 50% FBS, RPMI III, 10% DMSO at -80°C. FBS was inactivated by incubation at 56°C for 45 minutes (min).

#### ***4.1.1 Cultivation of adherent and suspension cells***

Adherent tumor cells (HepG2, Hep3B and Huh-7) were split every two to three days using trypsin/EDTA for 5 min at 37°C to detach cells. The proteolytic cleavage reaction by trypsin was stopped by adding new FBS containing medium to the cells. For cells in suspension, new medium was added every two to three days.

The three cell lines HepG2, Hep3B and Huh-7 were used as an *in vitro* model system for HCC. These cell lines have been used for the analysis of functional features of liver cells, because they have different mutations. The hepatocellular carcinoma in different patients shows a molecular diversity (Hoshida *et al.*, 2010; Zucman-Rossi, 2010). HepG2 cells, which derived from the liver tissue of a 15 year old Caucasian American male with a well differentiated hepatocellular carcinoma, have a mutation in NRas (Q61L) leading to a constant activation of the MAPK pathway. The Hep3B cells, which were derived from a HCC of an 8 year old black male, have a deletion of p53 and are often used to analyze the effects of p53. Huh-7 cells, which were derived of a well differentiated HCC of a 57-year-old Japanese male, have a gain of function mutation in p53 (Y220C) leading to a lack of p53 transcriptional activity and more resistance to apoptosis (Muller *et al.*, 1998). Not much is known about the p53 (Y220C) mutation. It has been described by the group of Brachmann that the mutant p53 (Y220C) is uniquely localized to the cytoplasm in H1299 cells (Baroni *et al.*, 2004). These results suggest that p53 (Y220C) is not functional in activating p53 target genes.

#### ***4.1.2 Isolation of peripheral blood mononuclear cells (PBMCs)***

Isolation of PBMCs from blood of healthy donors or patients with HCC was performed using the polysaccharide Ficoll (Biochrom AG), which has a density of 1077 mg/ml (Noble and Cutts, 1967). Thus, the components of the blood were separated by Ficoll gradients according

to their density during centrifugation. The blood, which was collected in EDTA or heparin collection tubes, was diluted with PBS at a ratio of 1:2 and slowly placed on 15 ml Ficoll in a 50 ml tube. Then, the tube was centrifuged at 840 g for 25 min without brake. This caused the separation of the blood components according to their densities. PBMCs were in the white interphase, which can be found between the above blood plasma and the below Ficoll solution, and transferred into a fresh 50 ml tube and centrifuged. To remove the remaining erythrocytes, cell pellet was incubated with erythrocyte lysis buffer for 5 min at room temperature (RT). After two washing steps with PBS, cells were resuspended in RPMI III and cell number was determined by trypan blue staining and counting the living cells under the microscope.

#### ***4.1.3 Isolation of NK cells from PBMCs***

NK cells from PBMC were isolated using the magnetic Dynal-bead untouched human NK cells kit (Invitrogen/Dynal). The NK cells were isolated according the manufacture's protocol. In principle, a mixture of biotinylated monoclonal antibodies against the non-NK cells was added to PBMC. During a short incubation time, the depletion MyOne SA Dynalbeads bound the non-NK cells. The bead-bound cells were then separated from NK cells with a magnet. Bead-bound cells were discarded, and the remaining untouched NK cells used for further experiments. Purity of the NK cell fraction was checked by flow cytometry with CD3 and CD56 staining.

#### ***4.1.4 Treatment of hepatocellular carcinoma cells with MAPK inhibitors***

The MAPK signaling pathway in HCC cell lines was inhibited by using small molecule inhibitors. Five different inhibitors were used: sorafenib, PLX4720, U0126, AZD6244 and PD0325901 (Figure 7).

**Sorafenib**, also called Nexavar (Bayer AG), inhibits C-Raf (Raf-1), wild-type B-Raf, mutant-specific B-Raf<sup>V600E</sup> and receptor tyrosine kinases (e.g. VEGFR-2,3; PDGFR- $\alpha$ , Flt-3 and c-KIT), which leads to inhibition of MEK/ERK signaling (Gollob *et al.*, 2006; Wilhelm *et al.*, 2004). One pill of sorafenib (tosylated 200 mg, Bayer AG) was solved in 31.4 ml DMSO (stock solution, 10 mM) and used at final concentrations between 0.5 and 15  $\mu$ M, as indicated in figure legends.

**PLX4720** (Selleck Chemicals) preferentially inhibits mutated B-Raf<sup>V600E</sup> and with lower affinity to wild-type B-Raf (Tsai *et al.*, 2008). It is solved in DMSO (stock solution, 10 mM), and used at final concentrations between 2.5 and 10  $\mu$ M.

**U0126** (Promega) binds MEK1/2, inhibiting its catalytic activity and therefore activation of downstream kinases ERK1/2 (Favata *et al.*, 1998). It is solved in DMSO (stock solution, 10 mM), and used at final concentrations between 2.5 and 15  $\mu$ M.

**AZD6244**, also called selumetinib or ARRY-142886 (Astra Zeneca and Selleck Chemicals), is a selective, non-ATP competitive inhibitor of MEK1/2 and therefore activation of ERK1/2 (Davies *et al.*, 2007). It is solved in DMSO (stock solution, 10 mM), and used at final concentrations between 2.5 and 15  $\mu$ M.

**PD0325901** (Selleck Chemicals) is non-competitive with ATP and is specific and highly potent against MEK1/2 and therefore activation of ERK1/2 (LoRusso *et al.*, 2010). It is solved in DMSO (stock solution, 10 mM), and used at final concentrations between 5 and 10  $\mu$ M.

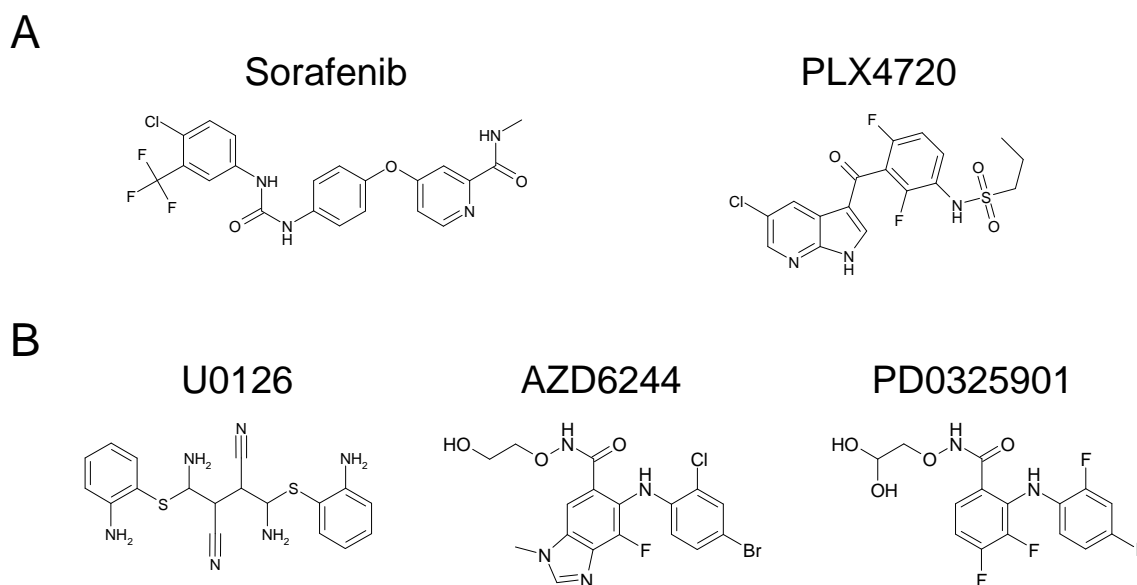


**Figure 7: Chemical structures of MAPK inhibitors.** (A) B-Raf inhibitors. (B) MEK inhibitors. Chemical structures were drawn with ISIS Draw 2.1.4.

In order to analyze short-term as well as long-term effects of MAPK inhibition, the following time points were chosen for analysis: 0, 30 min, 6, 12, 24, 48, 72 and 96 hours (h).  $1 \times 10^5$  HepG2, Hep3B and Huh-7 cells were seeded in 6-well plates, one 6-well plate for each time-point. Cells were seeded the day before treatment and allowed to adhere and grow for about 24 h. For treatment with MAPK inhibitors, the medium was discarded and 1.5 ml of the drug-containing medium was added. In addition to the inhibitors, cells were cultured in medium only and treated with DMSO as controls. Since most of the inhibitors are not stable and get degraded at 37°C, medium was changed after 48 h of treatment. After the respective incubation times, we harvested cell culture medium supernatants for the detection of chemokines and growth factors and lysed the cells using the cell lysis kit for phospho-protein detection (Bio-Rad).

For flow cytometry analysis, cells were seeded in 10 cm cell culture dishes 24 h before treatment. Then, medium was discarded and medium with inhibitors and DMSO control was added. After their respective incubation time, supernatant was collected and cells detached using trypsin/EDTA.

#### ***4.1.5 Preparation of protein lysates***

We used the cell lysis kit (Bio-Rad) for the preparation of tumor cell lysates, because this lysis procedure maintains the binding site for both, capture and detection antibody. The treatment with different small molecule inhibitors of the MAPK pathway was performed as described above. After treatment, the supernatant was collected for cytokine and chemokine detection, and cells were washed with 2 ml ice-cold PBS per well. After adding 150  $\mu$ l cold lysis buffer to each well, cells were detached with a cell scraper and lysates were transferred to 1.5 ml microcentrifuge tubes. Next, the tubes were incubated during gentle rotation at 4°C for 20 min, and then shock-frozen at -80°C to increase cell digestion. After thawing the lysates on ice, they were centrifuged at 15,000 g for 20 min at 4°C. The supernatants were transferred to new tubes, and stored at -80°C. 20  $\mu$ l lysate were used for detection of total protein concentrations.

#### ***4.1.6 Determination of protein lysate concentrations and adjustment to assay concentrations***

For the determination of protein concentration, we used the Pierce BCA Protein Assay Kit (Thermo Scientific). A standard dilution series using bovine serum albumin (BSA) was prepared. 10 µl of each standard dilution or sample was pipetted into a 96-well microtiter plate well in duplicates. 200 µl of the working reagent were added to each well, and mixed on a plate shaker for about 30 seconds (sec). The plate was covered and incubated at 37°C for 30 min. After the incubation time, the plate was cooled down to RT and the absorption was measured at 562 nm with an ELISA reader (TECAN sunrise). The Magellan software of the ELISA reader calculated the concentration of the protein lysates using the standard curve with a 4 parameter Marquardt algorithm. Protein concentrations were set to the lowest measured concentration amongst all lysates within one group, diluted with human serum diluent for the detection of cytokines and with assay buffer and lysis buffer in a 1:1 dilution for the detection of phosphorylated proteins.

## **4.2 Tissue Preparation**

### ***4.2.1 Preparation of tissue lysates***

For generation of tissue lysates we also used the cell lysis (Bio-Rad). Depending on the tissue size, 250 to 500 µl ice-cold lysis buffer were added to a 1.5 ml microcentrifuge tube. Frozen liver tissue was placed into a Petri dish, which lies on an ice-cold metal block. A small piece was cut off the frozen tissue sample and the rest was stored again at -80°C. The small tissue piece was chopped up as much as possible and transferred into the microcentrifuge tube containing the lysis buffer. After vortexing, the tissue was shock-frozen at -80°C to increase cell digestion. Thawing the lysates on ice, they were put in a cold ultrasonic bath (Bandelin electronics) for 10 min. To increase cell lysis, lysates were pipetted up and down. After repeated shock-freezing and thawing on ice, tissue lysates were ultrasonicated again and then centrifuged at 15,000 g for 20 min at 4°C. The supernatant was transferred into a new tube, and stored at -80°C. 20 µl lysate was used for detection of total protein concentrations as described above.

### ***4.2.2 Isolation of liver lymphocytes***

Liver lymphocytes were isolated according to Morsy *et al.* 2005. Freshly isolated hepatic tissue was washed once with HBSS medium (Invitrogen) to remove the remaining blood. The tissue was gently chopped up with a sterile blade into small pieces (1-2 mm<sup>3</sup>) and transferred into a 50 ml tube with HBSS-containing collagenase (500 mg/l (312 U/mg)), DNase I (50 mg/l) and FBS (2%). The tissue suspension was incubated at 37°C for 30 to 60 min and then passed through a 30 mm nylon mesh filter to remove cell clumps and undissociated tissue. To increase the amount of cells, a plunger from a 20 ml syringe was used to dissociate the tissue further. The nylon mesh was washed three times with HBSS medium. The filtered suspension was centrifuged at 500 g for 10 min at 4°C and the cell pellet washed twice in HBSS. To remove hepatocytes, the final pellet was resuspended in HBSS and centrifuged at 36 g for 1 min at 4°C. The resulting supernatant was transferred into a new 50 ml tube. The supernatant was centrifuged once again at 500 g for 10 min at 4°C. The pellet was resuspended in 15 ml HBSS medium and slowly added on 15 ml Ficoll in a 50 ml tube and centrifuged at 840 g for 25 min without brake. The white interphase containing the liver lymphocytes was transferred into a new tube and washed with HBSS medium. The pellet was resuspended in TM medium containing 100 U/ml IL-2, counted and a fraction was used for flow cytometry staining.

### ***4.2.3 Ex vivo treatment of liver tissue samples***

Explants from freshly isolated liver of HCC individuals were divided into small pieces, each having the same size, under sterile conditions and incubated with 1 ml medium with and without 5 µM sorafenib, PLX4720, U0126, AZD6244 or PD0325901 for 8 h at 37°C. After treatment, supernatants were transferred into 1.5 ml tubes and stored at -80°C until multiplex and ELISA analysis.

## 4.3 Flow Cytometry

### *4.3.1 Principle of flow cytometry*

Flow cytometry is used to simultaneously analyze large numbers of cells regarding to their size, granularity and surface expression of fluorescently stained molecules.

As a cell passes through the laser beam, it refracts or scatters light and subsequently is detected in two modes (forward and sideward scatter, FSC and SSC). FSC represents the amount of light that is scattered in the forward direction as laser light strikes the cell. The magnitude of forward scatter is roughly proportional to the size of the cell. SSC captures granularity and structural complexity of cells. Therefore, the cell size and the viability of the cells can be measured in these modes (Robinson, 2004). Moreover, fluorescent dyes or fluorochrome-labeled antibodies can be used to mark extrinsic properties of cells, which make it possible to distinguish between different cell populations, e.g. lymphocytes, monocytes and granulocytes, and to analyze membrane-expressed or intra-cytoplasmic molecules. Several dyes can be separated with one measurement. Since large numbers of cells are analyzed in a short time, statistically valid information about cell populations are quickly obtained (Robinson, 2004).

Flow cytometry analysis was used to characterize surface expression of ligands for NK and T cells, and adhesion molecules on hepatocellular carcinoma and hepatoma cell lines. In addition, PBMCs and subpopulations of hepatic lymphocytes were analyzed. HLA class I expression, CD155 expression and various other markers were used in indirect staining FACS assays to identify changes in surface expression following exposition to MAPK inhibitors. For cytotoxicity assays with NK cells, it was necessary to define the NK cell population, and other subpopulations within PBMC for specific analysis. CD107a staining was used as marker for detection of degranulating effector cells following contact with target cells. Measurements were performed with BD FACS Calibur or BD LSR II and analyzed using the BD CellQuest software and BD FACS Diva software, respectively.

### **4.3.2 Measurement of flow cytometry**

#### **Sample preparation for indirect staining**

For indirect staining, unlabeled primary antibodies were used. 50,000 to 200,000 cells were resuspended in 50  $\mu$ l FACS buffer per staining and transferred in a 96-well microtiter plate. 40  $\mu$ l of primary antibody (5  $\mu$ g/ml) or 50  $\mu$ l of hybridoma supernatant was then added to the cell suspension, and incubated on ice for 45 min. Following a washing step with FACS buffer, secondary goat or rabbit anti-mouse antibody conjugated with PE was added in 50  $\mu$ l FACS buffer. After a further incubation period of 20 min on ice in the dark, cells were washed in FACS buffer and measured immediately, or fixed with 1% PFA in PBS. Isotype control monoclonal antibodies were used to determine nonspecific background staining.

#### **Sample preparation for direct staining**

Direct antibody staining was performed in 96-well microtiter plates. 50,000 to 200,000 cells per sample were resuspended in 50  $\mu$ l FACS buffer, and respective antibodies in different combinations were added. After incubation on ice and in the dark for 30 min, cells were washed with 150  $\mu$ l FACS buffer, and if necessary, cells were fixed using 1% PFA in PBS. Isotype controls for each color were used to determine nonspecific background staining.

### **4.3.3 CD107a Degranulation assay**

During the killing process of target cells, NK and T cells release cytotoxic granules into the immunological synapse. With the fusion of the lysosomes to the cell membrane, lysosomal-associated membrane protein-1 (LAMP-1, CD107a), which is associated with the granula membrane, becomes transiently detectable at the cell surface of activated NK and T cells (Alter *et al.*, 2004). Specific antibodies were used to detect these CD107a expressing effector cells as a marker for target cell-induced cytotoxic activity.

Isolated NK cells from PBMC were stimulated for 24 h to 48 h with 500 U/ml IL-2. In 96-well plates target and effector cells were mixed in a 1:1 ratio in 200  $\mu$ l medium, and 10  $\mu$ l CD107a antibody (PE-labeled) per well was immediately added. After 1 h of incubation, 2 mM monensin (BD Bioscience) was added to prevent the acidification of endocytic vesicles, thus avoiding the degradation of reinternalized CD107a proteins from the surface,

and allowing the visualization of this marker following stimulation (Alter *et al.*, 2004). Three hours later, after a washing step, further antibody staining was used to characterize the effector cell population, with e.g. DNAM-1 FITC, CD3 PerCP, CD56 APC and CD16 Pacific blue, as previously described.

## 4.4 Detection of Cell Proliferation

### 4.4.1 Cell Count

Proliferation can be determined just by measuring the cell number. About  $1 \times 10^5$  cells were seeded into a 6-well plate and grown for 24 h. Then cells were treated with MAPK inhibitor at a concentration of 5  $\mu$ M. Cell number was analyzed at the time points 0, 24 h, 48 h, 72 h and 96 h. Cells were counted after trypan blue staining using a Neubauer counting chamber under a light microscope. Trypan blue is a vital stain used to selectively color dead cells. Live cells with intact membrane are not colored.

### 4.4.2 CFSE proliferation

Cell proliferation can be measured with carboxy-fluorescein diacetate succinimidyl ester (CFDA-SE). The non-fluorescent CFDA-SE has two acetate side chains, which makes the molecule highly membrane permeable (Figure 8). CFDA-SE is taken up by the cell, but could easily exit the cell again. Yet, in the cytosol, the two acetate side chains are removed by esterases. The potent carboxy-fluorescein succinimidyl ester (CFSE) is fluorescent; almost membrane impermeable and can covalently bind to intracellular molecules. CFSE reacts with amine groups, which then form a stable amine bond and stable fluorescent labeling of the cell is achieved (Parish, 1999; Weston and Parish, 1990). Proliferating cells sequentially halve the CFSE fluorescence upon each cell division, because CFSE gets equally distributed to the daughter cells (Figure 8) (Hasbold *et al.*, 1999; Lyons and Parish, 1994).

For CFSE proliferation assays, cells were centrifuged and the pellet was resuspended in 2.5  $\mu$ M CFSE in PBS. After incubation for 10 min at 37°C, cells were washed with PBS and the pellet was resuspended in 5 ml RPMI III + 10% human serum and incubated for 30 min at 37°C. After a washing step with medium, cells were adjusted to  $1 \times 10^5$  cells/ml and seeded

into a 6-well plate with 1 ml medium per well. After 24 h, cells were treated with 1 ml medium containing MAPK inhibitor at a concentration of 5  $\mu$ M. Cell proliferation was analyzed after 0 and 96 h by flow cytometry (FACS Calibur, BD).

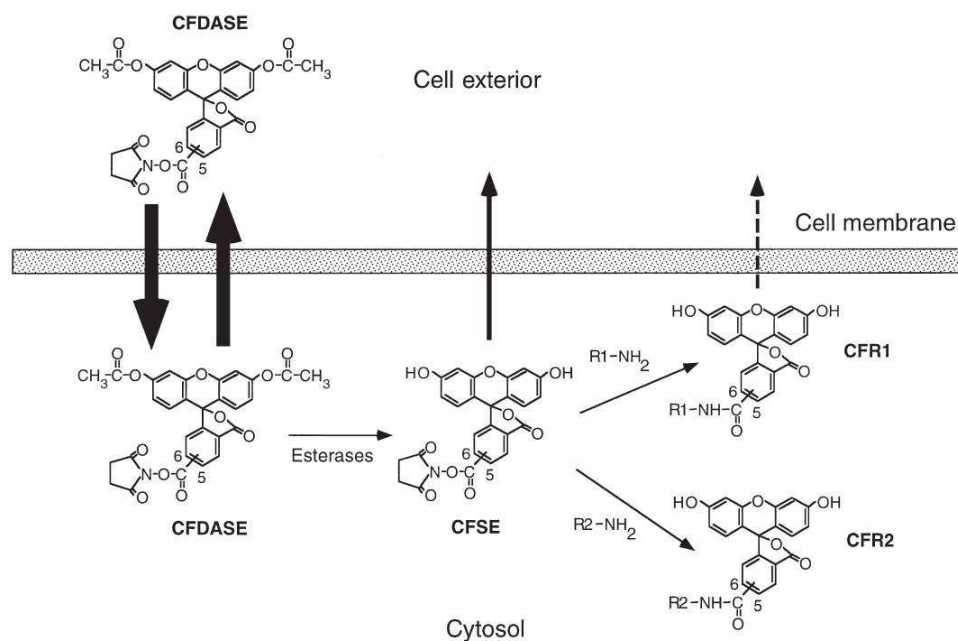


**Figure 8: CFSE labeling of the cell.** The non-fluorescent carboxy-fluorescein diacetate succinimidyl ester (CFDA-SE) is highly membrane permeable because of its two acetate side chains. CFDA-SE is taken up by the cell, but because CFDA-SE is highly lipophilic it can exit the cell again. In the cytosol the acetate side chains are removed by esterases, which make the fluorescent carboxy-fluorescein succinimidyl ester (CFSE) less membrane permeable and therefore CFSE exits from the cell at a slower rate. CFSE can covalently couple to molecules in the cytosol. It couples to molecules (R1-NH<sub>2</sub>) to form conjugates (CFR1), which can still exit from the cell or are rapidly degraded. CFSE can also be bound to long-lived molecules (R2-NH<sub>2</sub>) to form conjugates (CFR2), which cannot escape from the cell. Figure was adapted from (Parish, 1999).

#### 4.4.3 xCELLigence system

The xCELLigence system (Roche Diagnostic) monitors cellular processes such as proliferation, cytotoxicity and morphological changes (adhesion) in real-time without incorporation of labels or dyes. It utilizes an electronic readout called impedance across interdigitated micro-electrodes integrated on the bottom of microtiter plates called E-plates. The gold electrodes at the bottom of E-plates cover about 80% of the bottom of the wells (Atienza *et al.*, 2005; Kirstein *et al.*, 2006).

The presence of adherent cells on the electrode sensor surface will alter the local ionic environment at the interface between electrode and solution, leading to an increase in the impedance. The more cells attach to the bottom of the E-plate, the larger the increase in

electrode impedance (Figure 9). In addition, the impedance depends on the quality of the cell interaction with the electrodes. For example, increased cell adhesion or spreading will lead to a larger change in electrode impedance. To quantify cell status based on the measured cell-electrode impedance, a dimensionless parameter termed cell index (CI) is used. CI is derived as a relative change in measured electrical impedance to represent the status of cells in the wells. When cells are not present or do not adhere on the electrodes, the CI is zero. Under the same physiological conditions, when cells attach on the electrodes, the CI value increases. Thus, CI is a quantitative measure of cell number present in a well. Additionally, changes in cell status, such as cell morphology, cell adhesion, or cell viability will lead to changes in CI. Thus, the CI can be used to monitor cell viability, cell number, morphology, and degree of adhesion. However, it is not possible to discriminate between these events.

In the xCELLigence system the real-time cell analyzer dual plate (RTCA DP) instrument was used, which composes slots for three E-plates 16, to perform proliferation assays, measure the effects of MAPK inhibitors, and the extent of NK cell killing. The instrument was placed in an incubator set to 37°C and 5% CO<sub>2</sub>.

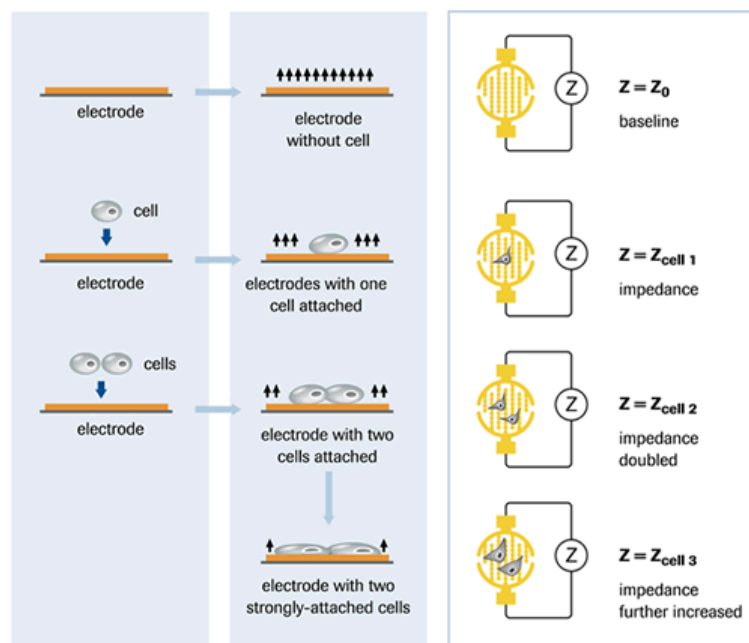


**Figure 9: xCELLigence technology and derivation of the cell index.** Cell index (CI) is a relative metric, and requires a background measurement as a starting point for evaluation. Changes in impedance by cell adhesion and proliferation lead to higher impedance and higher values of CI. Image used from Roche Diagnostics.

### **Monitoring of cell proliferation**

#### **Proliferation assays**

For proliferation tests, between 2500 and 10000 cells of HepG2, Hep3B and Huh-7 were seeded in duplicate or triplicate E-plate 16 wells for each cell line. Control wells contained only medium and the initial background measurement was performed with 100  $\mu$ l medium only in each well. After addition of the cells, they were allowed to sink for 30 min at RT, before initiating the measurement. Incubation of the cells occurred at 37°C and 5% CO<sub>2</sub> for the indicated times. In the absence of inhibitors or other drugs, increasing impedance correlates with cell proliferation.

#### **Monitoring of MAPK inhibitors on cell proliferation**

MAPK inhibitors aim to reduce cell proliferation and possibly induce cell death of tumor cells. The real-time monitoring technique of the xCELLigence system is especially suited to continuously analyze the effects of MAPK inhibition on cell status and proliferation without any further intervention over long incubation periods.

Cells were seeded in the E-plate 16 wells one day before addition of inhibitor or solvent control. After adjusting the background measurement with 100  $\mu$ l medium, 2500 to 5000 cells were added in a total volume of 50  $\mu$ l medium per well, and rested for 30 min at RT. Then the E-plate 16 was placed in the RTCA instrument and the measurement was started. After about 24 h, MAPK inhibitors were diluted in 50  $\mu$ l medium and added to the E-Plate wells. To test the concentration dependency of the MAPK inhibitors, concentrations from 2.5  $\mu$ M to 15  $\mu$ M were used. The measurement was immediately continued for 96 h.

## **4.5 Detection of Apoptosis**

### ***Sub-G1 staining (Nicoletti)***

A typical characteristic of apoptosis is the degradation of DNA by endonucleases leading to DNA fragments with the size of ~180 bp. The sub-G1 method is based on the fact that the small DNA fragments can be eluted following washing in sodium-citrate buffer, but which does not happen in vital cells. After staining the DNA with propidium iodide (PI), these

apoptotic cells that have lost the DNA will take up less stain and will appear to the left of the G1 peak as depicted in Figure 10 (Nicoletti *et al.*, 1991).

For the analysis of the apoptotic cells, HepG2 and Hep3B cells were treated with MAPK inhibitors as described in 4.1. After treatment, the supernatant was collected and transferred into a 1.5 ml tube. The remaining adherent cells were washed with ice-cold PBS and trypsinated. In the meantime, the 1.5 ml tube was centrifuged at 3,000 rpm for 8 min at 4°C and the supernatant was removed. The trypsinated cells were added to the microcentrifuge tube and centrifuged again. The cell pellet was washed with PBS. After centrifugation, the cell pellet was resuspended in 300 µl Nicoletti solution, which induced the elution of the small DNA fragments, containing 20 µg/ml PI and cells were measured within 30 min using the FACS Calibur.

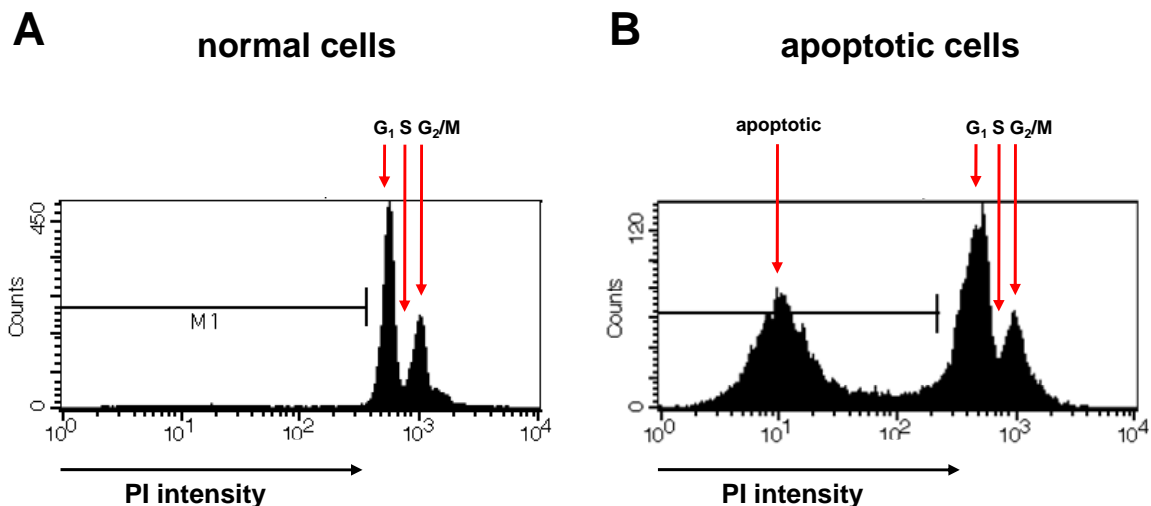


**Figure 10: Apoptosis measurement with sub-G1 peak method.** Profile of the DNA content in normal (A) and apoptotic cells (B), stained with PI. A prominent “sub-G1” peak appears in apoptotic cells, but not in normal cells.

## 4.6 Multiplex Analysis of Cytokines and Phosphorylated Proteins

### 4.6.1 Principle of multiplex analysis

The Luminex system is a bead based immunoassay and allows the simultaneous detection of several proteins, like cytokines, chemokines or kinases in cell culture supernatants or cell lysates respectively. This method uses a panel of up to 100 different fluorescence-labeled-

beads, which can be differentiated from another due to two different dyes by the Luminex machine (Figure 11). The bead sets are colored in different ratios of red dye and infrared dye. 10 different levels of fluorescence intensity for each dye create a panel of 100 beads; each is specific for a different target molecule. Thus, this bead set allows the simultaneous detection of different proteins within one sample. Each bead carries thousands of capture antibodies for one specific protein. Quantification of the protein of interest occurs by the addition of a second biotinylated specific antibody, which binds to another epitope of the protein of interest, and thus addition of streptavidin-PE (SAPE) enables quantification according to fluorescence intensity. The Luminex reader is equipped with two lasers, a classification laser (635 nm) which excites the beads and allocates them into specific regions, and a reporter laser (532 nm), which excites the molecular tags, i.e. PE. The amount of fluorescent intensity (reporter laser) is proportional to the amount of the captured molecule. For each analyte, 25 to 100 beads are measured, and the median fluorescence intensity of these beads is reported.

#### ***4.6.2 Quantification of cytokines, chemokines and growth factors***

The Luminex technique was used to create a cytokine and chemokine secretion profile for hepatocellular carcinoma cell lines and human liver tissue of healthy liver, resected liver tissue of colorectal metastases, cirrhotic tissue and HCC tissue, and to determine the effects of MAPK inhibition on this profile. Bio-Plex assays (Bio-Rad) contain standard concentrations of each analyte, and the calculation of respective standard curves allows the calculation of protein concentrations.

The assay was performed according to the manufacturer's protocol. In brief, lyophilized cytokine standard was resuspended in 500  $\mu$ l RPMI III, and incubated on ice for 30 min. Serial dilution series to generate standard curves for each cytokine, chemokine and growth factor of interest were performed. The bead mixture, specific for the analyzed cytokines, chemokines and growth factors, was incubated with 50  $\mu$ l supernatant in a 96-well filter plate for 30 min at RT. All incubation steps have been carried out on a plate shaker in the dark, to avoid bead aggregations, as well as bleaching of the beads and SAPE-labeled detection antibodies. Medium or lysis buffer served as background controls. Several washing steps were performed with 100  $\mu$ l wash buffer/well, to remove unbound proteins. We used a vacuum pump (Millipore) for all washing steps to remove the fluid in the wells. Since the beads are bigger than the filter pores, they remain in the wells. After addition of secondary biotinylated

antibody mix for 30 min at RT, and three more washing steps SAPE was added for 10 min at RT (1:100 dilutions). After three final washing steps and addition of 125  $\mu$ l assay buffer, standards and samples were analyzed for bead and SAPE fluorescence.

### Analysis of standard curves and samples

The Bio-Rad Manager 5.0 and 6.0 software was used for analysis. Standard curves are automatically calculated by the software using a 5 parameter logistic plot formula, which allows the calculation of protein concentrations in the samples (pg/ml), according to the linear relationship between fluorescent intensity and concentration. Only values within the linear regression range of the standard curves were qualified as concentrations.

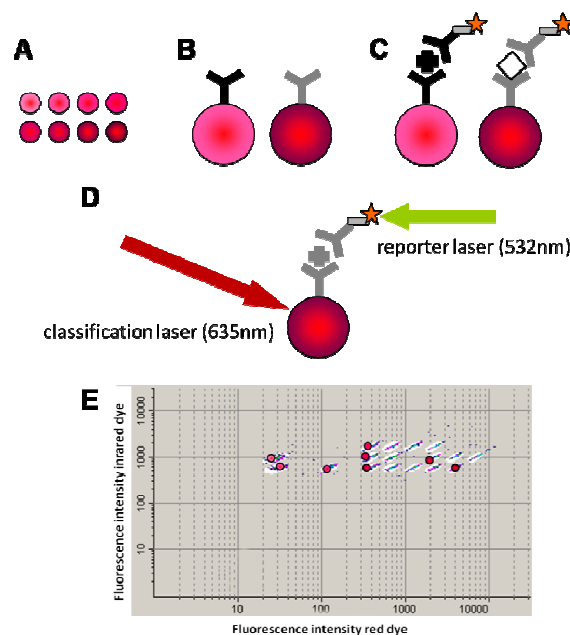


**Figure 11: Principle of multiplex analysis.** (A) The beads are based on a two-dye method with different ratios of red dye and infrared dye each containing 10 different levels creating a panel of 100 beads. (B) Dyed beads are conjugated to monoclonal antibodies which are specific for a target. (C) In the test samples, the antibodies bind to the proteins; reporter biotinylated secondary antibodies bind to the bound sample molecules. (D) The classification laser excites the beads; fluorescence of the beads identifies the region. (E) The reporter laser excites molecular tags, i.e. SAPE. The amount of fluorescence intensity is proportional to the amount of the bound protein. Figure was adapted from B. Simm.

### ***4.6.3 Phosphorylation of kinases and transcription factors***

With the multiplex technology, also phosphorylated proteins were measured according to the manufacturer's protocol. Bio-Rad does not provide standards with defined protein concentrations, but positive control lysates to test for general assay performance. The median fluorescence intensity of at least 50 beads for each analyte is a measure for the total or phosphorylated protein content in the samples. It is important to quantify changes in phosphorylated kinase protein in comparison with corresponding total protein content.

## **4.7 Enzyme-Linked Immunosorbent Assay (ELISA)**

ELISA is a widely used quantitative immunoassay. We used this method to detect human MICA/B and TGF $\beta$ . These sandwich ELISAs were performed according to the manufacturer's protocol (RnD Systems). In brief, first the 96-well microtiter plates were coated with the capture antibody diluted in PBS by incubating the plates overnight. For the assay procedure, the samples and standards were added to the wells and incubated for 2 h at RT. For the measurement of immuno-reactive TGF $\beta$ , the supernatant has to be acidulated with 1 M HCL prior the 2 h incubation. After washing, the detection antibody is added and incubated again for 2 h. Afterwards the working dilution of streptavidin-horseradish peroxidase (HRP) is added for 20 min. Then the substrate solution is pipetted to each well. After 20 min the stop solution is added and the optical density is determined using the TECAN sunrise microplate reader at a wavelength of 450 nm.

## **4.8 Western Blot Analysis**

### **SDS-Polyacrylamid gel-electrophoresis**

The samples were denaturated in Laemmli buffer and put them on ice after boiling them for 5 min at 95°C. Next, the samples were separated on NuPage gels, running at 150V constant for 50-90 min in 1x MOPS buffer.

### **Western Blot**

After SDS/PAGE proteins were transferred to a polyvinylidene difluoride (PVDF) membrane for 90 min at 200 mA in Western Blot transfer buffer. Prior to use, the PVDF membrane was activated in methanol and washed in transfer buffer. After blotting, the membrane was placed in blocking buffer for 2 h at RT or over night at 4°C. Primary antibody was then added and incubated over night at 4°C. After rinsing the membrane in wash buffer, the blot membrane was incubated with HRP-conjugated secondary antibody for 1 h at RT, and following a washing step, the blot membrane was developed in SuperSignal Substrate Working Solution for approximately 5 min. Band intensities were analyzed using the software Quantity One (BioRad).

### **4.9 Signaling Pathway Drawing**

The signaling pathway models were generated with the help of the pathway builder from [www.proteinlounge.com](http://www.proteinlounge.com).

### **4.10 Generation of Classification Trees**

Generation of the classification tree was performed by A. Skoeries (N. Halama, Bioquant Heidelberg) using the programming language R.

### **4.11 Statistics**

To determine the statistically significant differences between different treatments in HCC cell lines or between the cytokine milieu of healthy liver, resected liver of colorectal metastases, cirrhotic liver tissue and HCC tissue, the software GraphPad Prism 5 was used. Depending on whether data was distributed normally or not, student t-tests or Mann-Whitney U-tests were used respectively.

## 5 Results

### 5.1 Signaling Pathways in HCC and Small Molecule Inhibitors

In hepatocellular carcinoma, the MAPK pathway is often permanently activated, suggesting a pivotal role for this pathway in tumor development. This activation is often due to a mutation in one of the upstream molecules. It usually occurs by two main mechanisms, oncogenic mutations within the Ras or B-Raf gene or constitutive Raf activation due to either over-expression of growth factors or their receptors (e.g. VEGFR, EGFR, IGFR or c-Met) (Gollob *et al.*, 2006; Lachenmayer *et al.*, 2010).

Several strategies for blocking the Raf/MEK/ERK signaling pathway are now being evaluated as cancer therapies. A number of different small molecules, which are currently under clinical investigation, inhibit these pathways at different levels (Favata *et al.*, 1998; Friday and Adjei, 2008; Gollob *et al.*, 2006; Roberts and Der, 2007; Smith *et al.*, 2006).

To assess the effect of MAPK pathway inhibition on cell signaling, proliferation, apoptosis, cell surface molecule expression and immune cell recognition, the three cell lines HepG2, Hep3B and Huh-7 were used as an *in vitro* model system for HCC. These cell lines have been used for the analysis of functional features of liver cells. Since HCC in different patients shows a substantial molecular diversity, a more potential understanding requires studies on pathway analyses as well as functional tests (Hoshida *et al.*, 2010; Zucman-Rossi, 2010). The three cell lines, which derived from patients with HCC, have different mutations. HepG2 cells have a mutation in NRas (Q61L) leading to a constant activation of the MAPK pathway. The Hep3B cells have a deletion of p53 and are often used to analyze the effects of p53. Huh-7 cells have a gain of function mutation in p53 (Y220C) leading to a lack of p53 transcriptional activity and more resistance to apoptosis (Muller *et al.*, 1998). Therefore, these three cell lines represent different HCC tumors. In order to have a detailed analysis of the effects of the Raf inhibitor sorafenib on HCC, the three cell lines were treated with sorafenib and compared with mutation-specific B-Raf<sup>V600E</sup> inhibitor PLX4720 and three MEK inhibitors U0126, AZD6244 and PD0325901 (Figure 12).

In previous studies of MAPK inhibition in colorectal carcinoma and melanoma cell lines, we have shown that MAPK signaling disruption can have short-term effects, like inhibition of phosphorylation of downstream targets, but also long-term effects like alterations in HLA

class I expression and DNA methyltransferase activity (Sers *et al.*, 2009) (Dissertations Braun 2008; Massen submitted). In order to enable for treatment periods of up to 96 h for HCC cells, the inhibitor concentrations had to be downscaled to a concentrations that could be used for all cell lines. 5  $\mu$ M was chosen for all three cells lines for treatments up to 96 h with low toxic effects. By using the same concentration for all inhibitors, these compounds can be directly compared and the different sensitivities of the cell lines to these inhibitors can be determined. For several experiments, different concentrations were used to analyze the concentration dependent effects.

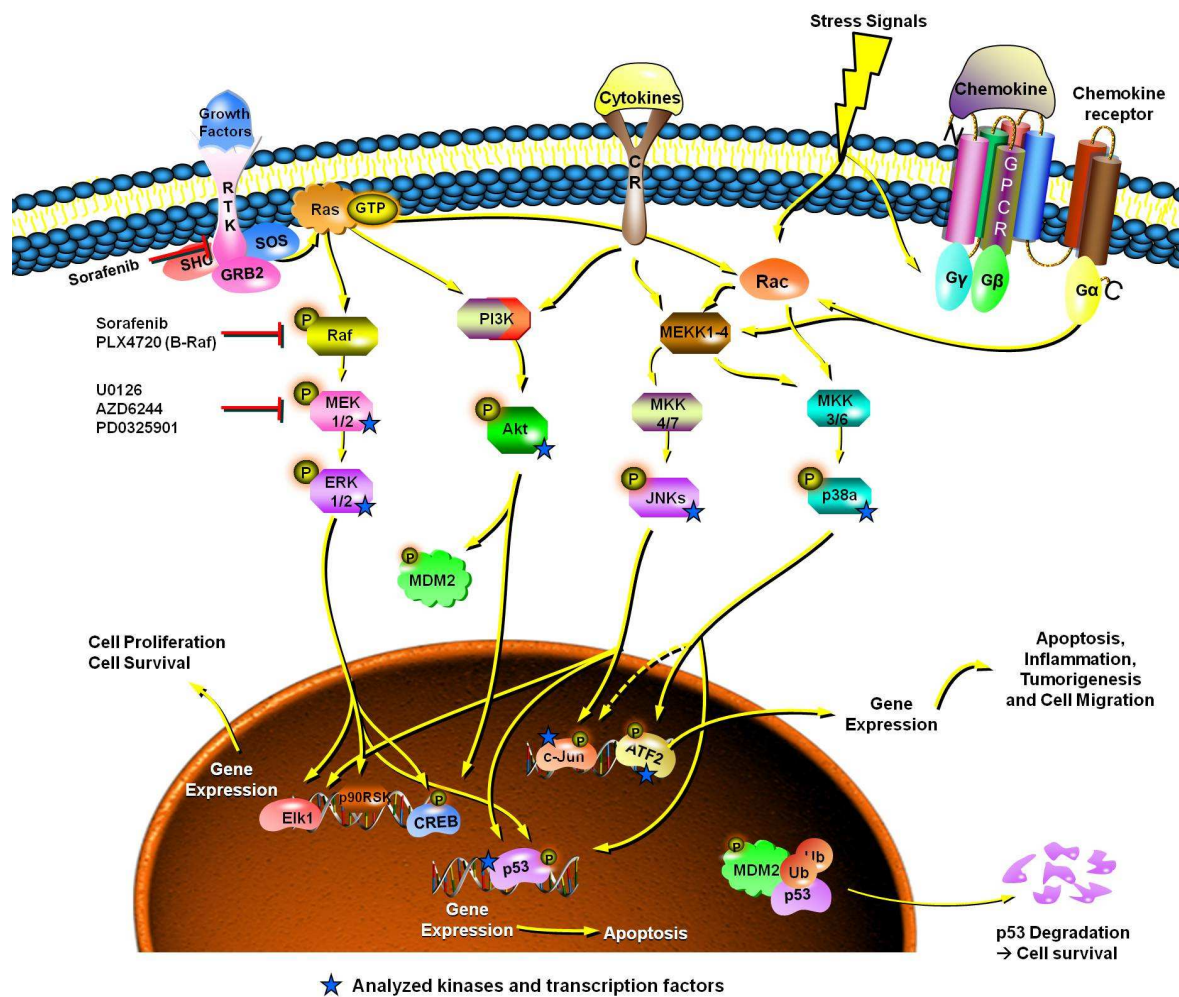


**Figure 12: MAPK family and Akt signaling pathway and inhibitors of the MAPK pathway.** The multi-kinase inhibitor sorafenib, the mutant-specific B-Raf<sup>V600E</sup> inhibitor PLX4720 and the MEK inhibitors U0126, AZD6244 and PD0325901 were used. Several different kinases and transcription factors like MEK1, ERK1/2, Akt, JNK, p38, c-Jun, ATF-2, and p53 were analyzed. Pathway was generated with the pathway builder from [www.proteinlounge.com](http://www.proteinlounge.com).

### 5.1.1 Comparison of MAPK inhibitors at the phosphorylation level

The efficiency of MAPK inhibitor is often measured according to the decreased phosphorylation of downstream kinases, mostly ERK1/2 at Thr202/Tyr204 and Thr185/Tyr187. Due to the assumed linear signaling within the MAPK pathway, blockage of B-Raf or MEK should both lead to a reduction of ERK phosphorylation.

It was tested whether the B-Raf inhibitors sorafenib and PLX4720 and the MEK inhibitors U0126, AZD6244 and PD0325901 efficiently inhibit MEK1 and ERK1/2 phosphorylation (Figure 12). For this, HepG2, Hep3B and Huh-7 cells were treated up to 96 h with these inhibitors or DMSO as a solvent control. Lysates were analyzed for phosphorylated and total MEK1 and ERK1/2 (Figure 13A,B).

The analysis of phosphorylated MEK1 (p-MEK1) and p-ERK1/2 revealed several differences between the inhibitors as well as the cell lines. While sorafenib led to a decreased phosphorylation of MEK1, the MEK inhibitors U0126, AZD6244 and PD0325901 resulted in an increase in phosphorylation (Figure 13A) (data not shown for PD0325901). The effect of U0126 was weaker in comparison to AZD6244 and PD0325901. Interestingly, in contrast to sorafenib, the mutant-specific B-Raf<sup>V600E</sup> inhibitor PLX4720 did not inhibit MEK1 phosphorylation, but rather led to a strong increase in phosphorylation in NRas-mutant HepG2 cells and to a moderate increase in NRas wild-type Hep3B cells (Huh-7 cells not tested).

At the ERK1/2 level, which is just downstream of MEK, differences in phosphorylation were also detected between the MAPK inhibitors and between the HCC lines (Figure 13A). AZD6244 and PD0325901 decreased phosphorylation already after 30 min with continued inhibition evident still at 96 h for all three cell lines. U0126 led to a continued decrease in phosphorylation in HepG2 cells, while in Hep3B and Huh-7 cells ERK1/2 phosphorylation went back to the DMSO control level after 12 h. Sorafenib showed differential effects between the three cell lines. In HepG2 cells, sorafenib reduced ERK1/2 phosphorylation within the first 12 h, but then in a “rebound” effects, it increased ERK1/2 phosphorylation, although MEK1 phosphorylation was still inhibited. In Hep3B and Huh-7 cells, ERK1/2 was almost completely and constantly inhibited by sorafenib. Only after 72 h, ERK phosphorylation was back to the DMSO level. In sharp contrast to sorafenib and the MEK inhibitors, PLX4720 elevated the ERK1/2 phosphorylation in HepG2 and partly in Hep3B cells (Huh-7 not tested).



**Figure 13: Modulation of MEK1 and ERK1/2 after treatment with MAPK inhibitor.** HepG2, Hep3B and Huh-7 cells were treated with 5  $\mu$ M MAPK inhibitor or DMSO as control for up to 96 h. (A) Phosphorylation of MEK1 and ERK1/2. (B) Total protein concentration of MEK1 and ERK1/2. Total MEK1 was not tested (n.t.) for treatment with PLX4720. Shown is one representative experiment of up to three independent experiments. For each experiment, protein concentration was adjusted to 500  $\mu$ g/ml and a minimum of 50 beads was measured and MFI was calculated. The readout of the phosphoplex is the MFI of > 50 beads detecting either phosphorylated or total kinase protein.

---

This contradictory effect on a mutant-specific B-Raf inhibitor was so far only shown for NRas-mutant melanoma lines but not for other tumor cells (Heidorn *et al.*, 2010; Kaplan *et al.*, 2011). This effect results from a drug-driven heterodimerization of B- and C-Raf in which C-Raf continues to signal and, thereby, phosphorylates MEK1. This can only occur because PLX4720 does not simultaneously inhibit C-Raf. This is not seen in sorafenib treated cells, since sorafenib is also a C-Raf inhibitor. In melanoma, this perplexing Plexicon effect was assigned to NRas-mutant melanoma cells, but I could show that even in NRas wild-type Hep3B cells this phenomenon was observed.

These findings already demonstrate that inhibitors of the same molecule can have differential effects upstream as well as downstream of the original target.

Besides the phosphorylated kinases, also the total amount of MEK1 and ERK1/2 was measured (Figure 13B). All three cell lines had a high constitutive basal level of total MEK and ERK as indicated with the DMSO control. U0126 treatment did not change substantially total-MEK1 (t-MEK1) levels. Sorafenib only showed a slight degradation of t-MEK after 72 h, but AZD6244 induced a strong decline in the t-MEK1 levels. Interestingly, this decrease is in strong contrast with the high increase in p-MEK1 indicating that p-MEK1 may be resistant to degradation. Although U0126 and AZD6244 inhibited both the MAPK at the MEK level, they have different binding sites at the MEK protein and therefore showed differences in the effect on phosphorylated and total MEK1. For technical reasons, t-MEK1 levels could not be tested for PD0325901 and PLX4720 treatment.

At the t-ERK1/2 level (Figure 13B), sorafenib led to a slight degradation in HepG2 cells, to a stronger degradation in Hep3B cells and equal levels in Huh-7 cells. In contrast, U0126 and AZD6244 did not have any effects on t-ERK1/2, even though AZD6244 mediated a strong decline in the t-MEK1 content. Surprisingly, PLX4720 reduced t-ERK1/2 in HepG2 cells although a strong increase in p-MEK1 and p-ERK1/2 was measured again indicating that phosphorylated kinases are not affected by degradation. This total-kinase degradation is not

mediated by cascades since treatment with pan-caspase inhibitor had no effect (not shown). In Hep3B cells phosphorylation of ERK1/2 was slightly reduced.

*In summary, sorafenib was the only inhibitor, which inhibited B- and C-Raf activity in the tested cells. U0126, AZD6244 and PD0325901 inhibited kinase activity of MEK, although they bind at different sites. MEK inhibition is not necessarily associated with a decrease in MEK phosphorylation itself. It seems that U0126, AZD6244 and PD0325901 stabilized MEK phosphorylation and therefore Raf was still able to phosphorylate MEK1. Although differences were seen at the p-MEK level, ERK phosphorylation was effectively inhibited with these inhibitors with some rebound effects seen with sorafenib. In sharp contrast, PLX4720 activated the MAPK pathway by phosphorylation of MEK and ERK. These results raises the question what effects these differences at the MEK and ERK levels have on other signaling cascades and on downstream molecules.*

### **5.1.2 Effects of MAPK inhibitors on other signaling pathways**

Other signaling pathways are closely linked to the MAPK cascade and regulated to some extent through the same upstream molecules (Figure 4). The JNK and the p38 kinases belong also to the family of the MAP kinases and can be activated by the Ras protein. JNK is involved in a broad range of cellular processes like apoptosis, negative regulation of cell proliferation and cytokine production. The p38 pathway is also involved in cell differentiation and apoptosis. Both, JNK and p38 pathways are mainly activated through stress stimuli, such as UV radiation, cytokines, inflammatory signals, heat shock and changes in the level of reactive oxygen species. Another important pathway, which is not directly linked to the MAPK pathway, but in close connection, is the PI3K/Akt pathway (Figure 4). It regulates many different cell functions like cellular survival, inhibition of apoptosis, angiogenesis and tumor development. Therefore, I wanted to know whether the inhibition of the MEK/ERK pathway influences other signaling pathways (Figure 12). In addition to MEK and ERK, phosphorylated and total protein of JNK, p38 and Akt were analyzed as shown in Figure 14 and in the appendix.

In HepG2 cells, phosphorylation of JNK was not affected by sorafenib, PD0325901 (data not shown) or AZD6244. Only U0126 and PLX4720 treatment resulted in an increased p-JNK. In Hep3B cells, a slight elevation of p-JNK was detectable after 6 h by sorafenib, U0126, PD0325901 (data not shown) and AZD6244 and a decline at a later time point was observed by sorafenib. In Huh-7 cells only AZD6244 treatment slightly increased p-JNK.

In contrast, the p38 pathway was not generally affected by the MAPK inhibitors, which nicely shows that the observed effects were specific for the other molecules. Sorafenib increased phosphorylation in HepG2 and Hep3B cells transiently between 6 and 24 h, while PLX4720 induced an increase of p-p38 in HepG2 and a decrease in Hep3B cells. The MEK inhibitors showed generally no effect and p-p38 in Huh-7 cells was not affected.

Although the Akt pathway is not directly linked to the MAPK pathway, it was altered by the MAPK inhibitors, but the effects differed between the cell lines. In HepG2 cells, the MEK inhibitors U0126, PD0325901 (data not shown) and AZD6244 permanently increased p-Akt at Ser 473 which is an important regulatory phosphorylation site of Akt, while sorafenib and PLX4720 decreased p-Akt. In Hep3B cells, U0126 and PLX4720 did not affect p-Akt, but sorafenib, PD0325901 and AZD6244 led to late decline in phosphorylation with the strongest effects seen with sorafenib. In Huh-7 cells, sorafenib, AZD6244 and U0126 increased phosphorylation of Akt within the first 24 h, but at later time-points, p-Akt was below the DMSO control in sorafenib treated cells.

With these experiments, it was observed that the MAPK inhibitors sorafenib, U0126, AZD6244, PD0325901 and PLX4720 could affect the phosphorylation status of MEK/ERK and also of Akt, and only to a certain extent of JNK and p38 (Figure 14). Since these pathways play a major role for the regulation of many different transcription factors, I looked at the downstream effects, analyzing the transcription factors CREB (data not shown), c-Jun and ATF-2 after MAPK inhibition (Figure 15).

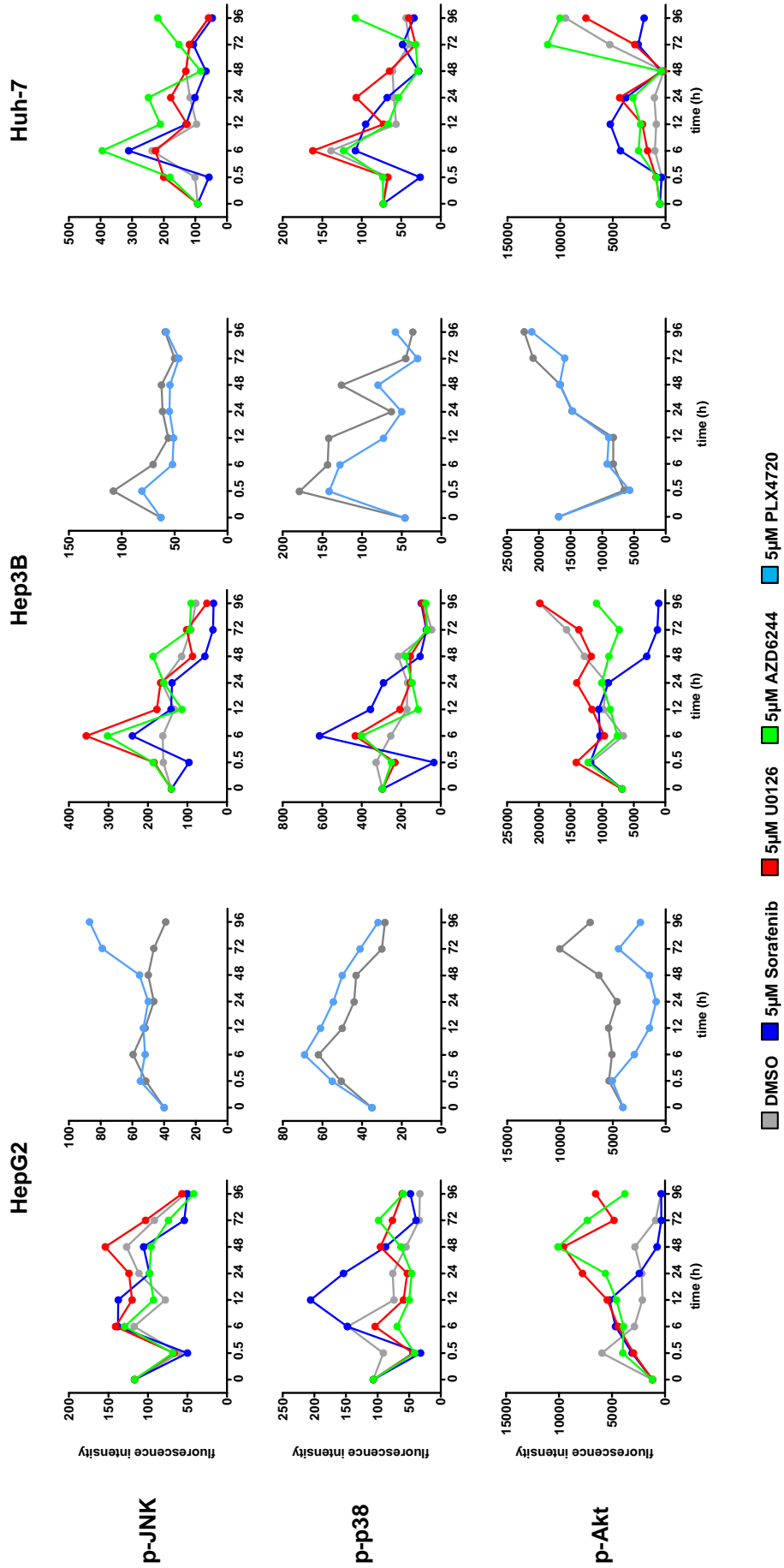


**Figure 14: JNK, p38 and Akt phosphorylation after treatment with MAPK inhibitor.** HepG2, Hep3B and Huh-7 cells were treated with 5  $\mu$ M MAPK inhibitor or DMSO as control for up to 96 h. The phosphorylation of JNK, p38 and Akt was measured. Effect of PLX4720 was not tested for Huh-7 cells. Shown is one representative experiment of up to three independent experiments. For each experiment, protein concentration was adjusted to 500  $\mu$ g/ml and a minimum of 50 beads was measured and MFI was calculated. The readout of the phosphoplex is the MFI of > 50 beads detecting phospho-kinases.

---

c-Jun, which is a component of the transcription factor activating protein 1 (AP-1) complex together with c-fos, is mainly activated by JNK, but can also be phosphorylated by p38 and ERK. Among many other activities, it is involved in the negative regulation of cell proliferation.

Sorafenib induced an increase in c-Jun phosphorylation in all three cell lines. PD0325901 (data not shown) and AZD6244 slightly decreased p-c-Jun in HepG2 cells for the first 48 h, but in Hep3B and Huh-7 cells they increased p-c-Jun (Figure 15). U0126 showed only slight elevation of phosphorylation in all three cell lines. In HepG2 but not in Hep3B cells p-c-Jun was also elevated by PLX4720. These observations suggest that AP-1 transcriptional regulation is influenced by MAPK inhibitors.

The transcription factor ATF-2, which is a member of the leucine zipper family, is activated primarily in response to signals that came on stress-activated protein kinases p38 and JNK. ATF-2 phosphorylation patterns were modulated by the MAPK inhibitors similarly to c-Jun with upregulation by sorafenib in all three cell lines and by AZD6244 in Huh-7 cells (Figure 15). In HepG2 cells, U0126 and AZD6244 also resulted in an increase of p-ATF-2. Upregulation through PD0325901 was also detected for the first 24 h (data not shown). This modulation of ATF-2 suggests a link between ATF-2-driven transcription and MAPK inhibition.

In contrast to the phosphorylation levels, the total protein levels of c-Jun and ATF-2 remained constant after the treatment period (see appendix). Only sorafenib induced substantial degradation of ATF-2 in HepG2 cells, c-Jun and ATF-2 in Hep3B cells and c-Jun in Huh-7 cells. This finding supports the suggestion that apart from MAPK inhibition the stability and turnover of kinases and transcription factors is affected by sorafenib rather than by other small molecules inhibitors.

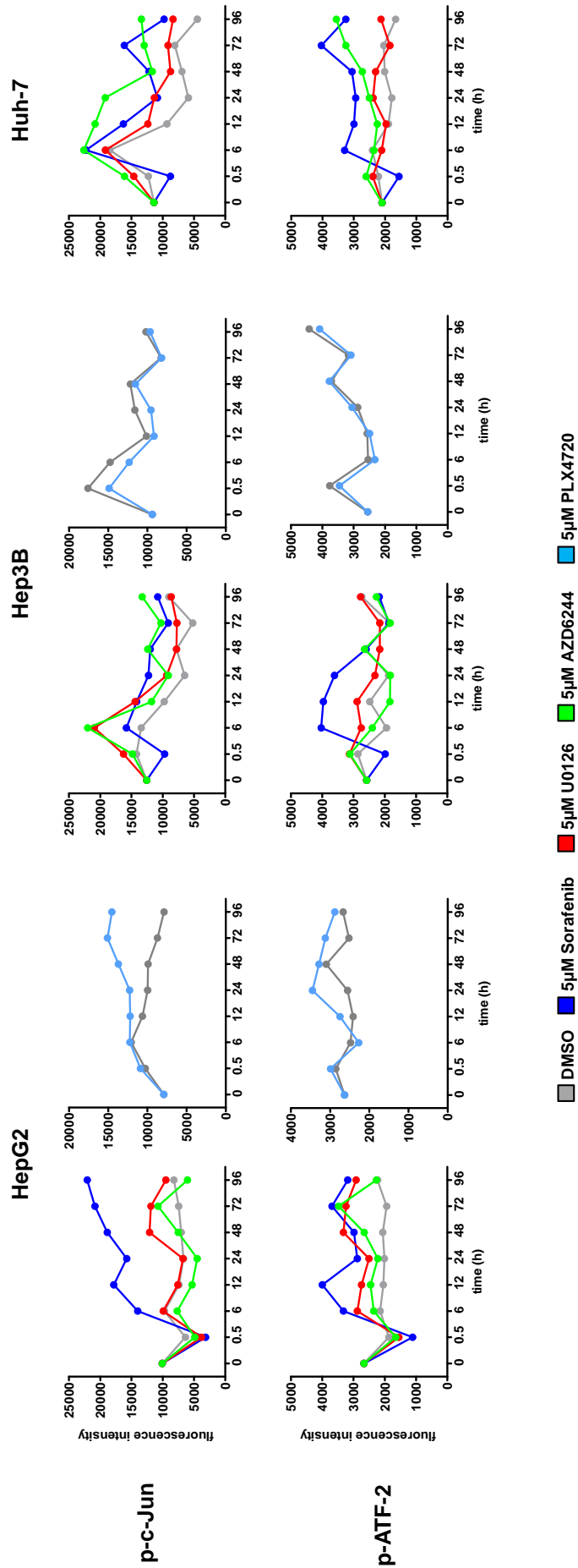


**Figure 15: c-Jun and ATF-2 phosphorylation after treatment with MAPK inhibitor.** HepG2, Hep3B and Huh-7 cells were treated with 5  $\mu$ M MAPK inhibitor or DMSO as control for up to 96 h. Phosphorylation of c-Jun and ATF-2 was measured. Shown is one representative experiment of up to three independent experiments. For each experiment, protein concentration was adjusted to 500  $\mu$ g/ml and a minimum of 50 beads was measured and MFI was calculated. The readout of the phosphoplex is the MFI of > 50 beads detecting phospho-kinases.

---

*In summary, it could be observed that besides modulation of the MEK/ERK pathway, Akt, p38 and slightly JNK were also affected by MAPK inhibitors. Downstream transcription factors were also altered during drug treatment. In contrast, total protein levels of these signaling and transcription factor components remained mainly stable. These signaling pathways play a major role for cell survival and proliferation. Thereby, altering these signaling pathways by MAPK inhibitors would expect to have large-scale consequences for the cell that will be addressed with respect to surface expression of immune recognition molecules as well as secretion of chemokines and growth factors.*

### 5.1.3 MAPK inhibition limits proliferation of HCC cells

In order to study the impact of the MAPK pathways on cell proliferation, HepG2, Hep3B and Huh-7 cells were treated with sorafenib, PLX4720, U0126, AZD6244 and PD0325901. Since these inhibitors are in a straight line connected in the MAPK cascade, it was of great interest to see whether differences in proliferation and adhesion could be detected between inhibitors and cell lines, respectively. Due to the different mutation status, it was also of interest to see whether NRas mutations or mutations in the p53 gene may have an effect on cell proliferation during drug treatment.

Since significant reduction in the phosphorylation of the “surrogate” marker ERK1/2 was observed, it was expected to detect effects on proliferation during treatment with sorafenib, U0126, AZD6244 and PD0325901. Among this line, it was interesting to see whether the slight increase of p-ERK1/2 in HepG2 cells by sorafenib after 24 h would be visible at the level of cell proliferation. Because PLX4720 induced activation of the MEK/ERK pathway in HepG2 cells and to a certain extent also in Hep3B cells, an increase in cell proliferation in consequence would have been expected. Because the inhibitors have different affinities

towards their targets, the use of the same inhibitor concentrations should also show differences in inhibition of cell proliferation.

To analyze the effects of the MAPK inhibitors on cell proliferation, different methods were used. The easiest, though old fashioned, method is to count the cells at different time points (Figure 16). With a “real-time” measurement method as the xCELLigence system, adhesion and cell growth can be constantly monitored for days at intervals of min (Figure 17). Finally, to analyze cell division, the CFSE method was used, whereby serial dilutions for each division are visualized (Figure 18).

For analyzing cell proliferation, cells were grown for about 24 h before treatment. Looking at the effects of the five inhibitors on the cell number, it was observed that in all three cells lines treatment with 5  $\mu$ M sorafenib, AZD6244 and PD0325901 had the strongest inhibitory effect with no increase in the cell numbers over time, indicating a block in cell divisions (Figure 16). In Huh-7 cells, sorafenib and in Hep3B cells, sorafenib, AZD6244 and PD0325901 substantially decreased the cell number. U0126 had a weaker effect on cell proliferation with even slowly increasing cell numbers. The cell number did not really change with PLX4720 treatment in Hep3B and Huh-7 cells. Surprisingly, in the NRas-mutant cells, where PLX4720 induced hyperphosphorylation in MEK1 and ERK1/2, cell proliferation was blocked nevertheless to some extent by PLX4720 suggesting that increase in p-ERK alone is not sufficient to accelerate the cell cycle in these cells.

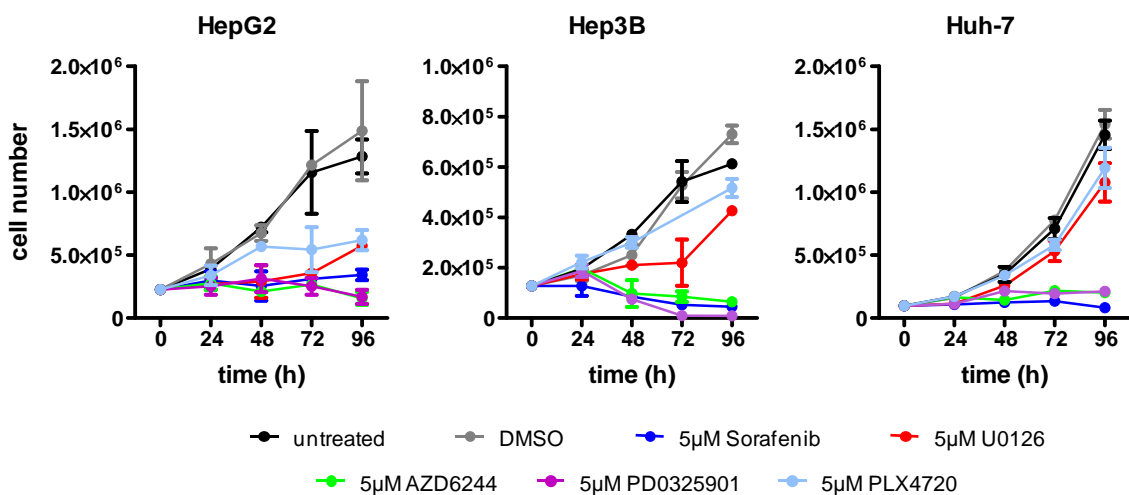


**Figure 16: Cell count of MAPK inhibitor-treated HCC cells.** Cell numbers of HepG2, Hep3B and Huh-7 cells were counted after treatment of 5  $\mu$ M MAPK inhibitors, DMSO and medium controls every 24 h for up to 96 h. Sorafenib, AZD6244 and PD0325901 induced strong inhibition of cell proliferation. U0126 has a slightly lesser effect in HepG2 and Hep3B, and barely inhibited cell proliferation in Huh-7 cells. PLX4720 induced reduction of cell number in HepG2 and Hep3B cells. n=2-3  $\pm$  SD.

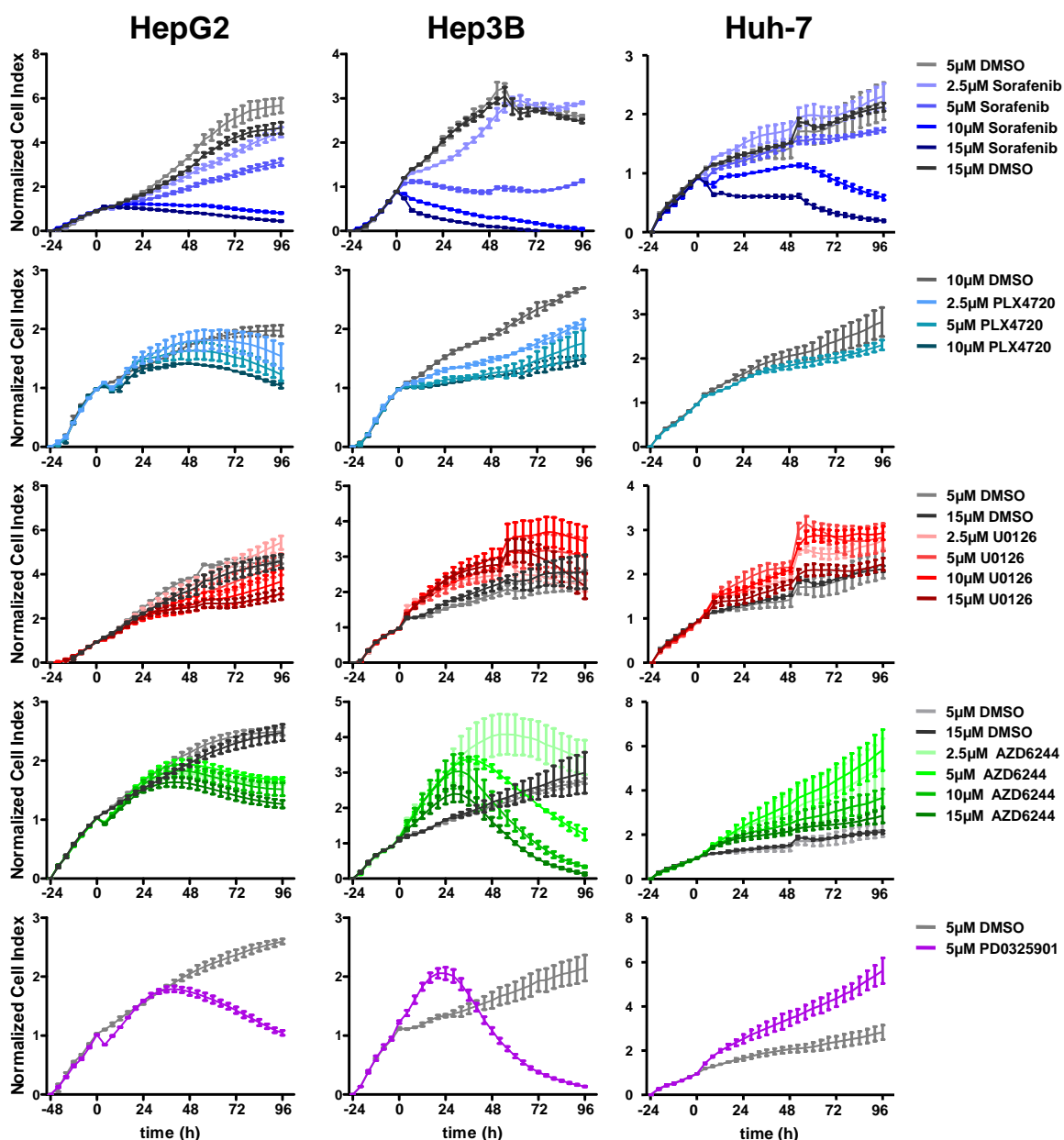


**Figure 17: xCELLigence profile of HCC cells treated with MAPK inhibitors.** HepG2, Hep3B and Huh-7 cells were grown for 24 or 48 h prior treatment with various concentrations of the MAPK kinase inhibitors sorafenib, U0126, AZD6244, PD0325901 and PLX4720 compared to DMSO controls for 96 h. Cell index was constantly measured and normalized to the start-point of treatment.  $n=3 \pm SD$ .

To further evaluate the anti-proliferative effects of the MAPK inhibitors, the xCELLigence system was used to monitor the inhibition in real-time in comparison to the cell counting method where only certain time points were verified (Figure 17). Quantification of the cell proliferation status is based on the measured cell-electrode impedance, a dimensionless parameter termed cell index (CI) is used. CI is derived as a relative change in measured electrical impedance to represent the status of cells in the wells. In order to visualize the

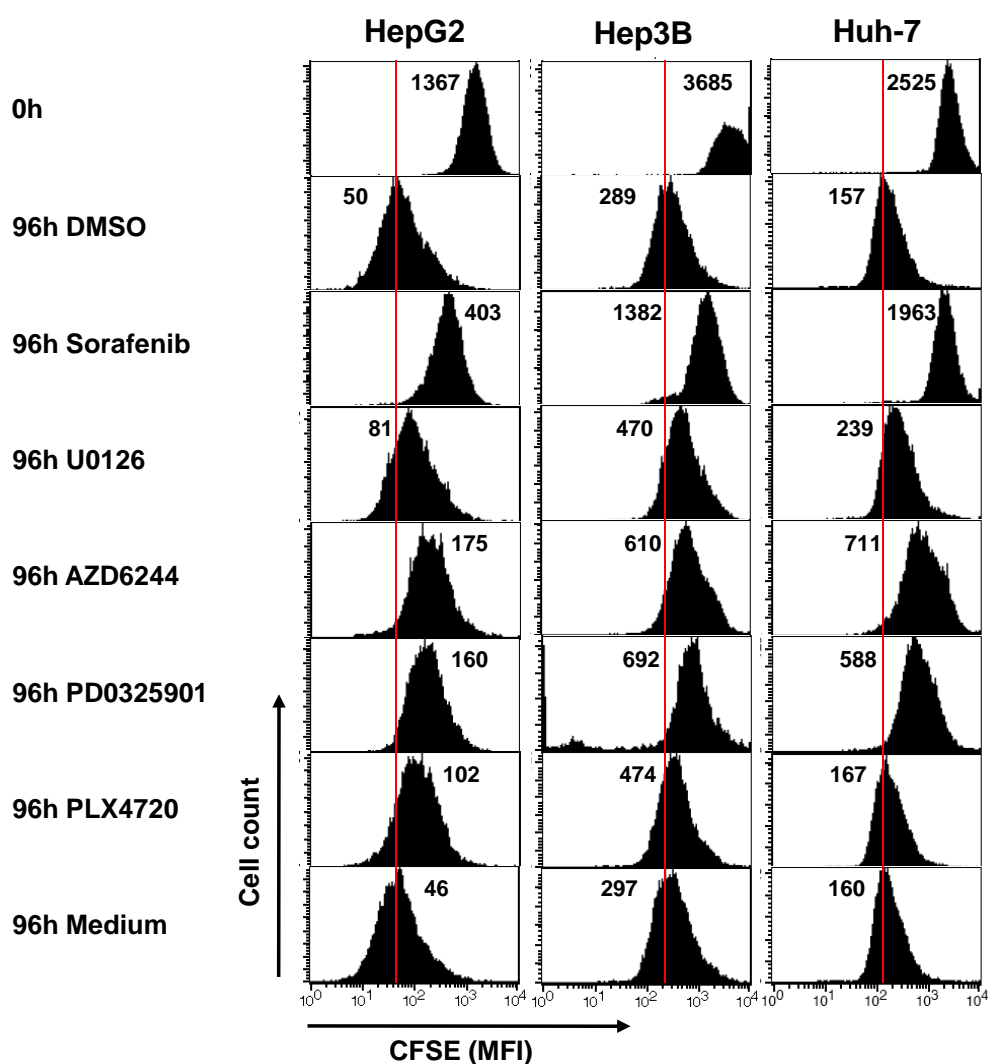
relative changes of the different MAPK inhibitors, the CI was normalized to the time-point of treatment and set to one (for more details see 4.4).

Figure 17 shows the effects of the MAPK inhibitors for HepG2, Hep3B and Huh-7 cells. Sorafenib nicely decreased proliferation in a concentration- and time-dependent manner in all three cell lines as indicated with a lower CI compared to DMSO treated cells. However, the effect of sorafenib differed between the cell lines. The strongest effect was observed in Hep3B cells, in which 5  $\mu$ M sorafenib already led to a stop in cell proliferation. This can be seen in stable CI values around CI=1, i.e. no change in impedance. Higher concentrations reduced the CI values which indicate decreased proliferation and detachment of the cells. In HepG2 cells, 5  $\mu$ M sorafenib reduced the proliferation to a lesser extent and only a slight effect was seen in Huh-7 cells. 10 and 15  $\mu$ M sorafenib dramatically inhibited cell proliferation in all three cell lines. Although increasing p-ERK, PLX4720 did not increase cell proliferation, but rather inhibited proliferation in a concentration dependent manner.

Interestingly, the MEK inhibitors U0126, AZD6244 and PD0325901 behaved differently in the xCELLigence system compared to sorafenib and PLX4720, and strong differences were seen between the cell lines. In HepG2 and Hep3B cells the MEK inhibitors decreased the CI in a concentration dependent manner at late time-points beyond 48 h. In Huh-7 cells treated with U0126, AZD6244 and PD0325901, the normalized CI curves did constantly raise and did not get below the DMSO control. This raise in CI in some MEK inhibitor treated cells was probably due to an enhanced cell adhesion which cannot be discriminated from proliferation by this method. Therefore, cell division was additionally analyzed by dilution of CFSE in flow cytometry in order to explain the effects in more detail.

Besides cell counting and using the xCELLigence system for cell adhesion and cell proliferation, the capability of the cells to divide was analyzed under the influence of MAPK inhibitors by using the CFSE method (Figure 18). Cells were stained with CFSE and treated with 5  $\mu$ M inhibitor for 96 h (see 4.4). CFSE intensity was not so strongly decreased when cells were treated with sorafenib indicating a strong inhibition of cell division. This effect was slightly less pronounced with AZD6244 and PD0325901. U0126 had only a weak effect on cell division indicated by strong CFSE dilution comparable to DMSO control. PLX4720 achieved almost no block of cell division with only a slight reduction in HepG2 cells.

A



B

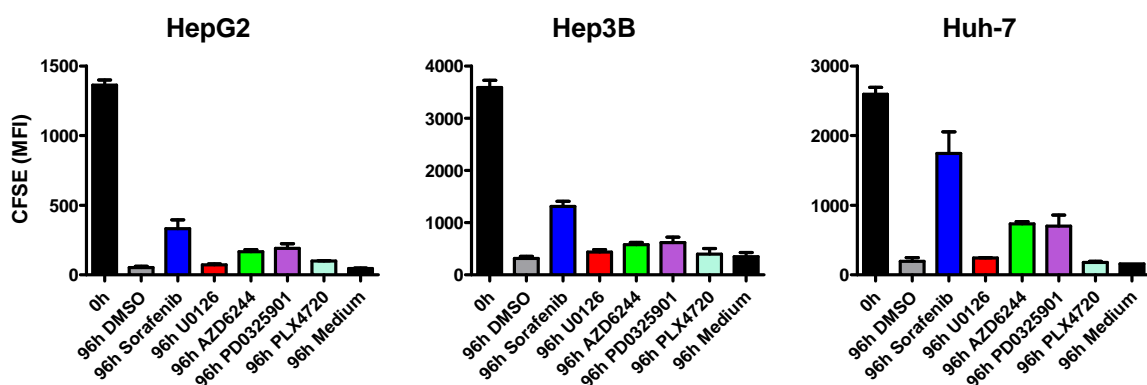


**Figure 18: MAPK inhibitor-mediated inhibition of cell division of HCC cells.** CFSE-labeled HepG2, Hep3B and Huh-7 cells were treated with 5  $\mu$ M sorafenib, U0126, AZD6244, PD0325901 and PLX4720 and compared to DMSO and medium controls. Cells were analyzed using flow cytometry. Sorafenib induced strong inhibition of cell division whereas AZD6244 and PD0325901 had a lesser effect. U0126 barely inhibited cell division and PLX4720 did not show any effects in Hep3B and Huh-7 cells but slightly in HepG2 cells. (A) Histogram layout (B) Analysis of two to three experiments. Shown are the median fluorescence intensities (MFI) of CFSE.

*In summary, the MAPK inhibitors except for PLX4720 nicely inhibited cell proliferation and cell division with differences in the effectiveness between the cell lines. Although sorafenib, AZD6244 and PD0325901 inhibited similarly cell proliferation regarding cell number, differences between sorafenib and the MEK inhibitors were observed for cell adhesion and the inhibition of cell division. While sorafenib effectively blocked cell division, the MEK inhibitors reduced cell proliferation through other mechanisms. Therefore, it was next analyzed whether MAPK inhibition induces apoptosis and modulates factors involved in the regulation of apoptosis.*

### **5.1.4 Some MAPK inhibitors induce apoptosis in HCC**

Besides regulating cell proliferation, the MAPK family is also a very important regulator of apoptosis. The MEK/ERK pathway is mainly involved in cell proliferation and cell survival, but it has also been shown to impinge on apoptosis. High levels of p-ERK1/2 can reduce the apoptosis rate by inhibiting cytosolic caspase activation and the pro-apoptotic molecule Bad (Krishna and Narang, 2008). It has recently been published that hyperactivation of the MEK/ERK pathway induced by PLX4720 in NRas-mutant melanoma cells leads to resistance against apoptosis (Kaplan *et al.*, 2011). On the basis of the phosphorylation data during drug treatment induction of apoptosis was addressed for the three cell lines during inhibitor treatment. To assess the role of the MAPK pathway for the induction of apoptosis in HCC, all five MAPK inhibitors were directly compared with a certain focus on sorafenib.

To measure the amount of apoptosis induced by MAPK inhibitor treatment, DNA fragmentation (sub-G1 peak) was analyzed in HepG2, Hep3B and Huh-7 cells. To analyze time- and dose-dependent effects, tumor cells were treated for 48 and 96 h with 5  $\mu$ M and 10  $\mu$ M inhibitor, respectively (Figure 19). Indeed, MAPK inhibitors induced apoptosis to a different extent and as expected from the p53 status, the three cell lines showed different sensitivities towards inhibitor treatment. In general, apoptosis was induced in a time- and dose-dependent manner. Interestingly, high rates in apoptotic cells were measured in Hep3B cells, which lack p53, after treatment with sorafenib, AZD6244, PD0325901 after 48 and 96 h with 5 and 10  $\mu$ M inhibitors. In these cells, U0126 induced apoptosis substantial to a lesser extent and PLX4720 did not induce apoptosis although a tendency towards more apoptosis was observed with 10  $\mu$ M.

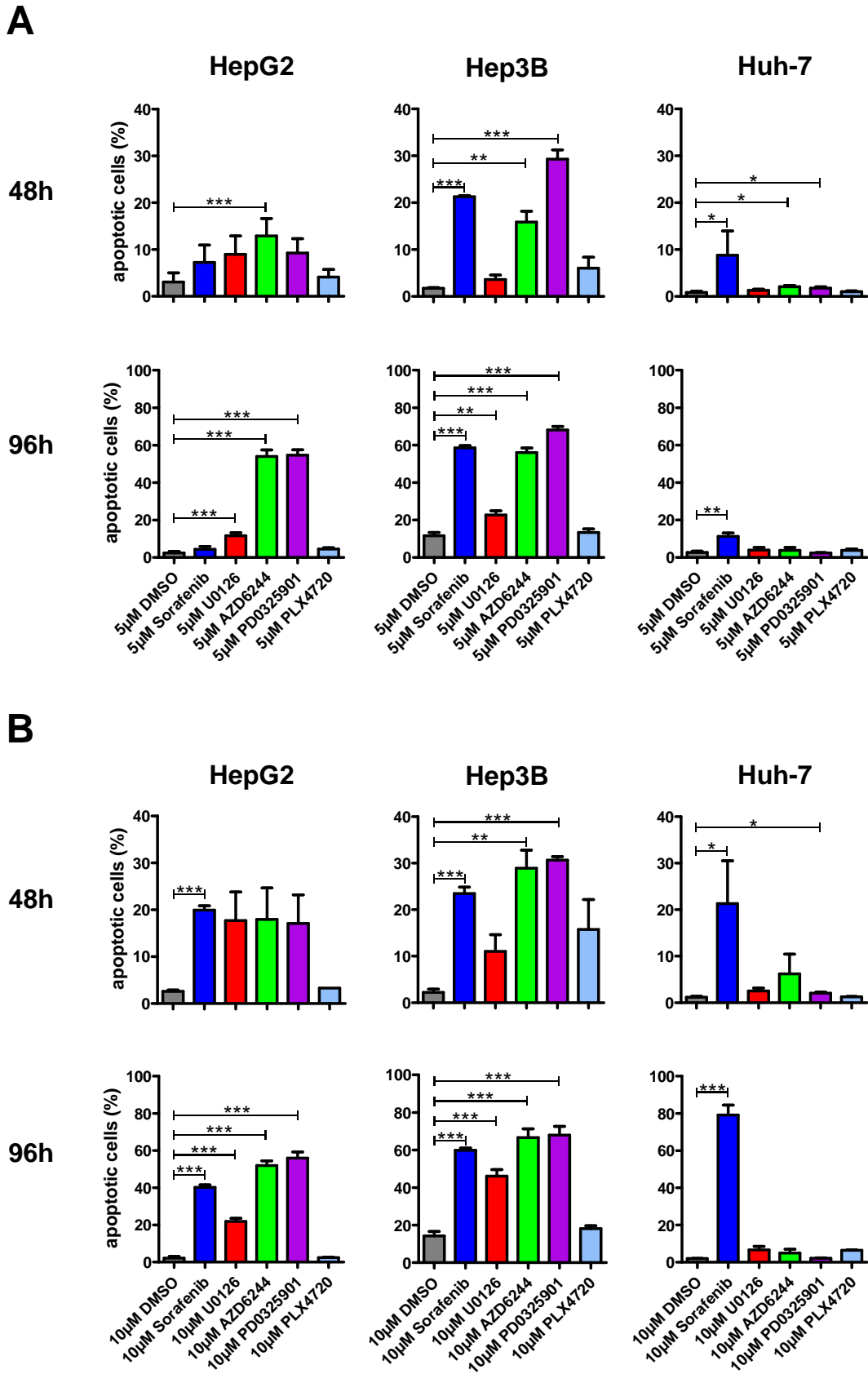


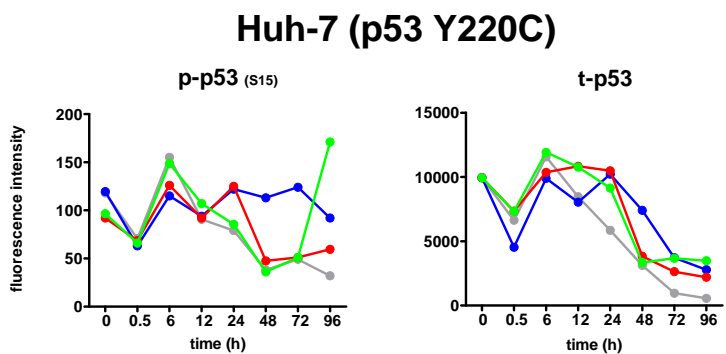
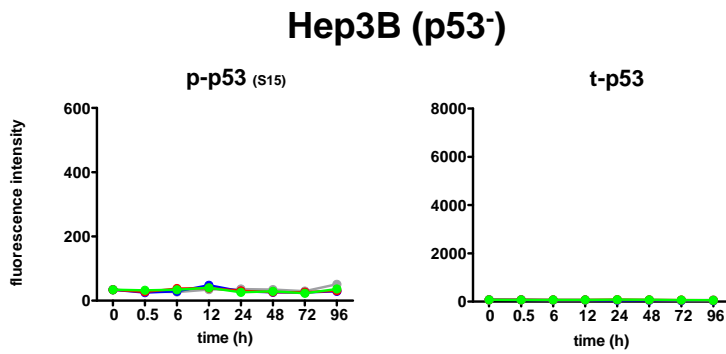
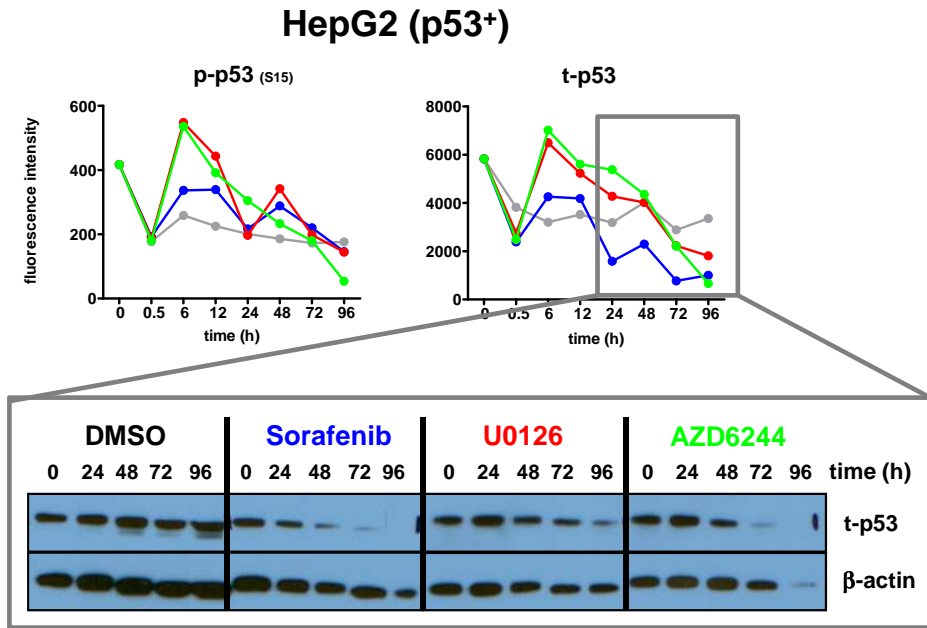
**Figure 19: MAPK inhibitors induce apoptosis in HCC cell lines to a different extent.** HepG2, Hep3B and Huh-7 cells were treated with 5  $\mu$ M (A) and 10  $\mu$ M (B) of MAPK inhibitors or DMSO control for 48 and 96 h. Apoptosis was determined by measuring the sub-G1 peak using PI.  $n \geq 3 \pm$  SD. \*:  $p < 0.05$ ; \*\*:  $p < 0.01$ ; \*\*\*:  $p < 0.0001$ .

In p53-wild-type HepG2 cells, longer treatment and higher concentrations were needed to induce significant apoptosis with the MAPK inhibitors except for PLX4720 that did not induce apoptosis at all (Figure 19). With a 5  $\mu$ M inhibitor concentration, primarily AZD6244 and PD0325901 but not sorafenib significantly induced apoptosis. As expected for a dose-dependent manner, 10  $\mu$ M sorafenib increased apoptosis to a similar level as 10  $\mu$ M AZD6244 and 10  $\mu$ M PD0325901. Thus, despite strong inhibition of p-ERK1/2 by all inhibitors, induction of apoptosis is regulated partly independently from MEK/ERK phosphorylation.

Remarkably, Huh-7 cells behaved differently compared to HepG2 and Hep3B cells. Huh-7 cells have a gain of function mutation in p53 (Y200C), which induces an increased half-life of p53, whereby this mutation is associated with increased apoptosis resistance (Puisieux *et al.*, 1995). Accordingly, Huh-7 cells seemed to be rather apoptosis resistant especially for the low inhibitor concentrations (Figure 19). However, sorafenib showed a strong induction of apoptosis in a time- and dose-dependent manner again strongly indicating that apoptosis is induced independently from the MEK/ERK phosphorylation status.

The regulation of apoptosis is complex and many different factors can be involved in different cell types. Apoptosis is regulated via several mechanisms coming from either the extrinsic or the intrinsic pathway. Therefore, it was analyzed to what extent the molecules of these pathways may be modulated during MAPK inhibition. A detailed analysis of the factors involved in apoptosis was mainly performed for sorafenib and in HepG2 and Hep3B cells. Some of the data were acquired in cooperation with the laboratory of Martina Müller-Schilling (University Hospital Heidelberg, Germany).

The tumor suppressor gene p53 has many important functions as regulating cell cycle, apoptosis, and gene stability which are all involved in prevention of malignant transformation. The tightly regulated p53 protein is induced by a variety of stress signals, including DNA damage, oxidative stress and activated oncogenes. Dysregulation of the p53 protein by MAPK inhibition might have effects on cell survival. Phosphorylated and total amounts of p53 were analyzed in HepG2, Hep3B and Huh-7 cells after MAPK inhibition by phosphoplex and western blot analysis (Figure 20, Figure 21). Figure 20 shows the kinetics of phosphorylated (Ser15) and total protein p53 levels in HepG2, Hep3B and Huh-7 cells after sorafenib, U0126 and AZD6244 treatment compared to DMSO control. In HepG2 cells, p-p53 was upregulated within the first 12 h by sorafenib and U0126 then went back to DMSO level and were



■ DMSO  
 ■ 5μM Sorafenib  
 ■ 5μM U0126  
 ■ 5μM AZD6244

p: phosphorylated

t: total

**Figure 20: p53 phosphoplex and WB analysis in HCC cells after MAPK inhibition.** HepG2, Hep3B and Huh-7 cells were treated with 5 μM sorafenib, U0126, AZD6244 or DMSO as control for up to 96 h. Western blot analysis confirmed the results obtained by phosphoplex analysis. β-actin was used as a loading control. p: phosphorylated protein; t: total protein.

increased again after 48 to 72 h, while during AZD6244 treatment, p-p53 was elevated within the first 48 h. Total protein levels were also increased by sorafenib during the first 12 h, but then decreased and dropped below the DMSO control. U0126 and AZD6244 induced an increase in t-p53 up to 48 h and then the curve also went below the DMSO control.

Hep3B cells lack p53 and therefore no signal was detected for p- and t-p53. In Huh-7 cells, sorafenib induced an increase of p-p53 after 48 h and in t-p53 after 24 h. U0126 slightly increased t-p53 levels and AZD6244 induced late elevation of p-53 and slight upregulation of t-p53.

Phosphoplex analysis is a rather recently established and sensitive method to analyze cell signaling. From the same lysates western blot analysis were performed to confirm our phosphoplex findings in HepG2 cells (Figure 20). Nice correlations were observed between phosphoplex and western blot analysis.

Additionally, p53 modulation was analyzed after PD0325901 and PLX4720 treatment besides sorafenib, U0126 and AZD6244 treatment in HepG2 cells (Figure 21). Indeed, p53 was increased in the first 12 to 24 h by PD0325901 as it was seen for sorafenib and the other MEK inhibitors. In contrast, PLX4720 did not change the p53 levels compared to DMSO. Thus, p53 was regulated by MEK and B-Raf inhibitors but in a drug-specific manner. Therefore, this p53 regulation is MEK/ERK independent.

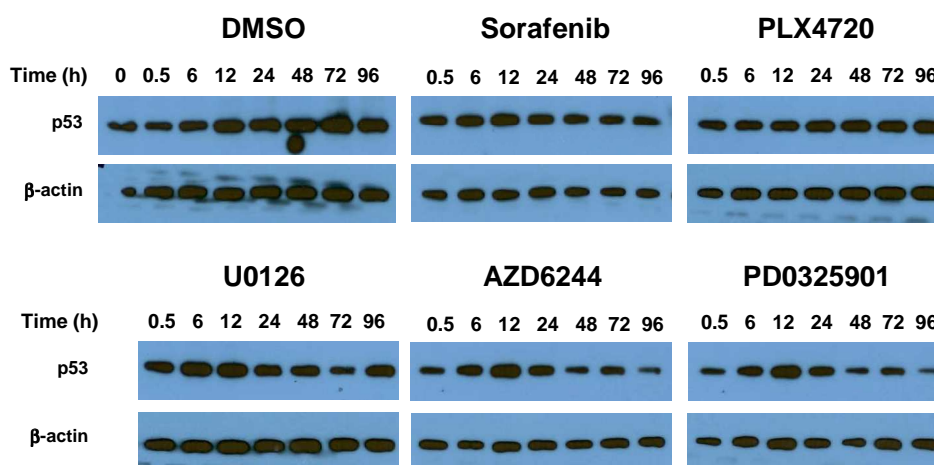


**Figure 21: p53 expression is modulated by MAPK inhibitors in HepG2 cells.** HepG2 cells were treated with 5  $\mu$ M sorafenib or DMSO control for up to 96 h and p53 expression was analyzed by western blot.  $\beta$ -actin was used as a loading control.

Besides p53, the proteins p63 and p73 also belong to the p53 family and have partially overlapping but also distinct functions. The proteins p63 and p73 are required for p53-dependent apoptosis in response to DNA damage (Flores *et al.*, 2002). Besides the normal full-length protein, several isoforms of p63 and p73 can exist. The N-terminally truncated  $\Delta N$  isoforms  $\Delta Np63$  and  $\Delta Np73$  have anti-apoptotic properties as intrinsic inhibitors and it has been recently published that  $\Delta Np63$  induces drug resistance in HCC (Mundt *et al.*, 2010) and  $\Delta Np73$  confers resistance to chemotherapy (Muller *et al.*, 2005). In order to get a more comprehensive view on the regulation of the p53 family, p63 and p73 were analyzed from the same samples used in phosphoplex.

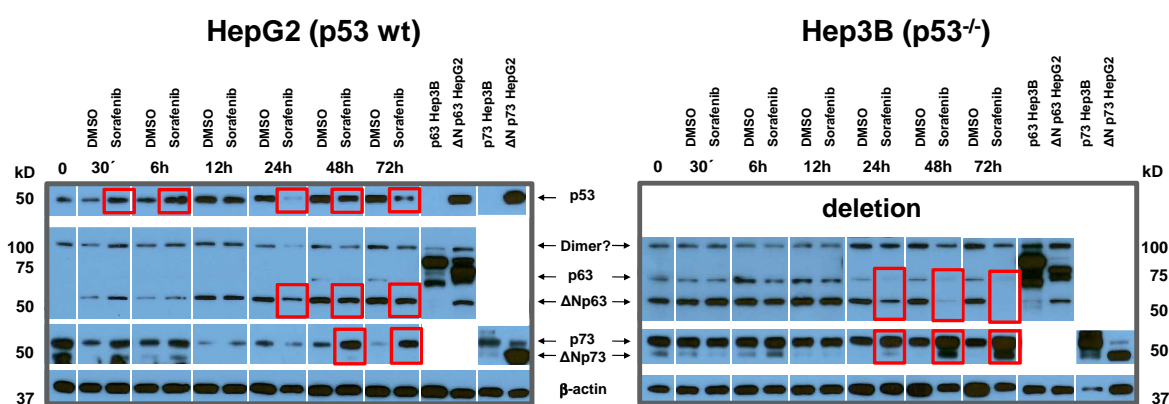


**Figure 22: p53 family members p53, p63 and p73 are altered by sorafenib.** HepG2 and Hep3B cells were treated with 5  $\mu$ M sorafenib or DMSO up to 72 h. As a positive control, lysates expressing p63, p73 and their  $\Delta N$  isoforms and as a loading control,  $\beta$ -actin were used

Due to the limited amount of lysates, only sorafenib treated cells were analyzed in detail. For analyzing p63 and p73 in HepG2 and Hep3B cells after sorafenib treatment, cells were treated up to 72 h and western blot analyses were performed (Figure 22). In HepG2 cells, the  $\Delta Np63$  isoform was induced after longer cultivation. Normal p63 was not detectable. Sorafenib treatment reduced the levels of  $\Delta Np63$  after 24 h. Treatment with sorafenib strongly increased the levels of p73 after 48 and 72 h. A similar effect of sorafenib was detected in Hep3B cells, which lack p53.  $\Delta Np63$  was strongly decreased after sorafenib treatment, although the slight p63 expression, which was detectable for the DMSO control, seemed to be also reduced by sorafenib. In contrast, p73 and also the  $\Delta N$  isoform were increased by sorafenib. These experiments demonstrate that sorafenib, in particular, mediates a differential regulation of the p53 family members, p63 and p73 as well as their  $\Delta N$  isoforms. Therefore, it is likely that this modulation also affects apoptosis induction.

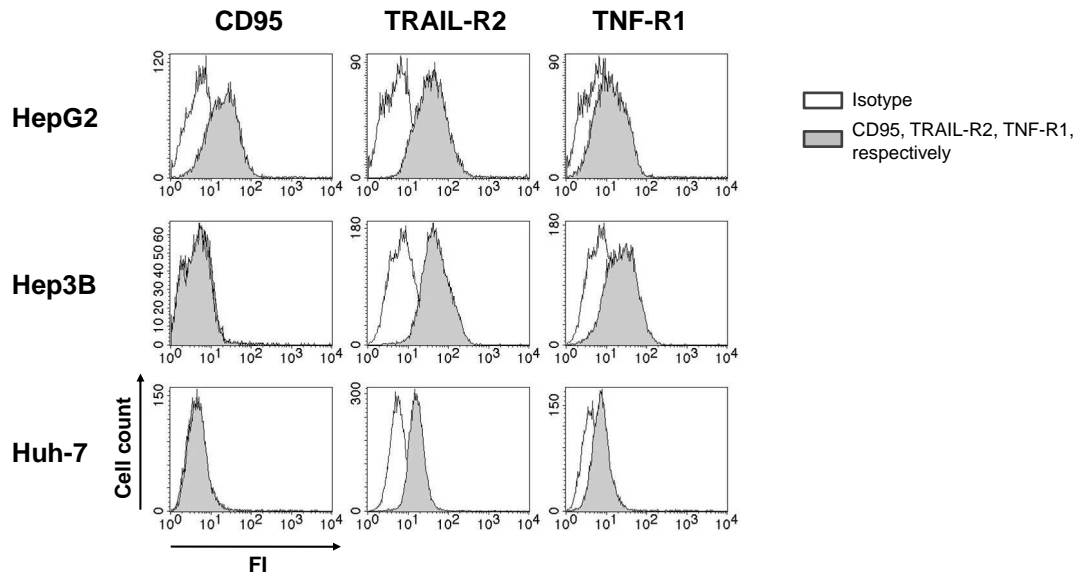


**Figure 23: Death receptor expression on HCC cells.** Cells were characterized for the expression of the death receptors CD95, TRAIL receptor 2 (TRAIL-R2), and TNF receptor 1 (TNF-R1). Only HepG2 cells express CD95, while Hep3B and Huh-7 cells are deficient in CD95, presuming as a consequence of p53 deficiency. TRAIL-R2 is detected on all three cell lines and TNF-R1 is only slightly expressed.

For the induction of apoptosis in tumor cells, various death receptors play a pivotal role. Therefore, we analyzed the expression of the cell surface death receptors CD95 (Fas), tumor necrosis factor receptor 1 (TNF-R1) and TNF related apoptosis inducing ligand receptor 2 (TRAIL-R2) (Figure 23). HepG2 cell expressed CD95 to a low to medium level and Hep3B and Huh-7 cells were CD95-deficient. In contrast, TRAIL-R2 and TNF-R1 were expressed on all three HCC lines.

MAPK pathway inhibition had an effect on surface expression of the death receptors CD95, TNF-R1 and TRAIL-R2. An increase of CD95 expression after 48 h was induced by sorafenib, AZD6244 and PD0325901, but not PLX4720 treatment in HepG2 cells (Figure 24). In Hep3B cells, which are deficient of CD95, no modulation was detected after treatment with these inhibitors (data not shown). Expression of TRAIL-R2 and TNF-R1 was only tested in HepG2 and Hep3B cells after 48 h sorafenib treatment. TRAIL-R2 was slightly increased in HepG2 and Hep3B cells, but TNF-R1 was not significantly modulated but showed a tendency of downregulation in both cell lines (data not shown).

To show that upregulation of CD95 and TRAIL-R2 was also modulated on the RNA level, PCR analysis was performed by the laboratory of M. Müller-Schilling (University Hospital Heidelberg). A significant increase of CD95 and TRAIL-R2 mRNA was observed in HepG2

cells, and an increase of TRAIL-R2 mRNA in Hep3B cells (data not shown). Moreover, we could see that the combination of sorafenib treatment with activation or stimulation of the death receptors increased the apoptotic rate indicating that sorafenib has sensitizes the death receptor signaling pathway (data not shown, manuscript in preparation).

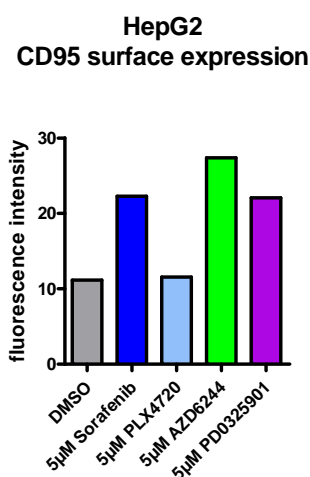


**Figure 24: MAPK inhibition increase CD95 expression in HepG2 cells.** HepG2 cells were treated with 5  $\mu$ M sorafenib, AZD6244, PD0325901, PLX4720 or DMSO for 48 h. Surface molecule expression of CD95 was measured by flow cytometry analysis using the FACS Calibur. Shown is one of three independent experiments.

To complete the picture of sorafenib-mediated apoptosis, the effects of sorafenib on the intrinsic apoptosis signaling pathway were also analyzed. In HCC, the anti-apoptotic molecules Mcl-1 and Bcl-xL are often overexpressed and play a pivotal role for resistance against apoptosis (Fleischer *et al.*, 2006; Sieghart *et al.*, 2006; Watanabe *et al.*, 2002; Watanabe *et al.*, 2004). Using western blot analysis, sorafenib was shown to effectively reduce Mcl-1 levels in HepG2 and Hep3B cells and Bcl-xL in Hep3B cells (Figure 25A). Western blot bands were also quantified by density measurements which nicely visualize Mcl-1 and Bcl-xL degradation (Figure 25B). Bcl-xL and Mcl-1 expression was also tested after U0126, AZD6244, PD0325901 and PLX4720 treatment in Hep3B cells (Figure 26). In contrast to sorafenib, U0126 and PLX4720 did not reduce Bcl-xL expression. However, treatment with AZD6244 reduced Bcl-xL after 24 h with a slight recovery after 72 and 96 h though still below the DMSO control. The MEK inhibitor PD0325901 decreased Bcl-xL levels substantially beginning at 24 h and a stable disappearance until 72 h.

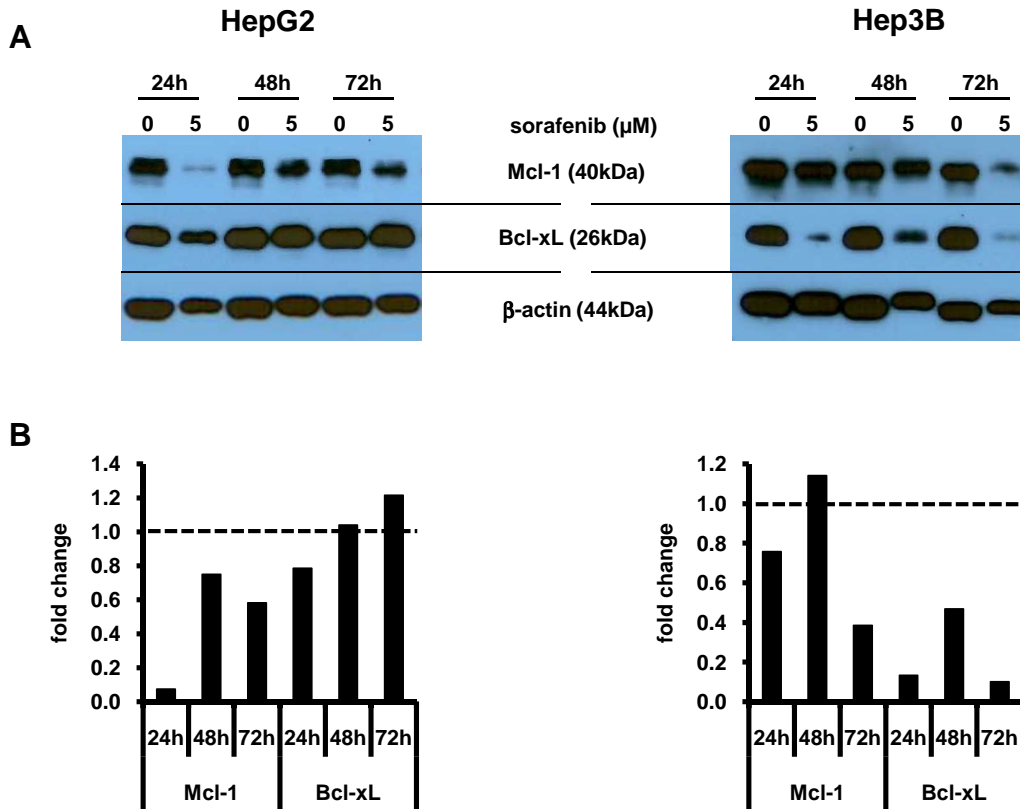


**Figure 25: Expression of Mcl-1 and Bcl-xL is reduced after sorafenib treatment.** HepG2 and Hep3B cells were treated with 5 μM sorafenib or DMSO control for 24, 48 and 72 h. (A) Western blot analysis shows a decrease in Mcl-1 and Bcl-xL in HepG2 and Hep3B cells. β-actin was used as a loading control. (B) Quantitative analysis of western blot analysis. Intensities were measured with Quantity One (BioRad), normalized to β-actin and treatment was compared to the DMSO control and depicted as fold change.

Compared to Bcl-xL, Mcl-1 regulation displayed different kinetics under MAPK inhibition with “waves” of enrichment and degradation (Figure 26). Mcl-1 levels in general increased over time in the DMSO treated cells as well as with PLX4720 and AZD6244, and U0126 but to a lesser extent. In contrast, weak Mcl-1 bands were detectable in PD0325901 treated cells suggesting that this MEK inhibitor impaired Mcl-1 stability more than the other MEK inhibitors. Only sorafenib seemed to reduce Mcl-1 expression in Hep3B cells, indicating that different MEK/B-Raf inhibitors can mediate opposite effects on Mcl-1. Thus these alterations are obviously independent of the MEK/ERK pathway and the small molecules exert different “side effects”.

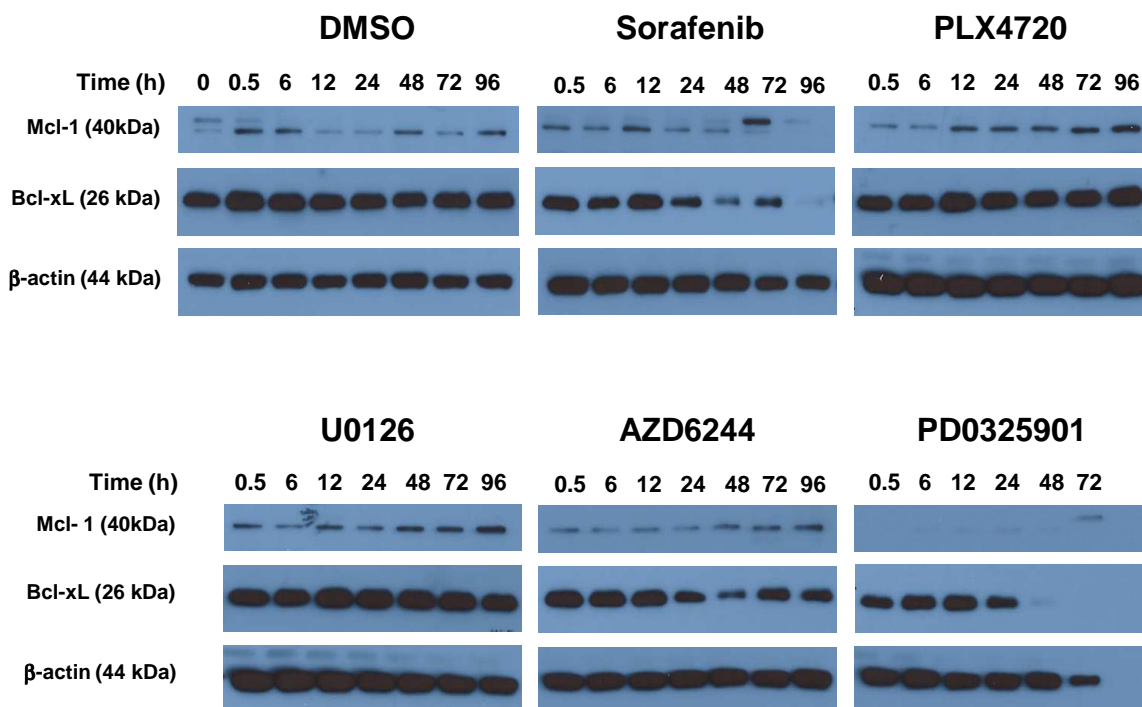


**Figure 26: Mcl-1 and Bcl-xL are partly modulated by MAPK inhibitors in Hep3B cells.** Hep3B cells were treated with 5  $\mu$ M sorafenib, PLX4720, U0126, AZD6244, PD0325901 or DMSO control for up to 96 h analyzed by western blot. Mcl-1 was decreased by sorafenib, but not by PLX4720, U0126 and AZD6244. Bcl-xL was mostly decreased by sorafenib, AZD6244 and PD0325901.  $\beta$ -actin was used as a loading control.

*In summary, several MAPK inhibitors induced apoptosis in liver tumor cells in a time- and dose dependent manner. However, remarkable differences were observed between cell lines as well as inhibitors. Therefore, it was of interest to address the nature of these differences in more detail. Looking at signal molecules involved in the regulation of apoptosis, it could be demonstrated that p53 and its family member p73 were partially stabilized and the anti-apoptotic isoforms  $\Delta$ Np63 and  $\Delta$ Np73 were decreased by the MAPK inhibitors, sorafenib in particular. The anti-apoptotic molecules Bcl-xL and Mcl-1 were partially downregulated by sorafenib and three MEK inhibitors, but not by the mutation-specific B-Raf<sup>V600E</sup> inhibitor PLX4720. Moreover, the three death receptors CD95, TRAIL-R2 and TNF-R1, which are important for the induction of apoptosis, were modulated by MAPK inhibition and, again, sorafenib differed from the other inhibitors, partly elevating death receptor surface expression which was in sharp contrast to PLX4720 and the MEK inhibitors. These observations point towards an ERK-independent side effect of certain MAPK inhibitors, sorafenib in particular, which may also account for the differences in clinical outcome of these drugs.*

## 5.2 Immunological Side Effects of MAPK Inhibitors

Many surface molecules, also those which are important for cell-cell interaction and recognition by the immune cells, were shown to be influenced by the MAPK and closely linked pathways. In terms of microenvironment, secretion of cytokines, chemokines and growth factors is also often regulated by these pathways. Therefore, I wanted to assess the effect of MAPK inhibition on cell surface expression of immunologically relevant molecules, immune cell recognition and cytokine/chemokine secretion. For this, the three cell lines HepG2, Hep3B and Huh-7 were treated with the MAPK inhibitors sorafenib, PLX4720, U0126, AZD6244 and PD0325901 and several parameters were addressed.

### 5.2.1 Characterization of hepatocellular carcinoma cell lines

In a first set of experiments, the surface molecule expression especially those which are important for recognition by T and NK cells were characterized in the three HCC cell lines. The expression of HLA class I and II, c-Met, ULBP1-4, MICA/B and adhesion molecules are shown in Figure 27 to Figure 29. All three cell lines showed strong expression of HLA class I. HepG2 cells were HLA-A2 and HLA-A24 positive, whereas Hep3B and Huh-7 are both negative for those HLA class I alleles. HepG2 and Hep3B cells were negative for the HLA class II molecule HLA-DR, but low expression was detected on Huh-7 cells.

In HCC, the c-Met receptor, which is an important receptor for the mitogen hepatocyte growth factor (HGF), is upregulated compared to non-malignant hepatocytes (Yang *et al.*, 2007). Accordingly, high c-Met expression was detectable in all three cell lines.

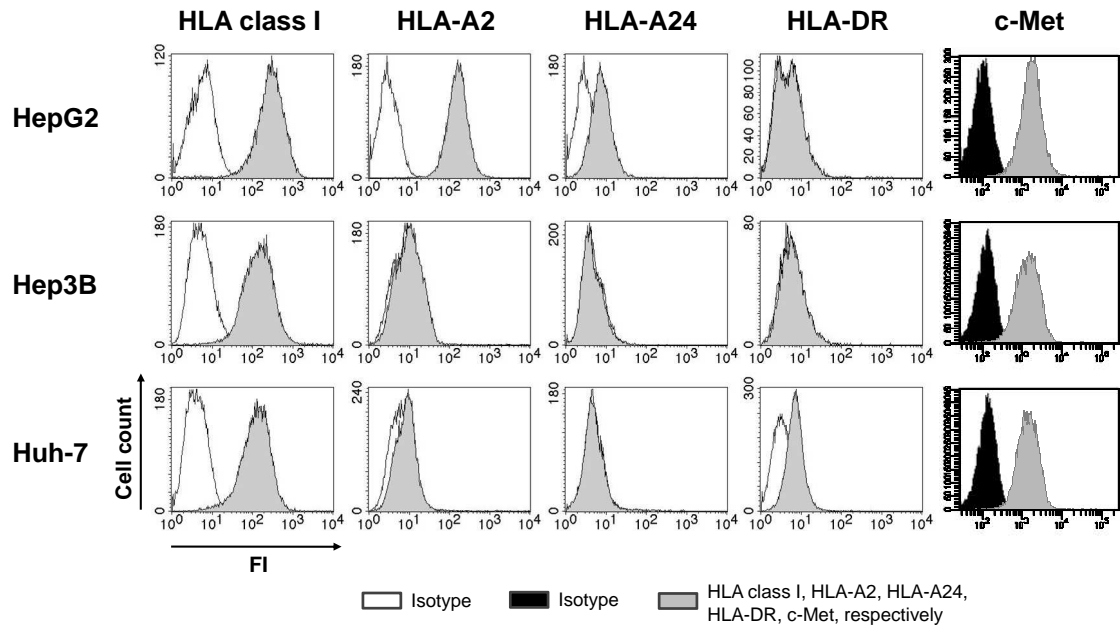


**Figure 27: HLA and c-Met surface molecule expression of HCC cells.** Untreated cells were characterized for the expression of HLA and c-Met using flow cytometry analysis. All three cell lines express HLA class I molecules (W6/32), whereas HepG2 are positive for HLA-A2 (HB54) and -A24 (0497HA). HLA-DR (L243) is only weakly expressed on Huh-7 cells. c-Met (95106) is expressed on all three cell lines. FI: fluorescence intensity measured in the PE and APC (c-Met) channel using the FACS Calibur and LSR II, respectively.

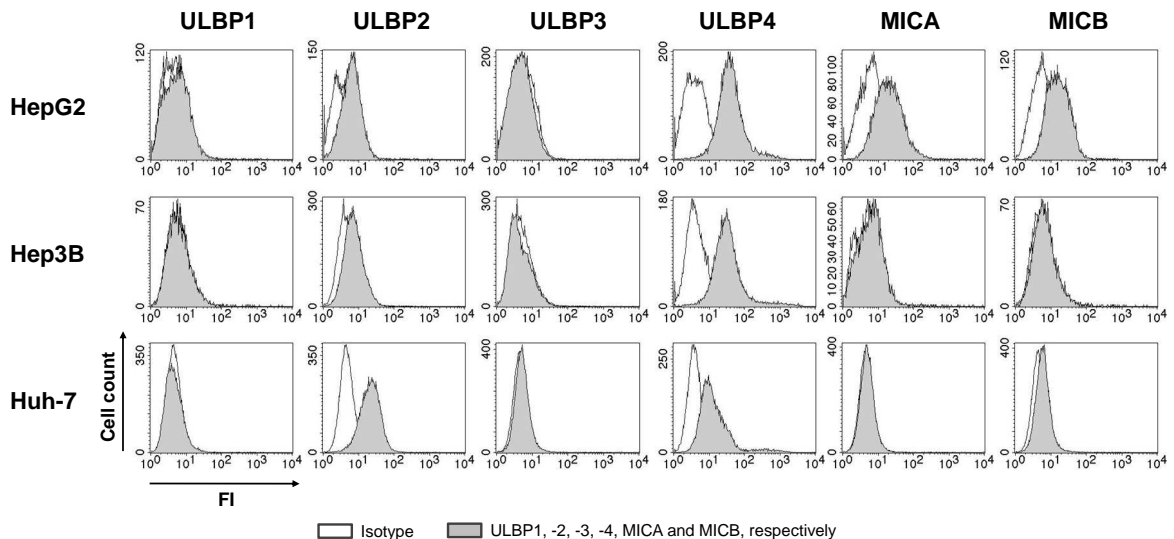


**Figure 28: NKG2D ligand surface molecule expression of HCC cells.** Cells were characterized for the expression of ULBP1-4 and MICA/B using flow cytometry analysis. All three cell lines express to a certain extent ULBP2 and ULBP4. HepG2 cells also express MICA and MICB whereas in Hep3B and Huh-7 showed only minimal to no expression. FI: fluorescence intensity measured in the PE channel using the FACS Calibur.

In addition to HLA, the expression of the ligands ULBP1-4 and MICA/B for the activating NK cell receptor NKG2D was analyzed (Figure 28). All three cell lines showed no expression of ULBP1 and -3, but low levels of ULBP2, whereas the expression on Huh-7 cells was low to medium. ULBP4 was expressed at low levels on Huh-7 cells and at intermediate levels on HepG2 and Hep3B cells. Because ULBP4 expression in liver carcinoma cell lines was recently described for HepG2 cells (Cao *et al.*, 2008), ULBP4 mRNA expression was confirmed in HepG2 cells with PCR (data not shown). MICA and MICB are only weakly expressed in HepG2 cells, while both molecules are absent in Hep3B and Huh-7 cells.

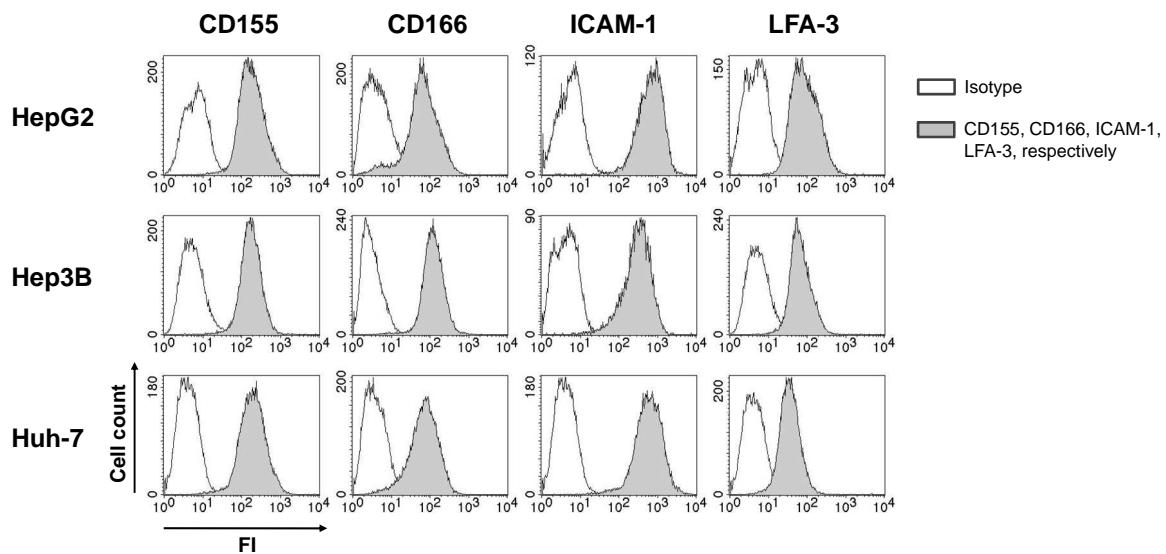


**Figure 29: CD155 (PVR) and adhesion molecule expression of HCC cells.** Cells were characterized for the expression of the adhesion molecules CD155, CD166, ICAM-1 and LFA-3 using flow cytometry analysis. All three cell lines express intermediate to high levels of these adhesion molecules. FI: fluorescence intensity measured in the PE channel using the FACS Calibur.

CD155 (PVR) is another important ligand for the recognition of many tumor cells by the immune cells. It is unique among NK receptor ligands because CD155 possesses its own signaling capacity and feeds into the MAPK pathway and probably others (Casado *et al.*, 2009; Chan *et al.*, 2010). CD155 binds to DNAM-1 (CD226) which is constitutively expressed on a majority of T and NK cells and mediates NK cell activation primarily. As shown in Figure 29, CD155 was strongly expressed on all three cell lines.

In general, adhesion molecules play an important role for the interaction between tumor cells and immune cells. Therefore, the cell lines were also analyzed for the expression of ICAM-1 (Inter-Cellular Adhesion Molecule 1), LFA-3 (Lymphocyte Function-associated Antigen 3) and CD166 (ALCAM). All three cell lines showed similar expression of these three adhesion molecules with high levels of ICAM-1 and intermediate levels of LFA-3 and CD166.

### 5.2.2 Influence of MAPK inhibition on HLA, NK receptor ligands and adhesion molecule expression

For the recognition of tumor cells by the most relevant effector cells, i.e. T and NK cells, surface molecule expression on the tumor cells play an important role. Tumor cells often change their surface molecules in order to escape immune recognition. To see whether MAPK modulation also influences cell surface molecules relevant for immune recognition, HLA class I, c-Met, the NKG2D ligands MICA/B, ULBP2 and ULBP4, the DNAM-1 ligand CD155 and the adhesion molecules CD166, LFA-3 and ICAM-1 were analyzed. HepG2, Hep3B and Huh-7 cells were treated for 48 h with 5  $\mu$ M sorafenib, U0126, AZD6244, PD0325901 and PLX4720 and surface molecules were measured using FACS analysis.

HLA class I was differently modulated by the MAPK inhibitors and between the cell lines (Figure 30). No alteration in the expression was observed with U0126 and PLX4720 for all three cell lines, AZD6244 in HepG2 and sorafenib in Hep3B cells. While in HepG2 cells HLA class I was weakly downregulated by sorafenib, it was upregulated in sorafenib treated Huh-7 cells. In contrast, HLA class I expression was increased by AZD6244 in Hep3B and Huh-7 cells and strongly elevated by PD0325901 in all three cell lines.

#### HLA class I

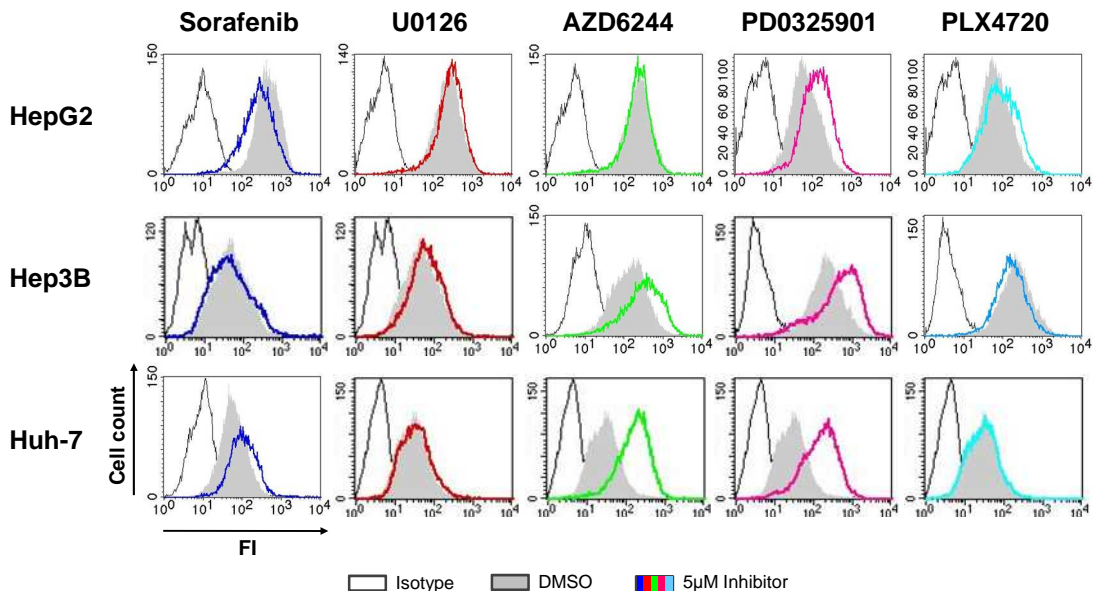


**Figure 30: HLA class I is altered by certain MAPK inhibitors in HCC cells.** Tumor cells were treated with 5  $\mu$ M sorafenib, U0126, AZD6244, PD0325901 or PLX4720 for 48 h and HLA class I expression (W6/32) was analyzed. FI: fluorescence intensity measured in the PE channel using the FACS Calibur.

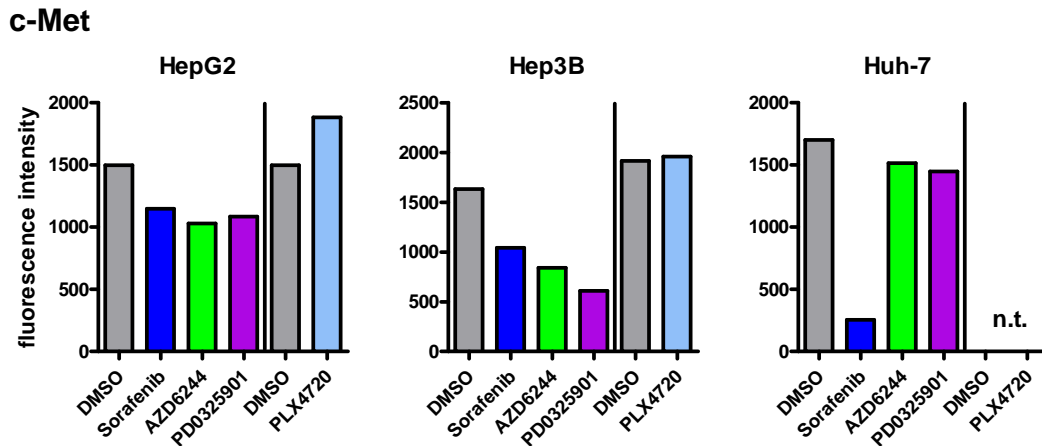


**Figure 31: c-Met surface molecule expression is altered by MAPK inhibitors in HCC cells.** Tumor cells were treated with 5  $\mu$ M sorafenib, U0126, AZD6244, PD0325901 or PLX4720 for 48 h and c-Met expression was analyzed. Fluorescence intensity measured in the APC channel using the LSR II.

The c-Met receptor is often overexpressed in HCC and correlates with a shorter 5-year survival (Ueki *et al.*, 1997). The high c-Met expression seen in HepG2, Hep3B and Huh-7 cells (5.2.1) was decreased by sorafenib, AZD6244 and PD0325901 (Figure 31) while PLX4720 treatment upregulated c-Met receptor in HepG2 but not in Hep3B cells (Huh-7 cells not tested).

The NKG2D ligand ULBP2 was not substantially altered with MAPK inhibitors (Figure 32). A small upregulation was observed with sorafenib, AZD6244 and PD0325901 in HepG2 and with AZD6244 in Huh-7 cells. In contrast, in Hep3B and Huh-7 cells sorafenib seemed to downregulate ULBP2. Also ULBP4 expression was modulated by the MAPK inhibitors. It was upregulated after sorafenib, AZD6244 and PD0325901 treatment in HepG2 and Hep3B cells, but not with PLX4720 (Huh-7 cells not tested). MICA and MICB were differently modulated after MAPK inhibitor treatment in all three cells lines (data not shown).

In addition to the NKG2D ligands, CD155, which binds to the activating receptor DNAM-1 on NK and T cells, was elevated in HepG2 and Huh-7 cells by sorafenib, AZD6244 and PD0325901, while in Huh-7, U0126 seemed to slightly increase CD155 expression (Figure 33).

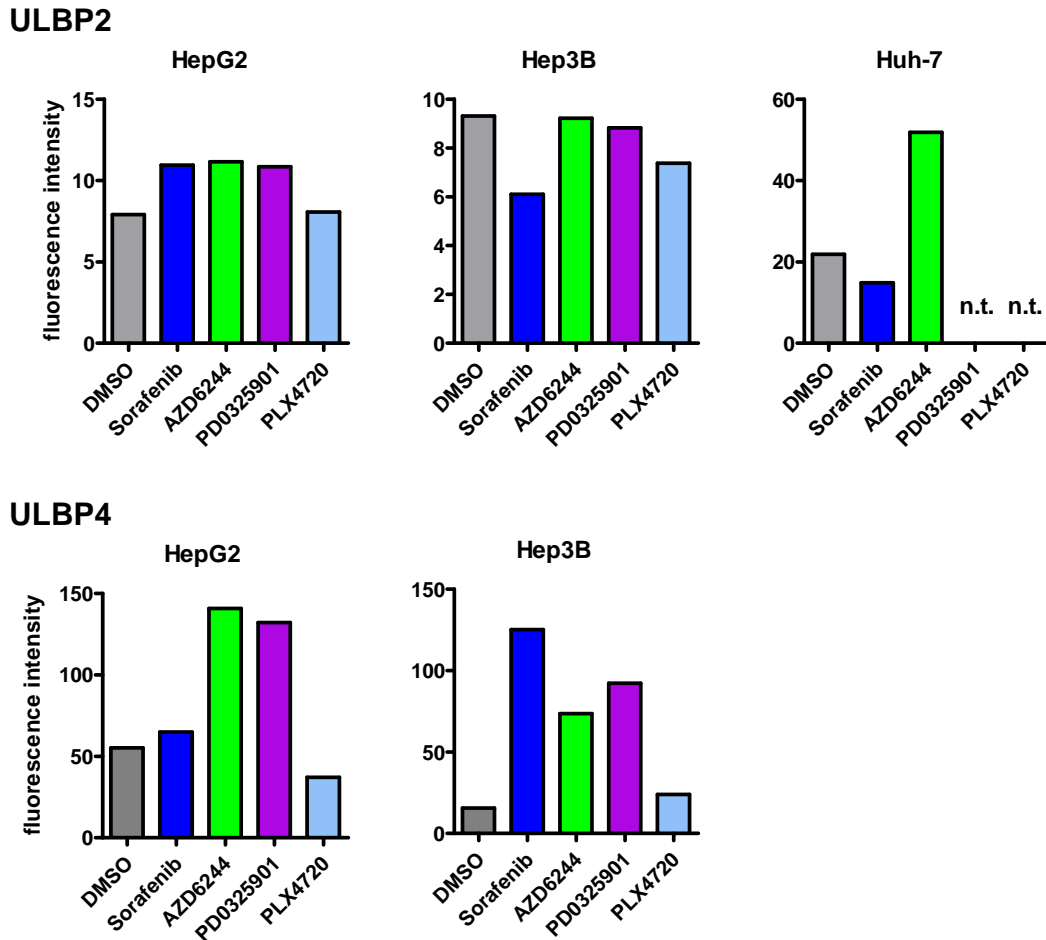


**Figure 32: ULBP2 and ULBP4 expression is altered by MAPK inhibitors in HCC cells.** Tumor cells were treated with 5  $\mu$ M sorafenib, U0126, AZD6244, PD0325901, PLX4720 or DMSO for 48 h and ULBP2 and ULBP4 expression was analyzed by flow cytometry. Fluorescence intensity measured in the PE channel using the FACS Calibur. Shown is one representative experiment.

For the recognition of tumor cells by NK and T cells, adhesion molecules play an important role. MAPK inhibition altered the expression of the adhesion molecules CD166, LFA-3 and ICAM-1. CD166 (ALCAM), which is a ligand for the CD6 receptor on NK and T cells, was upregulated by sorafenib, U0126, AZD6244 and PD0325901 in HepG2 and Huh-7 cells while no alteration was observed in Hep3B cells (Figure 34). PLX4720 did not influence CD166 expression indicating that CD166 is negatively regulated via MEK/ERK signaling. LFA-3 is differently regulated in the three cell lines (Figure 34). While sorafenib and the MEK inhibitors downregulated LFA-3 expression in HepG2 and Hep3B cells, they induced an upregulation of LFA-3 in Huh-7 cells. In NRas-mutant HepG2 cells, PLX4720 treatment led

to an increase in LFA-3 expression, indicating that LFA-3 is regulated via the MEK/ERK pathway.

Regulation of the adhesion molecule ICAM-1 was different between sorafenib and the MEK inhibitors (Figure 34). While the MEK inhibitors AZD6244 and PD0325901 induced a downmodulation of ICAM-1 in all three cell lines, sorafenib treatment led to a slight upregulation of ICAM-1. Again this demonstrates that opposite effects can occur during treatment with sorafenib and the MEK inhibitors. PLX4720 also induced an elevation of ICAM-1 on HepG2, but not on Hep3B cells.

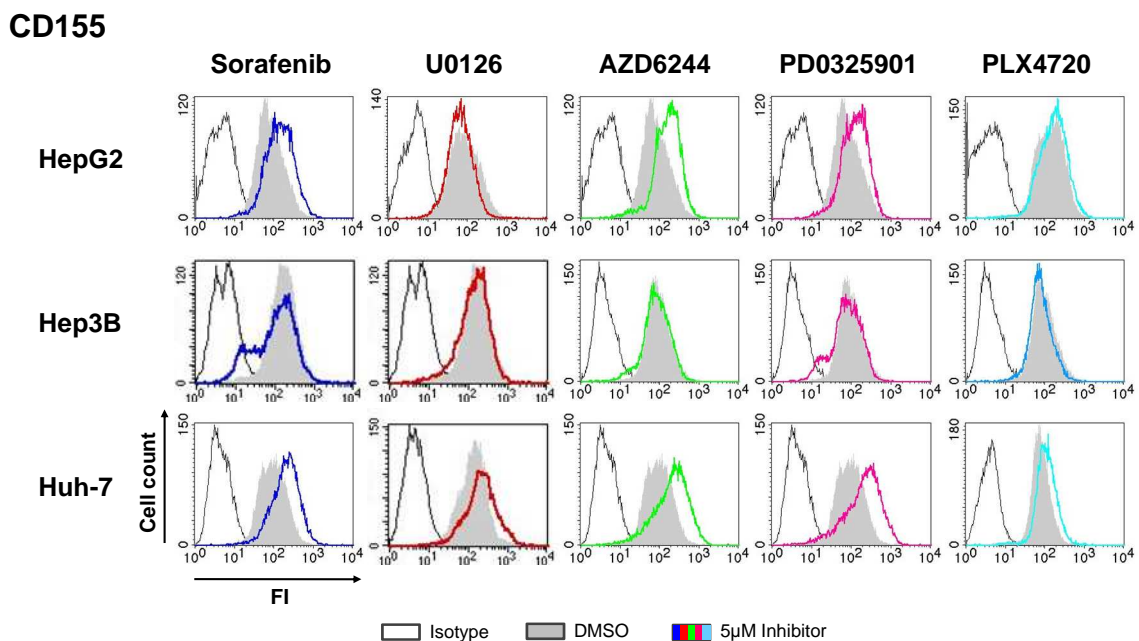


**Figure 33: CD155 expression is partly increased by sorafenib, AZD6244 and PD0325901 treatment.** Cells were characterized for the expression of CD155 after treatment with 5 µM sorafenib, U0126, AZD6244, PD0325901 and DMSO for 48 h using flow cytometry analysis. All three cell lines express CD155. Sorafenib, AZD6244 and PD0325901 partly increased CD155 expression on HepG2 and Huh-7 cells. FI: fluorescence intensity measured in the PE channel using the FACS Calibur.

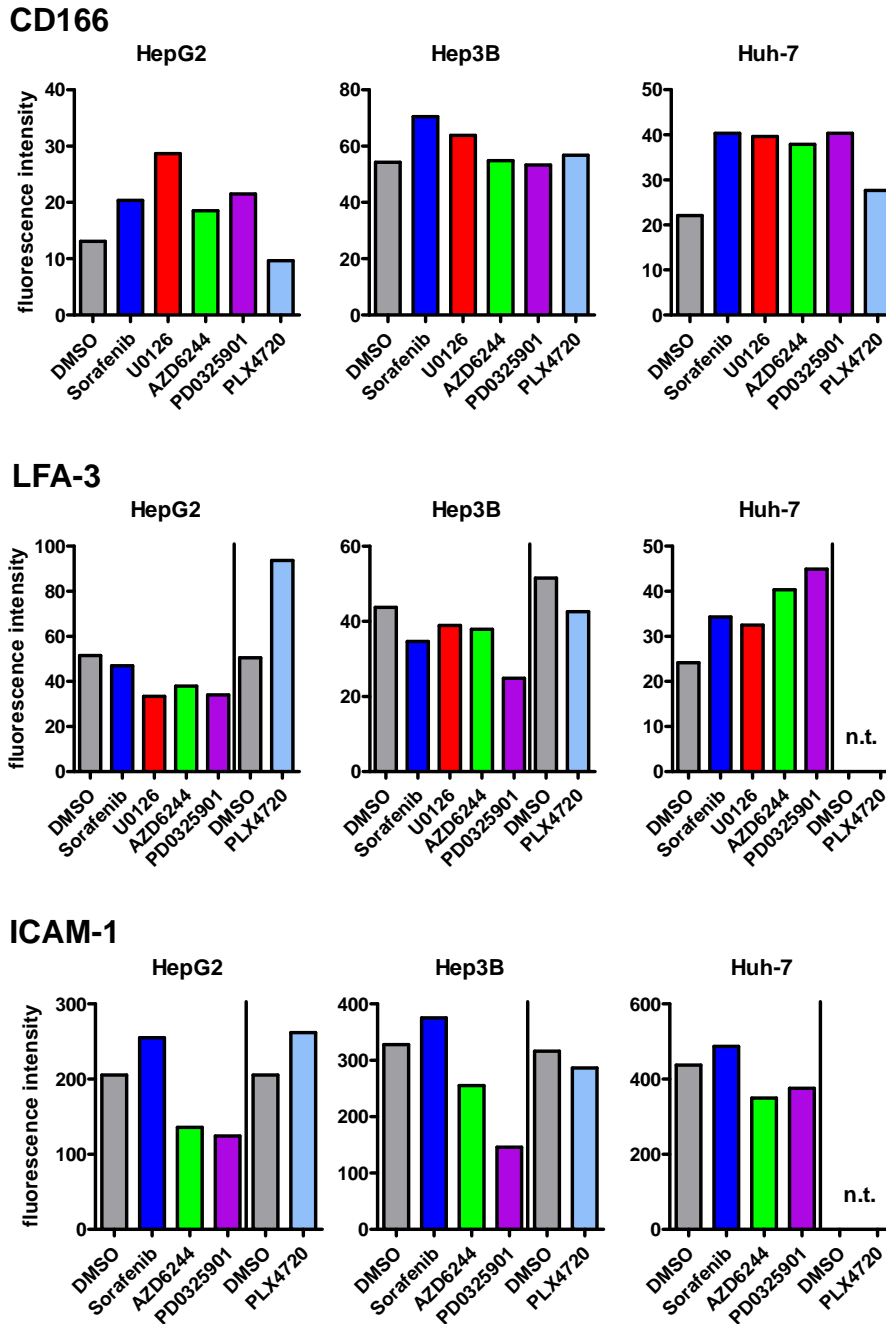


**Figure 34: Adhesion molecules are altered by MAPK inhibitors in HCC cells.** Tumor cells were treated with 5  $\mu$ M sorafenib, U0126, AZD6244, PD0325901, PLX4720 or DMSO for 48 h and CD166, LFA-3 and ICAM-1 expression was analyzed by flow cytometry. Fluorescence intensity measured in the PE channel using the FACS Calibur.

*In summary, expression of several surface molecules was modulated in HCC cell lines after MAPK inhibitor treatment. The repeated observation that surface expression of NKG2D ligands CD155 and HLA in particular, was not always modulated by these MAPK inhibitors*

*in the same direction strongly suggests that this modulation occurs independently from suppression of ERK phosphorylation shown in Figure 13. In consequence of this observation, one has to postulate side effects resulting from off-target effects of these substances that either are directly mediated at the protein expression and stabilization (CD155 for example) or indirectly via concerted expression machineries (HLA peptide /  $\beta$ 2m complex, for instance). Since most of these surface molecules are important for recognition by immune cells, like NK cells, it was of interest to know whether these changes in surface molecule expression also affect the recognition by NK cells.*

### **5.2.3 Consequences of altered HLA class I and NK ligand expression for NK cell degranulation**

As shown previously, MAPK inhibition modulated the surface molecule expression on tumor cell lines (5.2.2). Several of these surface molecules are important for the recognition and killing by NK cells. The crucial question is whether these alterations have a measurable impact on the recognition and lysis of the tumor cells by the immune effector cells. To try to answer this question, NK cell recognition of the three liver carcinoma cell lines with and without MAPK inhibition was analyzed.

As a measurement for the cytotoxic activity of NK cells, the CD107a degranulation assay was used. Cytotoxic NK cells, which were activated through receptor engagement by ligands on their target cells, release granula into the immunological synapse. During this process, the NK cell lysosomes, which contain perforin and granzyme, fuse with the plasma membrane and LAMP-1, also called CD107a, becomes temporarily exposed at the surface of activated NK cells. This molecule can be fixed and stained and is used as a marker for active, ongoing degranulation.

IL-2 pre-activated PBMCs from healthy donors were used as effector cells. Since degranulation assays are analyzed by flow cytometry, it was not necessary to isolate the NK cells, because NK cells can be defined as CD3<sup>-</sup> and CD56<sup>+</sup> cells and the presence of CD107a positive NK cells were quantified. As positive control, the HLA class I negative cell line K562 was used as target cells and for spontaneous degranulation, PBMCs were also cultured alone for 4 h.

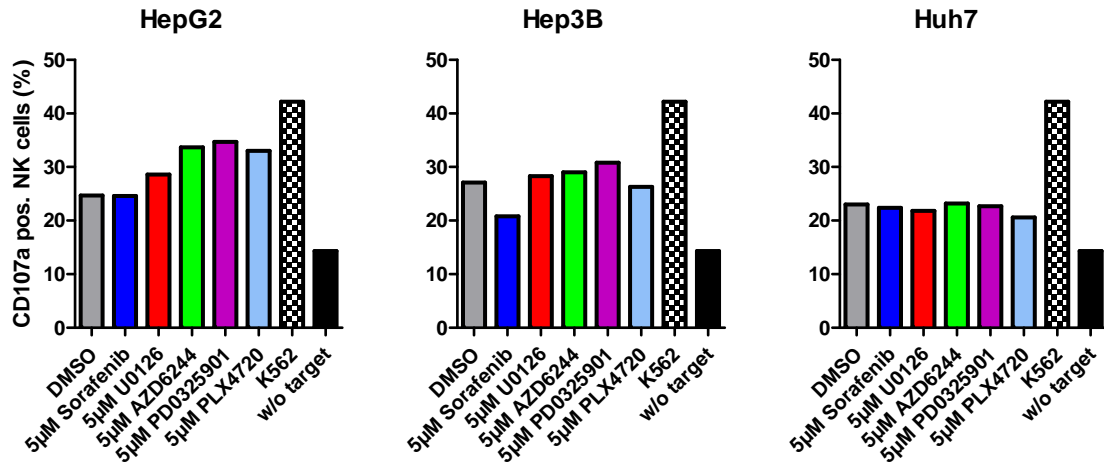


**Figure 35: Degranulation of NK cells against HCC cells treated with MAPK inhibitors.** HepG2, Hep3B and Huh-7 cells were treated with 5 µM MAPK inhibitors for 48 h and then used as target cells for NK cell degranulation. PBMCs were isolated from healthy donors, pretreated with IL-2 (500 U/ml) for 48 h and co-cultured with HepG2, Hep3B and Huh-7 cells for 4 h. The amount of CD107a on NK cells was measured. The HLA class I negative cell line K562 was used as positive control. Background degranulation was measured without the target cells. No significant modulation of NK cell degranulation was observed with MAPK inhibitors in HepG2 and Hep3B cells. Shown is one representative experiment.

Degranulation of NK cells by transient CD107a staining was tested with PBMCs of healthy donors against HepG2, Hep3B and Huh-7 cells treated with different MAPK inhibitors (Figure 35). First of all, it could be observed that NK cells degranulated, as indicated with a transient increased CD107a expression, when co-cultured for 4 h with the target cells. Degranulation of NK cells against HepG2, Hep3B and Huh-7 cells was similar indicating that pre-activated NK cells are able to recognize these HCC cells and become subsequently activated. Degranulation against K562 cells was even higher, because K562 cells are HLA class I-negative but express ligands for activating receptors like NKG2D. Although some modulation of HLA class I and NK ligand surface expression was detectable, MAPK inhibition of these tumor cells did not significantly alter degranulation of NK cells. In a donor-dependent way, MEK inhibitors and also the B-Raf<sup>V600E</sup> inhibitor PLX4720 slightly elevated degranulation in HepG2 cells, but not in Hep3B and Huh-7 cells. This observation that MAPK inhibitor treatment did not substantially alter NK cell activity against HCC cells nicely demonstrates the balance between activation and inhibition in NK cells.

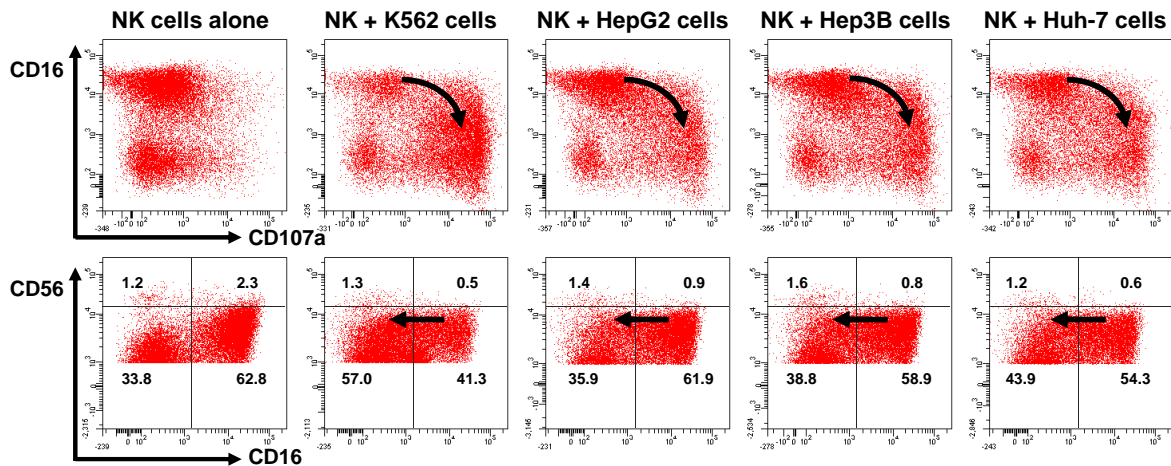


**Figure 36: Degranulating NK cells downregulate CD16 expression.** PBL were isolated from PBMCs of healthy donors, pretreated for 48h with IL-2 (500 U/ml) and co-cultured with HepG2, Hep3B and Huh-7 cells for 4 h. The expression of CD16, CD56 and the amount of CD107a was measured on gated NK cells. The HLA class I negative cell line K562 was used as positive control. CD16<sup>+</sup> degranulating NK cells downregulate the expression of CD16.

In addition to CD107a, NK cells were also stained for CD56 and CD16 in order to evaluate the NK subsets defined by these markers. We could previously show that CD56<sup>dim</sup> CD16<sup>+</sup> NK cells loose/downregulate CD16 expression in the process of degranulation, e.g. when co-cultured with K562 cells (Dissertation M. Braun 2008). To test whether this is also the case during co-cultivation of NK cells with HCC cells, CD16 expression was analyzed in parallel with the degranulation assays (Figure 36). As expected degranulating (CD107a positive) NK cells at the same time decrease to some extent their levels of CD16 following exposure to all three cell lines HepG2, Hep3B and Huh-7, although to a lesser extend compared to co-culture with K562 cells. This difference nicely shows the correlation between CD107a degranulation and CD16 loss. Moreover, we could see that degranulated cells are members of the CD56<sup>dim</sup> NK cell population.

To analyze long-term effects of the co-culture, HCC target cells and isolated IL-2 activated NK cells were cultured together for 48 h (Figure 37). This long-term co-culture of NK cells alone alters already their phenotype regarding CD56 and CD16 expression. Although the culture started with highly enriched NK cells (d0), after 2 days most of the NK cells became CD56 and CD16 negative indicating that IL-2 culture activated NK cells and, thereby, modulates CD16 and CD56 surface expression. In contrast co-cultivation with HepG2 and Hep3B cells led to an increase of the CD56<sup>dim/bright</sup> CD16<sup>-</sup> population. A larger proportion of CD56<sup>dim</sup> CD16<sup>+</sup> NK cells remained in this setting. Co-culture with Huh-7 cells resulted in an even higher representation of CD16<sup>+</sup> NK cells suggesting that the three HCC lines are

recognized by different NK subsets. Co-culture with K562 cells also resulted in a mixture of NK cells with a higher percentage of CD16<sup>+</sup> NK cells. Thus, contact with HCC lines shifted the NK cell repertoire towards CD16<sup>+</sup> as well as CD56<sup>bright</sup> NK cells. This composition is closely related to the intrahepatic NK population (5.2.4).

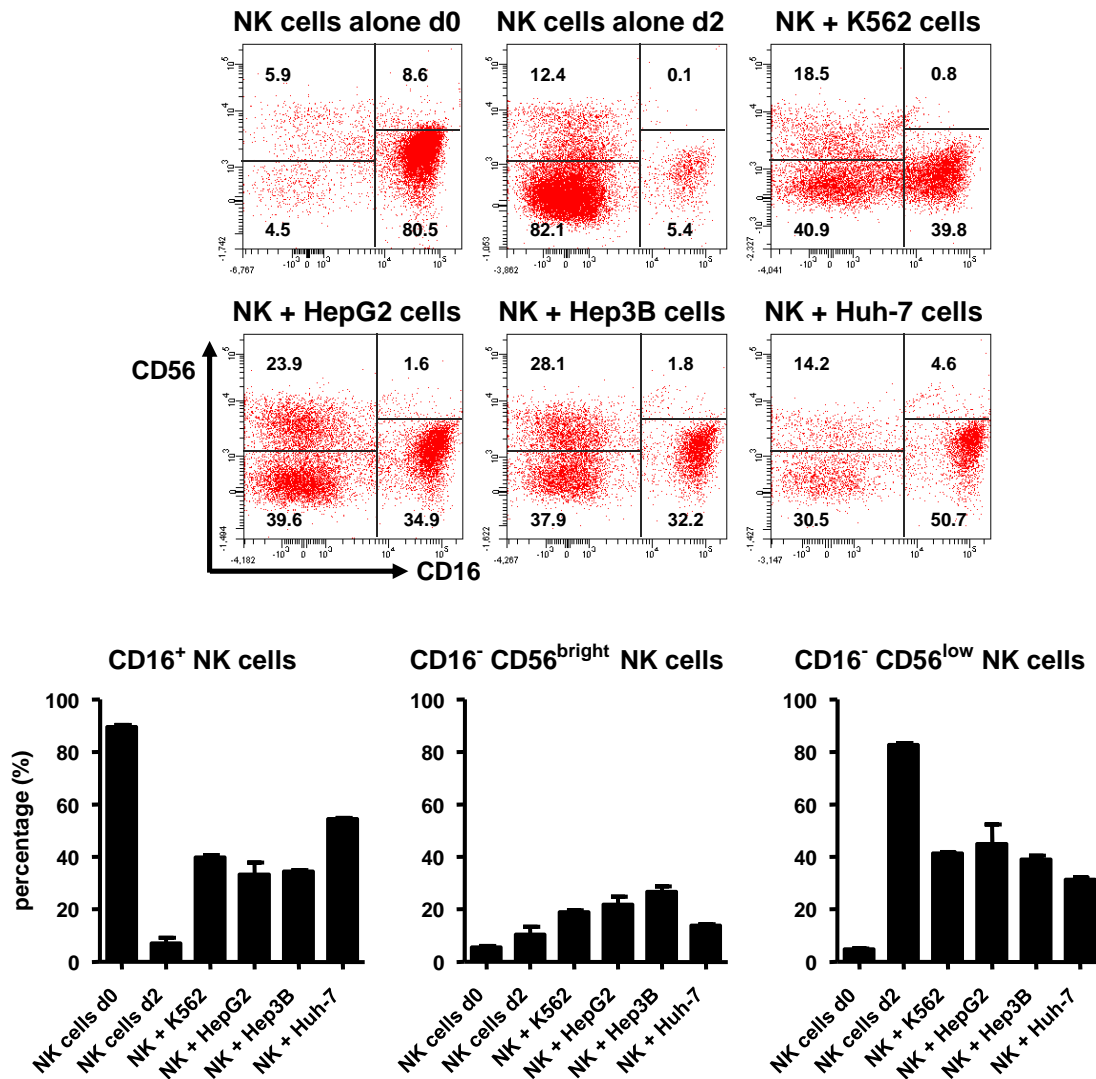


**Figure 37: CD16 and CD56 phenotype of NK cells is altered after long-term co-cultivation with HCC cells.** NK cells were isolated from PBMCs of healthy donors, co-cultured with HepG2, Hep3B, Huh-7 and K562 cells for 48 h with 100U/ml IL-2. The expression of CD16, CD56 on NK cells was measured. After day 2, NK cells lose CD16 and CD56 expression when cultivated alone. In the presence of tumor cells the CD56<sup>dim</sup> CD16<sup>-</sup> population gets enriched with co-cultivation with HepG2 and Hep3B cells. n=2

*In summary, treatment of HCC cells with MAPK inhibitors resulted in modulation of HLA and NK ligand surface expression. However, this alteration did not significantly impinge on NK cell degranulation. This minimal influence on degranulation can be explained by the*

balance between activating and inhibitory receptors on NK cells which results from slight modulations of ligand expression due to the integration of the different signals. Degranulation also altered the phenotype of NK cells, i.e. degranulating  $CD56^{dim} CD16^+$  NK cell and to some extent down-modulate  $CD16$  surface expression following co-culture with HCC cells. However, long-term culture of NK cells with HCC cells changed the  $CD56 CD16$  phenotype towards the maintenance of  $CD16^+$  NK cells and  $CD56^{bright}$  NK cells. It would be interesting to see whether the NK cell phenotype is also altered in HCC tumor tissue. Therefore, the hepatic NK cell compartment was investigated in detail. The next question was whether MAPK inhibitors induce the tumor cells to change their chemokine secretion pattern, which then in turn might influence the attraction of NK cell subsets towards the tumor tissue.

#### 5.2.4 Lymphocytes in normal, cirrhotic and HCC liver

Infiltration of immune cells into the tumor is dependent on chemokine and cytokine milieu. In chapter 5.3.1, it will be described in detail that the chemokine milieu differs significantly in healthy vs. cirrhotic and HCC tissue. The liver has also been described as a “lymphoid organ”, having important functions in innate and adaptive immunity (Crispe, 2009; Parker and Picut, 2005).  $CD8^+$  T cells, NK cells and NKT cells are enriched in the liver compared to other organs (Morsy *et al.*, 2005). Here, the composition of NK and T cells was investigated exemplarily in normal, cirrhotic and HCC tissue in comparison to peripheral blood lymphocytes. As shown in 5.2.3, co-culture of peripheral NK cells with HCC lines reserved the composition significantly. As expected, the proportion of NK and T cells are modulated in liver tissue.

<b>A</b>			<b>B</b>		
<b>PBL</b>	<b>NK cells</b>	<b>T cells</b>	<b>PBL</b>	<b>CD4 T cells</b>	<b>CD8 T cells</b>
<b>Healthy</b>	10.6 ± 7.0	68.9 ± 6.2	<b>Healthy</b>	60.6 ± 2.3	39.4 ± 2.3
<b>HCC</b>	17.7 ± 9.2	42.9 ± 11.9	<b>HCC</b>	71.5 ± 16.5	28.5 ± 16.5

**Table 15: Proportion of peripheral blood NK and T cells in HCC.** Lymphocytes were isolated from blood of healthy donors and patients with HCC and analyzed by flow cytometry. (A) Proportions of NK ( $CD3^+$ ,  $CD56^+$ ) and T ( $CD3^+$ ) cells were determined. (B) Gating on T cells, the expression of  $CD4^+$  T helper cells vs.  $CD8^+$  cytotoxic T cells was calculated.  $n=3 \pm SD$ .

In sharp contrast, the distribution of NK cells in liver tissue differed substantially to peripheral blood. The healthy liver was enriched in NK cells and made up to about 30% of hepatic lymphocytes (Table 16). As depicted in Figure 38, NK cell phenotype regarding CD56 and CD16 expression was significantly altered. The difference was due to a higher proportion of CD56<sup>bright</sup> CD16<sup>-</sup> NK cells and reduced CD56<sup>dim</sup> CD16<sup>+</sup> hepatic NK cells compared to PBMC. The NK cell number and phenotype changed even more in cirrhotic liver, non-malignant liver tissue of HCC patients and HCC tumor tissue (Figure 38). In cirrhosis, CD56<sup>bright</sup> NK cells were drastically increased with even less CD16<sup>+</sup> NK cells, but the total NK cell proportion was slightly reduced. Remarkably, NK cells were virtually absent in HCC tumor tissue. However, in adjacent non-malignant tissue, the proportion of NK cell was highly increased. The majority of these NK cells displayed a CD56<sup>dim</sup>/CD56<sup>bright</sup> CD16<sup>-</sup> phenotype.

We have recently shown that the scavenger receptor CD6 is differentially expressed by a subpopulation of peripheral CD56<sup>dim</sup> but not CD56<sup>bright</sup> NK cells (Braun *et al.*, 2010). In the periphery most CD56<sup>dim</sup> CD16<sup>+</sup> NK cells also express CD6. However, in liver tissue, regardless of a malignant, cirrhotic or healthy origin, the NK cell population expressing CD6 was strongly reduced compared with the blood counterparts and the most prominent reduction was observed in the cirrhotic tissue (Figure 38).

The proportion of T cells was also changed in the liver tissue compared to PBMC of healthy individual and patients (Table 16). In the normal liver, T cells made up about 40% of liver lymphocytes. In cirrhotic and tumor tissue, this proportion was increased to about 50% and 80%, respectively. This shows that in the tumor tissue, T cells are still present while NK cells are absent although the mechanism for the disappearance of NK cells still remains elusive.

A			B			
Tissue	NK cells	T cells	CD4 T cells	CD8 T cells	CD4 <sup>+</sup> CD8 <sup>-</sup> T cells	CD4 <sup>+</sup> CD8 <sup>+</sup> T cells
Normal Liver	31.5	38.5	39.9	46.9	12.7	0.5
Cirrhosis	27.1	52.8	31.7	59.4	8.2	0.6
HCC Normal	55.9	25.6	53.4	33.8	9.1	3.7
HCC Tumor	1.5	83.4	20.5	75.9	1.7	1.9

**Table 16: Proportion of hepatic NK and T cells in healthy, cirrhotic and tumor tissue.**

Lymphocytes were isolated from healthy liver, cirrhotic liver, healthy party of HCC liver, HCC tumor liver tissue. Lymphocytes were analyzed by flow cytometry and gated on (A) NK cells (CD3<sup>-</sup>, CD56<sup>+</sup>) and T cells (CD3<sup>+</sup>), and (B) T cells were further analyzed for the expression of CD4 and CD8. n=1

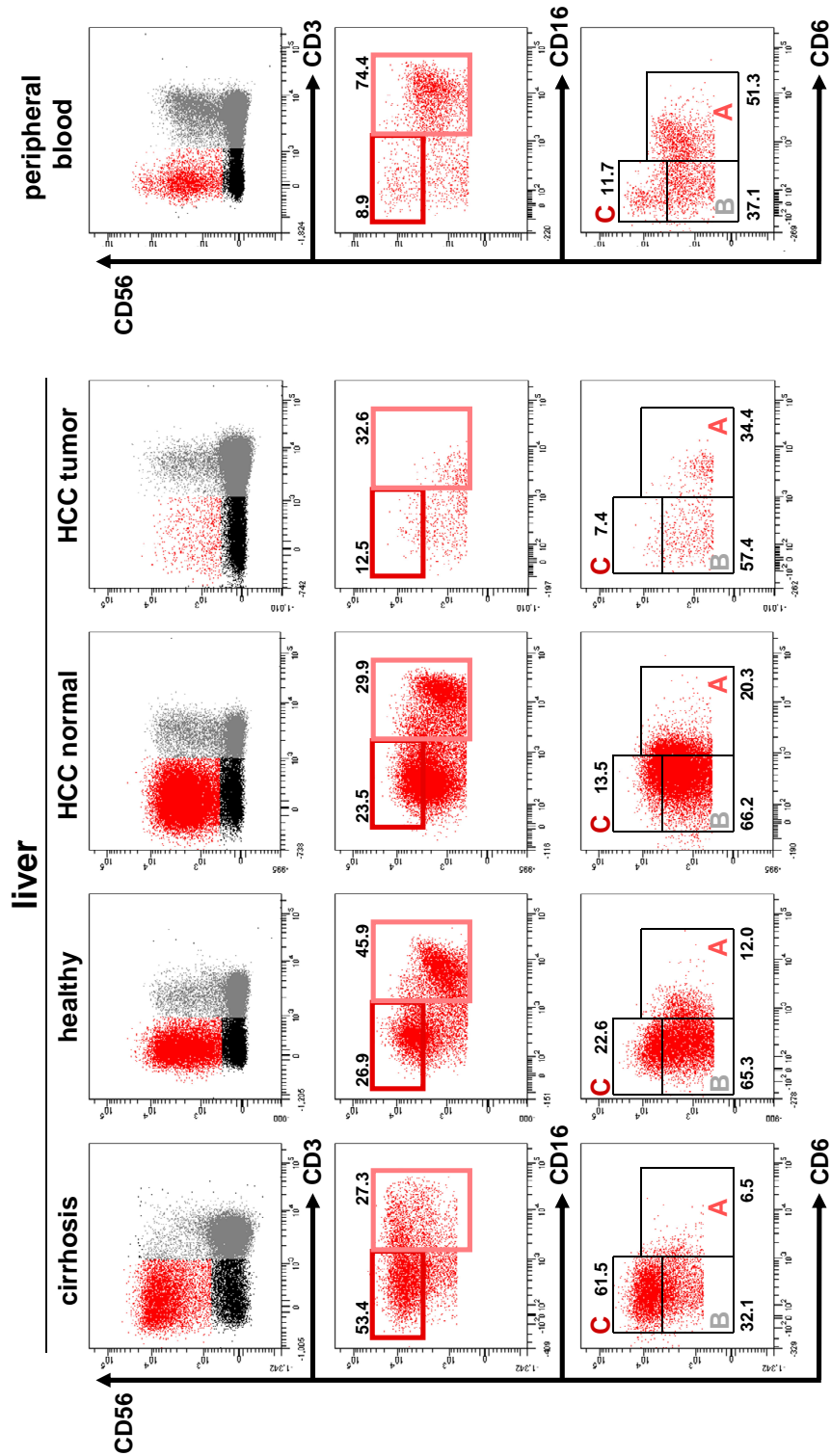


**Figure 38: Hepatic NK cells differ to peripheral NK cells regarding CD16 and CD6 expression.** Lymphocytes were isolated from healthy liver, cirrhotic liver, healthy party of HCC liver, HCC tumor liver tissue and from peripheral blood of a healthy donor. Lymphocytes were analyzed by flow cytometry: CD16 and CD6 expression were determined on gated NK cells (CD3<sup>+</sup>, CD56<sup>+</sup>). In the liver, more NK cells are CD16<sup>-</sup> and CD6<sup>-</sup> compared to peripheral NK cells. In cirrhotic liver an increase in CD56<sup>bright</sup> NK cells was detected and in HCC tumor most NK cells are lost.

The 2:1 ratio of CD4<sup>+</sup> T helper cells to CD8<sup>+</sup> cytotoxic T cells, which was observed in peripheral blood, was nearly switched to a 1:2 ratio in normal liver tissue (Figure 39). Even more CD8<sup>+</sup> T cells were found in cirrhosis and in HCC tumor tissue. The adjacent healthy HCC tissue contained more CD4<sup>+</sup> than CD8<sup>+</sup> T cells.

This reversed distribution of CD4<sup>+</sup> vs. CD8<sup>+</sup> T cells in healthy as well as in cirrhotic and malignant liver tissue is rather unique and may result from a special hepatic microenvironment which is described in the section 5.3.1.

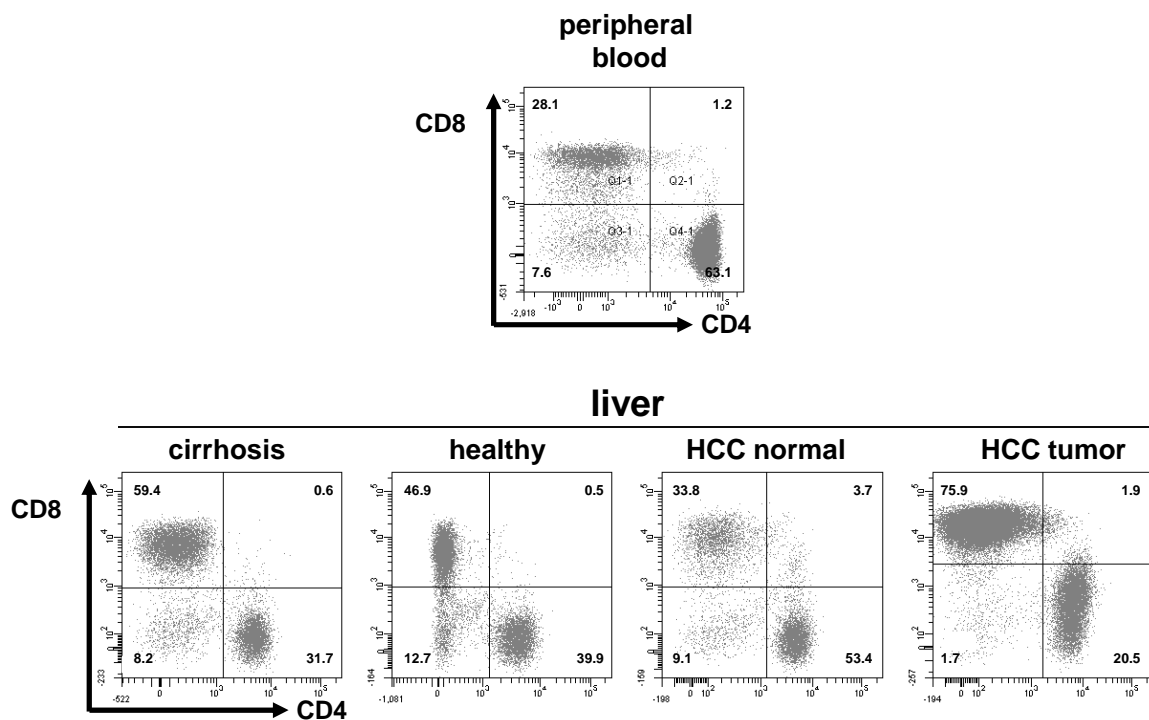


**Figure 39: Hepatic T cells differ to peripheral T cells regarding the ratio between CD4<sup>+</sup> and CD8<sup>+</sup> T cells.** Lymphocytes were isolated from healthy, cirrhotic, healthy part of HCC liver, HCC tumor liver tissue and from peripheral blood. Lymphocytes were analyzed by flow cytometry. Proportion of CD8 and CD4 expression on gated T cells (CD3<sup>+</sup>) were determined. Compared to the CD4 to CD8 ratio of 2:1 in peripheral blood, CD8<sup>+</sup> T cells are increased in the liver.

*In summary, the proportion and the phenotype of hepatic NK and T cells were changed compared to the blood counterparts. Liver NK cells showed a reduced expression of CD16 and CD6. The ratio of CD4<sup>+</sup> to CD8<sup>+</sup> T cells was almost switched from 2:1 in peripheral blood to 1:2 in liver tissue. In cirrhotic liver tissue, NK cells showed an increased activated (CD56<sup>bright</sup>) phenotype and CD8<sup>+</sup> T cells were enriched. In HCC tumor tissue, NK cells were absent and mostly CD8<sup>+</sup> T cells were present. It would be of great interest to see whether these compositions and phenotypes would change in HCC patients treated with sorafenib or other MAPK inhibitors.*

## 5.2.5 MAPK inhibitors modulate chemokine and growth factor secretion in HCC cells

In the tumor microenvironment many different cytokines, chemokines and growth factors are secreted by a variety of immune and parenchymal, endothelial cells. The release of the chemokines by the tumor cells can lead to a “reprogramming” of the tumor surrounding often favoring a pro-angiogenic and anti-immune situation. Infiltration of immune cells into a tumor is dependent on the chemokine and cytokine milieu. Therefore, we hypothesized that modulation of the tumor cells by small molecules does not only change the tumor cell activity itself, but also has an influence on the microenvironment. By using the three cell lines HepG2, Hep3B and Huh-7, the different chemokines and growth factors produced by these cells and the impact of the different MAPK inhibitors were analyzed. For this analysis, cells were cultured for 48 h with and without MAPK inhibitors. The multiplex method was used to simultaneously quantify up to 50 different cytokines, chemokines and growth factors. For the detailed analysis of the secretion profile by the HCC cell lines, a selection of chemokines and growth factors was addressed for the effects of MAPK inhibition (Figure 40 - Figure 42).

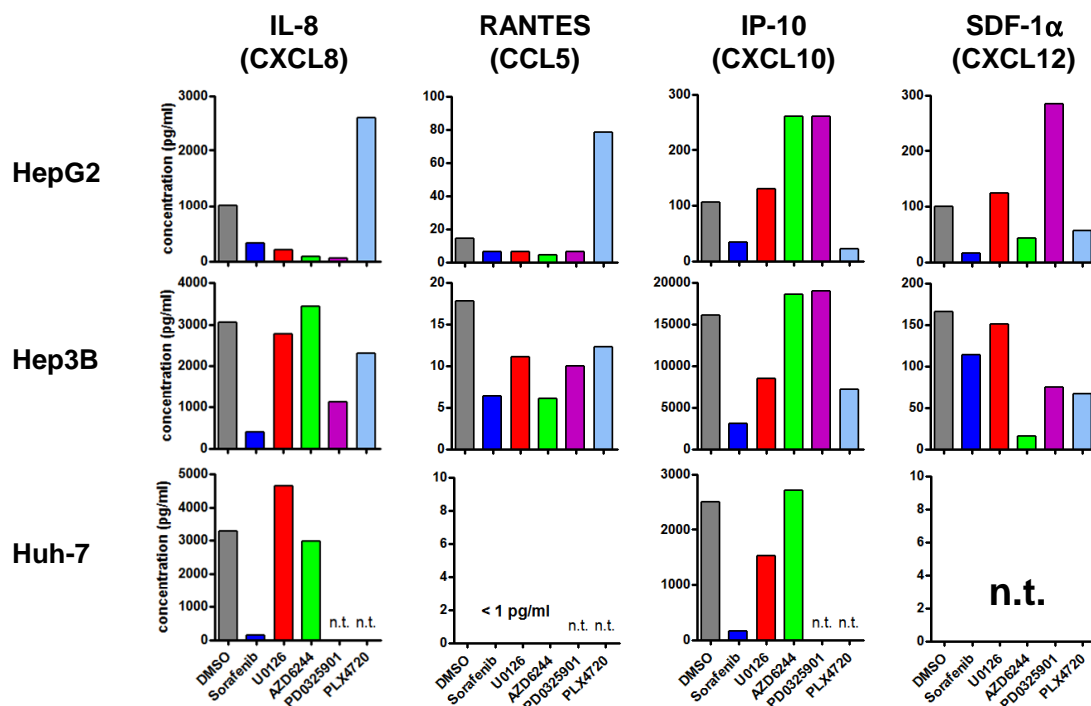


**Figure 40: Secretion of chemokines is modulated by MAPK inhibitors.** HepG2, Hep3B and Huh-7 cells were treated with 5  $\mu$ M MAPK inhibitors or DMSO control for 48 h and supernatant was analyzed for chemokines.

The three cell lines secreted a variety of different chemokines and growth factors. High amounts of the chemokines IL-8 (CXCL8), IP-10 (CXCL10), the angiogenic factor VEGF, the growth factor TGF $\beta$  and the soluble adhesion molecule ICAM-1 were secreted. The chemokine SDF-1 $\alpha$  (CXCL12), M-CSF, the growth factor SCGF and MIF were released to a medium level. The chemokine RANTES (CCL5) and the growth factor HGF, as well as soluble IL-1 receptor antagonist (IL-1RA) and adhesion molecule VCAM-1 were only secreted to a small amount. Substantial differences in the amount of the factors were seen between the cell lines. For example, the highest secretion of CXCL10 was detected for Hep3B cells, but 8-fold less CXCL10 was secreted in Huh-7 cells and another 20-fold less in HepG2 cells. In the supernatant of Huh-7 cells, no CCL5, M-CSF and IL-1RA were detected.

The chemokines CXCL8, CCL5 and CXCL10 were differently modulated by the MAPK inhibitors and differences were also seen between the three cell lines (Figure 40). Sorafenib reduced the secretion of these three chemokines in all cell lines. In HepG2 cells, the MEK inhibitors U0126, AZD6244 and PD0325901 inhibited secretion of CXCL8 and CCL5, but not CXCL10, where a substantial increase was detected. In Hep3B cells, PD0325901 reduced CXCL8 secretion, all MEK inhibitors reduced CCL5 secretion. Interestingly, U0126 reduced, but AZD6244 and PD0325901 increased CXCL10 secretion, suggesting that even different MEK inhibitors can have opposite effects on CXCL10 secretion. In Huh-7 cells, U0126 but not AZD6244 treatment led to a higher amount of CXCL8 while CXCL10 secretion was not affected by AZD6244 but reduced by U0126.

Most remarkably, the increase in MEK and ERK phosphorylation by PLX4720 was reflected by chemokine secretion of CXCL8 and CCL5 suggesting that these two chemokines are directly influenced by the NRas mutation. In contrast, a downregulation of CXCL10 was observed in HepG2 cells, and PLX4720 generally reduced all three chemokines in Hep3B cells.

The patterns for the growth factors VEGF and M-CSF in HepG2 cells after treatment were similar to CXCL8 and CCL5 (Figure 41). Sorafenib, U0126, AZD6244 and PD0325901 reduced and PLX4720 increased secretion again indicating a strong direct regulation by the oncogene-driven MAPK pathway. Although sorafenib and PLX4720 had opposite effects on the phosphorylation of ERK, both inhibitors increased secretion of the c-kit ligand SCGF (Figure 41), indicating that this growth factor is not directly regulated by the MAPK pathway.

In Hep3B cells, only sorafenib could inhibit VEGF and M-CSF secretion, while the other inhibitors had only minor effects. SCGF secretion was only weakly influenced by the inhibitors. In Huh-7 cells, the growth factor VEGF is reduced by sorafenib and AZD6244, but not by U0126 treatment while sorafenib increased secretion of SCGF. In all three cell lines TGF $\beta$  secretion is slightly reduced with sorafenib, U0126 and AZD6244 (PD0325901 and PLX4720 not tested), indicating that TGF $\beta$  secretion is influenced but not dependent on the MAPK pathway (Figure 41).

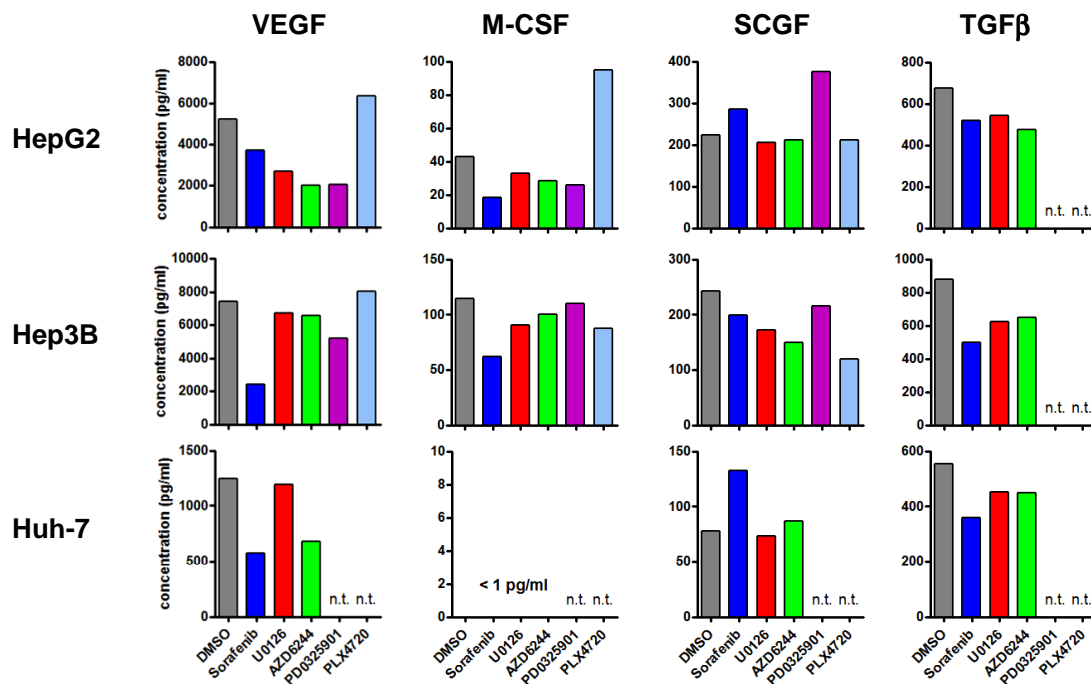


**Figure 41: Secretion of growth factors is modulated by MAPK inhibitors.** HepG2, Hep3B and Huh-7 cells were treated with 5  $\mu$ M MAPK inhibitors or DMSO control for 48 h and supernatant was analyzed for growth factors.

The three cell lines also differed substantially in the secretion of IL-1RA with the highest amount secreted by HepG2 and no detection in Huh-7 cells (Figure 42). While sorafenib, U0126, AZD6244 and PD0325901 reduced IL-1RA secretion in HepG2 cells, PLX4720 led to an increase. In Hep3B cells, the weak IL-1RA secretion was slightly enhanced by U0126 and AZD6244 with the exception of PLX4720. Soluble ICAM-1 was strongly decreased by MAPK inhibitors across the cells with the exception of PLX4720 in HepG2 cells.

In strong contrast to chemokine and growth factors, an increase in secretion by the four inhibitors was only seen for MIF (Figure 42). In HepG2 cells, U0126, AZD6244 and PD0325901 induced MIF even stronger than sorafenib. In Hep3B cells, PD0325901 treatment

led to the highest raise in MIF. In contrast to HepG2 and Hep3B, sorafenib induced a strong increase in the secretion of MIF in Huh-7 cells whereas U0126 and AZD6244 only raised MIF concentration to a slight amount (PD0325901 was not tested). Since MIF has a number of tumor protective functions, this upregulation may be associated with an acquisition of severe resistance mechanisms by the tumor cells.

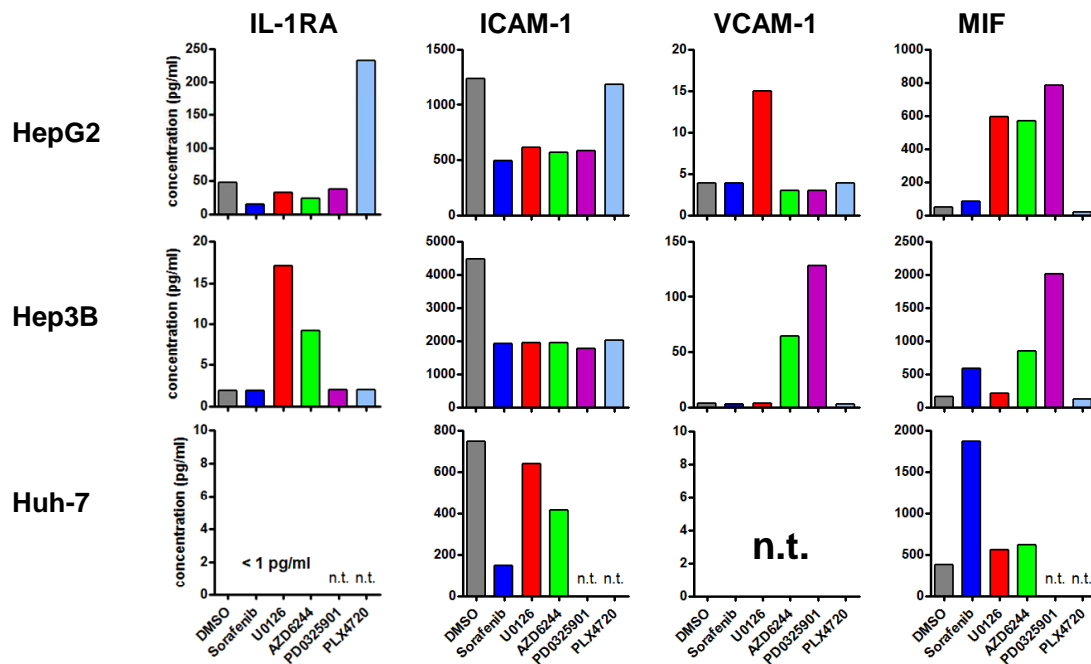


**Figure 42: Secretion of soluble adhesion molecules is modulated by MAPK inhibitors.** HepG2, Hep3B and Huh-7 cells were treated with 5  $\mu$ M MAPK inhibitors or DMSO control for 48 h and supernatant was analyzed for soluble adhesion molecules and other factors such as soluble receptors (IL-1RA).

In addition to NKG2D ligand surface expression, soluble variants were also addressed. These soluble MICA (sMICA) and MICB (sMICB) are formed by metalloprotease-mediated cleavage. Soluble MICB is increased in sera of cancer patients and are postulated to impair anti-tumor immune responses by downregulating expression of NKG2D on T and NK cells (Tamaki *et al.*, 2010). Soluble MICA was not detected for HepG2, Hep3B and Huh-7 cells, probably due to alleles that are not recognized by the used ELISA. Soluble MICB was measured, with higher concentrations in HepG2 and no detection in Huh-7 cells (Figure 43). Treatment with 5 $\mu$ M MAPK inhibitors almost completely inhibited sMICB secretion in HepG2, but in Hep3B cells only sorafenib showed strong reduction of sMICB. This differential effect of MAPK inhibitors between HepG2 and Hep3B cells may be linked to a different dependency of metalloproteases (MMPs) by the MEK/ERK pathway.

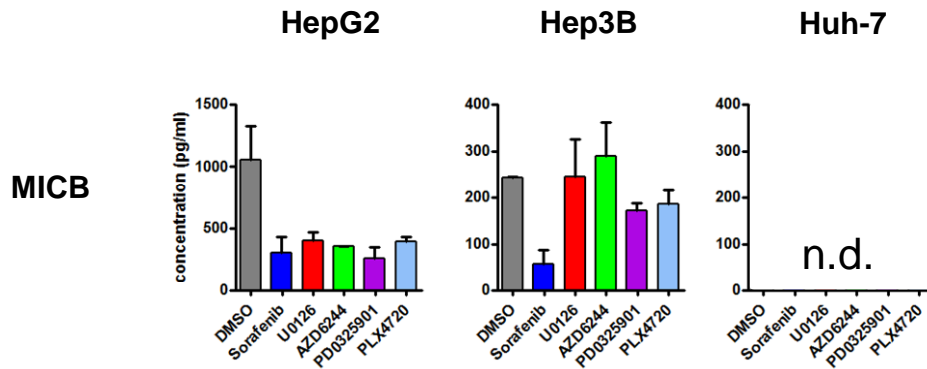


**Figure 43: Soluble MICB secretion is partially reduced by MAPK inhibitors.** HepG2, Hep3B and Huh-7 cells were treated with 5  $\mu$ M MAPK inhibitors for 48 h. Supernatant was collected and sMICB was measured by ELISA. In HepG2 cells, sMICB is reduced with all MAPK inhibitors including PLX4720. In Hep3B cells, only sorafenib and only partly PD0325901 and PLX4720 show an inhibition of sMICB. In Huh-7 cells, sMICB was not detected. Shown is one representative experiment out of two independent experiments.  $n=2 \pm$  SD

*In summary, it was detected that the three cell lines HepG2, Hep3B and Huh-7 secrete different chemokines and growth factors to an individual degree. Treatment with the B-Raf inhibitor sorafenib and the MEK inhibitors U0126, AZD6244 and PD0325901 mostly reduced the secretion of chemokines like CXCL8 for instance. Nevertheless, an increase in chemokine secretion was also detected, but remarkably not in all cell lines and for all inhibitors. The degree of inhibition varied between the cell lines and inhibitors. However, the strongest correlation between pathway inhibition and reduction in secretion was observed for CXCL8 and VEGF indicating that these strong tumor promoting factors are tightly linked to the oncogenic MAPK pathway. Remarkably, MIF was the only factor, which was increased with sorafenib and the MEK inhibitors, but effects were dependent on the cell line. The specific B-Raf inhibitor PLX4720 behaved partially different. For several factors like CXCL8, CCL5, VEGF and IL-1RA a strong increase in secretion was detected. In the NRas-mutant HepG2 cell line, this effect was most pronounced.*

*Although all these inhibitors except PLX4720 were shown to inhibit the MAPK pathway in section 5.1.1, they show different effects in the three different cell lines. Since hepatocellular carcinoma varies substantially between patients, it is of great interest to see whether these inhibitors have also different effects in the patients regarding the microenvironment in tumor tissue. Therefore, I analyzed HCC tissue in collaboration with H. Bantel (Hannover Medical School, Germany).*

## 5.3 Modulation of MAPK Pathway in Healthy and HCC Tissue

### 5.3.1 Hepatic microenvironment

Before analyzing the effect of MAPK pathway inhibition on the tumor microenvironment, the cytokine, chemokine and growth factor milieu was determined in liver tissue samples of healthy liver, healthy liver tissue derived during resection of colorectal metastases, cirrhotic liver tissue and HCC, respectively. The healthy liver tissue was derived from two donor liver that finally were not transplanted and from a hemangioma. Using the multiplex method, 50 cytokines, chemokines and growth factors were simultaneously measured in tissue lysates and some results are depicted in Figure 44 and Figure 45.

Chemokines, which are separated into four families, the C, CC, CXC and CX<sub>3</sub>C chemokines, play a pivotal role for the recruitment of circulating immune cells, but also a variety of them have many other important functions involved in angiogenesis and carcinogenesis (Keeley *et al.*, 2011; Simpson *et al.*, 2003).

For the CXC chemokines, it could be detected that the protein expression of CXCL8 (IL-8), CXCL9 (MIG) and CXCL10 (IP-10) was already increased in resected liver tissue of colorectal metastases, cirrhosis and HCC, although the increase of CXCL10 in liver tissue of patients with colorectal metastases and cirrhosis was not significant. The significant differences between healthy liver tissue and liver tissue obtained in the course of colon metastases resection demonstrate that the microenvironment in the metastatic situation is already influenced by the primary colon tumor. The levels of CXCL1 (Gro- $\alpha$ ) and CXCL12 (SDF-1 $\alpha$ ) did not significantly differ between the patient groups.

The CC chemokines CCL2 (MCP-1) and CCL4 (MIP-1 $\beta$ ) showed a tendency of increased levels in resected liver tissue from colorectal metastases, liver tissue of cirrhosis and HCC patients. The profile in cirrhosis and HCC seemed to be separated in two populations, one increased and one reduced for CCL3 (MIP-1 $\alpha$ ), CCL7 (MCP-3) and CCL27 (CTACK). This subgroup formation in a high vs. a low concentration group was also observed for other proteins; however, the basis for this distribution remains elusive. For resected liver tissue from colorectal metastases, the CCL3 and CCL27 chemokine levels were increased. The chemokine CCL5 (RANTES) showed a tendency of higher levels in resected liver tissue of colorectal metastases and cirrhotic liver, but not in HCC.

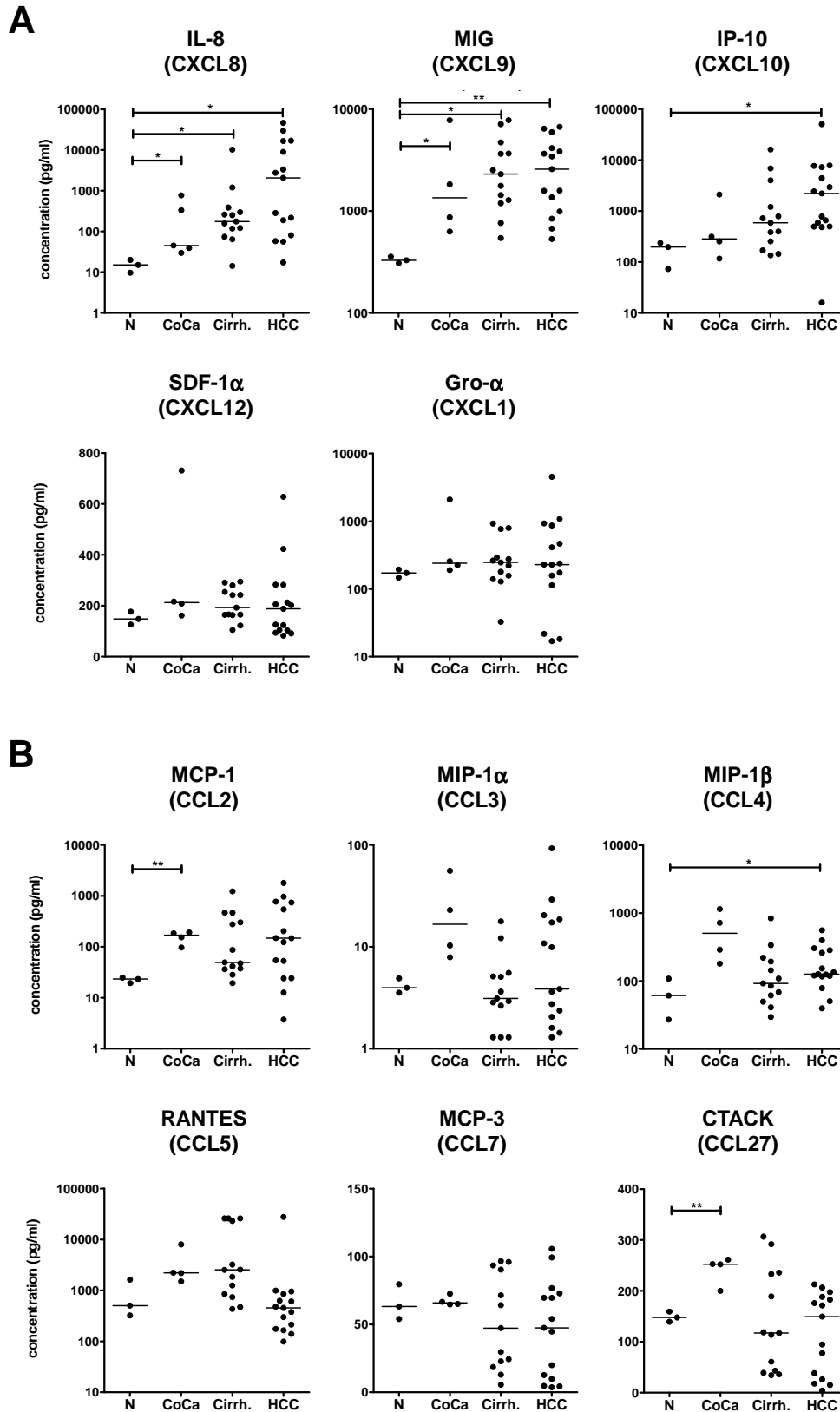


**Figure 44: Chemokine milieu in healthy liver, liver resection of colorectal metastases, cirrhosis and HCC.** Lysates were generated from frozen liver tissue and protein concentration was set to 1500  $\mu\text{g/ml}$ . CXC chemokine (A) and CC chemokine (B) concentrations were simultaneously measured by multiplex analysis. N: Normal healthy tissue (n=3), CoCa: resected liver tissue of colorectal metastases (n=4), Cirrh: cirrhotic tissue (n=13), HCC: HCC tissue (n=15).

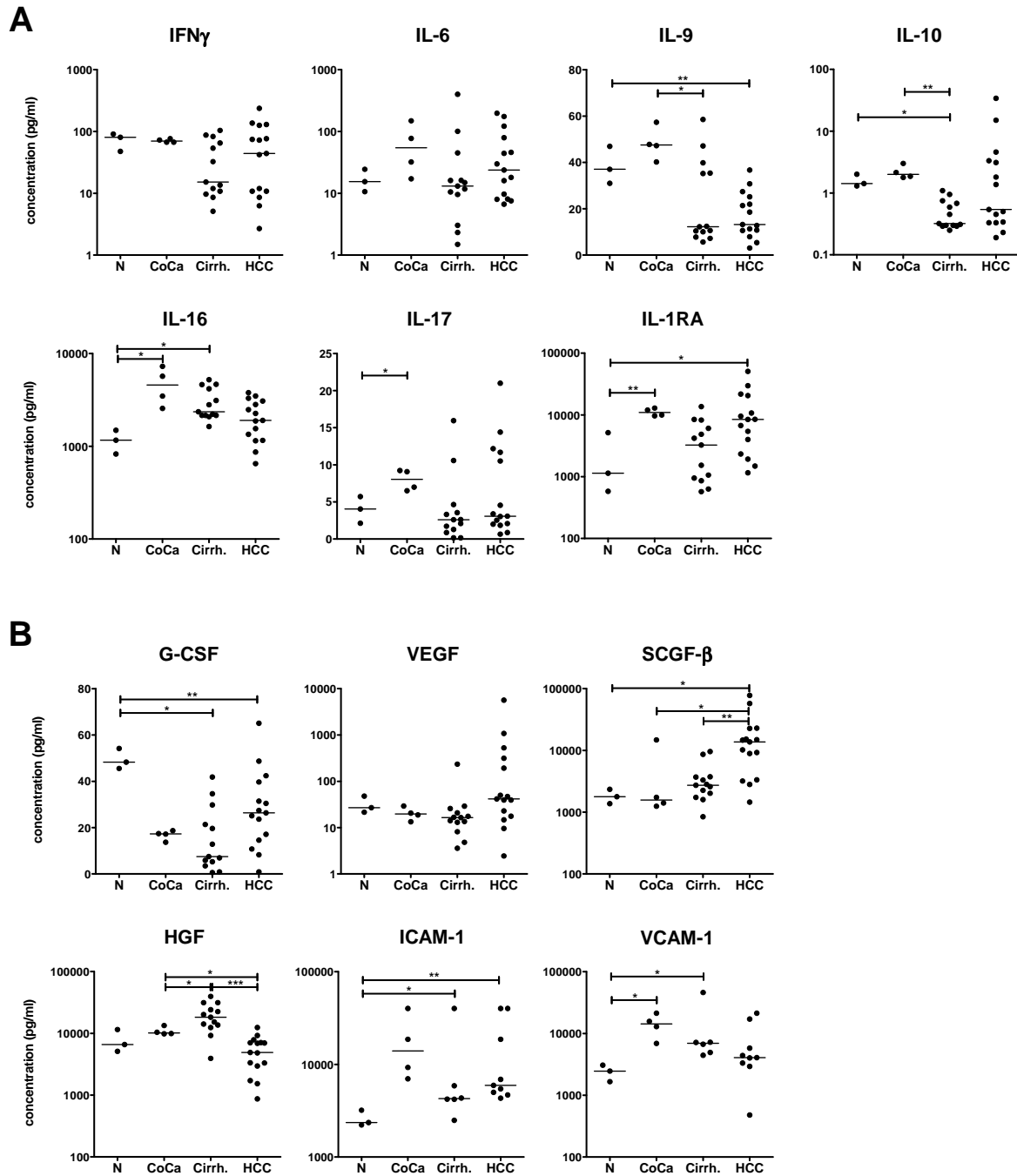


**Figure 45: Cytokine milieu and adhesion molecules in healthy liver, liver resection of colorectal metastases, cirrhosis and HCC.** Lysates were generated from frozen liver tissue and protein concentration was set to 1500  $\mu\text{g/ml}$ . IFN $\gamma$  and interleukin (A) and growth factor and adhesion molecule (B) concentrations were simultaneously measured by multiplex analysis. N: Normal healthy tissue (n=3), CoCa: resected liver tissue of colorectal metastases (n=4), Cirrh: cirrhotic tissue (n=13), HCC: HCC tissue (n=15).

Interferons and interleukins, which are cytokines and act as mediators between cells, were also differently accumulated in the different tissue. IFN $\gamma$ , the most important effector interferon, was partly reduced in cirrhosis and HCC, compared to healthy and resected liver tissue of colorectal metastases, suggesting that effector functions are reduced in these tissues. Remarkably, IL-6 levels were increased in resected liver tissue of colorectal metastases and HCC by not a significant extend as expected from the literature where IL-6 is postulated to drive the tumor microenvironment (Germano *et al.*, 2008; Yang *et al.*, 2011). In contrast, IL-9 and IL-10 surprisingly were reduced in cirrhosis and HCC, but not in resected liver tissue of colorectal metastases, which is unexpected because IL-10 is postulated to protect tumor tissue by counteracting an IFN $\gamma$ -mediated effector milieu. An increased level of IL-1RA and IL-16 was observed for liver tissue of colorectal metastases resection, cirrhosis and HCC. There were also interleukins, which were not altered in liver tissue of colorectal metastases resection, cirrhosis and HCC. IL-2, IL-4, IL-5 and IL-13 secretion was at a very low level in all four different liver tissues (data not shown). Other interleukins like IL-12 and IL-18 were secreted to a medium amount, but also no real differences were observed in the different tissues (data not shown) indicating that these interleukins do not seem to play a role in the development of cirrhosis and HCC.

Stimulating factors and growth factors play an important role in carcinogenesis since growth factors are often overexpressed in tumor tissue. As expected, the growth factors VEGF and SCGF- $\beta$  were both increased in HCC, and SCGF- $\beta$  was also increased in the cirrhotic tissue. Since both growth factors were shown to be secreted by HCC cells (5.2.5), these high amounts could be indeed be produced by tumor cells. Interestingly, HGF was only significantly increased in cirrhotic tissue, but not in HCC, indicating that HGF is not needed for the maintenance of HCC but maybe for the development into HCC. In contrast, G-CSF was reduced in resected liver tissue, cirrhosis and HCC.

Soluble adhesion molecules like ICAM-1 and VCAM-1 are often found to be increased in patients with tumors. It could be detected that in resected liver tissue of colorectal metastases, in cirrhotic and HCC tissue the concentrations of ICAM-1 and VCAM-1 was increased compared to healthy liver tissue.

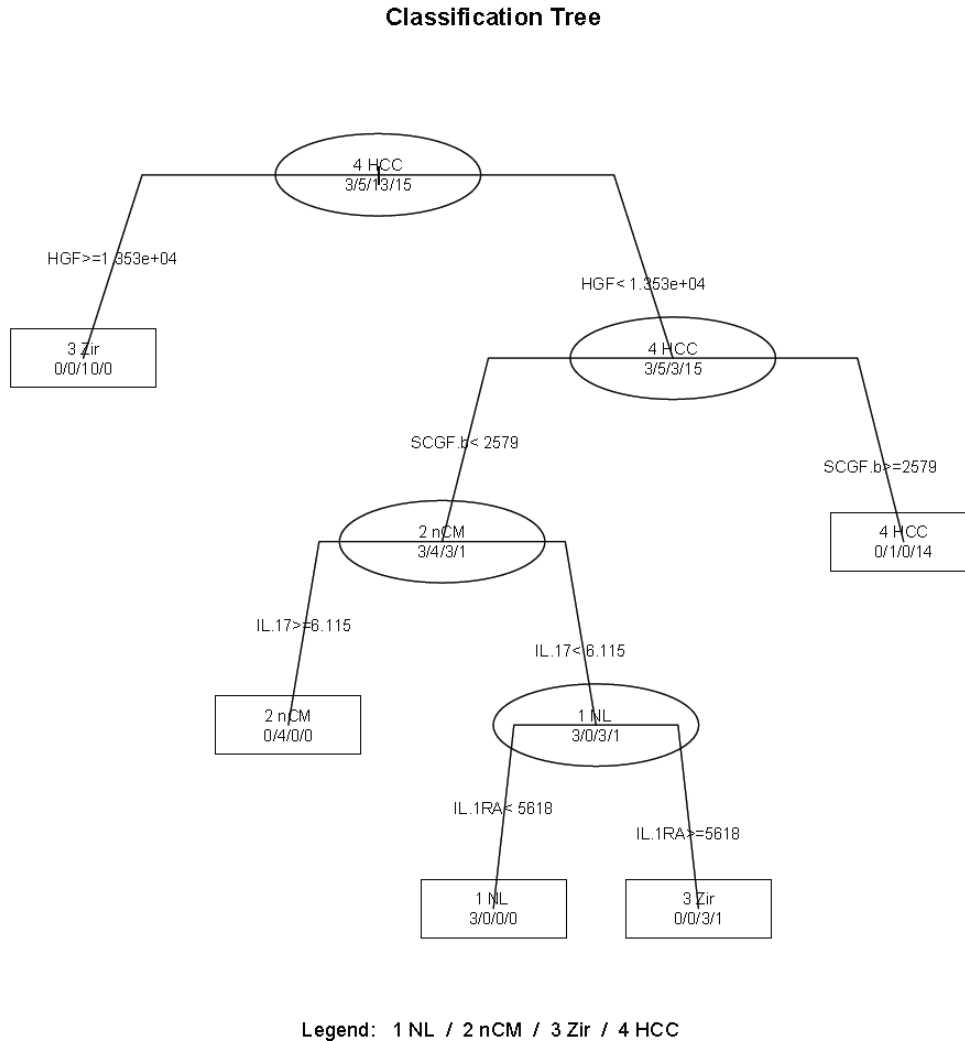


**Figure 46: Classification tree of analyzed cytokines, chemokines and growth factors.** Classification tree was generated by using the 50 different measured cytokines, chemokines and growth factors. NL: Normal healthy tissue (n=3), nCM: resected liver tissue of colorectal metastases (n=4), Zir: cirrhotic tissue (n=13), HCC: HCC tissue (n=15). Analysis was performed by A. Skoeries (Hamamatsu TIGA Center, University of Heidelberg).

The multiplex analysis generated a huge amount of data, because 50 different factors were measured in four different types of liver tissue. In cooperation with Anne Skoeries (Niels Halama, Hamamatsu TIGA Center, University of Heidelberg), a bioinformatic approach was used to analyze differences and possible classifications of the healthy liver, resected liver tissue of colorectal metastases, cirrhosis and HCC.

A classification tree of cytokines, chemokines or growth factors was generated to predict the pathological state of the liver whether it is healthy, cirrhotic, HCC or comes from a colorectal metastasis, on the basis of the cytokine and chemokine milieu (Figure 46). The classification tree showed that using around four different factors, the different liver tissues can be grouped

and predicted. An important classification factor is HGF, where high levels of HGF nicely separate the majority of the cirrhotic tissue from the rest. From the remaining samples, HCC tissue can be classified by using high levels of SCGF- $\beta$ . Normal healthy liver and histological “healthy” liver tissue from patients with colorectal metastasis can be distinguished by using IL-17, where IL-17 levels are lower in healthy liver, and IL-1RA can be further used to clearly separate the healthy liver tissue. This method shows that the classification tree is a very helpful tool to interpret large amount of data, which were generated by the multiplex analysis.

*In summary, several CXC but not so much CC chemokines were increased in cirrhotic and HCC liver tissue compared to healthy liver tissue. Some CC chemokines showed a tendency of decreased levels in the tumor tissue. Interleukins were differentially altered in cirrhotic and HCC tissue. Tissue concentrations of growth factors and adhesion molecules were elevated in cirrhotic and HCC tissue. With the help of a classification tree, HGF, SCGF- $\beta$ , IL-17 and IL-1RA can be used to predict the status of the liver tissue.*

*These results raise the question whether treatment of HCC tumor with small molecules like sorafenib and the MEK inhibitors would normalize the cytokine and chemokine milieu in HCC tumor tissue. Moreover, it is interesting to analyze whether these alterations of the microenvironment have an effect in the composition of immune cells in cirrhotic and HCC liver compared to healthy liver, as indicated in section 6.2.2.*

### 5.3.2 Modulation of cytokine and chemokine secretion by MAPK inhibitors in *ex vivo* hepatic tissue

As described in 5.3.1, several different cytokines, chemokines and growth factors can be detected in liver tissue and the composition seems to vary substantially according to the condition, i.e. healthy, cirrhosis, HCC. The microenvironment in HCC tissue is associated with an increase in several chemokines and growth factors. In addition, the chemokine secretion of tumor cells was modulated by MAPK inhibitors *in vitro* (5.2.5). Most of the factors which were increased in the tumor were downregulated with these inhibitors. In order to analyze the effects of the MAPK inhibitors on *ex vivo* liver tissue, which consist a variety of different cells, fresh liver tissue samples from patients with HCC or normal liver were treated *in vitro* for 8 h with medium or 7.5 µg/ml sorafenib. In a first experiment also the MEK inhibitors U0126, AZD6244 and PD0325901 and the B-Raf<sup>V600E</sup> inhibitor PLX4720 were used for tissue treatment (data not shown). After 8 h, tissue lysates of these HCC and normal liver tissues were prepared and both supernatants and tissue lysates were analyzed in parallel for 50 cytokines, chemokines and growth factors. Parts of these parameters are depicted in Figure 47 to Figure 50. These experiments were performed in cooperation with Kristin Wahl (Laboratory H. Bantel, Hannover Medical School, Germany).

The chemokines CXCL8, CXCL9, CXCL10 and CCL4 were significantly upregulated and CXCL1, CCL2 and CCL3 were partly increased in HCC tissue as described in 5.3.1. Treatment of HCC tissue for 8 h with sorafenib clearly reduced the secretion of the CXC chemokines CXCL8, CXCL9, CXCL10 and CXCL1 in both tissue and supernatant (Figure 47). In contrast, for CXCL1 and CXCL9 one and two out of the six tissue samples showed a significantly increase in concentration after sorafenib treatment indicating that these chemokines are independently regulated in tissues.

With respect to CC chemokines, CCL2 and CCL4 secretion was inhibited by sorafenib in tissues and supernatants with only one exception (Figure 47B). The content of CCL5, CCL7 and CCL27 was not significantly altered by sorafenib treatment. For CCL5, a tendency of downregulation in four out of six samples was detectable, while in supernatants the high CCL5 levels were reduced and low levels were increased after sorafenib treatment. The difference between tissue and supernatants may be due to different modes of chemokine secretion into interstitial tissue which may be easily “washed out” into the supernatant. Other chemokines, however, may be rather cell-bound and not released into the supernatant.

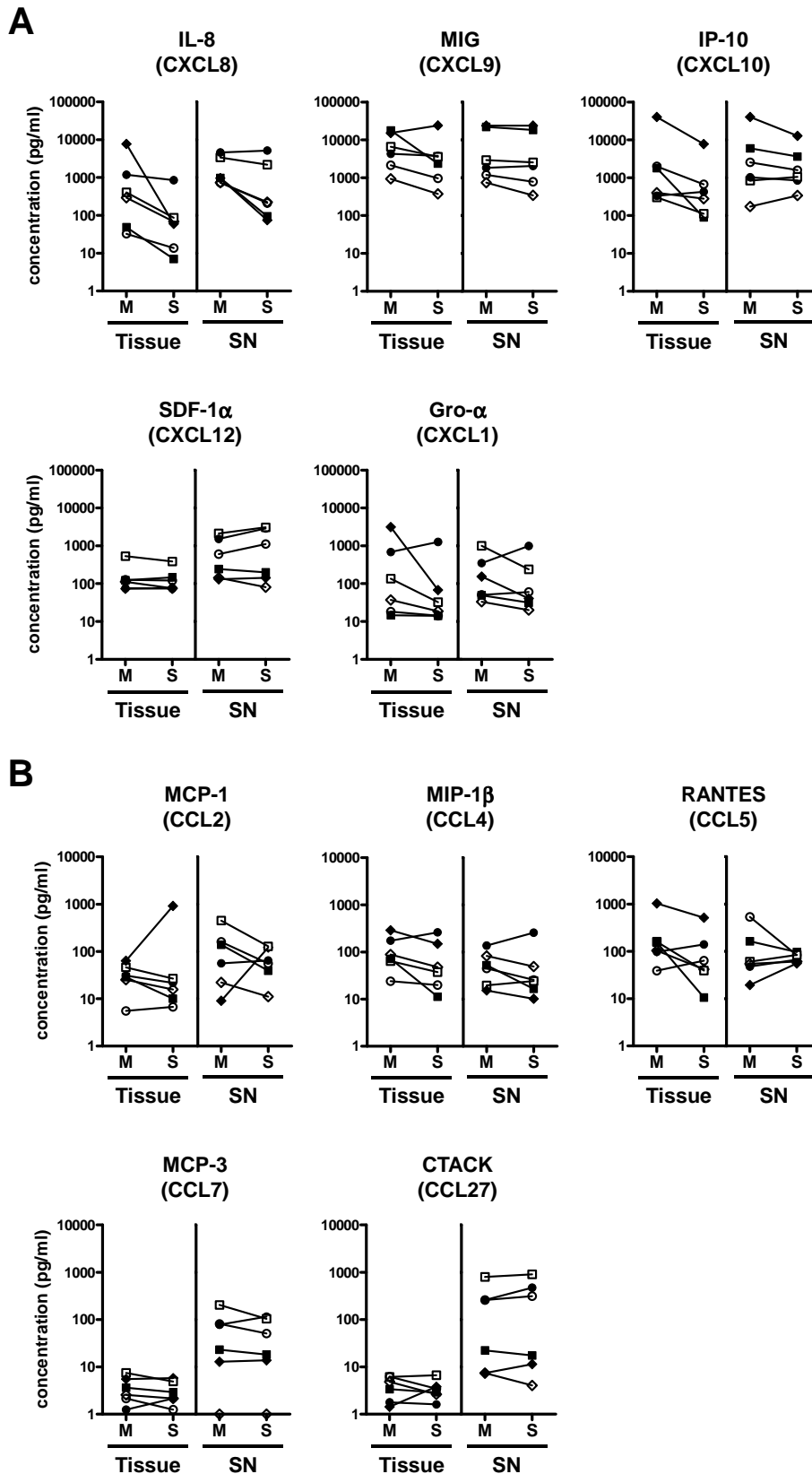


**Figure 47: Sorafenib alters the chemokine milieu in HCC tissue.** Fresh HCC tissue was treated *in vitro* with medium or 7.5  $\mu\text{g/ml}$  sorafenib for 8 h <sup>(\*)</sup>. Supernatant (SN) was collected, tissue lysates were generated and protein concentration was set to 500  $\mu\text{g/ml}$ . CXC chemokine (A) and CC chemokine (B) concentrations of supernatants and tissue lysates were simultaneously measured by multiplex analyses. M: medium; S: sorafenib; n=6.

<sup>(\*)</sup> Treatment was performed by Kristin Wahl (H. Bantel, Hannover Medical School).

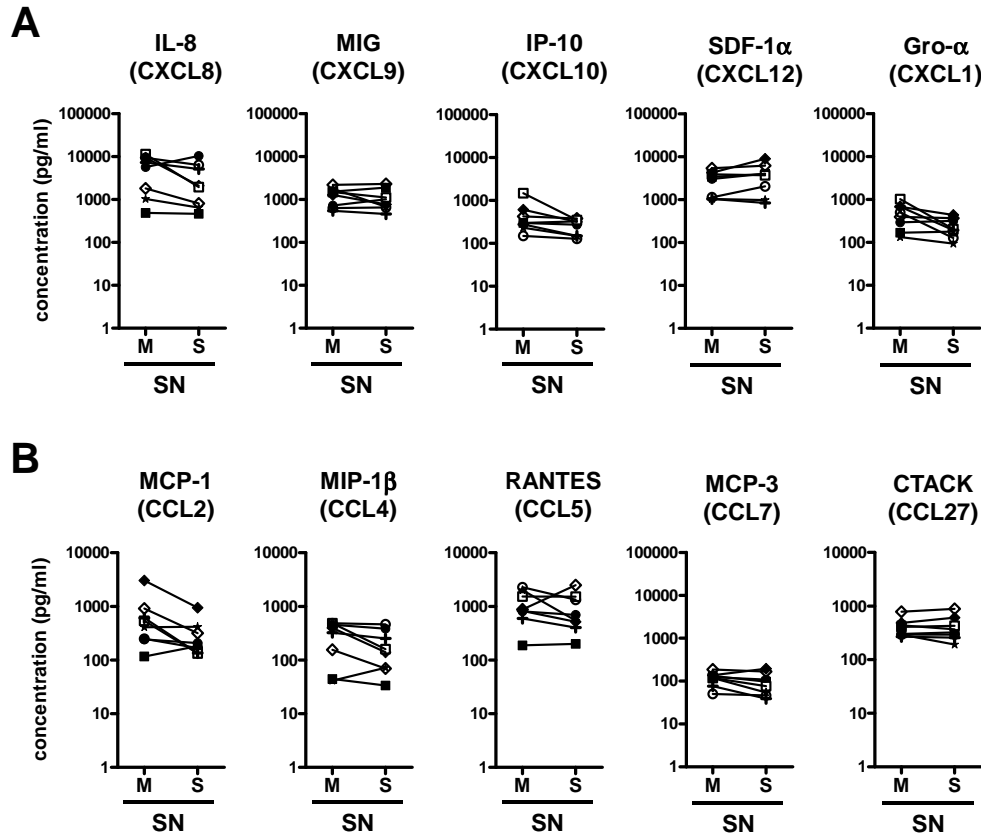


**Figure 48: Sorafenib alters the chemokine milieu in healthy liver.** Fresh healthy liver tissue was treated *in vitro* with medium or 7.5  $\mu$ g/ml sorafenib for 8 h and supernatant (SN) was collected (\*). CXC chemokine (A) and CC chemokine (B) concentrations were simultaneously measured by multiplex analyses. M: medium; S: sorafenib; n=8.

(\* Treatment was performed by Kristin Wahl (H. Bantel, Hannover Medical School).

Alterations of the chemokines after treatment with sorafenib were also seen in the supernatant of healthy liver tissue (Figure 48). Due to the limited tissue material, only supernatants of healthy liver tissue was available. Similar to HCC, CXCL8, CXCL10 and CXCL1 were downregulated after sorafenib treatment with one exception for CXCL8, where an increased concentration was detected. In contrast to HCC tumor tissue, CXCL9 showed no substantial alteration after treatment. Again similar to HCC tissue, CXCL12 was mostly upregulated following sorafenib exposure. Overall in healthy liver, it seems that sorafenib has more consistent effects on CC chemokines than in HCC where the etiology may have a more dominant impact. The secretion of CCL2, CCL4, CCL5 and CCL7 was rather inhibited while CCL27 could be modulated in both directions.

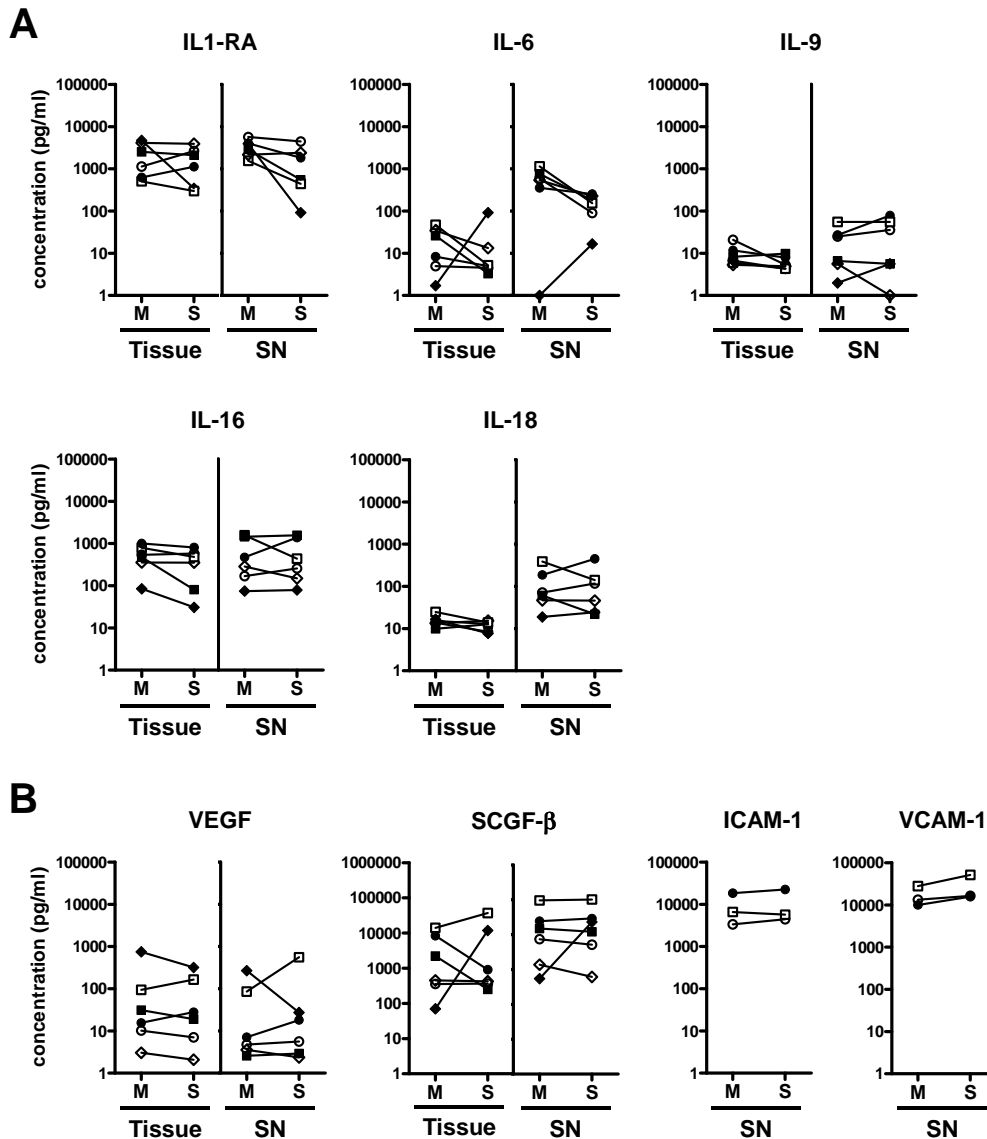


**Figure 49: Sorafenib alters the cytokine milieu and adhesion molecules in HCC.** Fresh HCC tissue was treated *in vitro* with medium or 7.5  $\mu\text{g/ml}$  sorafenib for 8 h <sup>(\*)</sup>. Supernatant (SN) was collected, tissue lysates were generated and protein concentration was set to 500  $\mu\text{g/ml}$ . Interleukin (A), growth factor and adhesion molecule (B) concentrations were simultaneously measured by multiplex analyses. M: medium; S: sorafenib; n=6. For ICAM-1 and VCAM-1 only the supernatants were analyzed (n=3).

<sup>(\*)</sup> Treatment was performed by Kristin Wahl (H. Bantel, Hannover Medical School).

Besides the chemokines, also interleukins, growth factors and adhesion molecules were analyzed after sorafenib treatment (Figure 49 for HCC and Figure 50 for healthy liver). IL-1RA is an inhibitor of the pro-inflammatory cytokine IL-1. In HCC tissue, high amounts of IL-1RA were detectable (5.3.1). Treatment with sorafenib decreased IL-1RA in the supernatant, while in tissue lysates, it could be modulated in both directions. IL-6, which acts as a pro- and as an anti-inflammatory cytokine, seems to be highly soluble, because it is found in HCC supernatant. Sorafenib treatment reduced IL-6 in the supernatants with one exception.

The Th2 response inducing cytokine IL-9 was found in low concentrations and was reduced in tissue lysates by sorafenib. Similarly, IL-16 and IL-18 were both reduced in the tissue lysates after treatment, while no tendency was observed in supernatants.

Growth factors were not clearly modulated by sorafenib treatment of HCC. The concentrations of VEGF in tissue showed a broad range that was influenced in both directions which, again, may be influenced by the HCC etiology. The two adhesion molecules ICAM-1 and VCAM-1 were highly concentrated in supernatants and even elevated by sorafenib.

In healthy tissue, in general, alteration of interleukins, growth factors and adhesion molecules were also observed, but appeared to be more homogeneous. IL-1RA, IL-6 and IL-16 were mainly decreased by sorafenib treatment, while somewhat higher concentrations of IL-9 and IL-18 were measured. VEGF concentrations were not influenced by sorafenib treatment and SCGF- $\beta$  was elevated in some samples and decreased in others.

Interestingly, the effect of sorafenib on the adhesion molecules ICAM-1 and VCAM-1 was different in healthy liver compared to HCC tumor tissue. While in HCC, sorafenib induced an elevation of ICAM-1 and VCAM-1, they were rather decreased in healthy liver.

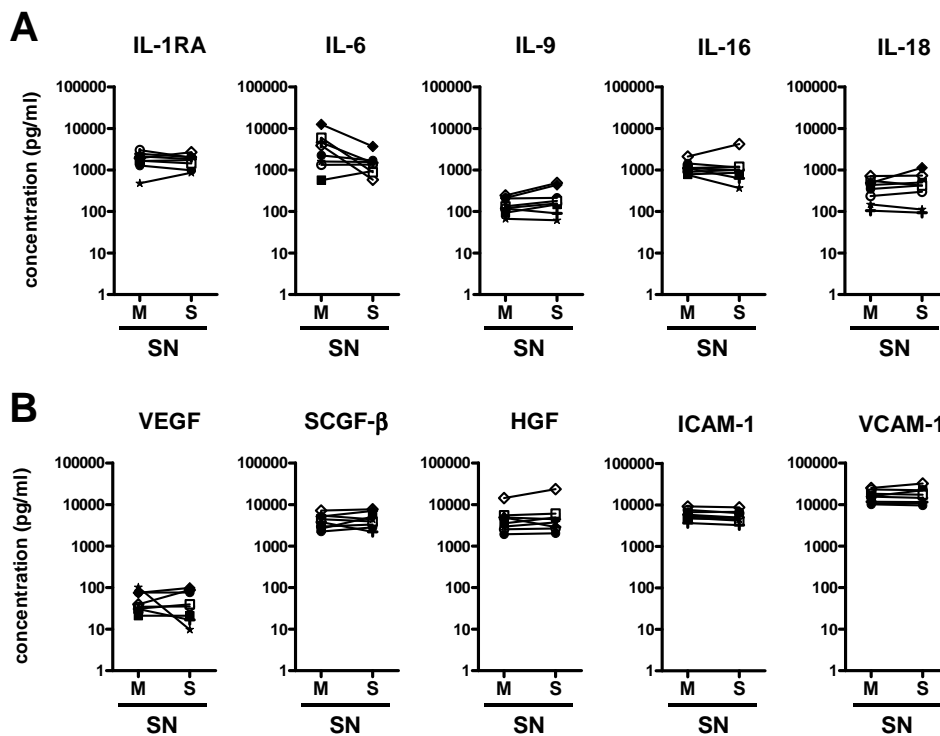


**Figure 50: Sorafenib alters the cytokine milieu and adhesion molecules in healthy liver.** Fresh healthy liver tissue was treated *in vitro* with medium or 7.5  $\mu\text{g/ml}$  sorafenib for 8 h and supernatant (SN) was collected (\*). Interleukin (A), growth factor and adhesion molecule (B) concentrations were simultaneously measured by multiplex analyses. M: medium; S: sorafenib; n=8. (\*) Treatment was performed by Kristin Wahl (H. Bantel, Hannover Medical School).

*In summary, in HCC tumor tissues, several chemokines and cytokines were found to be present of higher concentrations compared to non-malignant liver tissue. This observation supports the assumption that the hepatic microenvironment is comprised by tissue- and etiology-specific mixture of soluble mediators like cytokines, chemokines and growth factors. This dynamic composition can be influenced by viruses, cirrhotic and, finally malignant transformation and also by inhibition of signaling pathways.*

*Treatment with sorafenib mostly reduced the secretion of several CXC and CC chemokines in the tumor tissue, which nicely resembles the observation with HCC cell lines. In healthy tissue these chemokines were also partly reduced in a homogeneous fashion. Rather rarely, chemokines were elevated after sorafenib treatment indicating that the MAPK pathway is involved in chemokine secretion at various positions. Sorafenib also reduced interleukin and growth factor secretion in tumor tissue, but increased the release of adhesion molecules into supernatant. In healthy tissue, these effects were less pronounced suggesting that the malignant transformation into HCC impinges on the microenvironment, presumably driven by mutations as well as the individual etiology.*

*Since the microenvironment is important for the composition, recruitment and infiltration of immune cells into the liver tissue, it would be of great interest to see whether treatment with these MAPK inhibitors has an effect on the immune cell infiltration into the tumor site and the adjacent tissue. To date, no such immune monitoring is performed in the clinical trials, unfortunately.*

## 6 Discussion and Conclusions

Hepatocellular carcinoma is one of the most prevalent tumors worldwide. The MAPK pathway plays a central role in carcinogenesis and seems to be a good therapeutic target. So far, sorafenib is the only treatment option with some stabilization of the disease, but survival benefits are not sustained with only three to four months longer compared to non-treated patients. Although sorafenib treatment cannot cure HCC, it is very important to gain detailed insights in the action of sorafenib and other MAPK inhibitors. With this knowledge, more effective drugs could be developed or new combinations of drugs might be administered to achieve the desired effects, e.g. prolongation of survival.

To comprehensively analyze the effects of the MAPK pathway and the effects of its inhibition in hepatocellular carcinoma, sorafenib was compared to other MAPK inhibitors used in clinical and pre-clinical evaluations for the treatment of HCC. Therefore, the effects were determined regarding the impact on (1) signaling pathways, (2) proliferation and apoptosis, (3) surface molecule expression involved in NK cell recognition, (4) secretion of chemokines and growth factors by tumor cells, (5) the hepatic microenvironment upon exposure to MAPK inhibitors, sorafenib in particular.

### 6.1 Signaling Pathways

Cellular behavior and cell fate is regulated through diverse signaling pathways rather than regulated by just one pathway. Often, it is a combination of different signaling pathways which determines the cellular response. In tumor development, often one or more of these pathways are constantly activated. In HCC, The MAPK pathway, in particular, is often over-activated because it plays a pivotal role for cell proliferation and survival. Constant activation of the MAPK pathway is frequently due to mutations in components upstream of the pathway. Through these mutations, often other signaling pathways are also affected in compensatory or feedback loops. Because different signaling pathways are connected to some extent through these cross-talk or feedback connections, it is very important to perform a broad analysis when analyzing signaling pathways and effects of signaling inhibitors like sorafenib. Because of its contribution to tumorigenesis, tumor progression and disease metastasis formation,

intensive research has been performed on the MAPK pathway as a therapeutic target (Friday and Adjei, 2008; Leicht *et al.*, 2007). Still, the systemic effects of MAPK inhibition in tumor and non-tumor cells are poorly understood.

### 6.1.1 MEK/ERK signaling in HCC cells

Increased MAPK expression and activity has been described in primary human hepatocellular carcinoma, which is normally measured as phosphorylation of MEK1 at Ser217/Ser221 and ERK1/2 at Thr202/Tyr204 and Thr185/Tyr187. This is often due to a mutation in the receptor tyrosine kinases or the Ras protein (Downward, 2003; Gollob *et al.*, 2006). The HepG2 cell line has an NRas (Q61L) mutation leading to an activation of the MAPK pathway. Although Hep3B and Huh-7 cells do not have a mutation directly in the MAPK pathway, the phospho-MEK/ERK levels were at the level of HepG2 cells indicating that Hep3B and Huh-7 cells can constantly activate the MEK/ERK pathway through other mechanisms. This activation can be inhibited by the treatment with the Raf inhibitor sorafenib and the MEK inhibitors U0126, AZD6244 and PD0325901 and is depicted in a schematic diagram in Figure 51. Inhibition is demonstrated by an immediate and sustained decrease in phosphorylation of ERK1/2. Sorafenib binds and thereby inhibits Raf which is upstream of MEK (Figure 12) and as a consequence, MEK phosphorylation is blocked (Figure 13). The MEK inhibitors U0126, AZD6244 and PD0325901, in contrast, bind to and inhibit the MEK kinase (Figure 13). Although they inhibit MEK, they do not necessarily block the phosphorylation site of MEK, meaning that Raf can still phosphorylate MEK. Due to a block in the kinase activity of MEK, the phosphate group is not transferred to downstream ERK. Thus, p-MEK accumulates which is in accordance with earlier reports (Hennig *et al.*, 2010; Huynh *et al.*, 2007). Huynh *et al.* also described that AZD6244 was even able to activate B-Raf which then led to an increase in p-MEK.

Remarkably, ERK phosphorylation was not always constantly inhibited by the concentrations of 5  $\mu$ M sorafenib and U0126. Although p-MEK1 was inhibited by sorafenib in HepG2 cells and p-MEK1 was increased by U0126, p-ERK was elevated after 24 h in HepG2 cells. Maybe MEK1 inhibition was not complete, so that some MEK1 or even MEK2 can still transfer the phosphate group to ERK1/2. When using higher concentrations of sorafenib (10  $\mu$ M), no increase of p-ERK1/2 was detected in HepG2 cells (data not shown). It still has to be

determined whether this increase is just an effect of the concentration or whether resistance to drug treatment has already occurred, because it was described that Hep3B cells showed signs of resistance during treatment with U0126 (Yip-Schneider *et al.*, 2009).

In contrast to sorafenib and the MEK inhibitors, the mutation-specific B-Raf<sup>V600E</sup> inhibitor PLX4720, which also inhibits to some extent the wild-type B-Raf, induced a hyperactivation of p-MEK1 and p-ERK1/2 in the tested NRas-mutant HepG2 and NRas-wild-type Hep3B cells (Figure 13). PLX4720 is currently tested for melanoma treatment, where the B-Raf has often a point mutation at position 600 leading to a strong MAPK activation (Tsai *et al.*, 2008). In mutant B-Raf<sup>V600E</sup> cells, the MAPK pathway is inhibited by PLX4720, but it has been reported that PLX4720 induces hyperactivation of the MEK/ERK pathway in NRas-mutant melanoma cells (Heidorn *et al.*, 2010; Kaplan *et al.*, 2011). Because PLX4720 is only inhibiting B-Raf and not C-Raf, it is speculated that C-Raf dimerizes with B-Raf and is taking over the part of the inhibited B-Raf, and, thereby, activates the MEK/ERK pathway (Figure 51). This could explain the results for the NRas-mutant HepG2 cells. Interestingly, in NRas-wild-type Hep3B cells a slight increase of MEK and ERK was also detected indicating that the described hyperactivation induced by PLX4720 is not limited to NRas-mutant cells.

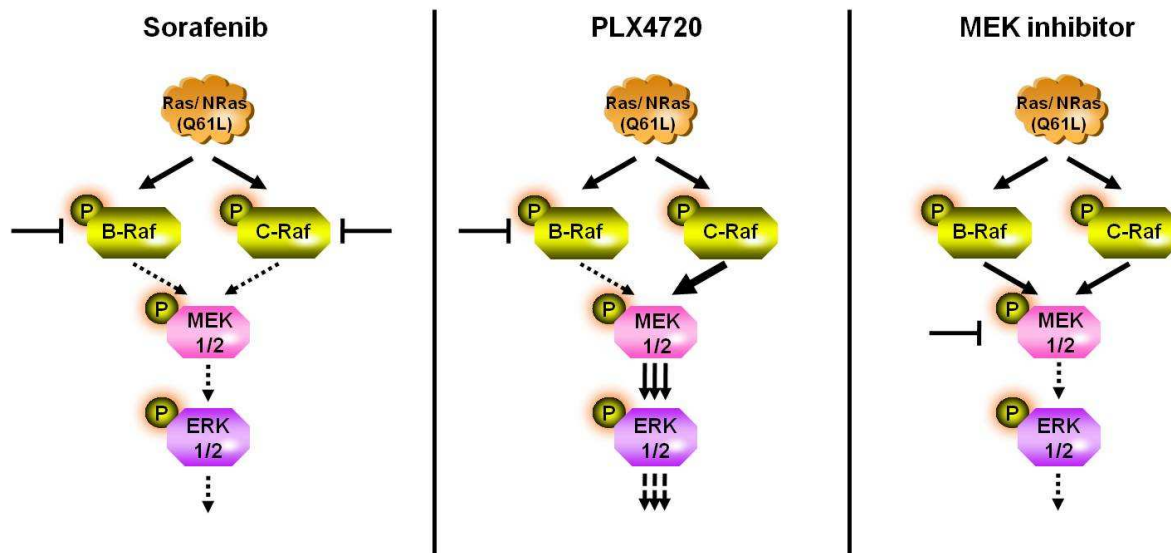


**Figure 51: Effects of MAPK inhibitors on MEK/ERK signaling in HCC cells.** Sorafenib inhibits both B- and C-Raf leading to an inhibition of downstream MEK and ERK. PLX4720 inhibits B-Raf, but not C-Raf leading to an activation of MEK and ERK via C-Raf in NRas-mutant and NRas-wild-type HCC cells. U0126, AZD6244 and PD0325901 inhibit the MAPK pathway at the MEK level and downstream ERK is inhibited. Pathway was generated with the help of the pathway builder from [www.proteinlounge.com](http://www.proteinlounge.com).

Besides analyzing the phosphorylated kinases, it is also important to measure the total amount of kinases to see whether degradation has taken place. Treatment with sorafenib, U0126 and AZD6244 showed different effects on the total MEK levels which may be associated with their different mechanisms of action. Degradation of MEK1 was extreme with AZD6244 treatment and only low with sorafenib and U0126. The differences between the two MEK inhibitors U0126 and AZD6244 might be explained by their different binding sites to MEK1. This strong decrease of t-MEK is in contrast to the strong increase of p-MEK. In contrast, the total amount of the downstream ERK levels was not substantially changed indicating that the modulation of total kinases was not due to different protein concentrations.

Our findings indicate that AZD6244 and PD0325901 have a high efficacy for the inhibition of the MEK/ERK pathway even better than sorafenib, the currently used treatment for HCC. These findings are in accordance to other reports, where it was described that PD0325901 and AZD6244 are specific MEK inhibitors leading to a blockage of the conversion of ERK to its activated, phosphorylated form (Hennig *et al.*, 2010; Huynh *et al.*, 2007).

### **6.1.2 Akt, JNK and p38 signaling pathways**

Because different signaling pathways are often closely connected, possible side-effects of MAPK inhibition on linked signaling pathways, i.e. JNK, p38 and Akt, were evaluated. The JNK and the p38 pathways can mainly be activated through stress stimuli, such as UV radiation, cytokines, inflammatory signals, heat shock and changes in the level of reactive oxygen species and also be activated by the Ras protein (Krishna and Narang, 2008). JNK has been reported to be a double-edged sword with pro- and anti-apoptotic functions (Liu and Lin, 2005). In general, low levels of phosphorylated JNK were observed in all three cell lines (Figure 14). Increase in phosphorylation was mostly seen in Hep3B and Huh-7 cells with the MEK inhibitors, indicating that the MEK inhibitors induce a link to JNK phosphorylation, which might be induced through stress signals.

For the p38 kinase it has been reported that it is negatively regulated by the MEK/ERK pathway (Chen *et al.*, 2000). We could observe that in HCC cell lines, the basal p38 levels were in general low (Figure 14). Only sorafenib treatment shortly induced p38 phosphorylation in HepG2 and Hep3B cells indicating that in HCC cells p38 is not closely linked to the constitutive MEK/ERK pathway.

Both JNK and p38 regulate several transcription factors like c-Jun and ATF-2. Activated c-Jun, in turn, can regulate gene expression together with c-Fos by forming one of several different AP-1 complexes at the DNA AP-1 binding site, which regulate several target genes involved in differentiation, cell migration, cytokine production, apoptosis and wound healing (Shaulian, 2010). c-Jun is also a double-edged sword with pro- and anti-apoptotic functions (Bossy-Wetzel *et al.*, 1997; Eferl *et al.*, 2003; Shaulian, 2010). In HCC cell lines, c-Jun activation does not correlate with JNK and p38 activation, indicating that c-Jun is regulated by other mechanisms. Basal c-Jun levels were high in these cell lines showing an already constitutive activation (Figure 15). While in Hep3B and Huh-7 cells, c-Jun gets even more activated by sorafenib and the MEK inhibitors, in HepG2 cells only sorafenib induced a strong phosphorylation of c-Jun suggesting different regulation mechanisms in the cell lines. The transcription factor ATF-2, which is regulated by JNK and p38, can form homodimers or heterodimers with c-Jun and the complex stimulates CRE-dependent transcription (De Cesare *et al.*, 1995). The increase in p-ATF-2 cannot be explained by JNK or p38 activation, indicating that other molecules are also responsible for ATF-2 phosphorylation. These results suggest that there might be a negative feedback loop between the MEK/ERK pathway and c-Jun and ATF-2, but both transcription factors seem to be regulated by some MEK/ERK-independent mechanisms.

In several tumor cells, the PI3K/Akt pathway is connected to the MAPK pathway. Both MEK/ERK and PI3K/Akt pathways can be regulated by Ras and interact with each other for the regulation of cell growth, but also tumorigenesis (Figure 4) (McCubrey *et al.*, 2007). In addition, Akt is also activated independently of Ras through RTKs and PI3Ks. The PI3K/Akt pathway is stimulated through growth factors and survival factors and regulates many different cell functions like cellular survival, inhibition of apoptosis, angiogenesis and tumor development (Osaki *et al.*, 2004). In HCC cell lines, intermediate p-Akt was observed in HepG2 and Huh-7 cells, but high basal levels in Hep3B cells (Figure 14). During MAPK inhibitor treatment, differences were especially seen in HepG2 cells where MEK inhibitors induced long-term activation of Akt while sorafenib initially increased phosphorylation but then inhibited p-Akt. These results show that sorafenib and the MEK inhibitors have partially opposite effects on p-Akt. The inhibition of RTKs by sorafenib but not by the MEK inhibitors might contribute to the different effects observed for the regulation of Akt. It has been reported that constitutive activation of the Raf-MAPK pathway causes negative feedback

inhibition of PI3K/Akt (Menges and McCance). This may explain why Akt phosphorylation was decreased by PLX4720 in HepG2 cells.

Akt phosphorylation has been implicated in early HCC recurrence and high p-Akt<sup>Ser473</sup> is associated with poor prognosis (Whittaker *et al.*, 2010). For the treatment of HCC, the MEK inhibitors AZD6244 and PD0325901 are currently under clinical and pre-clinical evaluation, respectively. Both induced phosphorylation of Akt in the NRas-mutant HepG2 cells indicating that the combination of NRas mutation and inhibition of ERK lead to increased Akt phosphorylation. Moreover, it raises the question whether this Akt phosphorylation has an influence on the progression of tumor growth, prognosis and tumor recurrence. There are several studies indicating that an increase in p-Akt leads to resistance towards MAPK inhibition (Balmanno *et al.*, 2009; Chen *et al.*, 2011; McCubrey *et al.*, 2006). Therefore, it would be of great interest to see whether increased Akt phosphorylation, early HCC recurrence and NRas mutations can be correlated in HCC patients.

In conclusion, our analyses showed that inhibition of Raf as well as of MEK affects other signaling pathways (JNK, Akt, p38) and downstream transcription factors (c-Jun, ATF-2), but the exact mechanisms are still unclear.

### 6.1.3 Proliferation

Since the MAPK pathway plays a prominent role for cell proliferation and migration (Katz *et al.*, 2007), it is not surprising that inhibition of the MAPK pathway led to a decrease in cell proliferation (Figure 16). The decrease in cell number was comparable in sorafenib, AZD6244 and PD0325901 treated cells, while U0126 had weaker effects. It has recently been described that sorafenib, U0126, AZD6244 and PD0325901 inhibit cell proliferation in HepG2, Hep3B and primary HCC cells (Hennig *et al.*, 2010; Huynh *et al.*, 2007; Liu *et al.*, 2006). I could also detect that cell division was inhibited mainly by sorafenib and to a lesser extent by the MEK inhibitors (Figure 18), indicating that regulation of cell division is only partly dependent on the MEK/ERK pathway (Figure 52). It has been reported by Liu *et al.* that sorafenib treatment of HepG2 cells lead to a downregulation of cyclin D1 (Liu *et al.*, 2006), which is regulated through MEK/ERK and PI3K/Akt (Figure 52). They described the downregulation of cyclin D1 as MEK/ERK dependent, since U0126 also induced inhibition of cyclin D1.

In contrast to sorafenib and the MEK inhibitors, the B-Raf<sup>V600E</sup> inhibitor PLX4720 induced hyperactivation of the MEK/ERK signaling pathway in the NRas-mutant HepG2 cells and to some extent also in the NRas-wild-type Hep3B cells (Figure 52). Despite this hyperactivation, no enhanced but rather decreased proliferation was detected. This is in agreement with a recent study where in NRas-mutant melanoma cells PLX4720 induced hyperactivation of the MEK/ERK pathway, but did not enhance cell cycle properties (Kaplan *et al.*, 2011). In another study, Menges and McCance could show that the constitutive activation of the MEK/ERK pathway causes cellular arrest through the ephrin type-A2 receptor (Menges and McCance, 2008).

In addition to the MEK/ERK pathway, the PI3K/Akt pathway plays also an important role for cell cycle regulation. Akt can phosphorylate p21 and p27 and inhibits their anti-proliferative effects, the inhibition of the cyclin D1/Cdk4 complex (Figure 52) (Osaki *et al.*, 2004). We could detect that phosphorylation of Akt<sup>Ser473</sup> is decreased and Akt is degraded by sorafenib after 24 h. This decrease in Akt would cause an increase in p21 and p27 and an inhibition of the cyclin/Cdk complex leading to a cell cycle arrest which indeed was recently described by Huynh *et al.* (Huynh *et al.*, 2009).

The group of Erwin Wagner has published that p38 $\alpha$  negatively regulates cell proliferation by antagonizing the JNK–c-Jun pathway in multiple cell types and in liver cancer development (Hui *et al.*, 2007). We could observe that phosphorylation of p38 was mainly upregulated by sorafenib in the first 6 to 24 h in HepG2 and Hep3B cells which might contribute to the inhibition of cell proliferation.

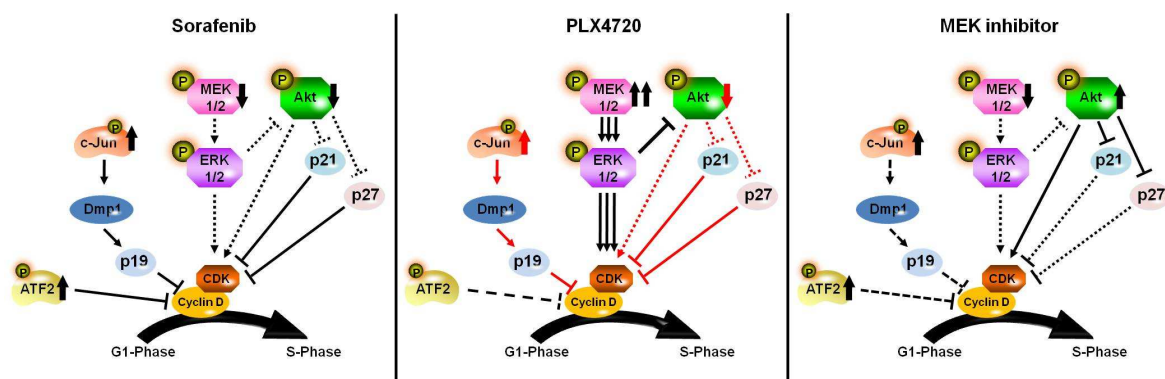


**Figure 52: Effects of MAPK inhibitors on cell cycle progression.** Sorafenib probably induces cell cycle stop via inhibition of the MEK/ERK and PI3K/Akt signaling pathway and activation of c-Jun and ATF-2 in HCC cells. PLX4720 induces hyperactivation of the MEK/ERK pathway and in NRas-mutant HepG2 cells, Akt signaling was reduced and c-Jun increased. MEK inhibitors inhibited MEK/ERK signaling, but increased Akt and slightly ATF-2 leading to a partial inhibition of the cell cycle. Red arrows indicate that the observed effects were in mutant N-Ras HepG2 cells only. Pathway was generated with the help of the pathway builder from [www.proteinlounge.com](http://www.proteinlounge.com).

While c-Jun has mostly been implicated as an enhancer of proliferation and tumor promoter, several studies have also shown that c-Jun can prevent tumorigenesis (Shaulian, 2010). It was described that in HRas-mutant cells, c-Jun is able to upregulate the transcription of the tumor suppressor Dmp1, which in turn increases the expression of the tumor suppressor p19<sup>ARF</sup> (Figure 52) (Sreeramaneni *et al.*, 2005). This tumor suppressor can directly repress cyclin D1 transcription and can also increase p53 stabilization. In HCC cells, c-Jun was highly expressed and phosphorylated and the phosphorylated form was increased by treatment with sorafenib and MEK inhibitors. PLX4720 also increased c-Jun in the NRas-mutant HepG2 cells, but not in Hep3B cells (Figure 52). Since cell proliferation and cell division was decreased by MAPK inhibitors, c-Jun seems to be implicated as an inhibitor rather than an activator of cell proliferation in HCC cells.

Besides c-Jun, an increase in p-ATF-2 induced by MAPK inhibitors could be also observed. For the regulation of proliferation, it has been reported that high levels of p-ATF-2 inhibit the G1/S phase transition of the cell cycle and, thereby, can decrease the proliferation rate (Crowe and Shemirani, 2000). Moreover, it has been shown that activated ATF-2 can inhibit the transcription of CDK4 (Xiao *et al.*, 2010). CDK4 regulates together with cyclin D the progression of the G1 phase into the S phase (Figure 52). In my system, sorafenib induced the highest induction of p-ATF-2 which might explain why sorafenib induced the most prominent cell cycle arrest.

### 6.1.4 Apoptosis

The goal of tumor treatment is besides inhibition of tumor growth the induction of apoptosis in tumor, but not in normal cells. Although several studies have been published about the effects of sorafenib, the molecular links towards apoptosis remain not completely understood. The problem we are facing in tumor therapy is that tumor cells are often resistant towards apoptosis induction. The Ras/Raf/MEK/ERK and PI3K/Akt pathways are often enhanced in many HCC cells, leading to resistance against apoptotic stimuli (Fabregat, 2009). HCC cell lines with different mutations revealed to have different apoptosis sensitivities upon MAPK inhibition in a concentration and time-dependent manner (Figure 19). In cooperation with Martina Müller-Schilling (University Hospital Heidelberg), we could show that sorafenib did not induce apoptosis in isolated primary human hepatocytes even by increasing the concentration, indicating tumor selective effects of sorafenib (manuscript in preparation). The

effects of the other MAPK inhibitors still have to be tested on primary human hepatocytes. Of the three analyzed HCC cell lines, the p53-deficient Hep3B cells were the most responsive cells for inducing apoptosis with 5  $\mu$ M sorafenib or MEK inhibitor U0126, AZD6244 and PD0325901. In contrast, the p53-mutant (Y220C) cell line Huh-7 was resistant to apoptosis induction by MEK inhibitors, but not by sorafenib in a dose-dependent manner. These data suggest that in Huh-7 cells, apoptosis is induced independently of the MEK/ERK pathway, since also AZD6244 and PD0325901 strongly decreased proliferation. Because these two inhibitors only inhibited cell cycle to a certain extent, the decrease in cell number seems to have other reasons. By using the xCELLigence system, which detects cell impedance, I could observe that especially in Huh-7 cells, the MEK inhibitors induced an increase in cell attachment and cell size. Therefore, MEK inhibitors seem to induce rather necrotic than apoptotic cell death in Huh-7 cells since necrosis is characterized by a gain in cell volume (Kroemer *et al.*, 2009).

In the p53 wild-type and NRas-mutant HepG2 cells, apoptosis was induced by the MAPK inhibitors, but to a lesser extent compared to Hep3B cells. At concentrations of 5  $\mu$ M, mainly the MEK inhibitors but not sorafenib significantly induced apoptosis. 5  $\mu$ M sorafenib did not seem to be as effective for the inhibition of the MEK/ERK pathway, which might explain the differences in the induction of apoptosis. In contrast, 10  $\mu$ M sorafenib constantly inhibited ERK phosphorylation over 96 h (data not shown) and similar apoptosis rates as by 10  $\mu$ M of the MEK inhibitors were also observed. Therefore, it seems that in NRas-mutant HepG2 cells using 5  $\mu$ M of the inhibitor sorafenib inhibits cell proliferation and cell division more effectively than the MEK inhibitors, but the MEK inhibitors induced more apoptosis. This indicates that in HepG2 cells, regulation of proliferation is less dependent on the MEK/ERK pathway than the induction of apoptosis. This is in contrast to Huh-7 cells, where apoptosis and cell proliferation regulation seems to be at least partly MEK/ERK independent.

While sorafenib and the MEK inhibitors did not have strong effects on JNK and p38 phosphorylation, they induced differences for Akt and the transcription factor ATF-2. Sorafenib reduced the level of Akt phosphorylation and induced phosphorylation of ATF-2. Moreover in Hep3B and Huh-7 cells, only sorafenib, but not the MEK inhibitors induced degradation of total Akt. Our data suggest that Akt plays an important role for the induction of apoptosis in some but not all HCC cells. In a study by Chen *et al.*, it was shown that downregulation of p-Akt leads to an overcome of apoptosis resistance (Figure 53) (Chen *et*

*al.*, 2008). This group recently demonstrated that activation of Akt in Huh-7 cells leads to resistance against sorafenib induced apoptosis (Chen *et al.*, 2011). This nicely fits with my findings where sorafenib seems to induce apoptosis through inhibition of Akt. The role of Akt for apoptosis resistance in Huh-7 cells against the MEK inhibitors will be further analyzed in our lab.

There are many regulators for apoptosis (Figure 53), among them the tumor suppressor p53, which is central player for the cell. The high induction of apoptosis in Hep3B cells was surprising, because p53-deficient cancer cells are often reported to be less responsive to chemotherapy (Alsafadi *et al.*, 2009). In Hep3B cells, the other p53 family members p63 or p73 might be able to take over the proapoptotic function of p53. We could observe that Hep3B cells express p63 and p73 and during sorafenib treatment, p73 was upregulated (Figure 22). In p53 wild-type HepG2 cells, p53 protein was modulated, i.e. phosphorylated at Ser15 by sorafenib and the MEK inhibitors, but not by PLX4720. An early induction in phosphorylation and, thus, stabilization, was observed by sorafenib and the MEK inhibitors, however, p53 was partially degraded after 24 to 48 h (Figure 20, Figure 21). It was published that c-Jun can antagonize the activity and repress p53 (Eferl *et al.*, 2003; Stepniak *et al.*, 2006). This could explain the decrease of p53 at the late time point, due to increased phospho-c-Jun levels. In Huh-7 cells, sorafenib but not the MEK inhibitors induced slight upregulation of p53 indicating that p53 regulation in Huh-7 cell is independent of the MEK/ERK pathway. In cooperation with Martina Müller-Schilling, we could detect that blocking p53, p63 and p73 reduced sorafenib-induced apoptosis in HepG2 and Hep3B cells (data not shown). Our results show that the p53 family plays an important role for the induction of apoptosis in HCC cells.

Besides p53, many pro- and anti-apoptotic molecules are involved in the regulation of apoptosis, such as the anti-apoptotic molecules Bcl-xL and Mcl-1 (Figure 53). Both are regulated via the PI3K/Akt and the MEK/ERK pathway. Akt and also ERK can phosphorylate and, thereby, block the pro-apoptotic molecule Bad (Krishna and Narang, 2008; Whittaker *et al.*, 2010). Normally, Bad can bind to the anti-apoptotic molecules Bcl-2, Bcl-xL and Mcl-1, and inhibit their function by the induction of their degradation. Moreover, Bad influences the integrity of the mitochondrial membrane and, therefore, leads to a release of cytochrome C. This release induces apoptosis by the activation of caspase 9. In addition, Akt and ERK1/2 can phosphorylate Bim, which binds and inhibits the anti-apoptotic molecules Bcl-xL, Mcl-1

and Bcl-2 (Figure 53) (Balmanno and Cook, 2009; McCubrey *et al.*, 2007). This phosphorylation leads to the dissociation of Bim with the anti-apoptotic molecules, its ubiquitination and degradation by proteasomes.

We detected that Bcl-xL and Mcl-1 were altered by both sorafenib and MEK inhibitor treatment. In HepG2 cells, Bcl-xL was slightly degraded by sorafenib treatment (Figure 25). This may be explained by an early, though weak dephosphorylation of ERK and inhibition of p-Akt after 24 h. In Hep3B cells, Bcl-xL was mainly decreased by sorafenib, along with inhibition of ERK1/2 and strong dephosphorylation and degradation of Akt (Figure 14, Figure 26 and Appendix). Interestingly, the MEK inhibitors did not show any effects on Akt phosphorylation and Bcl-xL expression. In HepG2 and Hep3B cells, sorafenib induced partial degradation of Mcl-1, which is consistent with a previous report showing that sorafenib, in contrast to the MEK inhibitor U0126, downregulates Mcl-1 in HepG2 and PLC/PRF/5 cells (Liu *et al.*, 2006).

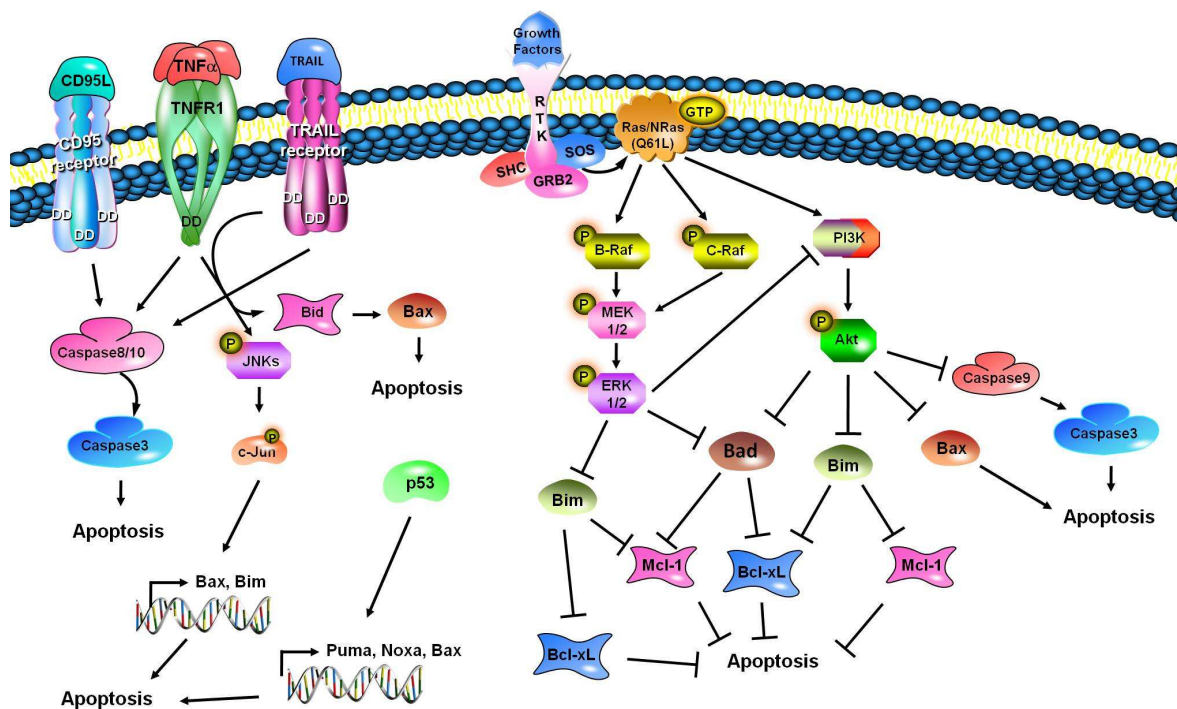


**Figure 53: Schematic drawing of regulation of apoptosis by MAPK and death receptor signaling pathways.** Pathway was generated with the help of the pathway builder from [www.proteinlounge.com](http://www.proteinlounge.com).

The mutant-specific B-Raf inhibitor PLX4720, which induced hyperactivation of the MEK/ERK pathway, slightly enhanced the levels of the pro-survival proteins Mcl-1 and Bcl-xL. This indicates that PLX4720 could promote tumor progression in NRas-mutant HCC cells, which is in accordance with a recent publication where Mcl-1 was upregulated by PLX4720 and conferred resistance to apoptosis (Kaplan *et al.*, 2011). I could observe that although PLX4720 did partly inhibit cell proliferation, it did not significantly induce apoptosis. It has been reported that C-Raf is able to directly prolong cell survival and inhibit apoptosis by Mcl-1 stabilization and inhibition of Mcl-1 degradation (Gollob *et al.*, 2006). This could explain why in Hep3B cells, only sorafenib inhibits Mcl-1, but not the MEK inhibitors and PLX4720. In sorafenib-treated cells, B- and C-Raf are blocked and Mcl-1 can be degraded, which is not the case for PLX4720, where only B-Raf is inhibited. Moreover, Gollob *et al.* could show that C-Raf can inhibit the pro-apoptotic molecule Bad and activates the anti-apoptotic molecule Bcl-2. Thus, C-Raf could be a major regulator for apoptosis independent of the MEK/ERK pathway.

Besides downregulation of the anti-apoptotic molecules Bcl-xL and Mcl-1 in HepG2 and Hep3B cells, we could observe in cooperation with Martina Müller-Schilling that sorafenib induced elevation of the pro-apoptotic molecules Bim, Bax, Noxa and Puma (Figure 53) (manuscript in preparation). Sorafenib induced at least partial phosphorylation of p38, JNK, p73 and p53, and inhibited p-ERK and p-Akt, which might lead to the increase of Bim, Bax, Noxa and Puma.

Treatment of HCC cells has not only an effect on intracellular signaling, but it also modulates death receptor expression, which play a role in the extrinsic apoptosis pathway. We could show CD95 expression was induced by sorafenib and the MEK inhibitors, but not by PLX4720, indicating that CD95 regulation is dependent on the MEK/ERK signaling pathway. It has been reported that increased c-Jun and ATF-2 levels, which was induced by sorafenib and the MEK inhibitors (Figure 15), can upregulate CD95 expression (Liu and Chang, 2010). Moreover, we could see that TRAIL-R2 was increased following sorafenib treatment. This could explain the results obtained by the El-Deiry group where sorafenib sensitizes the cell towards TRAIL (Ricci *et al.*, 2007). This is also in accordance to our results where sorafenib revealed a sensitizing effect towards TRAIL-R2-, CD95- and TNF-R1- mediated apoptosis (manuscript in preparation). Because many HCCs are resistance to apoptosis induced by CD95L (FasL) or TRAIL, treatment with sorafenib might overcome this resistance.

### 6.1.5 Conclusion

Taken together, our findings indicate that AZD6244 and PD0325901 have a high efficacy for the inhibition of the MEK/ERK pathway even better than sorafenib, the current treatment regimen for HCC. One reason for the poor survival benefit of sorafenib in patients with advanced HCC could be a suboptimal sorafenib concentration, which is not high enough for a sustained inhibition of the MEK/ERK pathway. Moreover, our analyses show that Raf as well as MEK inhibition affects other pathways like JNK, Akt, p38 and the transcription factors c-Jun and ATF-2, however the exact mechanisms have to be solved. The advantage of sorafenib compared to the MEK inhibitors is that it also inhibits the Akt pathway, which is very important for regulation of cell proliferation and apoptosis. Proliferation and apoptosis are regulated via MEK/ERK and Akt signaling. In addition, proliferation is also regulated in a MEK/ERK independent way in HCC cells. ATF-2 and c-Jun seem to be implicated as inhibitors of cell proliferation in HCC cells.

Moreover, the data show that sorafenib engages the intrinsic as well as the extrinsic apoptotic pathway. Inhibition of Akt seems to be very important for the induction of apoptosis in HCC. These results imply that for the treatment of HCC, it may be necessary to target both MEK/ERK and PI3K/Akt signaling pathways. The results indicate that the mutational status of the cancer cell is involved in the decision whether inhibition of the MEK/ERK pathway leads to apoptosis or not. Therefore, screening for the mutational status of HCC should be performed in future treatment strategies in order to improve the development of a more effective therapeutic intervention.

## 6.2 Immunological Side Effects

### 6.2.1 Modulation of immune cell recognition following MAPK inhibition

In addition to the inhibition of tumor growth and induction of apoptosis, new potential cancer therapeutics should also modulate the immune system in such a way that immune cells can recognize and kill the tumor. This is very difficult to achieve, because tumor cells have several immune escape mechanisms. Besides being resistant towards apoptosis, they can modulate their surface molecule expression at several levels to be less efficiently recognized by immune cells. For the recognition of tumor cells by T and NK cells, HLA class I, MICA/B, ULBPs, CD155 and several adhesion molecules are important. While in HCC cells HLA class I molecules were still expressed, several NKG2D ligands like MICA/B, ULBP1-3 were only weakly expressed or even absent (Figure 27, Figure 28). This constellation of weak NK cell ligands and normal HLA class I molecules implies that HCC cells are poorly recognized by NK cells. Thus, killing experiments using the CD107a degranulation assays showed that indeed HCC cells can be weakly killed by NK cells. Treatment of tumor cells with MAPK inhibitors only partially influenced the degranulation capacity of NK cells (Figure 35). These observations demonstrate that minor changes in surface expression do not always lead to substantial changes in NK cell degranulation.

Treatment of HCC cells with MAPK inhibitors modulated the expression of surface molecules, which are important for cell growth and recognition by NK cells (Figure 29, Figure 32). The growth factor receptor c-Met is often highly expressed in HCC and overexpression has been associated with increased tumor grade and poor prognosis (Ueki *et al.*, 1997; Whittaker *et al.*, 2010). I could detect that c-Met was highly expressed in HepG2, Hep3B and Huh-7 cells. This is in accordance with a previous publication showing that c-Met is highly expressed in HepG2 and Hep3B cells and HGF treatment induced slight increase in cell growth through c-Met (Lee *et al.*, 2008b). They also described that activation of the HGF/c-Met signaling pathway via the MAPK pathway leads to an enhanced cell motility and invasion through extracellular matrix substrates. Treatment of HCC cells with sorafenib and the MEK inhibitor reduced the expression of c-Met, while activation of the MEK/ERK pathway by PLX4720 led to enhanced expression of c-Met indicating that c-Met can be positively regulated via the MEK/ERK pathway (Figure 54). Inhibition of the MEK/ERK pathway by sorafenib and the MEK inhibitors suggest reducing cell motility and cell invasiveness and therefore, prevents formation of metastasis.

It was previously shown by Monika Braun that in the KRas-mutant colorectal cancer cell line HCT116, HLA class I and ULBP1-3 expression was increased by the inhibition of the MAPK pathway (Sers *et al.*, 2009). In this system, increased HLA class I expression was accompanied by enhanced tumor killing by T cells. In the HCC system, a decrease of HLA class I was only seen by sorafenib in HepG2 cells, but an increase in HLA class I expression was achieved by the MEK inhibitors in Huh-7 cells. Most importantly, modulation of HLA class I did not correlate with degranulation of NK cells. These results indicate that in contrast to colon carcinoma, looking at the HLA class I molecule expression after MAPK inhibitor treatment does not directly correlate with NK cell cytotoxicity. Therefore, other factors or activating molecules might have a stronger influence on NK cell cytotoxicity.

There are several ligands, which bind to the activating receptors on NK cells. The NKG2D receptor represents one of the most important activating receptors and it binds to a variety of molecules, which include ULBP1-6 and MICA/B (Eagle *et al.*, 2009a; Eagle *et al.*, 2009b; Nausch and Cerwenka, 2008). HepG2, Hep3B and Huh-7 cells express ULBP2 and 4, but not ULBP1 and 3 (Figure 27). To my knowledge we are the first to report that ULBP4 is expressed in Hep3B and Huh-7 cells. While sorafenib and the MEK inhibitors induced an increase in ULBP4 on HepG2, Hep3B and Huh-7 cells, PLX4720 reduced ULBP4 expression indicating a MEK/ERK dependent regulation of ULBP4 (Figure 54). The expression of ULBP2 was not substantially modulated by MAPK inhibitors. The observation that NKG2D ligands are modulated in both directions by different inhibitors demonstrates the complexity of their regulation which is not only influenced by the MAPK pathway alone.

Also soluble forms of MICA and MICB, which can be shedded from the cell surface by metalloproteases like ADAM7 and ADAM9 (Kohga *et al.*, 2010; Salih *et al.*, 2006), contribute to the immune regulation. Soluble MICA and B were described to be often elevated in the sera of HCC cancer patients {Kohga, 2008 #1940;Salih, 2006 #489}. In the soluble form, they can impair the antitumor activity by downregulating the expression of the activating receptor NKG2D on T and NK cells (Kohga *et al.*, 2010; Tamaki *et al.*, 2010). HepG2 and Hep3B secrete soluble MICB and the secretion was inhibited by the MAPK inhibitors, thereby reducing the potency of tumor cells to inhibit the immune response. It has to be further analyzed to what extend downregulation of soluble MICB helps the immune system to fight against the tumor.

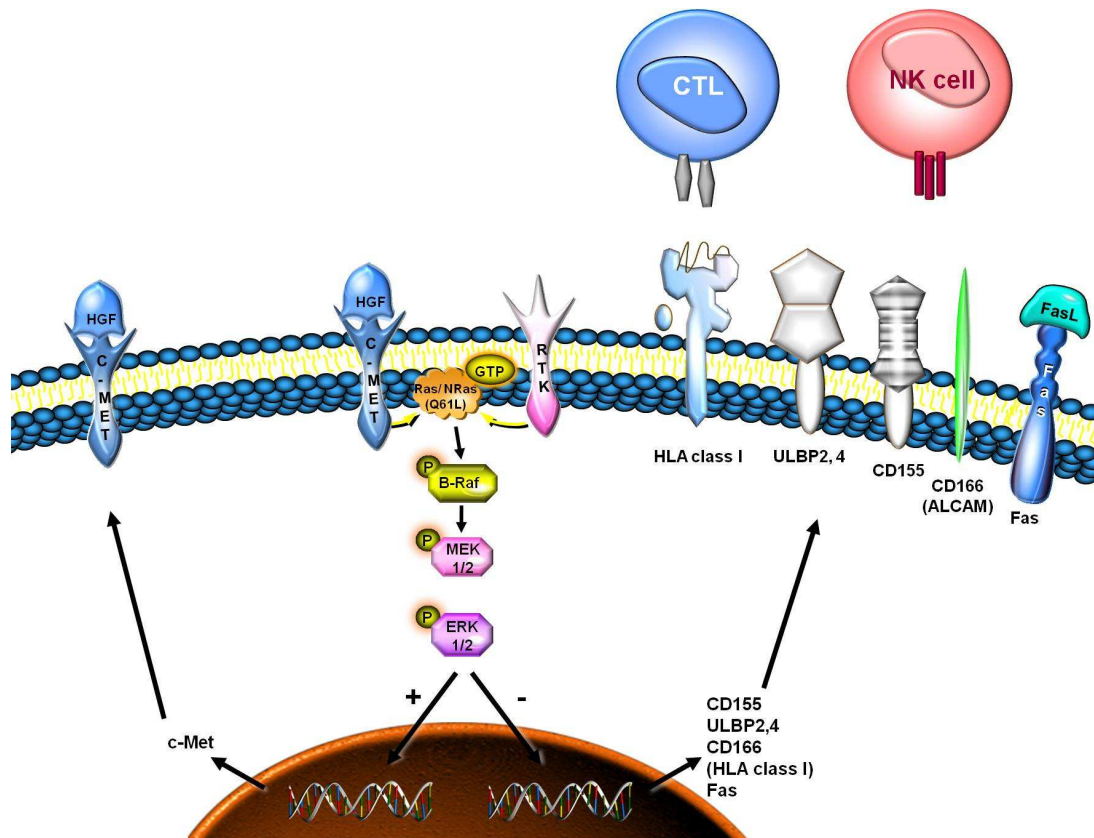


**Figure 54: Scheme of surface molecule expression regulated by MAPK pathway.** Several surface molecules like HLA class I, ULBPs, CD155, CD166 and Fas are negatively regulated by the MAPK pathway in HCC cells. Some molecules like c-Met are positively regulated by the MAPK pathway. Pathway was partly generated with the help of the pathway builder from [www.proteinlounge.com](http://www.proteinlounge.com) and some molecules were adapted and modified from C. Falk.

Another important activating receptor on NK and T cells is DNAM-1 (CD226) with its ligand CD155. In HCC, the role of CD155 for the recognition by NK and T cells is still unclear. Here, we show for the first time that the three HCC cell lines express CD155. So far, it has been described that TuAg1/TagE4, which is the rat ortholog of the human poliovirus receptor CD155, is expressed on a high percentage of rat hepatocellular carcinomas and is induced during rat liver regeneration and acute liver injury (Erickson *et al.*, 2006). In my studies, CD155 expression could be increased by sorafenib and MEK inhibitors in HCC cells, indicating that CD155 expression is regulated via the MEK/ERK signaling pathway (Figure 54). In a SFB project, we will further analyze whether CD155 is an important ligand for the activation of NK cells in the liver. Using melanoma cell lines, we could observe that downregulation of CD155 reduced the levels of NK cell degranulation (Dissertation S. Maßen 2010), indicating the importance of the interaction of CD155 on the tumor cell with DNAM-1 on the NK cells. Moreover, it has been reported that NK cells require DNAM-1 for the elimination of tumor cells (Gilfillan *et al.*, 2008). On the other hand it could be shown that

primary ovarian carcinoma cells, which express CD155, can impair tumor targeting by the downregulation of DNAM-1 on NK cells (Carlsten *et al.*, 2009). In this setting, DNAM-1 contributes to the immune escape and plays a crucial role in NK cell-mediated recognition of several types of human tumors (Carlsten *et al.*, 2009). Moreover, CD155 has been implicated in tumor cell invasion and migration suggesting that CD155 itself contributes to tumorigenesis via its own signaling capacity (Sloan *et al.*, 2004). This shows that CD155 can have pro- and anti-tumorigenesis functions.

Overall, these data show that ligands for the inhibitory and activation receptors are mostly upregulated by MAPK inhibitors (Figure 54). Depending on the balance between activating and inhibitory receptors, NK cell cytotoxicity is increased or decreased.

Adhesion molecules are also important for the interaction between tumor and immune cells. They play an important role for cancer progression, tumor invasion and metastasis. Moreover, they are important for signal transduction, cell proliferation, morphogenesis and many other functions.

The adhesion molecule CD166 (ALCAM), which binds to CD6, was highly expressed on HepG2, Hep3B and Huh-7 cells, which has not been described so far. In a study from Horst *et al.* CD166 is defined as a surface marker associated with colorectal cancer stem cells (Horst *et al.*, 2009). Increased CD166 expression in colorectal carcinoma has been correlated with shortened patient survival (Weichert *et al.*, 2004). I could observe that treatment of HepG2, Hep3B and Huh-7 cells with sorafenib and MEK inhibitors, but not PLX4720, resulted in an upregulation of CD166 expression, indicating a negative regulation through the MEK/ERK pathway (Figure 54). Whether increased CD166 leads to a shortened patient survival in HCC is still unclear.

The adhesion molecule ICAM-1 is also important for the adhesion of tumor cells to and recognition by NK and T cells via their LFA-1 complex (Bryceson *et al.*, 2006; Sirim *et al.*, 2001). Interestingly, while sorafenib and PLX4720 increased, MEK inhibitors decreased ICAM-1 expression on HCC cells. A decrease in this ICAM-1/LFA-1 interaction would lead to presumably weaker immune cell recognition. Although the MEK inhibitors mediated a decrease of ICAM-1, a slight increase in NK cell degranulation against HepG2 cell was still seen, indicating that the adhesion is still good enough for inducing NK cell cytotoxicity.

Taken together, my results show that inhibition of the MAPK pathway modulates expression of several surface molecules (Figure 54). Due to the complex interaction between HCC and

NK cells, these changes of the surface molecules result in rather slight alterations of NK cell degranulation against HCC cells.

### 6.2.2 Hepatic NK and T cells

As described in the introduction, the liver has important functions in innate and adaptive immunity (Crispe, 2009; Parker and Picut, 2005). Interestingly, in the liver, the proportion and the phenotype of NK and T cells were different compared to the blood counterparts (Table 15+16; Figure 38+39). In healthy liver tissue, NK and CD8<sup>+</sup> T cells were enriched, which is accordance to a previous report (Morsy *et al.*, 2005; Norris *et al.*, 1998).

Despite the enrichment, the NK cell phenotype was different in the liver compared to peripheral blood counterparts (Figure 38). Liver NK cells showed a reduced proportion of CD56<sup>dim</sup> NK cells expressing CD16 and CD6, which is somewhat in accordance to a previously study where it was shown that liver NK cells have a higher proportion of CD16<sup>-</sup> NK cells (Burt *et al.*, 2009). Still, the mechanisms contributing to the regulation of the different NK cell composition is unclear. One possibility could be that at the endothelial cell layer there is a stop signal for CD56<sup>dim</sup> CD16<sup>+</sup> NK cells (Figure 55) or there are factors in the liver which contribute to a change of the NK cell phenotype. For the constellation of the immune cells in the liver, the microenvironment seems to play an important role (Crispe, 2009; Parker and Picut, 2005).

It has been described that TGFβ can promote the conversion of CD16<sup>+</sup> peripheral blood NK cells into CD16<sup>-</sup> NK cells (Keskin *et al.*, 2007). In the liver, LSECs, Tregs, MDSCs and HCC cells can secrete TGFβ, which may induce this conversion. In co-culture of peripheral NK cells with HCC cell lines, I could observe that the proportion of CD16<sup>+</sup> NK cells was reduced. It has to be further analyzed whether CD16 is downregulated on CD56<sup>dim</sup> NK cells or whether HCC cells differentially stimulate the CD16<sup>-</sup> NK fraction. Moreover, it has to be determined whether the reduced proportion of CD16<sup>+</sup> NK cells has an effect on the cytotoxicity. It has been reported that hepatic NK cells with fewer CD16<sup>+</sup> NK cells have a reduced cytotoxicity compared with their peripheral blood counterparts (Burt *et al.*, 2009). In contrast, it has been described that hepatic NK cells can spontaneously lyse NK-sensitive K562 target cells showing that hepatic NK cells are still cytotoxic (Doherty *et al.*, 1999). Although it was generally classified that CD56<sup>bright</sup> CD16<sup>-</sup> NK cells are mainly cytokine and chemokine producer and less cytotoxic (Di Santo, 2006), we could observe that both peripheral CD56<sup>bright</sup>

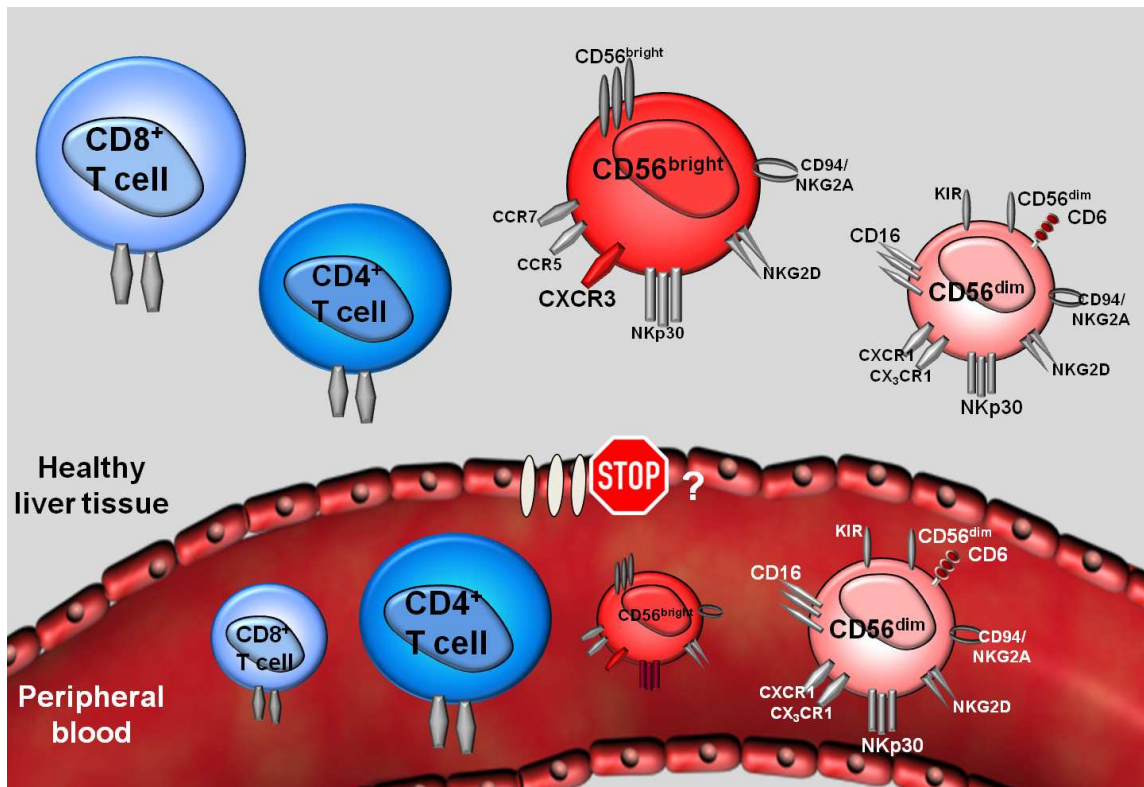


**Figure 55: Schematic diagram of T and NK cell population in liver tissue and peripheral blood.** While peripheral blood consist of ~10% CD56<sup>bright</sup> and CD16<sup>-</sup> NK cells and ~90% CD56<sup>dim</sup> CD16<sup>+</sup> NK cells, the liver tissue has a higher proportion of CD56<sup>bright</sup> CD16<sup>-</sup> NK cells and reduced proportion of CD56<sup>dim</sup> CD16<sup>+</sup> NK cells. The 2:1 ratio of CD4<sup>+</sup> to CD8<sup>+</sup> T cells in the blood was nearly switched to a 1:2 ratio in the liver tissue. The mechanisms, which lead to this altered NK and T cell proportions, are still unknown. Blood vessel was adapted from pathway builder from [www.proteinlounge.com](http://www.proteinlounge.com) and cells were adapted from C. Falk.

CD16<sup>-</sup> and CD56<sup>dim</sup> CD16<sup>+</sup> NK cells can degranulate to the same extent when they were stimulated with IL-2 and co-cultured with HLA class I negative target cells (Dissertation M. Braun 2008).

During cirrhosis and HCC, the composition of NK and T cells changed in the liver tissue. In cirrhosis a strong increase of CD56<sup>bright</sup> CD16<sup>-</sup> NK cells was detected. While in HCC tumor tissue NK cells were significantly reduced, higher percentages of NK cells were found in the surrounded “healthy” HCC tissue, indicating that the invasion of NK cells into the tumor tissue may be blocked. In a previous report it was observed that HCC patients displayed a substantial reduction in peripheral CD56<sup>dim</sup> CD16<sup>+</sup> NK cells compared with healthy subjects (Cai *et al.*, 2008). In contrast, CD8<sup>+</sup> T cell migration into the tumor tissue was not blocked, but rather enriched compared to CD4<sup>+</sup> T cells. These results are similar to the situation of NK and T cells in colorectal carcinoma tumor tissue. There, we could show that migration of NK cells into colorectal carcinoma tumor tissue is impaired during tumor development by

mechanisms that do not affect T cell infiltration and despite high levels of chemokines and cytokines (Halama *et al.*, 2011). In HCC tissue, CCL4 concentration was elevated, indicating that CCL4 might be involved in increased CD8<sup>+</sup> T cell recruitment into the tumor tissue. In cirrhotic and HCC tissue, high chemokine levels like CXCL8, 9 and 10 were also observed. These chemokines are ligands for the chemokine receptor CXCR3, which is highly expressed on CD56<sup>bright</sup> CD16<sup>-</sup> NK cells and only to a low level on CD56<sup>dim</sup> CD16<sup>+</sup> NK cells, but expression levels also depend on the activation status (Robertson, 2002). This high concentration can be an explanation for the strong increase of CD56<sup>bright</sup> CD16<sup>-</sup> NK cells in cirrhotic tissue, but not for the absence in the tumor tissue. CCL5 is increased in cirrhotic tissue, but not in HCC tumor tissue, which might explain the increase in CD56<sup>bright</sup> NK cell in the cirrhotic liver tissue, because CCR5, the receptor for CCL5, is higher expressed on CD56<sup>bright</sup> NK cells. Another possibility could be that the concentrations of some chemokines like CXCL10 were too high in HCC tissue leading to an inhibition of NK cell migration. In a recent publication it was shown that CXCL10 might block the migration of NK cells to the liver (Hintermann *et al.*, 2010). This group could show that CXCL10 is implicated in liver fibrosis, where NK cells are also reduced. Using CXCL10 deficient mice, they observed reduced fibrosis with less B- and T cells infiltration, but increased NK cells in the liver indicating that CXCL10 negatively regulates NK cell migration in this model. Besides the regulation by chemokines, it has been reported that MDSCs and Tregs are enriched in tumor tissue (Cao *et al.*, 2008). It was shown that addition of Tregs from HCC patients efficiently inhibited the anti-tumor ability of autologous NK cells in vitro (Cai *et al.*, 2008). MDSCs can inhibit NK cells in patients with HCC via the NKp30 receptor (Hoechst *et al.*, 2009). Interestingly, it has been reported that sorafenib treatment decrease MDSC and Treg numbers in the liver (Cao *et al.*, 2008). It has to be analyzed whether these cells also contribute to the blockage of NK cell migration into the tumor and whether sorafenib treatment increases NK cell numbers in the tumor tissue.

These results indicate that just the presence or absence of a chemokine is not enough to decide whether NK cells are recruited to the liver or not. Recruitment of NK cells into the liver seem to be differently regulated compared to the recruitment of T cells. The mechanisms of how NK cells are impaired in HCC tumor tissue is still unknown and has to be determined in the future. Moreover, the role of chemokines for the recruitment of NK cells has to be further analyzed. Due to the importance of NK cells for fighting against the tumor and it was reported

that higher NK cell numbers in HCC patients correlate with longer survival (Chew *et al.*, 2010). Therefore, it can be a successful approach to modulate the chemokine milieu towards infiltration of NK cells into the tumor tissue. It has to be shown, whether the reduced chemokine levels induced by sorafenib has an impact on the recruitment of NK cell into the tumor tissue.

### 6.2.3 Secretion of chemokines and growth factors by HCC cells

Features of tumorigenesis are uncontrolled growth, the development of new blood vessels and downregulation of the immune response. For this purpose, tumor cells secrete a variety of chemokines and growth factors. It could be observed that HCC cells secrete high amounts of CXCL8, CXCL10, VEGF, TGF $\beta$  and ICAM-1 and to intermediate level CXCL12, M-CSF, SCGF- $\beta$  and MIF (Figure 40 – Figure 42). Many of these factors are involved in angiogenesis and tumor escape mechanisms.

Because several chemokines are regulated via the MAPK pathway (Liu *et al.*, 2008; Whittaker *et al.*, 2010), I wanted to know how chemokine and growth factor secretion is affected by inhibition of MAPK pathway. Although there are several reports about the MAPK inhibitors, only a few have analyzed their effects on some chemokine secretion. I could observe that in HCC cells, CCL5, VEGF, M-CSF, TGF $\beta$  and soluble ICAM-1 were positively regulated via the MAPK pathway and, therefore, were significantly reduced by MAPK inhibitors. In HepG2 cells, also CXCL8 and IL-1RA seemed to be positively regulated by the MEK/ERK pathway. Curry *et al.* could show that M-CSF induces secretion of VEGF through the MEK/ERK signaling pathway (Curry *et al.*, 2008). In trophoblast cells, CCL5 was inhibited by the MEK inhibitor U0126 but also by the JNK inhibitor SP600125 (Renaud *et al.*, 2009). The p38 and ERK pathway inhibitors SB203580 and U0126 revealed that MAPK signaling regulates CXCL10 and CXCL8 at the mRNA level (Lee *et al.*, 2008a; Tibbles *et al.*, 2002). CXCL8 was also inhibited by the MEK inhibitor PD98059, the p38 inhibitor SB203580 and the JNK inhibitor II (Liu *et al.*, 2008). These data show that dependent on the cell type the secretion of chemokines and growth factors is not regulated by the MEK/ERK pathway alone, but also by other signaling pathways like JNK or p38 (Figure 56).

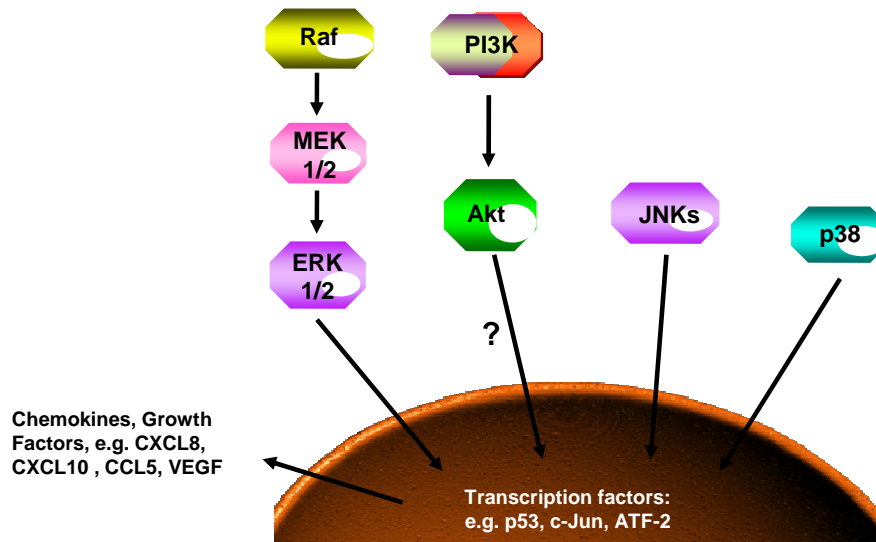


**Figure 56: Regulation of chemokines and growth factors by different signaling pathways.** Cytokines, chemokines and growth factors are often regulated by at least one of MEK/ERK, PI3K/Akt, JNK or p38 signaling pathways. Pathway was partly generated with the help of the pathway builder from [www.proteinlounge.com](http://www.proteinlounge.com).

Of the factors regulated by the MAPK pathway, CXCL8, CCL5, VEGF, M-CSF and TGF $\beta$  have been shown to be involved in angiogenesis. For their regulation, the hypoxia-inducible factor (HIF) seems to be a central regulator. HIF gets activated in the nucleus by several pathways like Ras/Raf/MEK/ERK, PI3K/Akt and by STATs (Whittaker *et al.*, 2010). Downregulation of these molecules by the MAPK inhibitors suggests a reduction in the potential for angiogenesis in HCC. In addition, it was reported that sorafenib blocks angiogenesis by inhibiting VEGFR and PFGFR, which resulted in reduced microvessels in the tumor (Liu *et al.*, 2006). Besides inducing angiogenesis, CXCL8 has also been shown to act as a growth promoter in several tumor cells. Therefore, inhibition of CXCL8 by sorafenib and the MEK inhibitors represent an important side effect for the treatment of HCC.

Thus, sorafenib seems to have broader and stronger effect on the inhibition of chemokines and growth factors than the MEK inhibitors. This indicates that other signaling pathways besides MEK/ERK play an important role for the regulation of chemokine and growth factor secretion (Figure 56). For some chemokines like CXCL10, their secretions seem to be differently regulated by sorafenib and the MEK inhibitors. Importantly, other factors like SCGF- $\beta$  were not altered by MAPK inhibitors indicating that the MAPK pathway specifically regulates some but not all chemokines and growth factors.

In contrast to the downregulation of many chemokines by MAPK inhibitors, the macrophage migration inhibitory factor (MIF) showed a different regulation, i.e. an upregulation by sorafenib and MEK inhibitors. In several tumors, such as colon cancer, melanoma and HCC, MIF is generally overexpressed (Han and Zhang, 2010; Lugrin *et al.*, 2009; Ren *et al.*, 2003). Among other effects, MIF is important for the development and progression of HCC and plasma MIF levels decreased after HCC resection. Thus, MIF is currently investigated as a prognostic marker for HCC (Han and Zhang, 2010; Zhao *et al.*, 2011). MIF has several different functions; it plays a pivotal role for cell proliferation, for inhibition of apoptosis, tumorigenesis, angiogenesis and inflammation (Baron *et al.*, 2011; Lugrin *et al.*, 2009). Moreover, it regulates the secretion of other cytokines, chemokines and growth factors. In HCC, it could be shown that MIF induced increased secretion of CXCL8 and VEGF (Ren *et al.*, 2003). For its mechanism of action, MIF binds to the CD74/CD44 receptor complex, which leads to activation of the MEK/ERK pathway, to activation or inhibition of the JNK pathway depending on the cell type, and to activation of p38 (Figure 57) (Baron *et al.*, 2011; Cheng *et al.*, 2010; Lue *et al.*, 2011). All these signals lead to an enhanced cell proliferation and cell survival (Lue *et al.*, 2011). Furthermore, MIF can act in an autocrine loop inducing the expression of angiogenic factors like CXCL8 and VEGF, and the migration of tumor cells, therefore, stimulating angiogenesis and metastasis in HCC (Ren *et al.*, 2003). Inhibition of the MEK/ERK pathway in MIF-treated cells reduces the secretion of the angiogenic factors CXCL8 and VEGF, which is in accordance with my results where CXCL8 and VEGF is reduced in HCC cells after MAPK inhibitor treatment (Lue *et al.*, 2011).

In tumor biology, MIF also contributes to tumorigenesis by providing a tumor escape mechanism by downregulating NKG2D on T and NK cells (Krockenberger *et al.*, 2008). Furthermore, MIF is a potent apoptosis inhibitor and a modulator of pro-oxidative stress-induced apoptosis, but the exact mechanisms are still unclear. It has been reported that MIF can suppress p53 activity (Fingerle-Rowson *et al.*, 2003; Han and Zhang, 2010; Hudson *et al.*, 1999), which could in part explain why p53 is decreased in HCC cells after MAPK inhibitor treatment.

Although all these aspects are known about the function of MIF, it is still unclear, how MIF secretion is regulated. I could observe that in all three HCC cell lines MIF secretion was rather enhanced and the profile of MIF concentrations with MAPK inhibitor treatment correlated with the profile of apoptosis induction (Figure 18 and Figure 36). The question is whether MIF secretion is induced by apoptosis or whether MIF is directly regulated by

signaling pathways like MEK/ERK and PI3K/Akt (Figure 57). It is interesting to see that in Huh-7 cells induction of apoptosis and secretion of MIF are only induced by sorafenib and not by the MEK inhibitors, indicating that the secretion of MIF and the induction of apoptosis follow the same regulatory mechanisms. Because MIF is implicated in cell proliferation, angiogenesis and inhibition of apoptosis, the secretion of MIF in apoptotic cells could be a rescue mechanism for other cells to become resistance against apoptosis or through the inhibition of immune cells by downregulation of NKG2D.

It will be further analyzed in our lab whether increased MIF lead to tumor escape through inducing resistance or whether MIF is “just” a factor in HCC cells correlating with apoptosis. Because MIF has been associated with tumor aggressiveness and metastasis (Lugrin *et al.*, 2009), increased MIF secretion might lead to the recurrence of the tumor in sorafenib-treated HCC patients. Therefore, it would be of great interest to see whether survival of sorafenib-treated HCC patients correlates with the plasma and/or tissue MIF levels and whether blocking of MIF could improve HCC therapy.

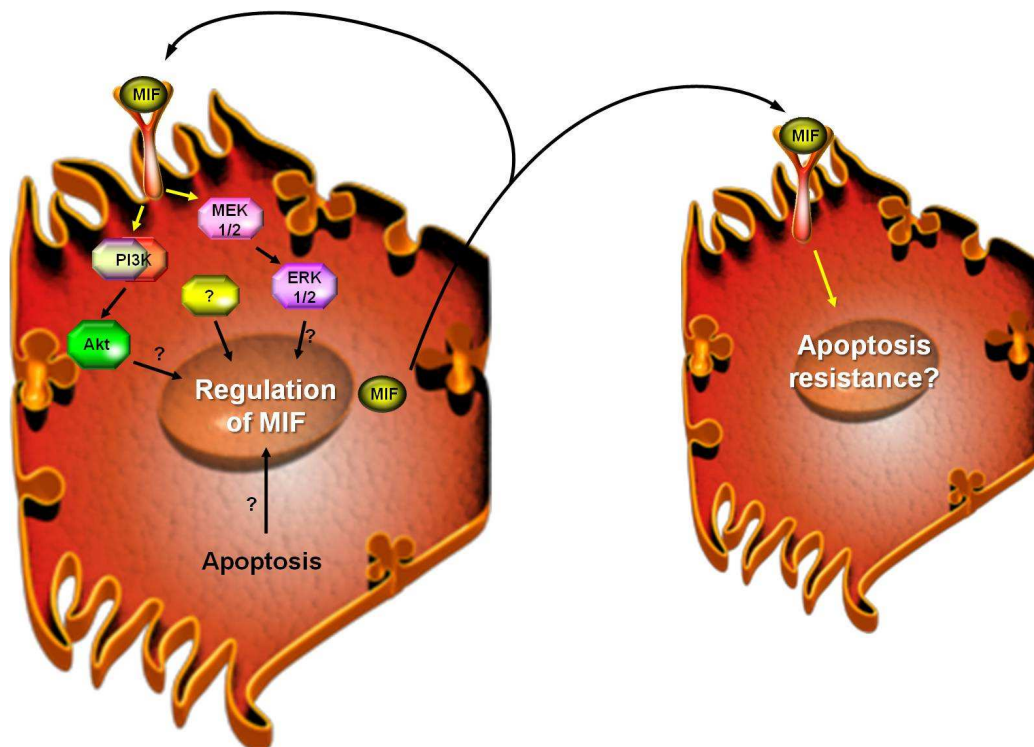


**Figure 57: Possible regulation mechanisms of MIF in HCC cells.** MIF might be regulated by MEK/ERK signaling, Akt signaling or other signaling pathways. Moreover, apoptosis could positively induce MIF secretion. Secreted MIF can stimulate the same cell in an autocrine loop or other cells in a paracrine loop. There, MIF might induce resistance against apoptosis. Pathway was partly generated with the help of the pathway builder from [www.proteinlounge.com](http://www.proteinlounge.com).

### 6.2.4 Conclusion

Taken together, my findings show that HCC cell lines highly express a variety of surface molecules which are associated with tumorigenesis and poor survival. In contrast, several ligands, which are important for NK cell cytotoxicity, are only slightly expressed or absent. Inhibition of the MAPK pathway modulates surface molecule expression with some ERK-independent side effect of certain MAPK inhibitors, in particular sorafenib. Due to the complex interactions with the balance of activating and inhibitory receptor ligands, it cannot be precisely defined which of these surface molecules influences NK and T cell cytotoxicity the most. Nevertheless, HCC cells induce NK cell killing to a certain extent, however, MAPK inhibition does not strongly improve the killing capacity of NK cells.

HCC tumor cells altered the phenotype of NK cells *in vitro* and NK cells were absent in HCC tumor tissue despite high chemokine levels indicating that NK cells might be a key effector cell type for fighting against HCC. Therefore, one goal for HCC treatment besides inducing apoptosis in tumor tissue and reducing angiogenesis should be to increase the number of activated NK cells in the tumor tissue.

Moreover, a variety of chemokines and growth factors are produced by HCC cells, which favor tumorigenesis and can induce angiogenesis. The chemokines produced by these tumor cells have been postulated as key factors in modulating immune response either against or in favor of tumorigenesis in the microenvironment. MAPK inhibition led to a downregulation of the cytokine, chemokine and growth factor secretion. Through this blockage, the potency of HCC cells to induce angiogenesis and tumor progression is reduced. Furthermore, MIF might be responsible for the resistance of the tumor against therapy suggesting a general resistance mechanism in cancer. Blocking of MIF might improve HCC treatment.

## 6.3 HCC and MAPK Pathway in the Tissue

### 6.3.1 Hepatic microenvironment

The hepatic microenvironment is heterogeneous with many different cytokines and chemokines, which are secreted by a variety of different cells (Chew *et al.*, 2010). During tumor development and progression, microenvironment is often changed in a pro-angiogenic and anti-immune situation. There, the chemokine milieu may be altered in the direction that immune cells cannot migrate into the tumor tissue. While in cirrhotic and HCC liver tissue some chemokines showed a tendency of decreased levels, other chemokines were increased, indicating distinct roles of chemokines for the development of cirrhosis and the progression towards HCC (Figure 44). It has been described that chemokines play an important role for several pathological conditions, including cancer (Platanias, 2005). For example, it has been shown that fibrosis can be induced by CXCL10 (Hintermann *et al.*, 2010). The chemokine CXCL8 is implicated in angiogenesis and was elevated in both cirrhotic and HCC tumor tissue. In a previous study, we could show that the concentration of several chemokines was higher in colorectal cancer than in the surrounding healthy tissue indicating a general mechanism for the progression of some tumors (Halama *et al.*, 2011). In cirrhotic and HCC tumor tissue, not all chemokines were elevated. For some chemokines like CCL3, CCL7 and CCL27 the profile in cirrhosis and HCC seemed to be separated in two populations with one increased and one decreased population showing the diversity of cirrhosis and HCC patients. Moreover, there are differences in the microenvironment between cirrhosis and HCC. For example, CCL5 seems to play a role for cirrhosis, but not for HCC.

Besides the chemokines, other factors like VEGF and PDGF also induce angiogenesis and are upregulated in HCC (Figure 45) showing that in HCC the angiogenic balance is disrupted. HCC has been described as a highly vascular tumor and angiogenesis seems to play a pivotal role for HCC development and progression (Whittaker *et al.*, 2010; Yang *et al.*, 2011).

There is currently the debate whether the HCC tumor microenvironment is pro- or anti-inflammatory (Schrader and Iredale, 2011). In general, the liver is rather tolerogenic than immunogenic, due to the immunosuppressive cytokines (Crispe, 2009). In HCC patients, it has been described that in the tumor tissue the number of Tregs and MDSCs are increased (Cai *et al.*, 2008; Hoechst *et al.*, 2009; Korangy *et al.*, 2010b). This enhancement of Tregs in

HCC has been associated with poor prognosis (Gao *et al.*, 2007). In cirrhosis and HCC, the pro-inflammatory molecules IFN $\gamma$  and TNF $\alpha$  were partly reduced indicating that the tumor is trying to evade immune recognition. This is probably achieved by recruited Tregs and MDSCs (Kao *et al.*, 2011). Moreover, it has been described that HCC patients, which have a predominant Th1 signaling (e.g IFN $\gamma$ , IL-2 and TNF $\beta$ ) in the tumor tissue, develop less frequently metastases indicating that a certain inflammatory microenvironment is favorable in controlling the tumor and enhancing survival of HCC patients (Chew *et al.*, 2010). In addition, an increased level of IL-1RA, which is an inhibitor of the pro-inflammatory cytokine IL-1, was observed in liver tissue of colorectal carcinoma resections, cirrhosis and HCC showing that anti-inflammatory factors are increased in HCC tumor development.

Not only inflammatory cytokines are reduced in cirrhosis and HCC, but also important anti-inflammatory cytokines like IL-10, indicating that it is not a clear shift towards anti-inflammatory or tolerogenic conditions. Other cytokines like IL-9 were also reduced in cirrhosis and HCC, but not in liver tissue of colorectal metastasis. IL-9 is mainly produced by CD4<sup>+</sup> T cells and implicated in Th2 responses and humoral immunity (Pilette *et al.*, 2002). In HCC and cirrhotic tissue, CD4<sup>+</sup> T cells are decreased and CD8<sup>+</sup> T cells increased compared to healthy liver tissue. This might explain the decreased level of IL-9. Besides IL-9, it has been described that CCL3 and CCL4 actively recruit CD8<sup>+</sup> T cells (Castellino *et al.*, 2006).

In contrast, the inflammatory and growth-promoting factor IL-6 was elevated in some HCC tissue samples and has been reported as a mediator for HCC progression in liver inflammation (Germano *et al.*, 2008; Yang *et al.*, 2011). On the other hand, it has been described that IL-6 together with CCL2 correlate positively with patient survival (Chew *et al.*, 2010). It has to be determined whether IL-6 tissue concentration correlates with progression of HCC. Besides IL-6, also the pro-inflammatory cytokine IL-16, which is mostly secreted by CD8<sup>+</sup> T cells was increased in resected liver tissue of colorectal metastases, cirrhosis and HCC, showing that not all pro-inflammatory cytokines are decreased in HCC.

Besides chemokines and cytokines, stimulating and growth factors play an important role in carcinogenesis. Growth factors like VEGF and SCGF- $\beta$  are often overexpressed in tumor tissue. SCGF- $\beta$  is a good marker for discriminating HCC tissue from healthy liver tissue and resected liver tissue of colorectal metastases (Figure 46). Interestingly, HGF was increased in cirrhotic tissue, but not in HCC tissue indicating that HGF plays a pivotal role in cirrhosis and seems to be necessary HCC pathogenesis (Yang *et al.*, 2011). HGF is mainly expressed by hepatic stellate cells and myofibroblasts, which get activated during fibrosis and cirrhosis and

then secrete HGF. With the help of a bioinformatic approach, we could detect that HGF is as a good prediction marker for cirrhosis.

Soluble adhesion molecules like ICAM-1 and VCAM-1 are often found to be increased in patients with tumors like colorectal carcinoma (Halama *et al.*, 2011). We could detect that in resected liver tissue of colorectal metastases, in cirrhotic and HCC tissue the concentrations of ICAM-1 and VCAM-1 were increased compared to healthy liver tissue. Increased levels of ICAM-1 and VCAM-1 have been associated with increased risk of invasion and metastasis. It shows that pathologic “healthy” liver tissue of patients with colorectal carcinoma resection has already a changed microenvironment favoring the migration of tumor cells into the liver, which is a preferred organ for metastasis of colorectal carcinoma.

### **6.3.2 Modulation of the microenvironment by MAPK inhibitors**

HCC tumor cells secrete a variety of chemokines and growth factors and their secretion was modulated by MAPK inhibition. In the tissue, there are several different cell types contributing to the microenvironment and it is more difficult to evaluate the effects of the MAPK inhibitors, since different cell types react differently to these inhibitors. In HCC tissue, several chemokines but also cytokines and growth factors were elevated probably contributing to the progression of HCC. *Ex vivo* tissue treatment with sorafenib for only 8 h already mediated a change in the microenvironment in the HCC tissue showing that the microenvironment can be rapidly modulated (Figure 47, Figure 49). Moreover, the microenvironment was also altered in the adjacent “healthy” tissue indicating that sorafenib has effects beyond the tumor tissue (Figure 48, Figure 50).

In the HCC tumor tissue, the increased angiogenic factors like CXCL8, VEGF and CXCL1 could be reduced with sorafenib treatment showing that sorafenib has angiostatic activity in the tumor tissue and that this effect seems to be partly MAPK independent. This indicates that for an effective inhibition of angiogenesis in HCC, specific MAPK inhibitors are not sufficient for HCC treatment.

Sorafenib reduced not only the concentration of factors involved in angiogenesis, but also some others. For example, IL-6, which has been implicated in the progression of HCC, was reduced after sorafenib treatment indicating that sorafenib has a broad effect for the fight against HCC. In HCC tumor tissue, CXC chemokines were increased and could be decreased

with sorafenib treatment. In the future, it has to be analyzed what consequence this modulation of chemokine has for the constellation of the immune cells of the liver.

In a first experiment, we could observe that the MEK inhibitors U0126, AZD6244 and PD0325901 had an effect on the microenvironment as well (data not shown). Already, the results clearly show that sorafenib and the other tested MAPK inhibitors have also an effect on the healthy liver tissue. Interestingly, even the mutant-specific B-Raf inhibitor PLX4720 seems to have an effect on the HCC tumor tissue and the healthy liver, indicating that the inhibition of the wild-type B-Raf is strong enough to induce an alteration of the microenvironment.

Our preliminary data show that sorafenib, the MEK inhibitors and the mutant-specific B-Raf inhibitor PLX4720 have some opposing effects suggesting partly independent effects of the MAPK pathway. Sorafenib seems to have broader “side effects” on other signaling pathways and for the regulation of cytokine and chemokine secretion in the tissue, which is in accordance to the *in vitro* studies. As other groups have shown, the JNK, p38 and NFκB pathways are important for the secretion of several cytokines, chemokines and growth factors (Kumar *et al.*, 2009; Nagai *et al.*, 2011; Venkatesha *et al.*, 2005; Wong *et al.*, 2005).

In the future it has to be analyzed to what extend the microenvironment is altered by the MAPK inhibitors and whether treatment of HCC normalize the cytokine and chemokine milieu in the tumor tissue. Moreover, it is interesting to analyze how these alterations of the microenvironment effect the composition of immune cells in HCC tumor tissue and what consequences this will have for the patient.

### 6.3.3 Conclusions

The tumor microenvironment is a very complex network and the progression towards cirrhosis and HCC changes the microenvironment in the liver. Several different cytokine and chemokine modifications are involved in liver diseases and the development into HCC, but the exact mechanisms are still to be solved. The data indicate that the cirrhotic and tumor microenvironment are not clearly shifted to a pro-inflammatory or an anti-inflammatory direction, but rather both pro- and anti-inflammatory sides are altered. The decrease of pro-inflammatory factors in HCC tumor tissue suggests that a partial inflammatory condition is essential to suppress tumor development in the liver. In the future, it has to be analyzed which cytokines and chemokines are the key players for regulating the immune system in the tumor tissue. Since HCC is different among patients, which is probably induced e.g. by etiology, it is difficult to unravel these key players for tumor development and progression. Thus, modulation of the tumor microenvironment might be one strategy for tumor treatment in the future. Sorafenib or MEK inhibitor treatment seems to be on the right way for the modulation of the microenvironment, since factors important for angiogenesis and tumor growth are reduced. However, the consequences of the reduction of the cytokine and chemokine milieu for the healthy and tumor liver tissue have to be revealed. Due to the broader effects of sorafenib on the modulation of the microenvironment, inhibition of only the MAPK pathway seems not to be sufficient. A combinational therapy targeting different pathways might be a more effective strategy for HCC treatment.

Alterations of the tumor but also the healthy microenvironment will have an effect on the migration and composition of intrahepatic lymphocytes like NK cells. Hopefully, alterations of the microenvironment (e.g. reduction of the chemokines induced by sorafenib), will reconstitute NK cell numbers in the tumor tissue.

In my opinion, it is an important approach to combine small molecule treatment like sorafenib with other drugs to trigger tumor cell death on the one hand and but also to alter the tumor microenvironment in such a way that lymphocyte migration into the tumor tissue is increased and the immune system is stimulated to recognize and kill the tumor cells. By this approach, the tumor is attacked by different mechanisms and it will be harder for the tumor to develop evasion or resistance mechanisms.

## 7 References

- Abou-Alfa GK, Johnson P, Knox JJ, Capanu M, Davidenko I, Lacava J *et al* (2010). Doxorubicin plus sorafenib vs doxorubicin alone in patients with advanced hepatocellular carcinoma: a randomized trial. *JAMA* **304**: 2154-60.
- Adams DH, Eksteen B (2006). Aberrant homing of mucosal T cells and extra-intestinal manifestations of inflammatory bowel disease. *Nat Rev Immunol* **6**: 244-51.
- Alsafadi S, Tourpin S, Andre F, Vassal G, Ahomadegbe JC (2009). P53 family: at the crossroads in cancer therapy. *Curr Med Chem* **16**: 4328-44.
- Alter G, Malenfant JM, Altfeld M (2004). CD107a as a functional marker for the identification of natural killer cell activity. *Journal of Immunological Methods* **294**: 15-22.
- Anfossi N, Andre P, Guia S, Falk CS, Roetynck S, Stewart CA *et al* (2006). Human NK cell education by inhibitory receptors for MHC class I. *Immunity* **25**: 331-42.
- Aravalli RN, Steer CJ, Cressman ENK (2008). Molecular mechanisms of hepatocellular carcinoma. *Hepatology* **48**: 2047-2063.
- Atienza JM, Zhu J, Wang X, Xu X, Abassi Y (2005). Dynamic monitoring of cell adhesion and spreading on microelectronic sensor arrays. *J Biomol Screen* **10**: 795-805.
- Balmanno K, Chell SD, Gillings AS, Hayat S, Cook SJ (2009). Intrinsic resistance to the MEK1/2 inhibitor AZD6244 (ARRY-142886) is associated with weak ERK1/2 signalling and/or strong PI3K signalling in colorectal cancer cell lines. *Int J Cancer* **125**: 2332-41.
- Balmanno K, Cook SJ (2009). Tumour cell survival signalling by the ERK1/2 pathway. *Cell Death Differ* **16**: 368-77.
- Baron N, Deuster O, Noelker C, Stuer C, Strik H, Schaller C *et al* (2011). Role of macrophage migration inhibitory factor in primary glioblastoma multiforme cells. *J Neurosci Res* **89**: 711-7.
- Baroni TE, Wang T, Qian H, Dearth LR, Truong LN, Zeng J *et al* (2004). A global suppressor motif for p53 cancer mutants. *Proc Natl Acad Sci U S A* **101**: 4930-5.
- Bossy-Wetzel E, Bakiri L, Yaniv M (1997). Induction of apoptosis by the transcription factor c-Jun. *EMBO J* **16**: 1695-709.
- Braun M, Muller B, Ter Meer D, Raffegerst S, Simm B, Wilde S *et al* (2010). The CD6 Scavenger Receptor Is Differentially Expressed on a CD56 Natural Killer Cell Subpopulation and Contributes to Natural Killer-Derived Cytokine and Chemokine Secretion. *J Innate Immun*.

- Breuhahn K, Longerich T, Schirmacher P (2006). Dysregulation of growth factor signaling in human hepatocellular carcinoma. *Oncogene* **25**: 3787-800.
- Bryceson YT, March ME, Ljunggren HG, Long EO (2006). Activation, coactivation, and costimulation of resting human natural killer cells. *Immunol Rev* **214**: 73-91.
- Burt BM, Plitas G, Zhao Z, Bamboat ZM, Nguyen HM, Dupont B *et al* (2009). The lytic potential of human liver NK cells is restricted by their limited expression of inhibitory killer Ig-like receptors. *J Immunol* **183**: 1789-96.
- Cai L, Zhang Z, Zhou L, Wang H, Fu J, Zhang S *et al* (2008). Functional impairment in circulating and intrahepatic NK cells and relative mechanism in hepatocellular carcinoma patients. *Clin Immunol* **129**: 428-37.
- Cao W, Xi X, Wang Z, Dong L, Hao Z, Cui L *et al* (2008). Four novel ULBP splice variants are ligands for human NKG2D. *International Immunology* **20**: 981-91.
- Carayannopoulos LN, Yokoyama WM (2004). Recognition of infected cells by natural killer cells. *Curr Opin Immunol* **16**: 26-33.
- Carlsten M, Norell H, Bryceson YT, Poschke I, Schedvins K, Ljunggren HG *et al* (2009). Primary human tumor cells expressing CD155 impair tumor targeting by down-regulating DNAM-1 on NK cells. *J Immunol* **183**: 4921-30.
- Casado JG, Pawelec G, Morgado S, Sanchez-Correa B, Delgado E, Gayoso I *et al* (2009). Expression of adhesion molecules and ligands for activating and costimulatory receptors involved in cell-mediated cytotoxicity in a large panel of human melanoma cell lines. *Cancer Immunol Immunother* **58**: 1517-26.
- Castellino F, Huang AY, Altan-Bonnet G, Stoll S, Scheinecker C, Germain RN (2006). Chemokines enhance immunity by guiding naive CD8+ T cells to sites of CD4+ T cell-dendritic cell interaction. *Nature* **440**: 890-5.
- Chan CJ, Andrews DM, McLaughlin NM, Yagita H, Gilfillan S, Colonna M *et al* (2010). DNAM-1/CD155 interactions promote cytokine and NK cell-mediated suppression of poorly immunogenic melanoma metastases. *J Immunol* **184**: 902-11.
- Chen G, Hitomi M, Han J, Stacey DW (2000). The p38 pathway provides negative feedback for Ras proliferative signaling. *J Biol Chem* **275**: 38973-80.
- Chen KF, Chen HL, Tai WT, Feng WC, Hsu CH, Chen PJ *et al* (2011). Activation of phosphatidylinositol 3-kinase/akt signaling pathway mediates acquired resistance to sorafenib in hepatocellular carcinoma cells. *J Pharmacol Exp Ther* **337**: 155-61.
- Chen KF, Yeh PY, Yeh KH, Lu YS, Huang SY, Cheng AL (2008). Down-regulation of phospho-Akt is a major molecular determinant of bortezomib-induced apoptosis in hepatocellular carcinoma cells. *Cancer Res* **68**: 6698-707.

- Cheng Q, McKeown SJ, Santos L, Santiago FS, Khachigian LM, Morand EF *et al* (2010). Macrophage migration inhibitory factor increases leukocyte-endothelial interactions in human endothelial cells via promotion of expression of adhesion molecules. *J Immunol* **185**: 1238-47.
- Chew V, Tow C, Teo M, Wong HL, Chan J, Gehring A *et al* (2010). Inflammatory tumour microenvironment is associated with superior survival in hepatocellular carcinoma patients. *J Hepatol* **52**: 370-9.
- Commins SP, Borish L, Steinke JW (2010). Immunologic messenger molecules: cytokines, interferons, and chemokines. *J Allergy Clin Immunol* **125**: S53-72.
- Crispe IN (2003). Hepatic T cells and liver tolerance. *Nat Rev Immunol* **3**: 51-62.
- Crispe IN (2009). The liver as a lymphoid organ. *Annual Review of Immunology* **27**: 147-63.
- Crowe DL, Shemirani B (2000). The transcription factor ATF-2 inhibits extracellular signal regulated kinase expression and proliferation of human cancer cells. *Anticancer Res* **20**: 2945-9.
- Curry JM, Eubank TD, Roberts RD, Wang Y, Pore N, Maity A *et al* (2008). M-CSF signals through the MAPK/ERK pathway via Sp1 to induce VEGF production and induces angiogenesis in vivo. *PLoS One* **3**: e3405.
- Davies BR, Logie A, McKay JS, Martin P, Steele S, Jenkins R *et al* (2007). AZD6244 (ARRY-142886), a potent inhibitor of mitogen-activated protein kinase/extracellular signal-regulated kinase kinase 1/2 kinases: mechanism of action in vivo, pharmacokinetic/pharmacodynamic relationship, and potential for combination in preclinical models. *Mol Cancer Ther* **6**: 2209-19.
- De Cesare D, Vallone D, Caracciolo A, Sassone-Corsi P, Nerlov C, Verde P (1995). Heterodimerization of c-Jun with ATF-2 and c-Fos is required for positive and negative regulation of the human urokinase enhancer. *Oncogene* **11**: 365-76.
- Deignan T, Curry MP, Doherty DG, Golden-Mason L, Volkov Y, Norris S *et al* (2002). Decrease in hepatic CD56(+) T cells and V alpha 24(+) natural killer T cells in chronic hepatitis C viral infection. *J Hepatol* **37**: 101-8.
- Di Santo JP (2006). Natural killer cell developmental pathways: a question of balance. *Annu Rev Immunol* **24**: 257-86.
- Doherty DG, Norris S, Madrigal-Estebas L, McEntee G, Traynor O, Hegarty JE *et al* (1999). The human liver contains multiple populations of NK cells, T cells, and CD3+CD56+ natural T cells with distinct cytotoxic activities and Th1, Th2, and Th0 cytokine secretion patterns. *J Immunol* **163**: 2314-21.
- Downward J (2003). Targeting RAS signalling pathways in cancer therapy. *Nat Rev Cancer* **3**: 11-22.

- Eagle RA, Flack G, Warford A, Martinez-Borra J, Jafferji I, Traherne JA *et al* (2009a). Cellular expression, trafficking, and function of two isoforms of human ULBP5/RAET1G. *PLoS One* **4**: e4503.
- Eagle RA, Traherne JA, Hair JR, Jafferji I, Trowsdale J (2009b). ULBP6/RAET1L is an additional human NKG2D ligand. *Eur J Immunol* **39**: 3207-16.
- Eferl R, Ricci R, Kenner L, Zenz R, David JP, Rath M *et al* (2003). Liver tumor development. c-Jun antagonizes the proapoptotic activity of p53. *Cell* **112**: 181-92.
- El-Serag HB, Rudolph KL (2007). Hepatocellular carcinoma: epidemiology and molecular carcinogenesis. *Gastroenterology* **132**: 2557-76.
- Erickson BM, Thompson NL, Hixson DC (2006). Tightly regulated induction of the adhesion molecule necl-5/CD155 during rat liver regeneration and acute liver injury. *Hepatology* **43**: 325-34.
- Fabregat I (2009). Dysregulation of apoptosis in hepatocellular carcinoma cells. *World J Gastroenterol* **15**: 513-20.
- Farazi PA, DePinho RA (2006). Hepatocellular carcinoma pathogenesis: from genes to environment. *Nat Rev Cancer* **6**: 674-87.
- Favata MF, Horiuchi KY, Manos EJ, Daulerio AJ, Stradley DA, Feeser WS *et al* (1998). Identification of a novel inhibitor of mitogen-activated protein kinase kinase. *J Biol Chem* **273**: 18623-32.
- Fernandez NC, Treiner E, Vance RE, Jamieson AM, Lemieux S, Raulet DH (2005). A subset of natural killer cells achieves self-tolerance without expressing inhibitory receptors specific for self-MHC molecules. *Blood* **105**: 4416-23.
- Fingerle-Rowson G, Petrenko O, Metz CN, Forsthuber TG, Mitchell R, Huss R *et al* (2003). The p53-dependent effects of macrophage migration inhibitory factor revealed by gene targeting. *Proc Natl Acad Sci U S A* **100**: 9354-9.
- Fleischer B, Schulze-Bergkamen H, Schuchmann M, Weber A, Biesterfeld S, Muller M *et al* (2006). Mcl-1 is an anti-apoptotic factor for human hepatocellular carcinoma. *Int J Oncol* **28**: 25-32.
- Flores ER, Tsai KY, Crowley D, Sengupta S, Yang A, McKeon F *et al* (2002). p63 and p73 are required for p53-dependent apoptosis in response to DNA damage. *Nature* **416**: 560-564.
- Fox SI (2006). *Human physiology*, 9th edn. McGraw-Hill: Boston, 1-770pp.
- Friday BB, Adjei AA (2008). Advances in targeting the Ras/Raf/MEK/Erk mitogen-activated protein kinase cascade with MEK inhibitors for cancer therapy. *Clin Cancer Res* **14**: 342-6.
- Gao B, Jeong WI, Tian Z (2008). Liver: An organ with predominant innate immunity. *Hepatology* **47**: 729-36.

- Gao Q, Qiu SJ, Fan J, Zhou J, Wang XY, Xiao YS *et al* (2007). Intratumoral balance of regulatory and cytotoxic T cells is associated with prognosis of hepatocellular carcinoma after resection. *J Clin Oncol* **25**: 2586-93.
- Germano G, Allavena P, Mantovani A (2008). Cytokines as a key component of cancer-related inflammation. *Cytokine* **43**: 374-9.
- Gershwin ME, Manns MP, Vierling JM. (2007a). *Liver Immunology Principles and Practice, Vol. Chapter 7*. Invernizzi P, Bianchi I, Locati M, Bonocchi R and Selmi C (eds). Humana Press Inc.: Totowa, NJ, pp 83 - 93.
- Gershwin ME, Manns MP, Vierling JM. (2007b). *Liver Immunology Principles and Practice, Vol. Chapter 3*. O'Farrelly CaD, D. (ed.). Humana Press Inc.: Totowa, NJ, pp 41 - 48.
- Gershwin ME, Manns MP, Vierling JM. (2007c). *Liver Immunology Principles and Practice, Vol. Chapter 2*. Knolle P (ed.). Humana Press Inc.: Totowa, NJ, pp 25 - 39.
- Gilfillan S, Chan CJ, Cella M, Haynes NM, Rapaport AS, Boles KS *et al* (2008). DNAM-1 promotes activation of cytotoxic lymphocytes by nonprofessional antigen-presenting cells and tumors. *J Exp Med* **205**: 2965-73.
- Gollob JA, Wilhelm S, Carter C, Kelley SL (2006). Role of Raf kinase in cancer: therapeutic potential of targeting the Raf/MEK/ERK signal transduction pathway. *Semin Oncol* **33**: 392-406.
- Greten TF, Korangy F, Manns MP, Malek NP (2009). Molecular therapy for the treatment of hepatocellular carcinoma. *Br J Cancer* **100**: 19-23.
- Gururaj A, Kumar R (2005). Polypeptide growth factors and their receptors. *Cancer Treat Res* **126**: 1-14.
- Halama N, Braun M, Kahlert C, Spille A, Quack C, Rahbari N *et al* (2011). Natural Killer Cells are Scarce in Colorectal Carcinoma Tissue Despite High Levels of Chemokines and Cytokines. *Clin Cancer Res* **17**: 678-689.
- Han Y, Zhang C (2010). Macrophage migration inhibitory factor plays a pivotal role in hepatocellular carcinoma and may be a noninvasive imaging target. *Med Hypotheses* **75**: 530-2.
- Hanahan D, Weinberg RA (2000). The hallmarks of cancer. *Cell* **100**: 57-70.
- Hanahan D, Weinberg RA (2011). Hallmarks of cancer: the next generation. *Cell* **144**: 646-74.
- Hasbold J, Gett AV, Rush JS, Deenick E, Avery D, Jun J *et al* (1999). Quantitative analysis of lymphocyte differentiation and proliferation in vitro using carboxyfluorescein diacetate succinimidyl ester. *Immunol Cell Biol* **77**: 516-22.

- Heidorn SJ, Milagre C, Whittaker S, Nourry A, Niculescu-Duvas I, Dhomen N *et al* (2010). Kinase-dead BRAF and oncogenic RAS cooperate to drive tumor progression through CRAF. *Cell* **140**: 209-21.
- Hennessy BT, Smith DL, Ram PT, Lu Y, Mills GB (2005). Exploiting the PI3K/AKT pathway for cancer drug discovery. *Nat Rev Drug Discov* **4**: 988-1004.
- Hennig M, Yip-Schneider MT, Wentz S, Wu H, Hekmatyar SK, Klein P *et al* (2010). Targeting mitogen-activated protein kinase kinase with the inhibitor PD0325901 decreases hepatocellular carcinoma growth in vitro and in mouse model systems. *Hepatology* **51**: 1218-25.
- Hintermann E, Bayer M, Pfeilschifter JM, Luster AD, Christen U (2010). CXCL10 promotes liver fibrosis by prevention of NK cell mediated hepatic stellate cell inactivation. *Journal of Autoimmunity* **35**: 424-35.
- Hoechst B, Voigtlaender T, Ormandy L, Gamrekelashvili J, Zhao F, Wedemeyer H *et al* (2009). Myeloid derived suppressor cells inhibit natural killer cells in patients with hepatocellular carcinoma via the NKp30 receptor. *Hepatology* **50**: 799-807.
- Horst D, Kriegl L, Engel J, Kirchner T, Jung A (2009). Prognostic significance of the cancer stem cell markers CD133, CD44, and CD166 in colorectal cancer. *Cancer Invest* **27**: 844-50.
- Hoshida Y, Toffanin S, Lachenmayer A, Villanueva A, Minguez B, Llovet JM (2010). Molecular classification and novel targets in hepatocellular carcinoma: recent advancements. *Semin Liver Dis* **30**: 35-51.
- Hudson JD, Shoaibi MA, Maestro R, Carnero A, Hannon GJ, Beach DH (1999). A proinflammatory cytokine inhibits p53 tumor suppressor activity. *J Exp Med* **190**: 1375-82.
- Hui L, Bakiri L, Mairhorfer A, Schweifer N, Haslinger C, Kenner L *et al* (2007). p38alpha suppresses normal and cancer cell proliferation by antagonizing the JNK-c-Jun pathway. *Nat Genet* **39**: 741-9.
- Hussain SP, Schwank J, Staib F, Wang XW, Harris CC (2007). TP53 mutations and hepatocellular carcinoma: insights into the etiology and pathogenesis of liver cancer. *Oncogene* **26**: 2166-76.
- Huynh H (2010). Molecularly targeted therapy in hepatocellular carcinoma. *Biochem Pharmacol* **80**: 550-60.
- Huynh H, Ngo VC, Koong HN, Poon D, Choo SP, Thng CH *et al* (2009). Sorafenib and rapamycin induce growth suppression in mouse models of hepatocellular carcinoma. *J Cell Mol Med* **13**: 2673-83.
- Huynh H, Nguyen TTT, Chow K-HP, Tan PH, Soo KC, Tran E (2003). Over-expression of the mitogen-activated protein kinase (MAPK) kinase (MEK)-MAPK in hepatocellular carcinoma: its role in tumor progression and apoptosis. *BMC Gastroenterol* **3**: 19-19.

- Huynh H, Soo KC, Chow PK, Tran E (2007). Targeted inhibition of the extracellular signal-regulated kinase kinase pathway with AZD6244 (ARRY-142886) in the treatment of hepatocellular carcinoma. *Mol Cancer Ther* **6**: 138-46.
- Janeway C, Travers P, Walport M, Shlomchik M (2005). *Immunobiology : the immune system in health and disease*, 6th edn. Garland Science: New York, xxiii, 823 p.pp.
- Kao J, Ko EC, Eisenstein S, Sikora AG, Fu S, Chen SH (2011). Targeting immune suppressing myeloid-derived suppressor cells in oncology. *Crit Rev Oncol Hematol* **77**: 12-9.
- Kaplan FM, Shao Y, Mayberry MM, Aplin AE (2011). Hyperactivation of MEK-ERK1/2 signaling and resistance to apoptosis induced by the oncogenic B-RAF inhibitor, PLX4720, in mutant N-RAS melanoma cells. *Oncogene*.
- Katz M, Amit I, Yarden Y (2007). Regulation of MAPKs by growth factors and receptor tyrosine kinases. *Biochim Biophys Acta* **1773**: 1161-76.
- Kawano T, Cui J, Koezuka Y, Toura I, Kaneko Y, Motoki K *et al* (1997). CD1d-restricted and TCR-mediated activation of valpha14 NKT cells by glycosylceramides. *Science* **278**: 1626-9.
- Keeley EC, Mehrad B, Strieter RM (2011). Chemokines as mediators of tumor angiogenesis and neovascularization. *Exp Cell Res* **317**: 685-90.
- Keshet Y, Seger R (2010). The MAP kinase signaling cascades: a system of hundreds of components regulates a diverse array of physiological functions. *Methods Mol Biol* **661**: 3-38.
- Keskin DB, Allan DS, Rybalov B, Andzelm MM, Stern JN, Kopcow HD *et al* (2007). TGFbeta promotes conversion of CD16+ peripheral blood NK cells into CD16- NK cells with similarities to decidual NK cells. *Proc Natl Acad Sci U S A* **104**: 3378-83.
- Kim S, Poursine-Laurent J, Truscott SM, Lybarger L, Song YJ, Yang L *et al* (2005). Licensing of natural killer cells by host major histocompatibility complex class I molecules. *Nature* **436**: 709-13.
- Kirstein SL, Atienza JM, Xi B, Zhu J, Yu N, Wang X *et al* (2006). Live cell quality control and utility of real-time cell electronic sensing for assay development. *Assay Drug Dev Technol* **4**: 545-53.
- Knolle PA, Gerken G (2000). Local control of the immune response in the liver. *Immunological Reviews* **174**: 21-34.
- Kohga K, Takehara T, Tatsumi T, Ishida H, Miyagi T, Hosui A *et al* (2010). Sorafenib inhibits the shedding of major histocompatibility complex class I-related chain A on hepatocellular carcinoma cells by down-regulating a disintegrin and metalloproteinase 9. *Hepatology*.
- Kohga K, Takehara T, Tatsumi T, Ohkawa K, Miyagi T, Hiramatsu N *et al* (2008). Serum levels of soluble major histocompatibility complex (MHC) class I-related chain A in patients

with chronic liver diseases and changes during transcatheter arterial embolization for hepatocellular carcinoma. *Cancer Sci* **99**: 1643-9.

Korangy F, Hochst B, Manns MP, Greten TF (2010a). Immune responses in hepatocellular carcinoma. *Dig Dis* **28**: 150-4.

Korangy F, Hochst B, Manns MP, Greten TF (2010b). Immunotherapy of hepatocellular carcinoma. *Expert Rev Gastroenterol Hepatol* **4**: 345-53.

Krishna M, Narang H (2008). The complexity of mitogen-activated protein kinases (MAPKs) made simple. *Cell Mol Life Sci* **65**: 3525-44.

Krockenberger M, Dombrowski Y, Weidler C, Ossadnik M, Honig A, Hausler S *et al* (2008). Macrophage migration inhibitory factor contributes to the immune escape of ovarian cancer by down-regulating NKG2D. *J Immunol* **180**: 7338-48.

Kroemer G, Galluzzi L, Vandenabeele P, Abrams J, Alnemri ES, Baehrecke EH *et al* (2009). Classification of cell death: recommendations of the Nomenclature Committee on Cell Death 2009. *Cell Death Differ* **16**: 3-11.

Kronenberg M (2005). Toward an understanding of NKT cell biology: progress and paradoxes. *Annu Rev Immunol* **23**: 877-900.

Kumar D, Hosse J, von Toerne C, Noessner E, Nelson PJ (2009). JNK MAPK pathway regulates constitutive transcription of CCL5 by human NK cells through SP1. *J Immunol* **182**: 1011-20.

Lachenmayer A, Alsinet C, Chang CY, Llovet JM (2010). Molecular approaches to treatment of hepatocellular carcinoma. *Dig Liver Dis* **42 Suppl 3**: S264-72.

Lee JW, Wang P, Kattah MG, Youssef S, Steinman L, DeFea K *et al* (2008a). Differential regulation of chemokines by IL-17 in colonic epithelial cells. *J Immunol* **181**: 6536-45.

Lee KH, Choi EY, Hyun MS, Jang BI, Kim TN, Lee HJ *et al* (2008b). Role of hepatocyte growth factor/c-Met signaling in regulating urokinase plasminogen activator on invasiveness in human hepatocellular carcinoma: a potential therapeutic target. *Clin Exp Metastasis* **25**: 89-96.

Leicht DT, Balan V, Kaplun A, Singh-Gupta V, Kaplun L, Dobson M *et al* (2007). Raf kinases: function, regulation and role in human cancer. *Biochim Biophys Acta* **1773**: 1196-212.

Liu J, Lin A (2005). Role of JNK activation in apoptosis: a double-edged sword. *Cell Res* **15**: 36-42.

Liu L, Cao Y, Chen C, Zhang X, McNabola A, Wilkie D *et al* (2006). Sorafenib blocks the RAF/MEK/ERK pathway, inhibits tumor angiogenesis, and induces tumor cell apoptosis in hepatocellular carcinoma model PLC/PRF/5. *Cancer Res* **66**: 11851-8.

- Liu WH, Chang LS (2010). Piceatannol induces Fas and FasL up-regulation in human leukemia U937 cells via Ca<sup>2+</sup>/p38alpha MAPK-mediated activation of c-Jun and ATF-2 pathways. *Int J Biochem Cell Biol* **42**: 1498-506.
- Liu Y, Kimura K, Yanai R, Chikama T, Nishida T (2008). Cytokine, chemokine, and adhesion molecule expression mediated by MAPKs in human corneal fibroblasts exposed to poly(I:C). *Invest Ophthalmol Vis Sci* **49**: 3336-44.
- Ljunggren HG, Karre K (1990). In search of the 'missing self': MHC molecules and NK cell recognition. *Immunol Today* **11**: 237-44.
- Ljunggren HG, Malmberg KJ (2007). Prospects for the use of NK cells in immunotherapy of human cancer. *Nat Rev Immunol* **7**: 329-39.
- Llovet JM, Bruix J (2008). Molecular targeted therapies in hepatocellular carcinoma. *Hepatology* **48**: 1312-27.
- Llovet JM, Burroughs A, Bruix J (2003). Hepatocellular carcinoma. *Lancet* **362**: 1907-17.
- Llovet JM, Ricci S, Mazzaferro V, Hilgard P, Gane E, Blanc J-F *et al* (2008). Sorafenib in advanced hepatocellular carcinoma. *N Engl J Med* **359**: 378-390.
- LoRusso PM, Krishnamurthi SS, Rinehart JJ, Nabell LM, Malburg L, Chapman PB *et al* (2010). Phase I pharmacokinetic and pharmacodynamic study of the oral MAPK/ERK kinase inhibitor PD-0325901 in patients with advanced cancers. *Clin Cancer Res* **16**: 1924-37.
- Lotze MT, Thomson AW (2010). *Natural killer cells : basic science and clinical application*. Elsevier/Academic Press: Amsterdam ; Boston ; London, **Chapter 27**, 345-357pp.
- Lue H, Dewor M, Leng L, Bucala R, Bernhagen J (2011). Activation of the JNK signalling pathway by macrophage migration inhibitory factor (MIF) and dependence on CXCR4 and CD74. *Cellular Signalling* **23**: 135-44.
- Lugrin J, Ding XC, Le Roy D, Chanson AL, Sweep FC, Calandra T *et al* (2009). Histone deacetylase inhibitors repress macrophage migration inhibitory factor (MIF) expression by targeting MIF gene transcription through a local chromatin deacetylation. *Biochim Biophys Acta* **1793**: 1749-58.
- Lyons AB, Parish CR (1994). Determination of lymphocyte division by flow cytometry. *J Immunol Methods* **171**: 131-7.
- Masson D, Jarry A, Baury B, Blanchardie P, Laboisie C, Lustenberger P *et al* (2001). Overexpression of the CD155 gene in human colorectal carcinoma. *Gut* **49**: 236-40.
- McCubrey JA, Steelman LS, Abrams SL, Lee JT, Chang F, Bertrand FE *et al* (2006). Roles of the RAF/MEK/ERK and PI3K/PTEN/AKT pathways in malignant transformation and drug resistance. *Adv Enzyme Regul* **46**: 249-79.

- McCubrey JA, Steelman LS, Chappell WH, Abrams SL, Wong EW, Chang F *et al* (2007). Roles of the Raf/MEK/ERK pathway in cell growth, malignant transformation and drug resistance. *Biochim Biophys Acta* **1773**: 1263-84.
- Mendez-Sanchez N, Vasquez-Fernandez F, Zamora-Valdes D, Uribe M (2008). Sorafenib, a systemic therapy for hepatocellular carcinoma. *Ann Hepatol* **7**: 46-51.
- Menges CW, McCance DJ (2008). Constitutive activation of the Raf-MAPK pathway causes negative feedback inhibition of Ras-PI3K-AKT and cellular arrest through the EphA2 receptor. *Oncogene* **27**: 2934-40.
- Moroso V, Metselaar HJ, Mancham S, Tilanus HW, Eissens D, van der Meer A *et al* (2010). Liver grafts contain a unique subset of natural killer cells that are transferred into the recipient after liver transplantation. *Liver Transpl* **16**: 895-908.
- Morsy MA, Norman PJ, Mitry R, Rela M, Heaton ND, Vaughan RW (2005). Isolation, purification and flow cytometric analysis of human intrahepatic lymphocytes using an improved technique. *Laboratory Investigation* **85**: 285-96.
- Muller M, Schilling T, Sayan AE, Kairat A, Lorenz K, Schulze-Bergkamen H *et al* (2005). TAp73/Delta Np73 influences apoptotic response, chemosensitivity and prognosis in hepatocellular carcinoma. *Cell Death Differ* **12**: 1564-77.
- Muller M, Schleithoff ES, Stremmel W, Melino G, Krammer PH, Schilling T (2006). One, two, three--p53, p63, p73 and chemosensitivity. *Drug Resist Updat* **9**: 288-306.
- Muller M, Wilder S, Bannasch D, Israeli D, Lehlbach K, Li-Weber M *et al* (1998). p53 activates the CD95 (APO-1/Fas) gene in response to DNA damage by anticancer drugs. *J Exp Med* **188**: 2033-45.
- Mundt HM, Stremmel W, Melino G, Krammer PH, Schilling T, Muller M (2010). Dominant negative (DeltaN) p63alpha induces drug resistance in hepatocellular carcinoma by interference with apoptosis signaling pathways. *Biochem Biophys Res Commun* **396**: 335-41.
- Nagai T, Arao T, Furuta K, Sakai K, Kudo K, Kaneda H *et al* (2011). Sorafenib inhibits the hepatocyte growth factor-mediated epithelial mesenchymal transition in hepatocellular carcinoma. *Mol Cancer Ther* **10**: 169-77.
- Nausch N, Cerwenka A (2008). NKG2D ligands in tumor immunity. *Oncogene* **27**: 5944-58.
- Nicoletti I, Migliorati G, Pagliacci MC, Grignani F, Riccardi C (1991). A rapid and simple method for measuring thymocyte apoptosis by propidium iodide staining and flow cytometry. *Journal of Immunological Methods* **139**: 271-9.
- Noble PB, Cutts JH (1967). Separation of blood leukocytes by Ficoll gradient. *Can Vet J* **8**: 110-1.

- Norris S, Collins C, Doherty DG, Smith F, McEntee G, Traynor O *et al* (1998). Resident human hepatic lymphocytes are phenotypically different from circulating lymphocytes. *J Hepatol* **28**: 84-90.
- Oo YH, Adams DH (2010). The role of chemokines in the recruitment of lymphocytes to the liver. *Journal of Autoimmunity* **34**: 45-54.
- Osaki M, Oshimura M, Ito H (2004). PI3K-Akt pathway: its functions and alterations in human cancer. *Apoptosis* **9**: 667-76.
- Parish CR (1999). Fluorescent dyes for lymphocyte migration and proliferation studies. *Immunol Cell Biol* **77**: 499-508.
- Parker GA, Picut CA (2005). Liver immunobiology. *Toxicol Pathol* **33**: 52-62.
- Paust S, Gill HS, Wang BZ, Flynn MP, Moseman EA, Senman B *et al* (2010). Critical role for the chemokine receptor CXCR6 in NK cell-mediated antigen-specific memory of haptens and viruses. *Nat Immunol* **11**: 1127-35.
- Pfizer I (2010). Pfizer Discontinues Phase 3 Trial of Sutent in Advanced Hepatocellular Carcinoma [http://media.pfizer.com/files/news/press\\_releases/2010/sun\\_1170\\_042210.pdf](http://media.pfizer.com/files/news/press_releases/2010/sun_1170_042210.pdf).
- Pilette C, Ouadrhiri Y, Van Snick J, Renauld JC, Staquet P, Vaerman JP *et al* (2002). IL-9 inhibits oxidative burst and TNF-alpha release in lipopolysaccharide-stimulated human monocytes through TGF-beta. *J Immunol* **168**: 4103-11.
- Platanias LC. (2005). *Chemokine and Cancer, Vol. Chapter 2*. Murooka TT, Ward SE and Fish EN (eds). Springer: New York, pp 15-44.
- Poulikakos PI, Zhang C, Bollag G, Shokat KM, Rosen N (2010). RAF inhibitors transactivate RAF dimers and ERK signalling in cells with wild-type BRAF. *Nature* **464**: 427-30.
- Puisieux A, Ji J, Guillot C, Legros Y, Soussi T, Isselbacher K *et al* (1995). p53-mediated cellular response to DNA damage in cells with replicative hepatitis B virus. *Proc Natl Acad Sci U S A* **92**: 1342-6.
- Racanelli V, Rehermann B (2006). The liver as an immunological organ. *Hepatology* **43**: S54-62.
- Raulet DH, Vance RE (2006). Self-tolerance of natural killer cells. *Nat Rev Immunol* **6**: 520-31.
- Ren Y, Tsui HT, Poon RT, Ng IO, Li Z, Chen Y *et al* (2003). Macrophage migration inhibitory factor: roles in regulating tumor cell migration and expression of angiogenic factors in hepatocellular carcinoma. *Int J Cancer* **107**: 22-9.
- Renaud SJ, Sullivan R, Graham CH (2009). Tumour necrosis factor alpha stimulates the production of monocyte chemoattractants by extravillous trophoblast cells via differential activation of MAPK pathways. *Placenta* **30**: 313-9.

- Ricci MS, Kim SH, Ogi K, Plastaras JP, Ling J, Wang W *et al* (2007). Reduction of TRAIL-induced Mcl-1 and cIAP2 by c-Myc or sorafenib sensitizes resistant human cancer cells to TRAIL-induced death. *Cancer Cell* **12**: 66-80.
- Roberts PJ, Der CJ (2007). Targeting the Raf-MEK-ERK mitogen-activated protein kinase cascade for the treatment of cancer. *Oncogene* **26**: 3291-310.
- Robertson MJ (2002). Role of chemokines in the biology of natural killer cells. *J Leukoc Biol* **71**: 173-83.
- Robinson JP (2004). Overview of flow cytometry and microbiology. *Curr Protoc Cytom Chapter 11*: Unit 11 1.
- Roger T, Chanson AL, Knaup-Reymond M, Calandra T (2005). Macrophage migration inhibitory factor promotes innate immune responses by suppressing glucocorticoid-induced expression of mitogen-activated protein kinase phosphatase-1. *European Journal of Immunology* **35**: 3405-13.
- Salih HR, Goehlsdorf D, Steinle A (2006). Release of MICB molecules by tumor cells: mechanism and soluble MICB in sera of cancer patients. *Human Immunology* **67**: 188-95.
- Schmitz KJ, Wohlschlaeger J, Lang H, Sotiropoulos GC, Malago M, Steveling K *et al* (2008). Activation of the ERK and AKT signalling pathway predicts poor prognosis in hepatocellular carcinoma and ERK activation in cancer tissue is associated with hepatitis C virus infection. *J Hepatol* **48**: 83-90.
- Schrader J, Iredale JP (2011). The inflammatory microenvironment of HCC - The plot becomes complex. *J Hepatol* **54**: 853-5.
- Seger R, Krebs EG (1995). The MAPK signaling cascade. *FASEB Journal* **9**: 726-35.
- Sers C, Kuner R, Falk CS, Lund P, Sueltmann H, Braun M *et al* (2009). Down-regulation of HLA Class I and NKG2D ligands through a concerted action of MAPK and DNA methyltransferases in colorectal cancer cells. *Int J Cancer* **125**: 1626-39.
- Severi T, van Malenstein H, Verslype C, van Pelt JF (2010). Tumor initiation and progression in hepatocellular carcinoma: risk factors, classification, and therapeutic targets. *Acta Pharmacol Sin* **31**: 1409-20.
- Shaulian E (2010). AP-1--The Jun proteins: Oncogenes or tumor suppressors in disguise? *Cell Signal* **22**: 894-9.
- Sieghart W, Losert D, Strommer S, Cejka D, Schmid K, Rasoul-Rockenschaub S *et al* (2006). Mcl-1 overexpression in hepatocellular carcinoma: a potential target for antisense therapy. *J Hepatol* **44**: 151-7.

- Simpson KJ, Henderson NC, Bone-Larson CL, Lukacs NW, Hogaboam CM, Kunkel SL (2003). Chemokines in the pathogenesis of liver disease: so many players with poorly defined roles. *Clin Sci (Lond)* **104**: 47-63.
- Sirim P, Zeitlmann L, Kellersch B, Falk CS, Schendel DJ, Kolanus W (2001). Calcium signaling through the beta 2-cytoplasmic domain of LFA-1 requires intracellular elements of the T cell receptor complex. *J Biol Chem* **276**: 42945-56.
- Sloan KE, Eustace BK, Stewart JK, Zehetmeier C, Torella C, Simeone M *et al* (2004). CD155/PVR plays a key role in cell motility during tumor cell invasion and migration. *BMC Cancer* **4**: 73.
- Smith RA, Dumas J, Adnane L, Wilhelm SM (2006). Recent advances in the research and development of RAF kinase inhibitors. *Curr Top Med Chem* **6**: 1071-89.
- Sreeramaneni R, Chaudhry A, McMahon M, Sherr CJ, Inoue K (2005). Ras-Raf-Arf signaling critically depends on the Dmp1 transcription factor. *Mol Cell Biol* **25**: 220-32.
- Steinke JW, Borish L (2006). 3. Cytokines and chemokines. *J Allergy Clin Immunol* **117**: S441-5.
- Stepniak E, Ricci R, Eferl R, Sumara G, Sumara I, Rath M *et al* (2006). c-Jun/AP-1 controls liver regeneration by repressing p53/p21 and p38 MAPK activity. *Genes Dev* **20**: 2306-14.
- Tamaki S, Kawakami M, Ishitani A, Kawashima W, Kasuda S, Yamanaka Y *et al* (2010). Soluble MICB serum levels correlate with disease stage and survival rate in patients with oral squamous cell carcinoma. *Anticancer Research* **30**: 4097-101.
- Tanaka S, Arii S (2010). Current status of molecularly targeted therapy for hepatocellular carcinoma: basic science. *Int J Clin Oncol* **15**: 235-41.
- Tibbles LA, Spurrell JC, Bowen GP, Liu Q, Lam M, Zaiss AK *et al* (2002). Activation of p38 and ERK signaling during adenovirus vector cell entry lead to expression of the C-X-C chemokine IP-10. *J Virol* **76**: 1559-68.
- Tsai J, Lee JT, Wang W, Zhang J, Cho H, Mamo S *et al* (2008). Discovery of a selective inhibitor of oncogenic B-Raf kinase with potent antimelanoma activity. *Proc Natl Acad Sci U S A* **105**: 3041-6.
- Ueki T, Fujimoto J, Suzuki T, Yamamoto H, Okamoto E (1997). Expression of hepatocyte growth factor and its receptor, the c-met proto-oncogene, in hepatocellular carcinoma. *Hepatology* **25**: 619-23.
- Venkatesha RT, Berla Thangam E, Zaidi AK, Ali H (2005). Distinct regulation of C3a-induced MCP-1/CCL2 and RANTES/CCL5 production in human mast cells by extracellular signal regulated kinase and PI3 kinase. *Mol Immunol* **42**: 581-7.
- Vivier E, Raulet DH, Moretta A, Caligiuri MA, Zitvogel L, Lanier LL *et al* (2011). Innate or adaptive immunity? The example of natural killer cells. *Science* **331**: 44-9.

- Watanabe J, Kushihata F, Honda K, Mominoki K, Matsuda S, Kobayashi N (2002). Bcl-xL overexpression in human hepatocellular carcinoma. *Int J Oncol* **21**: 515-9.
- Watanabe J, Kushihata F, Honda K, Sugita A, Tateishi N, Mominoki K *et al* (2004). Prognostic significance of Bcl-xL in human hepatocellular carcinoma. *Surgery* **135**: 604-12.
- Weichert W, Knosel T, Bellach J, Dietel M, Kristiansen G (2004). ALCAM/CD166 is overexpressed in colorectal carcinoma and correlates with shortened patient survival. *J Clin Pathol* **57**: 1160-4.
- Weiler-Normann C, Rehermann B (2004). The liver as an immunological organ. *Journal of Gastroenterology and Hepatology* **19**: S279-S283.
- Weston SA, Parish CR (1990). New fluorescent dyes for lymphocyte migration studies. Analysis by flow cytometry and fluorescence microscopy. *Journal of Immunological Methods* **133**: 87-97.
- Whittaker S, Marais R, Zhu AX (2010). The role of signaling pathways in the development and treatment of hepatocellular carcinoma. *Oncogene*.
- Wilhelm S, Carter C, Lynch M, Lowinger T, Dumas J, Smith RA *et al* (2006). Discovery and development of sorafenib: a multikinase inhibitor for treating cancer. *Nat Rev Drug Discov* **5**: 835-44.
- Wilhelm SM, Carter C, Tang L, Wilkie D, McNabola A, Rong H *et al* (2004). BAY 43-9006 exhibits broad spectrum oral antitumor activity and targets the RAF/MEK/ERK pathway and receptor tyrosine kinases involved in tumor progression and angiogenesis. *Cancer Res* **64**: 7099-109.
- Winau F, Quack C, Darmoise A, Kaufmann SH (2008). Starring stellate cells in liver immunology. *Curr Opin Immunol* **20**: 68-74.
- Wong CK, Wang CB, Ip WK, Tian YP, Lam CW (2005). Role of p38 MAPK and NF- $\kappa$ B for chemokine release in coculture of human eosinophils and bronchial epithelial cells. *Clin Exp Immunol* **139**: 90-100.
- Xiao L, Rao JN, Zou T, Liu L, Yu TX, Zhu XY *et al* (2010). Induced ATF-2 represses CDK4 transcription through dimerization with JunD inhibiting intestinal epithelial cell growth after polyamine depletion. *Am J Physiol Cell Physiol* **298**: C1226-34.
- Yang H, Magilnick N, Nouredin M, Mato JM, Lu SC (2007). Effect of hepatocyte growth factor on methionine adenosyltransferase genes and growth is cell density-dependent in HepG2 cells. *Journal of Cellular Physiology* **210**: 766-73.
- Yang JD, Nakamura I, Roberts LR (2011). The tumor microenvironment in hepatocellular carcinoma: current status and therapeutic targets. *Semin Cancer Biol* **21**: 35-43.

Yeh TC, Marsh V, Bernat BA, Ballard J, Colwell H, Evans RJ *et al* (2007). Biological characterization of ARRY-142886 (AZD6244), a potent, highly selective mitogen-activated protein kinase kinase 1/2 inhibitor. *Clin Cancer Res* **13**: 1576-83.

Yip-Schneider MT, Klein PJ, Wentz SC, Zeni A, Menze A, Schmidt CM (2009). Resistance to mitogen-activated protein kinase kinase (MEK) inhibitors correlates with up-regulation of the MEK/extracellular signal-regulated kinase pathway in hepatocellular carcinoma cells. *J Pharmacol Exp Ther* **329**: 1063-70.

Zhao YM, Wang L, Dai Z, Wang DD, Hei ZY, Zhang N *et al* (2011). Validity of plasma macrophage migration inhibitory factor for diagnosis and prognosis of hepatocellular carcinoma. *Int J Cancer*.

Zucman-Rossi J (2010). Molecular classification of hepatocellular carcinoma. *Dig Liver Dis* **42 Suppl 3**: S235-41.

## Acknowledgements

First of all, I would like to thank my supervisor Prof. Dr. Christine Falk for giving me the opportunity to work in her lab on such an interesting project. Thank you Chris for transferring so much energy and enthusiasm to me that working in science makes so much fun. I had a great time during my PhD thesis working in your lab!

Also, I thank Prof. Dr. Stephan Urban for being a supportive member of my PhD committee and for the representation of this work at the biological faculty of the University of Heidelberg.

Many thanks go to the lab members Bernadette Müller, Susan Gottwald, Ludmila Umansky, Tina Lerchl and the former members Stefan Maßen, Monika Braun and Barbara Simm. I had a great time working together with you all! Particularly, I want to thank Ludmila for teaching and helping me with the western blots and the multiplex assays. Also, thank you Tina for performing the ELISAs. Moreover, I want to thank several friends and colleagues for having a fun and refreshing time during lunch breaks.

I am grateful to our collaboration partners. Thanks to the laboratory of Prof. Dr. Martina Müller-Schilling, University Hospital Heidelberg, for providing the antibodies for western blot analysis and for good cooperation. I want to thank Kristin Wahl and Prof. Dr. Heike Bantel, Hannover Medical School, for the incredible work on treated HCC tissue. Thanks to Dr. Katrin Hoffman, University Hospital Heidelberg, and PD Dr. Gernot Kaiser, University Hospital Essen, for providing liver tissue samples. Also great thanks to Anne Skoeries and Dr. Niels Halama from the Hamamatsu TIGA Center, University of Heidelberg, for performing the bioinformatic analysis.

Moreover, I want to thank the German Cancer Research Center (DKFZ) Heidelberg for providing the funding for the first three years of my work and the DKFZ PhD program for providing the huge amount of lectures, seminars, courses and support.

Also, I thank Chris, Miriam Breunig, Harold Fenby, Susan and Ludmila for reading and correcting my thesis or parts of my thesis.

I want to thank Konrad, Charlotte, Miriam, Peter and Fransiska Breunig, who encouraged me the whole time.

My special thanks go to my parents, my brothers Valentin and Florian and my relatives, who always supported me. This would not be possible without your help!

Finally, I want to thank Esther Breunig for her great support. Thank you so much! You are the best!

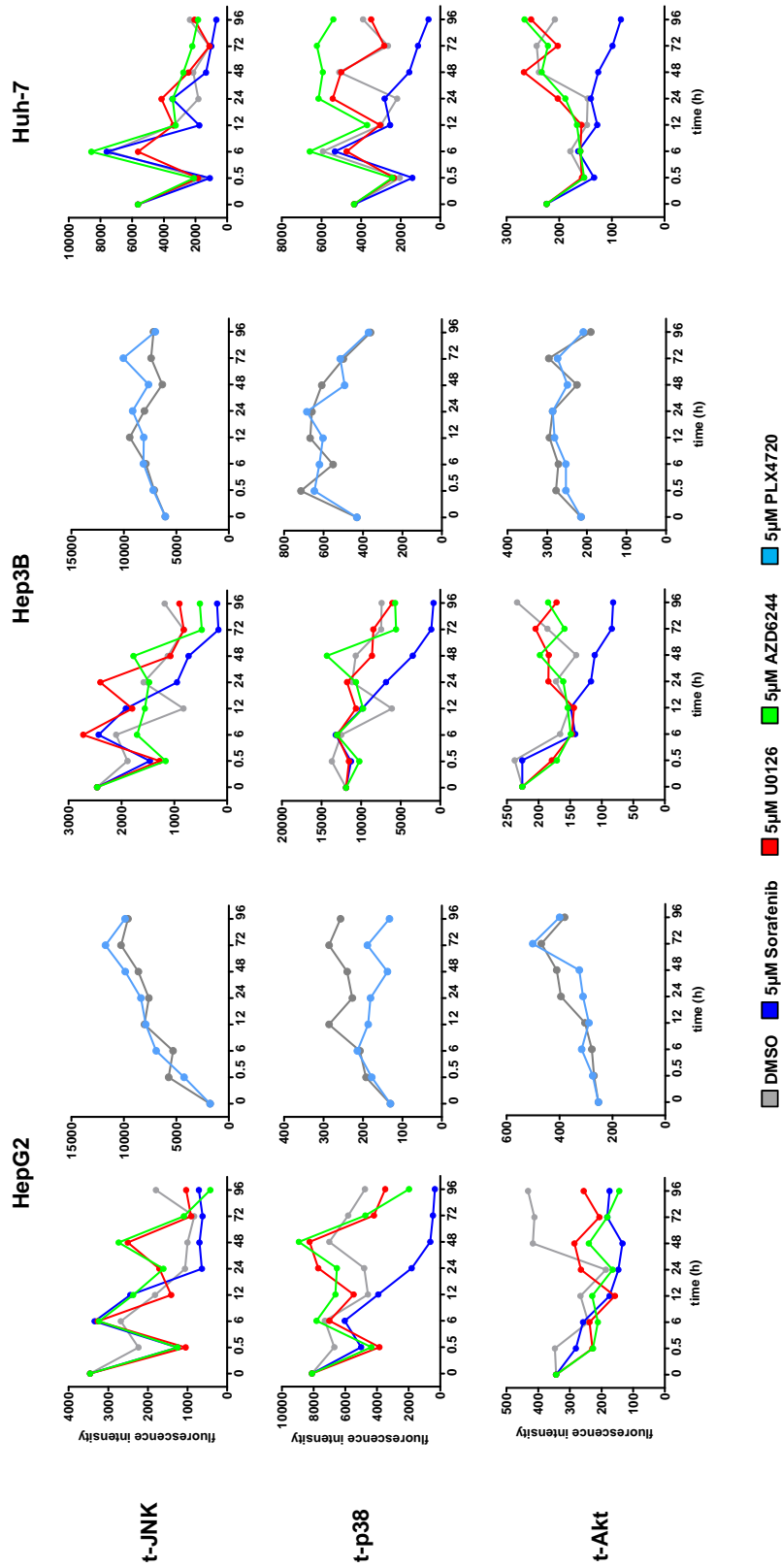
## List of Publications

- Winau F, **Quack C**, Dairmoise A, Kaufmann SH (2008). Starring stellate cells in liver immunology. *Curr Opin Immunol.* 20(1):68-74.
- Halama N, Braun M, Kahlert C, Spille A, **Quack C**, Rahbari N, Koch M, Weitz J, Kloor M, Zoernig I, Schirmacher P, Brand K, Grabe N, and Falk CS (2011). Natural killer cells are scarce in colorectal carcinoma tissue despite high levels of chemokines & cytokines. *Clin Cancer Res.* 17(4): 678-689
- Thomas A\*, **Quack C\***, Schilling T, Wahl K, Lehner F, Bantel H, Manns MP, Stremmel W, Falk CS and Müller M (manuscript in preparation). Sorafenib-induced apoptosis depends on p53 family function. (\*equally contribution)
- Quack C**, Umansky L, Lerchl T, Wahl K, Xiao Z, Hoffmann K, Bantel H, Falk CS (manuscript in preparation). Differential effects of MAPK inhibitors in hepatocellular carcinoma cells.

## Conference Abstracts

- **Translational Research in Chronic Liver Diseases**  
Heidelberg, Germany 2009
- **2<sup>nd</sup> European Congress on Immunology**  
Berlin, Germany 2009
- **EFIS – EJI Natural Killer Cell Symposium**  
Freiburg, Germany 2009
- **4<sup>th</sup> ENII – MUGEN Summer School on Immunology**  
Sardinia, Italy 2010
- **12<sup>th</sup> Meeting of the Society of Natural Immunity**  
Dubrovnik, Croatia 2010
- **7<sup>th</sup> Spring School on Immunology**  
Ettal, Germany 2011

# Appendix



**Appendix 1: Total amount of JNK, p38 and Akt after MAPK inhibitor treatment.** HepG2, Hep3B and Huh-7 cells were treated with 5  $\mu$ M MAPK inhibitor or DMSO as control for up to 96 h. The total level of JNK, p38 and Akt was measured. Effect of PLX4720 was not tested for Huh-7 cells. Shown is one representative experiment of up to three independent experiments. For each experiment, protein concentration was adjusted to 500  $\mu$ g/ml and a minimum of 50 beads was measured and MFI was calculated. The readout of the phosphoplex is the MFI of > 50 beads detecting total-kinases.

---

**Appendix 2: Total amount of c-Jun and ATF-2 after MAPK inhibitor treatment.** HepG2, Hep3B and Huh-7 cells were treated with 5  $\mu$ M MAPK inhibitor or DMSO as control for up to 96 h. The total level of c-Jun and ATF-2 was measured. Effect of PLX4720 was not tested for Huh-7 cells. Shown is one representative experiment of up to three independent experiments. For each experiment, protein concentration was adjusted to 500  $\mu$ g/ml and a minimum of 50 beads was measured and MFI was calculated. The readout of the phosphoplex is the MFI of > 50 beads detecting total-kinases.

---

